

# **Effect of Spatial Scale on Hydrologic Modeling in a Headwater Catchment**

by

Ryan Fedak

Thesis submitted to the Faculty of the  
Virginia Polytechnic Institute and State University  
in partial fulfillment of the requirements for the degree of

Master of Science  
in  
Civil Engineering

Dr. David F. Kibler, Chair  
Dr. G. V. Loganathan  
Dr. Tamim Younos

January 29, 1999  
Blacksburg, VA

# Effect of Spatial Scale on Hydrologic Modeling in a Headwater Catchment

by

Ryan Fedak

## ABSTRACT

In this study, two hydrologic models were applied to the mountainous Back Creek catchment, located in the headwaters of the Roanoke River in Southwest Virginia. The two models employed were HEC-1, an event based lumped model, and TOPMODEL, a continuous semi-distributed model. These models were used to investigate (a) the issue of spatial scale in hydrologic modeling, and (b) two approaches to modeling, continuous versus event based. Two HEC-1 models were developed with a different number of subareas in each. The hydrographs generated by each HEC-1 model for a number of large rainfall events were analyzed visually and statistically. No observable improvement resulted from increasing the number of subareas in the HEC-1 models from 20 to 81.

TOPMODEL was applied to the same watershed using a series of different size grid cells. The first step in applying TOPMODEL to a watershed involves GIS analysis which results in a raster grid of elevations used for the calculation of the topographic index,  $\ln(a/\tan \beta)$ . The hydrographs generated by TOPMODEL with each grid cell size were compared in order to assess the sensitivity of TOPMODEL hydrographs to grid cell size. An increase in grid cell size from 15 to 120 meters resulted in increased values of the watershed mean of the topographic index. However, hydrographs generated by TOPMODEL were completely unaffected by this increase in the topographic index. Analyses were also performed to determine the sensitivity of TOPMODEL hydrographs to several model parameters. It was determined that the parameters that had the greatest effect on hydrographs generated by TOPMODEL were the  $m$  and  $\ln(T_o)$  parameters.

The modeling performances of the event based HEC-1 and the continuous TOPMODEL were analyzed and compared visually and statistically for a number of large storms. The limited number of storms used to compare HEC-1 and TOPMODEL makes it difficult to determine definitively which model simulates large storms better. It does appear that perhaps HEC-1 is slightly superior in that regard. TOPMODEL was also executed as an event based model for two single events and the resulting hydrographs were compared to the HEC-1 and continuous TOPMODEL results. Both HEC-1 and TOPMODEL (when used as a continuous model) simulate large storms better than TOPMODEL (when used as an event based model).

# Acknowledgements

I would like thank Dr. David Kibler for serving as my advisor; his guidance, advice, and patience were invaluable. The insight and suggestions received from my other committee members, Dr. G.V. Loganathan and Dr. Tamim Younos, were greatly appreciated. The Virginia Tech Civil Engineering Department, and especially the Hydrosystems Division, have my gratitude for providing me with an excellent education. The Via Family deserves many thanks for assisting in providing funding for me, without which I could not have afforded graduate studies.

I would also like to thank my fellow Hydrosystems graduates students for their assistance, humor, and friendships. Finally, I would especially like to thank my family and Kimberly. Without their constant encouragement and faith in me, I could have never finished this project.

# Table of Contents

<b>1 Introduction</b> .....	1
1.1 Objectives.....	4
<b>2 Literature Review</b> .....	5
2.1 Evolution of Hydrologic Modeling.....	5
2.2 Predictive versus Investigative Models.....	6
2.3 Lumped versus Distributed Models.....	6
2.4 Geographic Information Systems (GIS) in Hydrologic Modeling.....	7
2.5 Continuous versus Event Based Models.....	9
2.6 Issue of Scale in Hydrologic Modeling.....	10
2.7 Recent Investigations into the Issue of Appropriate Grid Cell Size in TOPMODEL.....	11
<b>3 Watershed and Model Descriptions</b> .....	13
3.1 Watershed Description.....	13
3.2 Storm and Time Increment Selection.....	13
3.2.1 HEC-1.....	13
3.2.2 TOPMODEL.....	15
3.3 Model Descriptions.....	16
3.3.1 HEC-1.....	16
3.3.2 TOPMODEL.....	16
3.3.2.1 Assumptions.....	17
3.3.2.2 Basic Equations.....	21
3.3.2.3 Organization of Stores in TOPMODEL.....	24
3.3.2.4 Evapotranspiration.....	24
3.3.2.5 Overland Flow and Channel Routing.....	27
3.3.2.6 Specific version of TOPMODEL used in this study.....	30
3.3.2.6.1 History.....	30
3.3.2.6.2 Parameters.....	30
3.3.2.6.3 Input Files in DOS and Windows based versions of TOPMODEL.....	32

3.3.2.6.4 Initialization of Baseflow in the DOS and Windows Based Versions of TOPMODEL.....	35
3.3.2.6.5 GRIDATB .....	35
<b>4 Methodology .....</b>	<b>37</b>
4.1 HEC-1 .....	37
4.2 TOPMODEL .....	38
4.3 Model Calibration .....	38
4.3.1 HEC-1 .....	39
4.3.2 TOPMODEL .....	40
4.4 Analysis Techniques.....	41
<b>5 Results and Discussion.....</b>	<b>44</b>
5.1 TOPMODEL .....	44
5.1.1 Relationship between Topographic Index and Grid Cell Size .....	44
5.1.2 Effect of the $m$ Parameter on Simulated Hydrograph .....	44
5.1.3 Effect of the $\ln(T_o)$ Parameter on Simulated Hydrograph.....	51
5.1.4 Effect of the $ChVel$ Parameter on Simulated Hydrograph .....	55
5.1.5 Effect of Antecedent Moisture on Simulated Hydrograph.....	58
5.1.6 Effect of Grid Cell Size on TOPMODEL Simulated Hydrograph.....	60
5.2 HEC-1 .....	64
5.2.1 Effect of Spatial Scale on Simulated Hydrograph .....	64
5.3 Comparison of HEC-1 and TOPMODEL.....	68
5.3.1 Large storm modeling accuracy compared for TOPMODEL and HEC-1 .....	68
5.3.2 Continuous versus event based modeling.....	70
<b>6 Summary, Conclusions, and Future Research.....</b>	<b>76</b>
6.1 Summary .....	76
6.2 Conclusions .....	77
6.3 Future Research.....	78
<b>References .....</b>	<b>80</b>
<b>Appendix A: TOPMODEL Instructions.....</b>	<b>84</b>
<b>Appendix B: Sample GRIDATB Files.....</b>	<b>89</b>

<b>Appendix C:</b> GRIDATB Source FORTRAN Code .....	91
<b>Appendix D:</b> ArcView Instructions .....	99
<b>Appendix E:</b> 1995 TOPMODEL Hydrographs .....	129
<b>Appendix F:</b> 1996 TOPMODEL Hydrographs.....	139
<b>Appendix G:</b> 1997 TOPMODEL Hydrographs.....	149
<b>Appendix H:</b> HEC-1 Hydrographs.....	159
<b>Appendix I:</b> TOPMODEL Hydrographs Used for Comparison with HEC-1.....	164
<b>Appendix J:</b> Hydrographs for Water Years 1995, 1996, 1997, and the Beginning of 1998 .....	168
Vita .....	170

# List of Figures

Figure 1. Regional view including the Back Creek watershed outlined in black.....	14
Figure 2. Back Creek watershed with USGS gage station and IFLOWS rain gages .....	15
Figure 3. Directional weights for calculating contour length distance, cld, and upslope area per unit contour length, $a$ .....	18
Figure 4. Illustration of terms and concepts used in GRIDATB .....	20
Figure 5. Illustration of distribution of area in downslope directions used in GRIDATB .....	21
Figure 6. Simple graphical representation of the vertical storage in TOPMODEL. Modified from Beven <i>et al.</i> (1995).....	25
Figure 7. Yearly Evapotranspiration data used in TOPMODEL.....	26
Figure 8. Daily Evapotranspiration data used in TOPMODEL.....	26
Figure 9. Sample watershed to illustrate TOPMODEL routing method .....	28
Figure 10. Hydrograph from example problem demonstrating TOPMODEL routing procedure.....	29
Figure 11. Output form Windows based version of TOPMODEL.....	33
Figure 12. Output from DOS based version of TOPMODEL .....	33
Figure 13. Frequency distribution of the topographic index for varying grid cell sizes ....	45
Figure 14. Cumulative frequency distribution of the topographic index for varying grid cell sizes .....	45
Figure 15. Plot of mean value of topographic index for each grid cell size .....	46
Figure 16. (a-g) TOPMODEL hydrographs with varying values of $m$ .....	48
Figure 17. (a-e) TOPMODEL hydrographs with varying values of $\ln(T_o)$ .....	53
Figure 18. (a-c) TOPMODEL hydrographs with varying values of $ChVel$ .....	56
Figure 19 (a). November 1996 storm occurring at the end of a simulation period .....	59
Figure 19 (b). November 1996 event occurring at the beginning of a simulation period .....	59
Figure 20 (a). January 1996 event modeled with a 15 meter grid cell size .....	61
Figure 20 (b). January 1996 event modeled with a 120 meter grid cell size .....	61

Figure 21 (a). Original 15 meter topographic distribution and synthetic distributions shifted by increments of 10 .....	62
Figure 21 (b). Uniform topographic index distribution covering the same interval as the 15 meter distribution.....	63
Figure 22 (a). January 1996 event modeled with original 15 meter distribution.....	63
Figure 22 (b). January 1996 event modeled with synthetic distribution shifted by 30 .....	64
Figure 23. January 1995 event simulated using 20 subarea and 81 subarea HEC-1 Models .....	65
Figure 24 (a). August 1996 event; TOPMODEL continuous simulation .....	72
Figure 24 (b). August 1996 event; TOPMODEL event based simulation .....	72
Figure 24 (c). August 1996 event; HEC-1 event based simulation .....	73
Figure 25 (a). November 1996 event; TOPMODEL event based simulation .....	74
Figure 25 (b). November 1996 event; TOPMODEL continuous simulation .....	74
Figure 25 (c). November 1996 event; HEC-1 simulation .....	75

# List of Tables

Table 1. Topographic index statistics for varying grid cell sizes .....	46
Table 2. Comparison of HEC-1 peak flows generated by 81 and 20 subarea models .....	66
Table 3. Comparison of HEC-1 times to peak generated by 81 and 20 subarea models .....	67
Table 4. Comparison of HEC-1 flow volumes generated by 81 and 20 subarea models .....	68
Table 5. Comparison of HEC-1 and TOPMODEL peak flows.....	69
Table 6. Comparison of HEC-1 and TOPMODEL times to peak.....	69
Table 7. Comparison of continuous and event based simulation peak flows .....	73

# 1 Introduction

The early history of hydrology and hydraulic structures begins thousands of years ago when archeological evidence suggests that a dam was built across the Nile as early as 4000 B.C. Later a canal to transport fresh water was constructed between Cairo and Suez (Bedient and Huber (1992) and Biswas (1972)). The first serious students of hydrology were the Greek philosophers. Aristotle proposed the conversion of moist air into water deep inside mountains as the source of springs and streams. Flow measurement techniques based on the cross-sectional area were first attempted in the Roman water systems in 97 A.D. In the seventeenth century, Perrault made the first recorded measurements of rainfall and surface flow. He compared measured rainfall to the estimated flow of the Seine River to show that the two were related.

For appropriate design of hydraulic structures and flood control structures, information must be known about the hydrology of the system, such as peak discharge, runoff volume, and the time to peak of large storm events. Many design applications including dams, spillways, detention basins, culverts, and urban stormwater systems depend on this information. To accurately predict the peak discharge, runoff volume, and time to peak of design storms, the hydrological processes, which control the rainfall-runoff phenomenon, must be investigated.

It was not until relatively recently that attempts were made to model rainfall-runoff thus predicting runoff hydrographs, peak flow rates, and times to peak. Early models based on empirical equations predicted peak discharge and time to peak. In 1932, Sherman proposed the “unitgraph” or unit hydrograph technique. It was one of the first attempts to predict an entire hydrograph instead of just the peak flow and time to peak (Kilgore, 1997). Many researchers followed with increasingly complex models to improve the unit hydrograph shape. Although these techniques produced mathematically correct hydrographs, Todini (1988) states that their connections with the “real world” were lost. During the 1960’s and 1970’s, researchers focused their efforts on developing models with parameters having a physical interpretation. Due to limitations in the amount of available data and computing power, these physically based parameters were aggregated

or lumped together, thus greatly decreasing the amount of data to be processed. These models with aggregated parameters are termed *lumped parameter models*.

The rapid increase in computing power of the 1980's and 1990's has brought more complex models. Parameters no longer need to be lumped together because of computing limitations. *Distributed parameter models* are capable of incorporating information about the spatial variability of soils, land use, topography, or any other parameter in the modeling scenario. The improved availability of geographic information systems (GISs) aids in managing the large amounts of data required for distributed parameter models. GIS software can be combined with digital data such as soil type, vegetative cover, land use, and digital elevation models (DEMs) to create hydrologic models or input to hydrologic models.

The hydrologic processes, which both *lumped parameter* and *distributed parameter* models attempt to simulate, occur at a wide range of spatial scales; from a local scale of 1 meter, to a hillslope scale of 100 meters, to a catchment scale of 10 kilometers, to a regional scale of 1000 kilometers (Bloschl and Sivapalan, 1995). Heterogeneity in soil, vegetative cover, land use, etc. is present across all of these scales making understanding these hydrological processes difficult.

A major issue in hydrologic modeling is at what spatial scale does the model perform optimally. This performance can either refer to the ability of the model to preserve the essential runoff mechanisms, or the ability to produce a hydrologic response most similar to the observed response. This study is concerned primarily with the second issue. Generally, using smaller grid cell sizes or smaller subareas increases the amount of labor and computing time required for modeling. Therefore, to justify the increase in time and labor, the use of smaller grids or subareas should produce improved model performance. This is a primary research issue in this study.

This study investigates possible advantages of continuous models versus event based models. This study also investigates the effect of scale on two hydrologic models for a mountainous watershed in Southwest Virginia. The models include an event based lumped model (HEC-1) and a continuous semi-distributed model (TOPMODEL). The effect on hydrologic response of aggregating several subareas into larger subareas was

addressed in this study for HEC-1. These effects of spatial scale were determined by analyzing results obtained using various size subareas and grid cells. The effect on hydrologic response of using different size grids was addressed in this study for TOPMODEL. These effects of varying Digital Elevation Model (DEM) grid cell size were determined by analyzing results obtained using several different grid cell sizes.

## **1.1 Objectives**

The specific objectives of this research are:

- (1) To determine the effects of spatial scale on hydrologic simulation for a lumped and a continuous model.
- (2) To determine if model calibration based on a continuous simulation is an improvement over calibration based on several single events.
- (3) To investigate TOPMODEL, specifically, the routing procedure, parameter sensitivity, and the role of the topographic index.

## 2 Literature Review

### 2.1 Evolution of Hydrologic Modeling

Todini (1988) states that rainfall-runoff modeling began in the latter half of the 19<sup>th</sup> century in response to three main engineering problems: urban sewer design, land reclamation drainage systems design, and reservoir spillway design. The major goal of these first attempts at modeling was to estimate design discharge. Dooge (1977) comments that many of these first models were based on empirical equations developed under unique conditions and used in applications with similar conditions. Some models used the “rational method” to predict runoff peaks which he traces back to Mulvaney (1851). Early in the 20<sup>th</sup> century, hydrologists tried to improve the applicability of the rational method to large catchments with heterogeneity in rainfall and catchment characteristics (Todini, 1988).

Sherman (1932) introduced the “unitgraph” or unit hydrograph technique using the principle of superposition. This concept dominated hydrology for more than twenty-five years and is still in widespread use today (Anderson and Burt, 1985). The unit hydrograph was the first model to estimate the entire shape of the hydrograph rather than simply hydrograph peak values.

During the 1950s, hydrologists began to develop “conceptual models.” The 1960s brought the introduction of computers into hydrological modeling enabling complex water problems to be simulated as complete systems (Bedient and Huber, 1992). The first comprehensive hydrologic computer model, the Stanford Watershed Model, was developed at Stanford University (Crawford and Linsley, 1966). In the late 1960s, HEC-1 was developed by the Hydrological Engineering Center, U. S. Army Corps of Engineers. Real-time forecasting rainfall-runoff models were developed in the late 1970s and 1980s in response to the need of warnings in flood prone areas and as a tool for reservoirs or hydraulic structures management (Todini, 1988).

## **2.2 Predictive versus Investigative Models**

Hydrological models such as HEC-1 are primarily predictive models, meaning they obtain a specific answer to a specific problem. Other models, such as TOPMODEL, are developed to be investigative, meaning they increase our understanding of hydrological processes (O'Connell, 1991). The development of either type of model traditionally follows the same outline including the following steps: (1) collecting and analyzing data; (2) developing a conceptual model describing the important hydrological characteristics of a catchment; (3) developing a mathematical model from the conceptual model; (4) calibrating the model by adjusting coefficients to fit a portion of the historical data; (5) validating the model against a different portion of the historical data (Bloschl and Sivapalan, 1995).

## **2.3 Lumped versus Distributed Models**

Hydrologic models originally developed assuming watersheds to be fairly homogeneous, allowing weighted averages to be used as inputs. Because the inputs are averaged, or lumped, the models have come to be called “lumped” models. These lumped models, such as HEC-1, are generally expressed by ordinary differential equations, taking little or no account of spatial variability of watershed characteristics (Singh, 1995). They generally use spatially averaged or mean values to describe watershed characteristics such as soil type, land use, and slope.

Distinct from lumped models, distributed parameter models account for heterogeneity and spatial variability by considering variations in watershed characteristics across the entire area of the watershed. They are generally governed by partial differential equations. Obviously, to account for the spatial variability of model parameters requires large amount of data and computing power. With the increase in computing power in the 1980s and 1990s, hydrologists no longer have to settle for lumped models. They can now take advantage of this computing power to use distributed parameter models. Models, such as TOPMODEL, having characteristics of both lumped and distributed parameter models are referred to as semi-distributed, or quasi-distributed, models. Semi-distributed

models contain distributed parameters that take into account the heterogeneity and spatial variability, as well as lumped parameters that are spatially averaged.

Singh (1995) states that most models referred to as distributed models are not fully distributed, rather they are semi-distributed. In the majority of cases, watershed characteristics, input, many of the processes, and even boundary conditions are lumped, but some of the processes which are directly related to the output, for example the rainfall-runoff process, remain distributed. Distributed models commonly have a grid matrix with each grid cell containing a set of parameter values. Although an individual grid cell may be quite small compared to the total watershed area, a parameter value within that grid cell represents a spatial average of that parameter within the grid cell. In this sense, the distributed model could be said to have lumped characteristics.

## **2.4 Geographic Information Systems (GIS) in Hydrologic Modeling**

Sivapalan and Kalma (1995) write, “The greatest single advance in hydrological modelling in the past decade has probably been the availability and use of digitized topographic data.” The development of Geographic Information Systems (GIS) has vastly increased the quality and availability of data required for hydrological modeling. However, Wilson disagrees somewhat with Sivapalan and Kalma (1995) by observing that GIS software and databases have led to few improvements and/or new surface or subsurface models. Many hydrologic models that utilize GIS simply use it as a means of organizing model inputs and displaying model results. Notable exceptions are TOPMODEL and development of new terrain analysis methods for routing overland and channel flow. Maidment (1993) classifies the different uses of GIS in hydrology into four categories:

- A. Hydrological inventory and assessment,
- B. Hydrological parameter determination,
- C. Loosely coupled GIS and hydrological models,
- D. Integrated GIS and hydrological models.

*A. Hydrological inventory and assessment*

A GIS may be used to automatically derive information that would otherwise be painstakingly obtained from paper maps. A GIS can be used as a way to integrate, visualize, and derive spatial and non-spatial data (McDonnell, 1996).

*B. Hydrological parameter determination*

A very active area of research is the use of GIS for model parameter estimation. This role of GIS can be very beneficial for distributed parameter models which require large amounts of data. A GIS can be used to determine parameter values such as surface slope and contributing area above a point which are difficult to estimate using paper maps. TOPMODEL is an example of this type of model.

*C. Loosely coupled GIS and hydrological models*

Loosely coupled models have two distinct parts, a GIS component and a hydrological component. Generally, the two components do not share the same database, information must be exported between the components.

*D. Integrated GIS and hydrological models*

In integrated models, both the GIS component and the hydrologic component share the same database. Therefore, there is no export between the GIS and hydrologic components.

## 2.5 Continuous versus Event Based Models

Event based models, such as HEC-1, are designed to simulate hydrologic processes for only limited periods of time. The simulation generally begins corresponding to the start of a rainfall event and ends shortly after the hydrograph recession returns to baseflow. Event based models are not designed for long term prediction of baseflow, and, therefore, cannot be used to simulate extended low flow conditions in streams. Soil moisture accounting prior to an event is not performed by event based models, instead, parameters can be adjusted to reflect antecedent moisture conditions in the soil. In HEC-1, the curve number parameter that reflects antecedent moisture condition is also the same parameter that reflects hydrologic soil group and land use. The relationship between antecedent moisture condition and curve number is not easily defined, thus making adjustment of the curve number to reflect antecedent moisture condition quite difficult.

Continuous simulation models are generally based on long-term water balance equations. These continuous models, such as TOPMODEL, are theoretically designed to simulate hydrologic processes for indefinite lengths of time. However, due to limitations in computing power and in an attempt to make the output manageable and meaningful, simulations are generally performed for no longer than several years and for no shorter than a few weeks. Continuous models generally rely more on a short initialization period to simulate current soil moisture conditions rather than on user input initialization parameters. Because there often is a short period of initialization at the beginning of a simulation when hydrograph prediction can be poor, it is advantageous to minimize such initialization periods by simulating for longer periods. The TOPMODEL maximum simulation duration of 2500 time steps (about 3.5 months using a one hour time step) was used in this study. This is a relatively short simulation for a continuous model; it is common for continuous models to use one year or multiple year simulations.

A major advantage of continuous models over event based models is their soil moisture accounting capabilities. Continuous models can be used to simulate droughts and low flow periods in streams. The amount and timing of runoff generated from a rainfall event is very sensitive to amount of moisture already present in the soil before the event begins.

## 2.6 Issue of Scale in Hydrologic Modeling

According to Bloschl and Sivapalan (1995), scale refers to a characteristic time or length of a process, observation, or model. When large-scale models are used to make small-scale predictions, or vice versa, problems may arise. These scale issues in hydrology stem from the fact that the mathematical relationships describing a physical phenomenon are scale dependent (Gupta *et al.*, 1986). Due to increased environmental concern, scale issues in hydrology have increased in importance.

Hydrological processes occur at a wide range of scales and span about eight orders of magnitude in space and time (Klemes, 1983). For example, precipitation is an important component in the hydrologic cycle. Precipitation occurs at scales ranging from 1 m (cumulus convection) to 1000 km (frontal systems). Many hydrologic processes have similar length scales as precipitation but have delayed time scales. The time scale increases from infiltration excess to saturation excess to subsurface stormflow to groundwater controlled flows.

The transfer of information across scales is referred to as scaling. Scaling and its effects on hydrological modeling are linked to heterogeneity. This heterogeneity that affects scaling is small at small scales and large at large scales. The greater the degree of heterogeneity, the smaller the scale would have to be to represent such variability. Hydrologic models use parameters to represent entire watersheds, whereas data on watershed characteristics is collected only at a limited number of field locations (Singh, 1995). This field data is difficult to transform into a collective representation of the entire watershed. This brings about the question of what scale enables the best hydrologic simulation. As the spatial scale of model application increases from a small area to a large area, the hydrologic response becomes less sensitive to the spatial variability of the inputs. Singh (1995) defines scale as the size of a grid cell or subwatershed within which the hydrologic response can be treated as homogeneous. If this scale is too small, it will be dominated by local physical features, if it is too large, it will ignore significant hydrologic heterogeneity caused by spatial variability. Furthermore, model parameters may change as the degree of watershed disaggregation changes, and thus are scale-dependent. A

watershed's optimum scale reflects a compromise between the availability of hydrologic data and the complex, data dependent processes that generate hydrologic response.

## **2.7 Recent Investigations into the Issue of Appropriate Grid Cell Size in TOPMODEL**

Zhang and Montgomery (1994) calculated slope, drainage area per unit contour length, and the topographic index with grid cell sizes of 2, 4, 10, 30, and 90 m using ARC/INFO and spot elevation data obtained from low-altitude aerial photographs. They studied two watersheds in the western United States with moderate to steep terrain. Both the computed topographic parameters and hydrographs were significantly affected by the DEM grid cell size. The 10 m grid cell size produced substantially better results than the 30 m and 90 m grid cell sizes. However, the results obtained using grid cell sizes of 2 m and 4 m provided only slightly improved results. This may be due to the scale of the source data which was obtained at a scale of about ten meters or the use of a single flow direction algorithm to calculate drainage areas.

Quinn *et al.* (1995) computed drainage areas for a series of 5, 10, 25, and 50 m DEMs and found that: (1) small channels and catchment boundaries tend to become obscured or lost altogether as grid cell size increases, and (2) larger grid cell sizes exhibit a bias towards larger topographic index values (Wilson). It was concluded by Zhang and Montgomery (1994) and Quinn *et al.* (1995) that a grid cell size of 10 m or smaller was necessary to represent the variability of the topographic form in their study areas. To address the issue of spatial resolution versus required time, labor, and computing power, Zhang and Montgomery (1994) state, "... a 10-m grid cell size presents a reasonable compromise between increasing spatial resolution and data handling requirements for modelling surface processes..."

Moore (1996) found that the slope and topographic index values varied with grid cell size for scales ranging from 20 m to 680 m in three 100 km<sup>2</sup> study areas in southeastern Australia. Wolock and Price (1994) also studied the effect of DEM map scale and grid scale on the mean of the topographic index and the resulting simulated hydrograph. They found that the DEM source map scale and grid scale affected both the

$\ln(a / \tan \beta)$  distribution and the mean of the distribution. The simulated hydrograph was very sensitive to the mean of the  $\ln(a / \tan \beta)$  distribution. They state, however, that it should not be concluded from this that the coarse map scale or grid scale DEMs are inappropriate forms of topographic input for TOPMODEL. Because in TOPMODEL the water table configuration is related to ground surface topography, the water table surface may not be as variable as the ground surface, and, therefore, may be more closely related to coarser resolution topographic data.

## **3 Watershed and Model Descriptions**

### **3.1 Watershed Description**

Both TOPMODEL and HEC-1 models were developed for the Back Creek sub-watershed of the Upper Roanoke River Watershed in southwest Virginia. The Back Creek watershed, just south of Roanoke, Va., is an urbanizing watershed currently dominated by forest and pasture. This watershed was chosen for the study because it has a USGS streamflow gage station near the bottom of the watershed, the land use is relatively homogeneous, and the basin had been recently studied as part of a Dewberry and Davis Stormwater Management Project (1998). Henceforth in this study, the Back Creek watershed will be considered the portion of the watershed upstream of the gage station at Dundee (this neglects only a small area, 2.9 sq. mi., of the Back Creek watershed downstream of the gage). The remaining watershed area upstream of the gauge is 58.7 sq. mi. Figure 1 contains a regional view with the Back Creek watershed outlined in black. Figure 2 contains a map of the Back Creek watershed with the 20 subareas used in the HEC-1 model delineated.

### **3.2 Storm and Time Increment Selection**

#### **3.2.1 HEC-1**

The precipitation data for numerous events was obtained from the National Weather Service IFLOWS database. The precipitation data was obtained using a time step of fifteen minutes rather than one hour. A fifteen-minute time interval, as opposed to a one-hour time interval, should better represent the precipitation pattern of an actual storm. Due to the poor small storm modeling capability of HEC-1, the storms chosen for single event model comparison were the largest magnitude isolated storms during the 1995, 1996, 1997, and 1998 (only the beginning) water years. These water years were chosen because the streamflow data was readily available in digital form. In addition, a

large storm was chosen from the 1992 water year because the flow and precipitation data was easily accessible from Dewberry and Davis (1998).

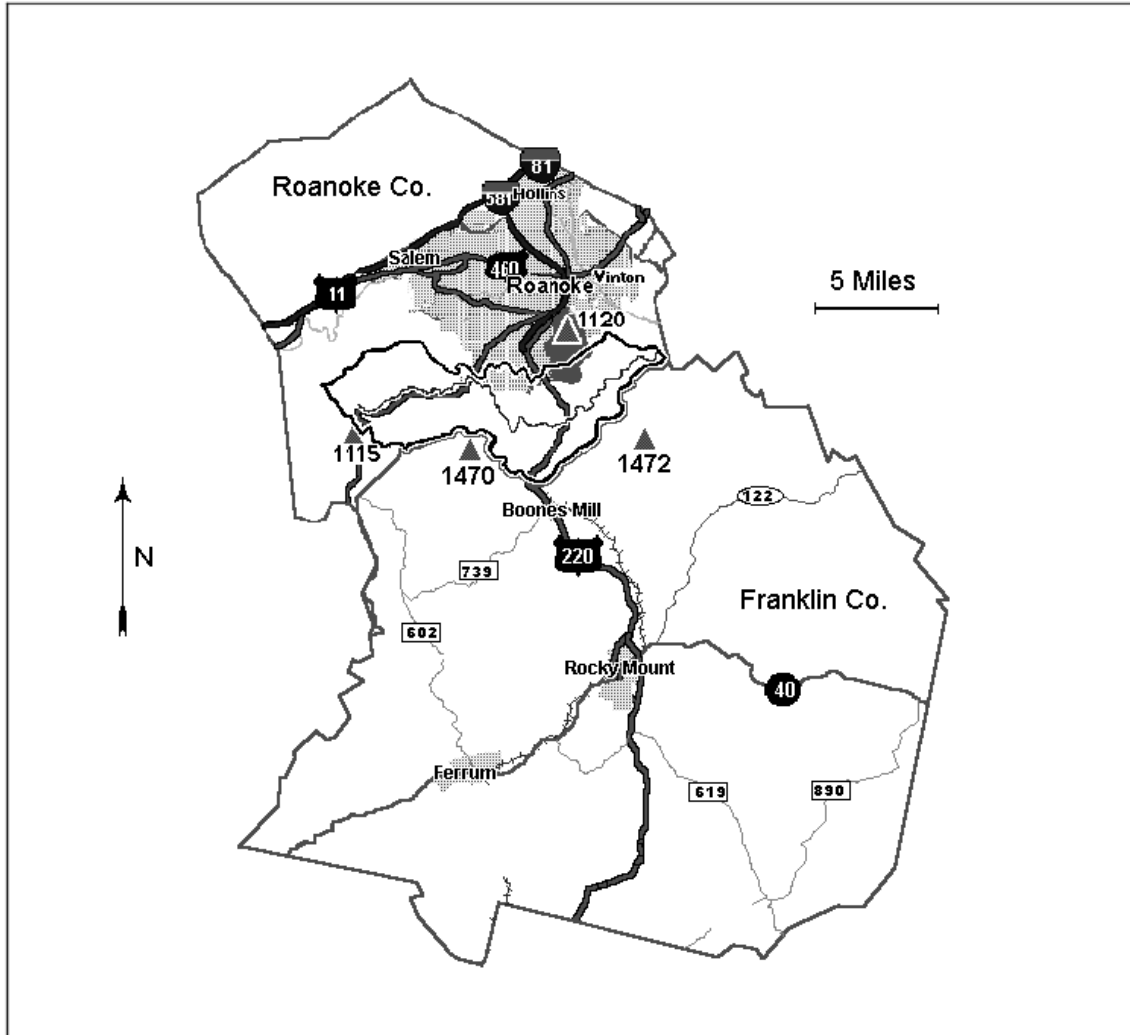


Figure 1. Regional view including the Back Creek watershed outlined in black.

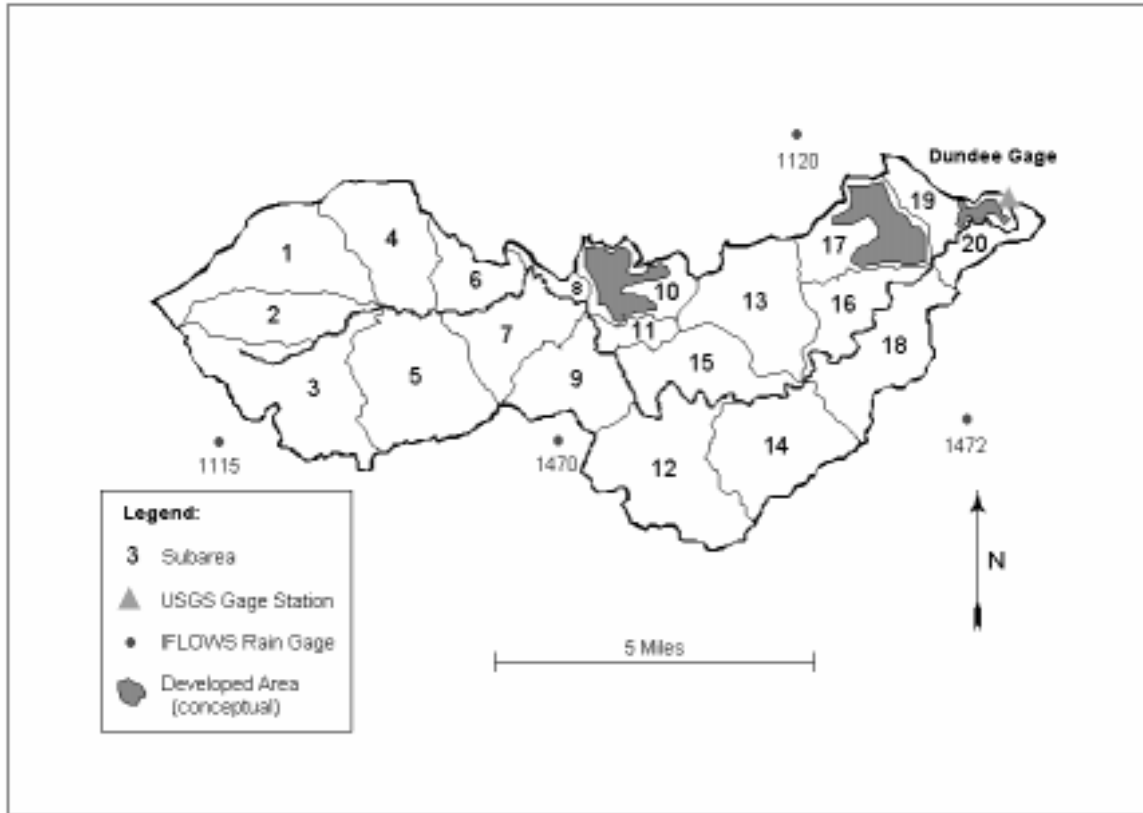


Figure 2. Back Creek watershed with USGS gage station and IFLOWS rain gages.

### 3.2.2 TOPMODEL

A time step of one hour, rather than fifteen minutes is used for TOPMODEL. This decision was made because TOPMODEL has the capacity to process only 2500 time steps per execution of the program. To calibrate the model for one year, a time step of fifteen minutes would necessitate the execution of TOPMODEL fifteen times, as opposed to only 4 executions required for a time step of one hour. Since the primary form of output from TOPMODEL is visual, the appearance of the output hydrographs was considered when choosing the time step. Hydrographs produced using a 15 minute time step had elongated time axes and were difficult to interpret visually. Perhaps the most compelling reason to use as few executions of TOPMODEL as possible involves the continuous soil moisture accounting of TOPMODEL. The simulated hydrograph response to a rainfall event is very sensitive to the amount of moisture already in the soil. The simulated hydrograph response at the beginning of a 2500 time step period may be poor because TOPMODEL may not have had sufficient time to estimate the amount of moisture in the soil.

### **3.3 Model Descriptions**

The two models investigated in this study are HEC-1 and TOPMODEL. HEC-1 is one of the most commonly used models for watershed simulation and flood analysis. It is an event based lumped model. TOPMODEL is of particular interest because it is a relatively new model and has not been thoroughly investigated. It allows the user to utilize Geographic Information Systems (GIS) for topographical data input. TOPMODEL is a physically based semi-distributed model that incorporates the effects of hillslope topography and variable-source-areas. TOPMODEL was developed primarily as a research tool, but has also been used in practical applications.

#### **3.3.1 HEC-1**

The U.S. Army Corps of Engineers, Hydrologic Engineering Center designed the Flood Hydrograph Package, HEC-1, to simulate surface runoff processes from precipitation and snowmelt over a watershed. Varying rainfall distribution and total storm rainfall can be applied to different portions of a watershed. HEC-1 simulates surface runoff response of a river basin to precipitation by representing the basin as a system of hydrologic and hydraulic components. A component may represent overland runoff, a stream channel, or a reservoir. Each component requires a set of parameters which correspond to that specific physical process (HEC, 1990). The watershed is divided into subareas so that lumped precipitation loss and watershed parameters can be used. Unit hydrograph and kinematic overland flow routing methods are used to transform precipitation excess to streamflow rate.

#### **3.3.2 TOPMODEL**

Topography is recognized as an important factor affecting the streamflow response of upland, forested watersheds to precipitation. Topography defines the effects of gravity on the movement of water in a watershed, and, therefore, it influences many aspects of the hydrologic system (Wolock and Price, 1994). TOPMODEL (Beven and Kirkby, 1979),

originally named TOPography MODEL, is a topography based model that uses variable contributing area concepts to model distributed hydrological responses. This variable source area concept states that overland flow is produced only over a small fraction of the total watershed area. The land-surface areas that produce overland flow are those that become saturated during precipitation events (Wolock and Price, 1994). They become saturated when the water table rises to the land surface.

### 3.3.2.1 Assumptions

TOPMODEL is generally considered to be relatively simple to apply because the effect of each parameter can be easily visualized. The mathematical starting points used to derive the fundamental TOPMODEL equations are the continuity equation and Darcy's law. The basic assumptions that govern TOPMODEL are (Holko and Lepisto, 1997):

- (1) The dynamics of the saturated zone can be approximated by successive steady-state representations.
- (2) The hydraulic gradient of the saturated zone can be approximated by the local surface topographic slope,  $\tan \beta$ ; groundwater table and saturated flow are parallel to the local surface slope.
- (3) The distribution of downslope transmissivity with depth is an exponential function of storage deficit or depth to the water table.
- (4) Grid cells with the same topographic index are hydraulically similar.

Topography is parameterized in TOPMODEL only as the statistical distribution of the topographic index  $\ln(a / \tan \beta)$ , where  $\ln$  is the Napierian logarithm,  $a$  is the upslope area per unit contour length, and  $\tan \beta$  is the surface slope gradient. The topographic index is an important hydrologic modeling component because it reflects the spatial distribution of soil moisture, surface saturation, and runoff generation processes (Zhang and Montgomery, 1994).

The grid based analysis is used *only* in calculating the statistical distribution of this topographic index. Once the distribution has been calculated, a grid based approach is

used only for display purposes and is not used in any runoff generation or routing procedures. The GRIDATB program, which calculates the topographic index for each cell and generates the statistical distribution, describes the method used to calculate  $a$ . A directional weight of 2 is used for the cardinal directions and a weight of  $2\sqrt{2}$  is used for the diagonal directions. See Figure 3. These weights are calculated using the following two steps:

- (a) calculate the distance between the corners of a 1 m grid cell in the appropriate direction (1 in the cardinal directions, and  $\sqrt{2}$  in the diagonal directions),
- (b) multiply the distance found in (a) by 2.

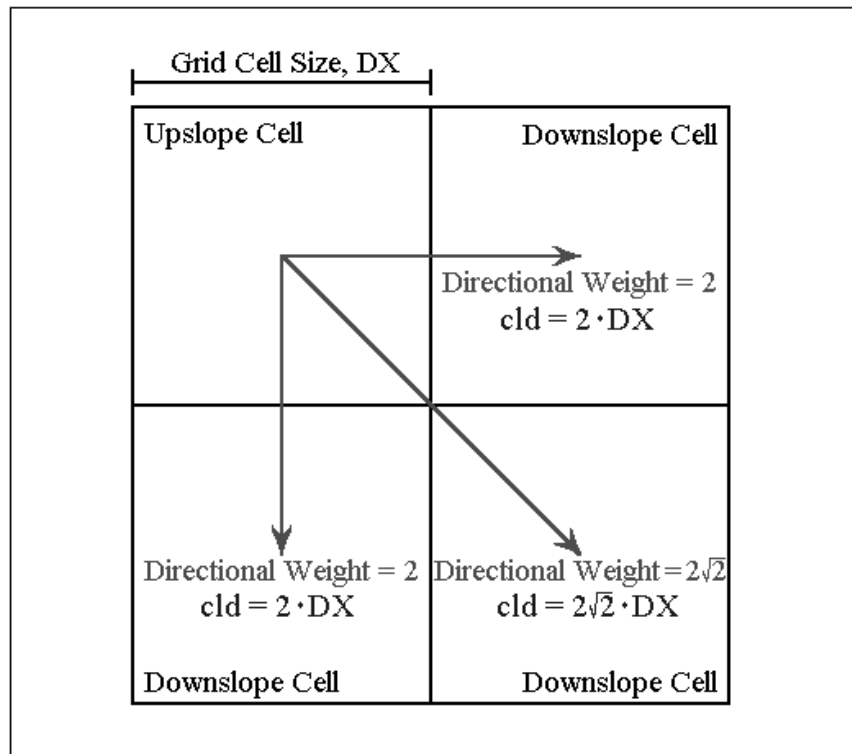


Figure 3. Directional weights for calculating contour length distance,  $cld$ , and upslope area per unit contour length,  $a$ .

The contour length distance, **cld**, is the means by which TOPMODEL assigns more contributing area to downslope grid cells in the cardinal directions and less area to those in the diagonal directions. The  $cld$  is calculated by multiplying the grid cell size,  $DX$ , by the directional weight. The value of  $a$  is determined by dividing the upslope

contributing area by the contour length distance. This procedure gives more weight to the cardinal directions and less weight to the diagonal directions. This means that if one downslope cell in a cardinal direction and one in a diagonal direction have the same elevation, about 1.4 times as much water will be routed in the cardinal direction.

The GRIDATB (see Section 3.3.2.6.5) program calculates the topographic index for each cell using the variables and equations that follow. The surface slope gradient from an upslope grid cell to a single downslope cell in the  $i$  direction is represented by  $(\tan \beta)_i$ . A multiple flow path algorithm is used to determine the downslope direction and proportion of surface runoff. The downslope flow directions are labeled 1, 2, 3, ... See Figures 4 and 5 for graphical clarification. Looking at the diagram in Figure 4, the surface slope gradient in *Direction 1*,  $(\tan \beta)_1$ , would be calculated by dividing the *Difference in elevation* by  $DX$ . Upslope contributing area ( $A$ ) (see Figure 5) is distributed in the downslope flow directions ( $A_1, A_2, A_3, \dots$ ), proportionally to  $\{(\tan \beta)_i * cld_i\}$  so that:

$$\begin{aligned} A &= A_1 + A_2 + A_3 \dots \text{downslope directions only} \\ &= C * \{(\tan \beta)_1 * cld_1 + (\tan \beta)_2 * cld_2 \dots\} \\ &\quad (C \text{ is a constant}) \end{aligned}$$

Therefore,

$$C = A / [\text{sum of } \{(\tan \beta)_i * cld_i\}]$$

and

$$\begin{aligned} A_1 &= A * C * (\tan \beta)_1 * cld_1 \\ A_2 &= A * C * (\tan \beta)_2 * cld_2 \quad \text{etc.} \end{aligned}$$

To calculate  $a/\tan \beta$  for a grid cell, a value of  $\tan \beta$  is first calculated based on the contour length distances so that:

$$\begin{aligned} \tan \beta &= \text{sum of } \{(\tan \beta)_i * cld_i\} / \text{sum of } cld_i \\ &\quad (\text{downslope directions only}) \end{aligned}$$

then the value of  $a/\tan \beta$  for this grid cell will be:

$$a/\tan \beta = A / \{\text{sum of } (cld_i) * (\tan \beta)\}$$

$$= A / [\text{sum of } \{(\tan \beta)_i * \text{cld}_i\}]$$

$$= C$$

The version of TOPMODEL employed in this study uses the value of  $\tan \beta$  in a *multiple* flow direction algorithm rather than a *single* flow direction algorithm. A single flow direction algorithm routes all runoff from one grid cell to the contiguous grid cell with the lowest elevation. A multiple flow direction algorithm divides the runoff between all contiguous downslope cells proportional to their relative slope gradients (Wolock, 1995).

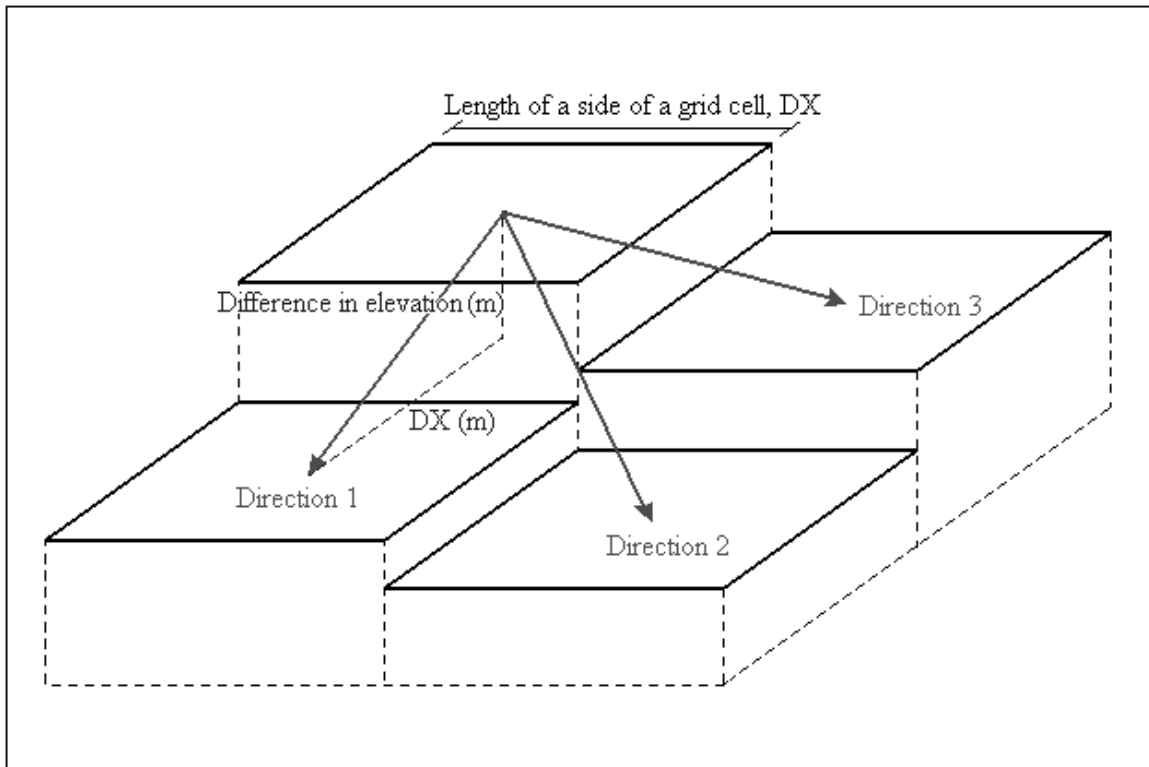


Figure 4. Illustration of terms and concepts used in GRIDATB.

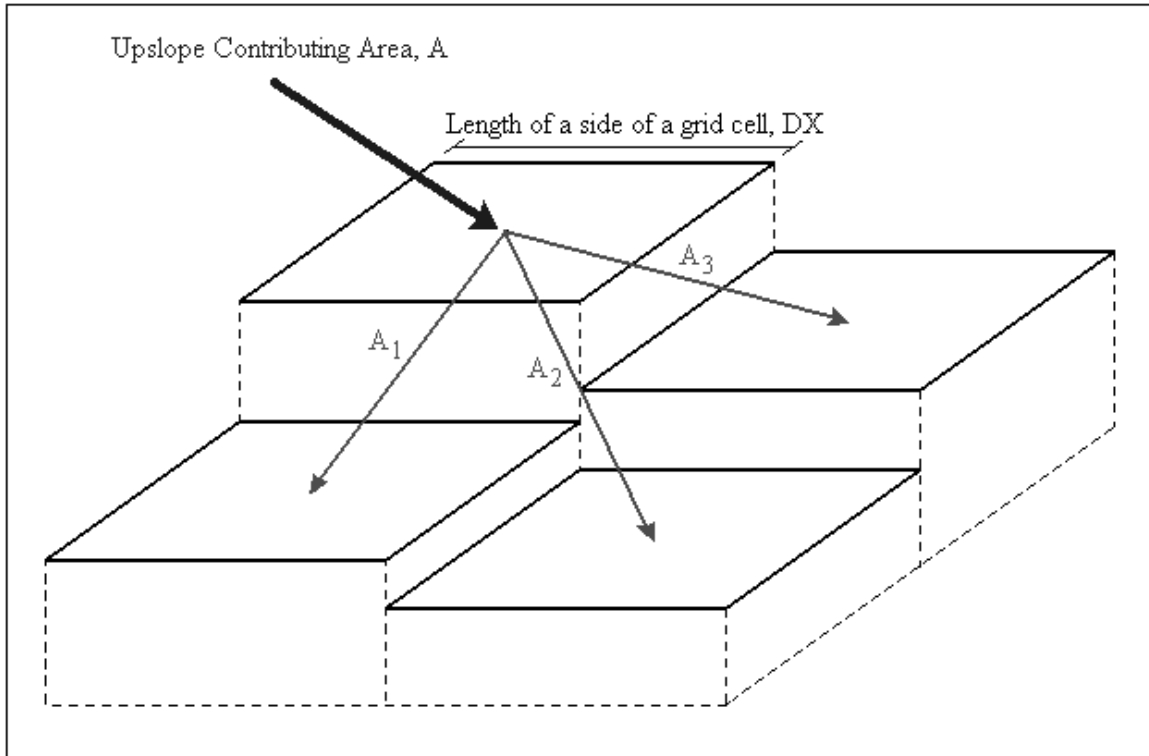


Figure 5. Illustration of distribution of area in downslope directions used in GRIDATB.

### 3.3.2.2 Basic Equations in TOPMODEL

Beven and Kirkby (1979) assumed a uniform recharge rate and a quasi-steady subsurface response to derive a function relating local soil moisture storage to the topographic index of a catchment:

$$S_i = S + m \{(\lambda - \ln(a / \tan \beta))_i - (\delta - \ln(T_i))\} \quad (1)$$

where:

- $S_i$  = local soil moisture deficit
- $S$  = mean soil moisture deficit of the catchment
- $m$  = model parameter that characterizes the decrease in soil hydraulic conductivity with depth
- $a$  = drainage area per unit contour length
- $\beta$  = slope

$T_i$	=	lateral transmissivity of the soil profile when the water table just intersects the ground surface
$\lambda$	=	mean value of $\ln (a / \tan \beta)$ for the catchment
$\delta$	=	mean value of $\ln (T_i)$ for the catchment

As in many applications of TOPMODEL, the version of TOPMODEL used in this study ignores the soil transmissivity terms in Eq. (1) because the spatial pattern of soil transmissivity is not known and therefore assumed to be constant over the catchment (Iorgulescu and Jordan 1994). Because  $S_i$  represents a negative soil moisture deficit, any location, or grid cell, with  $S_i \leq 0$  indicates that soil moisture store is full and surface saturation occurs. For grid cells where  $S_i > 0$ , the soil moisture store is not filled and there is no surface saturation (Zhang and Montgomery, 1994). As can be seen in Eq. (1), the value of the local soil moisture deficit,  $S_i$ , will decrease (thus increasing the likelihood of surface runoff) if there is an increase in the value of the topographic index in a cell.

During a model simulation, the mean soil moisture deficit of a catchment at time  $t$ ,  $S_t$ , is calculated by:

$$S_t = S_{t-1} + (q_{t-1} - r)\Delta t \quad (2)$$

where:

$S_t$	=	mean soil moisture deficit at time $t$
$S_{t-1}$	=	mean soil moisture deficit at time $t-1$
$q_{t-1}$	=	total catchment runoff at time $t-1$ divided by the catchment area (sum of $q_o$ and $q_b$ )
$r$	=	net recharge rate into the soil column
$\Delta t$	=	time interval used for the model simulation

The updated soil moisture deficit,  $S_i$ , at every grid cell in the catchment is then computed using Equation (1), and water is routed to the catchment outlet via (Wilson):

(a) subsurface runoff in areas with a soil moisture deficit larger than the precipitation added during a time step, (b) subsurface and infiltration excess overland flow in areas with rainfall intensities greater than the infiltration capacity, and (c) subsurface and saturation excess overland flow in areas with either a soil moisture deficit smaller than the incremental precipitation in a unit time step or that were saturated during the previous time step (Beven *et al.* 1984). The subsurface flow rate,  $q_b$ , is calculated by:

$$q_b = \exp(-(\lambda - \delta)) \exp(-S_t / m) \quad (3)$$

The saturation excess runoff,  $q_o$ , is the sum of excess soil moisture and direct precipitation that falls on the saturated areas (Zhang and Montgomery, 1994). This is expressed as:

$$q_o = (1 / A_t) \int_{A_s} \{-S_i / \Delta t + r\} dA \quad (4)$$

where:

$$\begin{aligned} A_t &= \text{total area of the catchment} \\ A_s &= \text{area of the catchment with surface saturation } (S_i \leq 0) \end{aligned}$$

Eq. 4 calculates the total saturation excess runoff,  $q_o$ , generated from all of the grid cells with saturation excess ( $S_i \leq 0$ ) and divides that flow rate by the total catchment area. This approach means that predicted soil moisture patterns will follow the outline of the topographic index and the predicted saturated source area will expand and contract as the water balance of the model changes (Quinn *et al.* 1995).

### 3.3.2.3 Organization of Stores in TOPMODEL

Routing water in TOPMODEL from the surface to the saturated zone is accomplished using a series of relatively simple stores. As in any series of stores, the discharge hydrograph will be most sensitive to the action of the least dynamic store (Kirkby, 1975 & Beven and Kirkby, 1979). This principal applies to a series of non-linear stores such as those perceived to exist in catchment hydrology. It is important to accurately represent the non-linearity of the most slowly responding store, while more dynamic stores may be approximated by simpler, linear representations (Beven, 1995). Kirkby (1975) presents data that suggests that the saturated zone is typically the slowest to respond. Therefore, TOPMODEL uses a non-linear store in the saturated zone, and a simple linear store in the dynamic zone. Figure 6 shows a simple graphical representation of the various stores. Two stores are referred to as ‘gravity’ controlled. The upper storage, *Vertical Drainage Storage (SUZ)*, controls the unsaturated zone while the lower storage, *Saturation Zone*, controls the saturated zone. This Vertical Drainage Storage is controlled by the saturation deficit,  $S_i$ , which is equivalent to the quantity of water required to completely fill this upper storage zone. Vertical flow,  $q_v$ , from the *SUZ* to the saturation zone will occur only when the moisture content of the root zone storage has exceeded the field capacity. The concept of *Non-active Moisture* reflects the idea that the field capacity of the soil must be filled before drainage will occur to the water table.

### 3.3.2.4 Evapotranspiration

Evapotranspiration data is an important, yet difficult to obtain, input component in continuous hydrologic models such as TOPMODEL. In TOPMODEL, hourly potential evapotranspiration is input by the user. This potential evapotranspiration, PET, can either be actual data from a nearby lake or reservoir, or the data series can be generated using a program called *Evap.exe* which can be downloaded with TOPMODEL. In this study, the *Evap.exe* program was utilized to generate a potential evapotranspiration data file based on annual and daily sine curves. *Evap.exe* is strictly an empirical method and does follow any well known PET methods such as those developed by Penman, Monteith, Jenson, Priestly, and Taylor. The program requires only the following input:

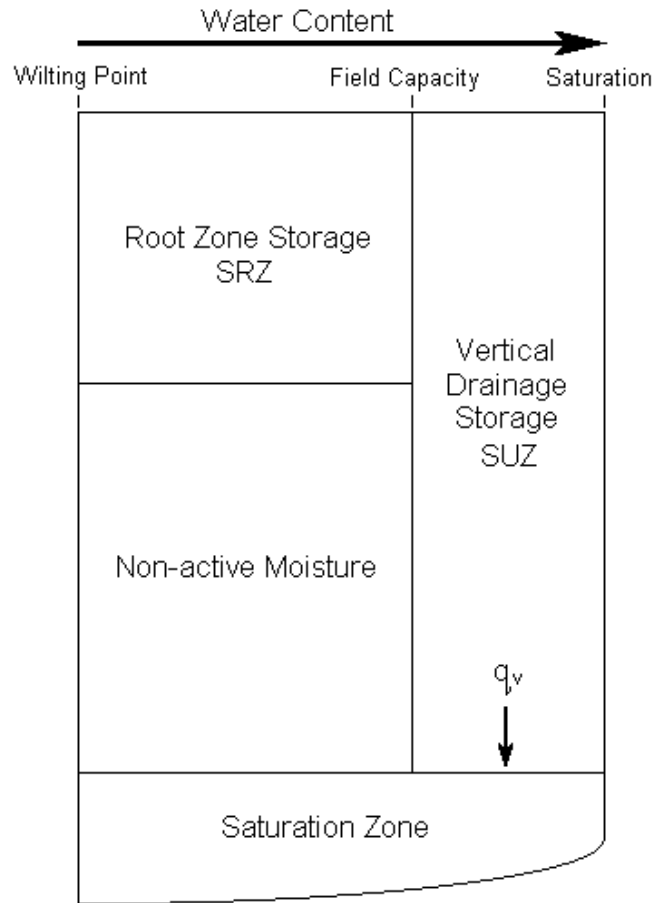


Figure 6. Simple graphical representation of the vertical storage in TOPMODEL.

Modified from Beven *et al.* (1995).

(a) start date, (b) number of days of data to generate, (c) time increment, (d) daily PET at summer maximum (mm/day), (e) daily PET at winter minimum (mm/day), and (f) name of output file. The values for (d) and (e) were calculated in the following manner: average daily mean values for the past 20 years were obtained from Gathright dam and scaled by monthly totals estimated by Roanoke County. The PET generated using *Evap.exe* was compared to actual PET estimated at a nearby lake and was determined to be acceptable. The same series of PET data was used for each year of simulation in TOPMODEL. Figure 7 shows a year of data as generated by *Evap.exe*. Note that the PET is minimum during the winter and maximum during the summer. Figure 8 shows four days worth of

PET data in the beginning of July. Note that the PET is minimum during the night and maximum during the middle of the day.

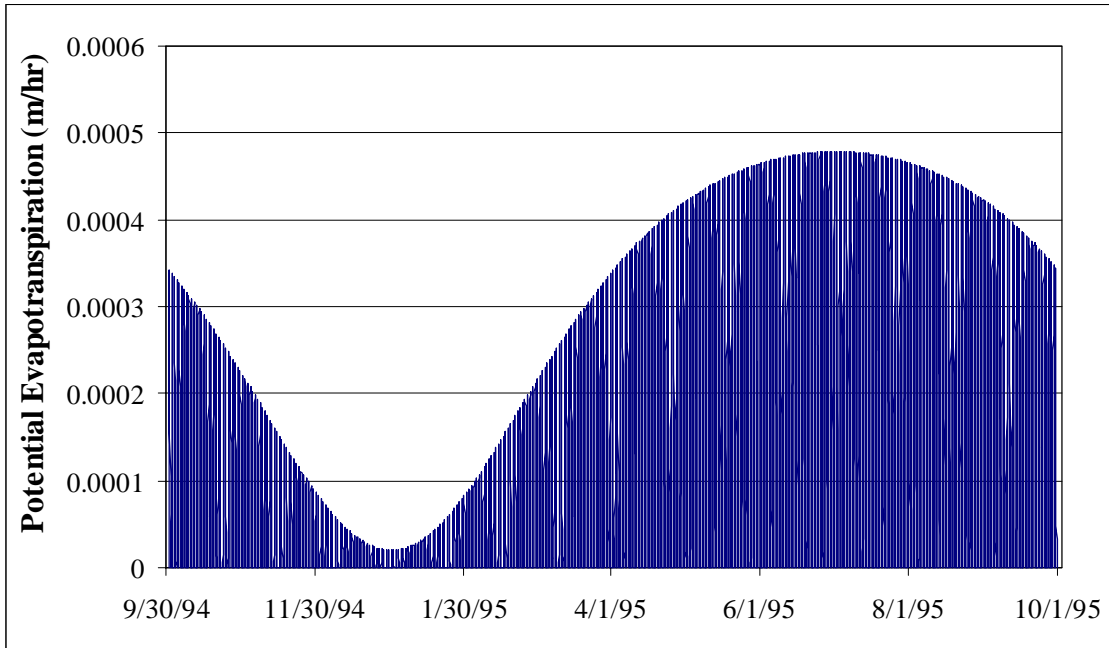


Figure 7. Yearly Evapotranspiration data used in TOPMODEL.

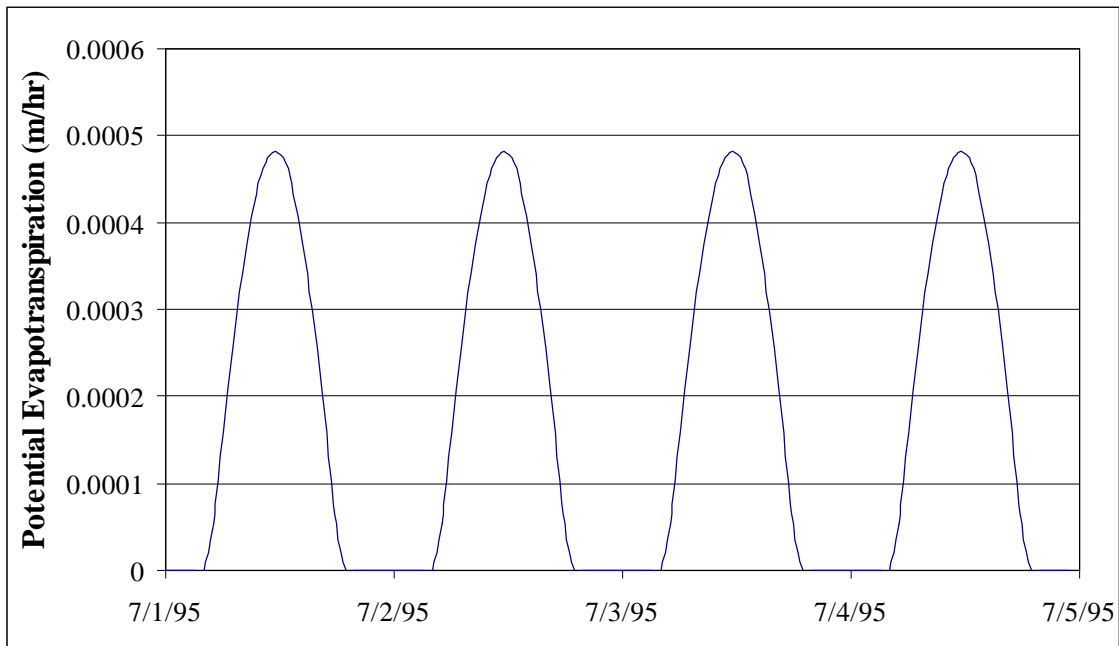


Figure 8. Daily Evapotranspiration data used in TOPMODEL.

### 3.3.2.5 Overland Flow and Channel Routing

For very small catchments, it may be acceptable to assume all surface runoff reaches the outlet in one time step. However, for large catchments, some type of routing of surface runoff is required. Beven and Kirkby (1979) incorporated an overland flow delay function and a channel routing function into TOPMODEL. For overland flow, the travel time,  $t$ , to the outlet from any point in the catchment can be calculated by:

$$t = \sum_{i=1}^N [x_i / (v \cdot \tan \beta_i)] \quad (5)$$

where:

- $x_i$  = length of the flow path containing  $N$  segments (m)
- $\tan \beta_i$  = slope of the  $i^{\text{th}}$  segment
- $v$  = velocity parameter (m/hr)

This method for routing overland surface runoff is not employed in the version of TOPMODEL used in this study. Overland and channel routing is combined into a simple constant wave speed routing algorithm. As discussed in Section 3.3.2.1, TOPMODEL does not use a grid based procedure for routing rainfall excess, or surface runoff, through a watershed. One of the input files for the TOPMODEL program includes a table containing the percent of the total catchment area downstream of the corresponding distance from the catchment outlet along the main channel. This data is used to route rainfall excess by delaying it from reaching the outlet. To simplify the method even further, the surface runoff is assumed to be generated uniformly over the entire catchment. This means that for routing purposes, surface runoff is generated as described in Section 3.3.2.2 based on the topographic index distribution and distributed uniformly over the entire watershed.

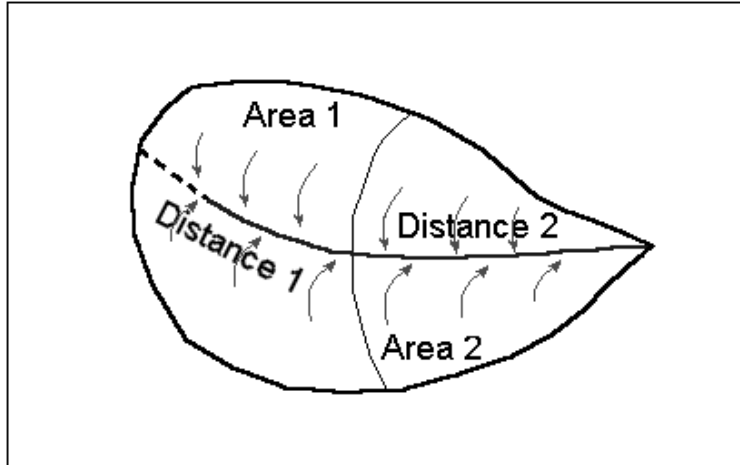


Figure 9. Sample watershed to illustrate TOPMODEL routing method.

To clarify this procedure, refer to Figure 9. Assume that *Area 1* represents 60% of the total area and *Area 2* represents 40% of the total area. Also assume that *Distance 1*, the distance along the main channel from the subarea divide to the watershed boundary, equals 900 meters, and *Distance 2*, the distance along the main channel from the outlet to the subarea divide, equals 1000 meters. The portion of the input file containing the routing data would look like this:

```

0.0    0.0    ← This indicates that 0% of the area is downstream of the outlet.
0.4    1000  ← Area 2
1.0    1900  ← Area 1

```

The first column is the percentage of the total area downstream of the corresponding main channel distance from the outlet. This main channel distance is in the second column. For example, looking at the second row, 40% of the total catchment area is downstream of a point 1000 meters up the main channel from the catchment outlet. This means that in the actual watershed, 40% of the total area drains into the portion of the main channel that is within 1000 meters of the outlet.

To understand how surface runoff is routed to the outlet, refer again to Figure 9. When precipitation excess or surface runoff is generated during a time interval, that runoff is distributed uniformly over the entire catchment. In the sample catchment, 60% of the

runoff would be assigned to Area 1 and 40% assigned to area 2. The travel time, in hours, to the outlet from each area is calculated by dividing the distance to the outlet by the main channel routing velocity parameter (this parameter is supplied by the user in one of the input files). For example, if the main channel routing parameter is 1000 m/hr, the travel time for Area 2 would be 1000 m / 1000 m/hr = 1.0 hours. The travel time for Area 1 would be 1900 m / 1000 m/hr = 1.9 hours. Therefore, 40% of the runoff produced from rainfall in a specific time step would be routed to the outlet one hour after the end of the rainfall time step. The remaining 60% of the runoff produced in the same time step would be routed to the outlet 1.9 hours, rounded to 2 hours, after the time step containing the rainfall. Figure 10 contains a hydrograph illustrating this example. This hydrograph assumes that there is no baseflow before or after the rainfall event.

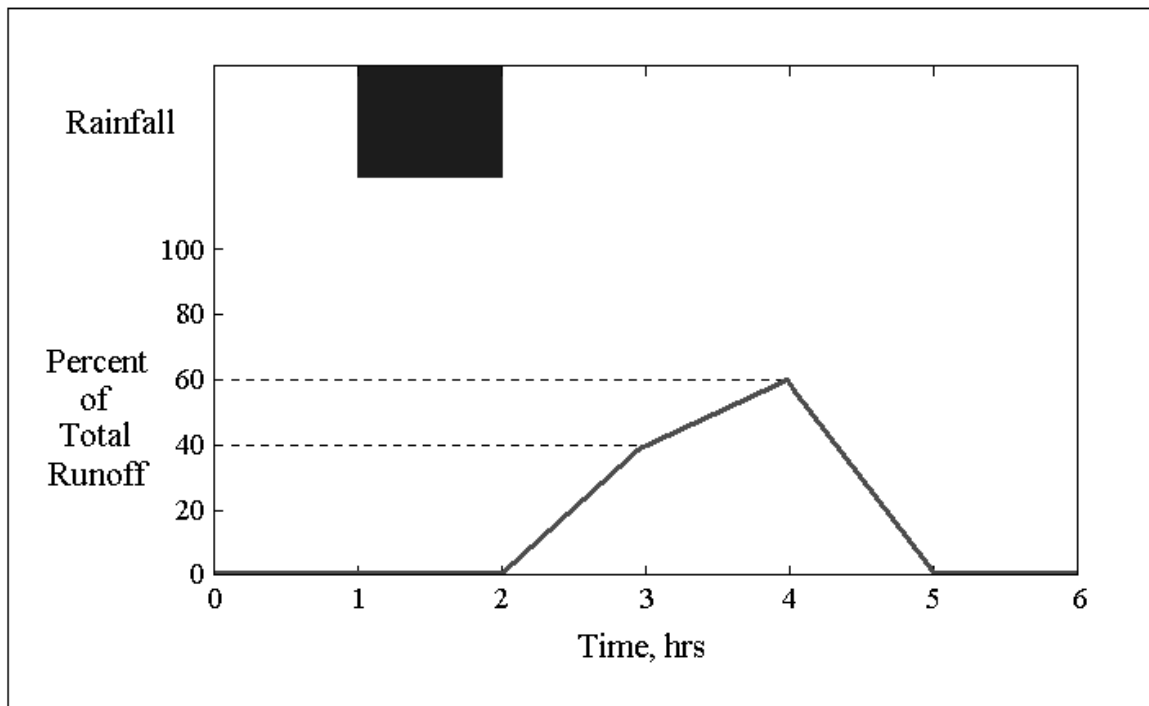


Figure 10. Hydrograph from example problem demonstrating TOPMODEL routing procedure.

### 3.3.2.6 Specific version of TOPMODEL used in this study

#### 3.3.2.6.1 History

In 1974, Professor Michael Kirkby, from the School of Geography, University of Leeds, used funding from the UK Natural Environment Research Council to initiate development of TOPMODEL (Beven *et al.* (95.02 Users Guide)). Keith Beven used punch cards to program the first versions in Fortran IV on an ICL 1904S mainframe computer. Since 1974 there have been many versions of TOPMODEL developed by various groups, but never a "definitive" version.

The version of TOPMODEL used in the study can be downloaded from one of the following web sites:

<http://es-sv1.lancs.ac.uk/es/research/hfdg/topmodel.html>

<http://www.es.lancs.ac.uk/es/Freeware/Freeware.html>

Available for download are a DOS based version of TOPMODEL and a Windows based version. In this study, the Windows based version was used predominantly instead of the DOS based version for several reasons: (a) improved graphical output, (b) the number of model parameters has been reduced, (c) model parameters can be adjusted quickly and easily, and (d) parameter sensitivity plots can be performed.

#### 3.3.2.6.2 Parameters

The twelve parameters in the DOS based version as described in *TOPMODEL and GRIDATB, A users guide to the distribution versions (95.02)* are:

$m$	=	the exponential storage parameter (m).
$T0$	=	the mean catchment value of $\ln(T0) \ln(m^2/h)$ .
$TD$	=	the unsaturated zone time delay per unit storage deficit (h).
$CHV$	=	the main channel routing velocity (m/hr).
$RV$	=	the internal subcatchment routing velocity (m/hr).

*SRMAX* = the maximum root zone water capacity (m).

There are also 2 initialization parameters

*Q0* = initial stream discharge, where by default *Q0* is set to the first observed discharge but may be changed by the user (m/time step).

*SRO* = initial value of root zone deficit (m).

For the *TMOD* program only, if the infiltration excess calculations are used, the additional parameters required in each subcatchment are:

*INFEX* = 1 to include infiltration excess calculations, otherwise 0.

*XK0* = surface hydraulic conductivity (*Ks* declines exponentially with depth) (m/hr).

*HF* = wetting front suction (m).

*DTH* = water content change across the wetting front.

In the Windows based version, the number of model parameters was reduced from twelve to five in order to simplify use of the model. These five parameters as described in *TOPMODEL Users Notes. Windows Version 97.01* are:

*m* = the parameter of the exponential transmissivity function or recession curve (units of depth, m).

$\ln(T_0)$  = the natural logarithm of the effective transmissivity of the soil when just saturated. A homogeneous soil throughout the catchment is assumed {units of  $\ln(m^2/h)$ }.

*SRmax* = the soil profile storage available for transpiration, i.e. an available water capacity (units of depth, m).

- SRinit* = the initial storage deficit in the root zone (an initialization parameter, units of depth, m).
- ChVel* = an effective surface routing velocity for scaling the distance/area or network width function. Linear routing is assumed (units of m/hr).

The  $m$  parameter in this study, as well as in the study performed by Beven and Kirkby (1979), proved to be very important and, therefore, requires a brief discussion. A physical interpretation of this parameter is that it controls the effective depth of the soil profile, or in other words, the depth of the soil down to the saturated zone. It does this in conjunction with the  $\ln(T_o)$  parameter, which defines the transmissivity of the soil profile when saturated to the surface. A larger value of  $m$  increases the active depth of the soil profile while a smaller value of  $m$  decreases the depth. A high value of  $\ln(T_o)$  when coupled with a small  $m$  results in a shallow effective soil with a pronounced transmissivity decay (Beven *et al.*, 1995).

#### **3.3.2.6.3 Input Files in DOS and Windows based versions of TOPMODEL**

The input files are similar for both the Windows based version and the DOS based version. Although the Windows based version was used to generate the data used in this study, the DOS based version was executed to ensure that both versions give similar results. The output from the two versions for one 500 hr period are included below. As seen in Figures 11 & 12, the results from the two models are quite similar. The Windows version is first, followed by the DOS version. Very small discrepancies between the two models exist for lower flow events.

(NOTE: The TOPMODEL windows contained in this work were taken from TOPMODEL Windows Version 97.01.)

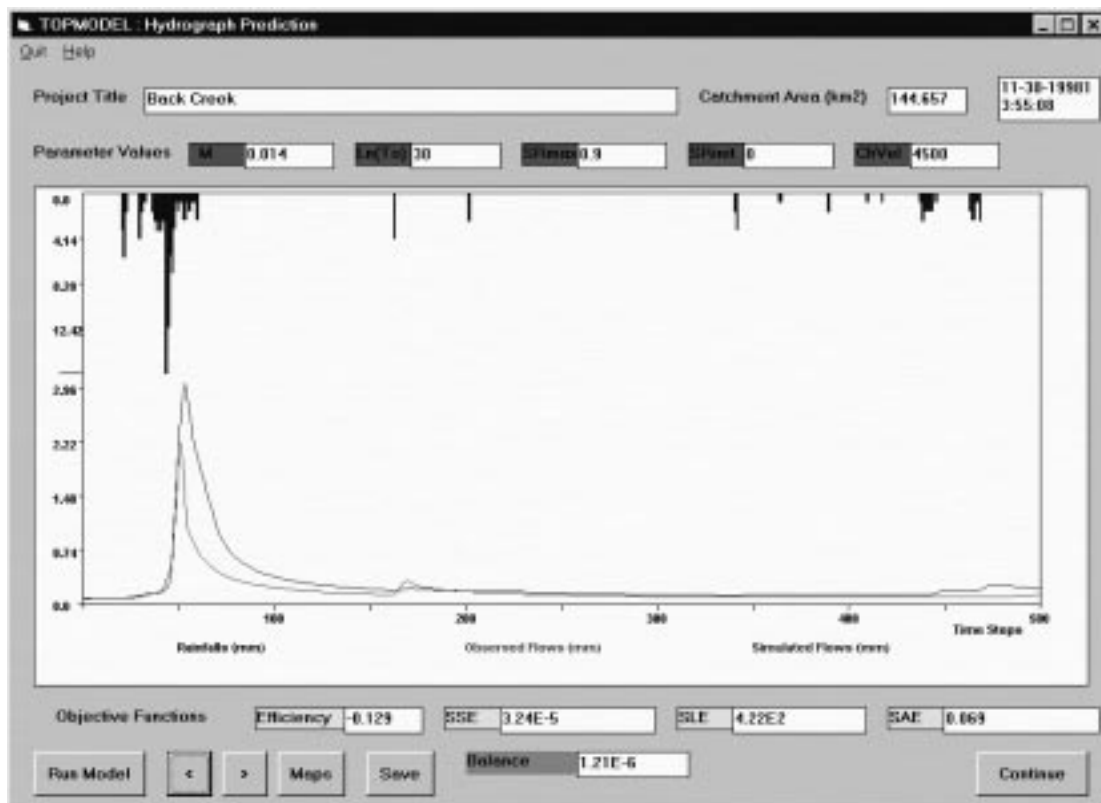


Figure 11. Output from Windows based version of TOPMODEL.

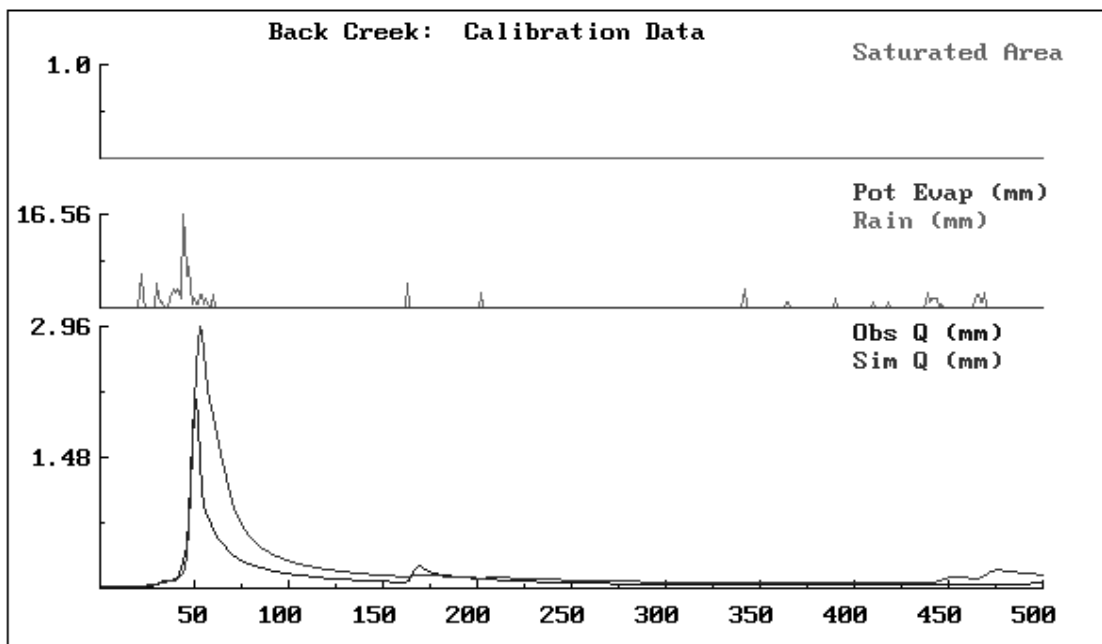


Figure 12. Output from DOS based version of TOPMODEL.

When executing the DOS based program, the parameters not included in the Windows based version were assigned the default values from the sample Slapton Wood Catchment problem which was downloaded with the TOPMODEL program. The exception is the initial flow parameter,  $Q_0$ , which was changed to reflect the first value of the flow from the observed record.

Appendix A contains sample files and instructions on how to use TOPMODEL. Some of the information in Appendix A is repeated from below. Four input files must be constructed before TOPMODEL will execute. The first file is called the project file which must be constructed for each catchment to be modeled. A sample file is included in Appendix A. This file contains only the four following lines:

1. Text description of application (i.e. Back Creek).
2. Catchment Data filename (i.e. \$catparm.dat).
3. Hydrological Input Data filename (i.e. \$inpt.dat).
4. Topographic Index Map filename (i.e. \$map.dat ) (may be left blank, but line must exist).

A sample Catchment Data file is included in Appendix A. The file contains a histogram of the percent of total area contained in each topographic index interval. The file also includes a table containing the percent of the total catchment area downstream of the corresponding distance from the catchment outlet along the main channel. At the end of the file is a value for each of the five parameters and a range of values for each parameter to be used in the Parameter Sensitivity Analysis.

A sample Hydrological Input Data file is included in Appendix A. The number of time steps and the duration of a time step are on the first line. The file also contains three columns of data. The columns from left to right are: incremental rain, evapotranspiration, and discharge rate per unit area. The units of each column are meters per hour.

A sample Topographic Index Map file is included in Appendix A. The format of this file is identical to the input file for the GRIDATB program (discussed below) except that it is limited to a grid size of 100 by 100 cells. A program named GRIDREDU, which

can be downloaded with TOPMODEL, can reduce the size of the grid by a reducing factor,  $N$ , specified by the user. The program selects every  $N^{\text{th}}$  cell in the matrix in both the x and y directions and creates a new, smaller file with these selected topographic index values. This file is used only for display purposes, so using the GRIDREDU program has no effect on the model simulation.

#### **3.3.2.6.4 Initialization of Baseflow in the DOS and Windows Based Versions of TOPMODEL**

The flow at the beginning of a simulation is initialized in different ways for the DOS based and Windows based versions. The DOS based version requires a parameter input by the user which indicates the flow for the first time step of the simulation. In this study, the initial flow parameter was assigned the value of the first observed flow for that simulation interval. The Windows based version does not have an initial flow parameter. Instead, the flow begins at a fraction of the observed flow and within ten hours of simulation, the program automatically increases the simulated flow until it approximately equals the observed flow.

#### **3.3.2.6.5 GRIDATB**

A program can be downloaded with TOPMODEL that computes the topographic index for each cell in an elevation raster grid. The input to the program is a raster grid file containing elevations (see small example input grid file in Appendix B). The output from the program consists of two files (see example output files in Appendix B). One of the files is a raster grid file containing the value of the topographic index for each grid cell. The second file consists of two parts. The first part is a list of the cells that the program has identified as sink or boundary nodes. The second part is a histogram representing the distribution of the topographic index. The GRIDATB program calculates the topographic index for each cell and arranges them into twenty-nine intervals. For each interval, the number of grid cells in that interval is divided by the total number of grid cells. This percentage of the total number of grid cells in each interval also equals the percentage of

the total area in each interval. This data is arranged in tabular form showing the percentage of the total area within each range of topographic index values.

The GRIDATB program could not be used as downloaded. The program was written to be used with grids of 200 cells by 200 cells or smaller. The largest grids used in this study were 1704 cells by 802 cells and had a grid cell size of 15 meters. The GRIDATB source FORTRAN code was downloaded and edited so it could process larger grids.

The first change to the source code was to increase the size of the two-dimensional arrays which store the elevations, topographic index values, and contributing areas. The second change was required because the contributing area was so large near the outlet of the watershed that a math error would occur. To remedy this problem, the size of the grid cell was decreased by eight orders of magnitude immediately upon being read from the input file. This prevents the contributing areas from becoming too large. However, the contributing area must be corrected when calculating the topographic index. Therefore, when calculating the topographic index, the natural log of  $1 \times 10^{16}$  (because the grid cell size is squared when calculating area) must be added to the natural log of  $(a/\tan \beta)$ . The corrections to the original code are in large bold type and can be seen in Appendix C. To ensure that the revisions did not change the output of the program, the original and revised versions of GRIDATB were both executed using the sample input file downloaded with the TOPMODEL program. This file is small enough to work with the both versions.

## 4 Methodology

### 4.1 HEC-1

A HEC-1 model for the Back Creek Watershed was developed using information from 7.5 minute USGS Quad Sheets and information from a Dewberry and Davis Stormwater Management Project (1998). The entire watershed was delineated into 81 subareas. The SCS Unit Hydrograph Method was selected for use in all HEC-1 modeling. Curve numbers were determined from TR-55 (SCS, 1986) for each subarea using information from Hydrologic Soil Condition and Land Use maps which were prepared as part of the Dewberry and Davis Stormwater Management Project. A default initial abstraction of  $.2*S$  was employed. The SCS lag time for each subarea was calculated by multiplying the time of concentration by  $.6$ . The segmental approach was used to determine the time of concentration. The 81 subareas were then aggregated into 20 subareas, and care was taken to ensure that parameters were determined using methods consistent with the calculations for the 81 subarea parameters. Area-weighted average curve numbers were calculated for each new subarea. SCS lag times and initial abstractions were calculated as before.

Theissen polygons were superimposed on the topographic map of the Back Creek watershed. If a subarea lies completely in one polygon, the precipitation distribution and storm total from that polygon's rain gage is applied to the subarea. If a subarea lies on the boundary between two or more polygons, the precipitation distribution is taken from the gage in the polygon in which the largest percentage of the subareas lies. Further, the storm total for the subarea is calculated by taking an areal-weighted average of all of the storm totals from all of the polygons in which the subarea lies. The precipitation distributions were not averaged because that tends to artificially reduce maximum storm intensities, thus not accurately representing the actual pattern. Several storms were input into both HEC-1 models using identical precipitation data. The hydrographs were graphed in Microsoft Excel.

## 4.2 TOPMODEL

Digital Elevation Models, DEMs, were downloaded from the USGS and used as topographic input for the topography-based rainfall runoff model, TOPMODEL. DEMs with a grid scale of 30 meters were obtained from 1:24000-scale maps (commonly referred to as 7½ minute maps). The model was calibrated at the 15-meter scale and those parameter values were used for all other scales. The calibration period was one year with an additional two years of validation. The model was run using grid cell sizes of 15, 30, 60, 90, and 120 meters. The computer program ArcView developed by ESRI, Environmental Systems Research Institute, Inc., (1996a) and the ArcView extension Spatial Analyst (ESRI, 1996b) were used to generate the DEMs with scales not directly obtained from the USGS. See Appendix D for ArcView instructions.

TOPMODEL cannot apply varying precipitation distributions or totals to different portions of a watershed. Therefore, an areal-weighted average of total precipitation was calculated for the entire watershed. The precipitation distribution from the most central rain gage, IFLOWS gage 1470, is scaled by this average total precipitation and applied to the entire watershed.

## 4.3 Model Calibration

Models enable hydrologists to study complex problems in an attempt to simulate and even predict hydrologic behavior. However, model results depend entirely on the model assumptions, inputs, and parameter estimates. Two problems which must always be addressed are selection of a suitable model and selection of parameters so that the model closely simulates the behavior of the catchment (Sorooshian and Gupta, 1995). “Calibration” is the process by which these parameters are selected. To calibrate a model, some aspect of watershed behavior which is to be matched must be selected. In this study, the model was calibrated based primarily on the prediction of peak flows and timing of the peaks for medium to large storms. To a lesser degree, the models were calibrated based on runoff volume and baseflow recession.

Most models typically contain two types of parameters, “physical” parameters and “process” parameters. Physical parameters are properties of a watershed that can be

physically measured. Examples of physical parameters are watershed area, the fraction of watershed area covered by impervious surface, the surface slope, and the contributing area above a point. Process parameters are properties of a watershed that cannot be directly measured. Examples of process parameters include average watershed effective transmissivity of the soil, effective surface routing velocity, decrease in hydraulic conductivity with depth, and SCS curve number.

The calibration process consists of two parts, parameter specification and parameter estimation (Sorooshian and Gupta, 1995).

- (a) **Parameter specification:** Prior knowledge of watershed properties and behavior is used to determine initial values for model parameters. Physical parameter estimates are obtained from field measurements or maps, and are typically fixed at these measured values and not adjusted. Values and ranges of possible values for process parameters are determined based on judgement, understanding of the hydrology of the watershed, and published values from studies performed on similar watersheds.
- (b) **Parameter estimation:** The initial estimates for process parameters previously discussed are adjusted within the range of possible values. These parameters are adjusted until the performance of the model more closely matches the behavior of the watershed. This adjustment can be done either manually or using computer based optimization methods.

#### 4.3.1 HEC-1

The 81 subarea HEC-1 model was calibrated for each storm that was used in HEC-1 modeling. This calibration was performed by slightly adjusting baseflow parameters for the entire watershed and the SCS Curve Number for each subarea until the calibration criteria was best fulfilled. The calibration criteria includes matching the simulated values with the observed values of peak flow, direct run-off (DRO) volume, time to peak, baseflow recession, and DRO duration. The initial abstraction was always assumed to be equal to the HEC-1 default of  $.2 \times S$ . Because the simulated time to peak

and direct runoff duration always closely matched the observed values, the SCS lag times were never adjusted after the initial values for each subarea were calculated. The calibrated set of parameters for each storm was then used for every other storm with the goal of determining which set of parameters best simulates all of the storms. The calibration criteria for every set of parameters used with every storm were evaluated and an optimum set of parameters was identified. The parameters for the 81 subarea model were used for the 20 subarea model.

#### 4.3.2 TOPMODEL

The version of TOPMODEL used does not have a routine for optimizing parameters. Instead, the distributors of the software encourage the user to manually change the parameters which requires the user to think about the effect of changing each parameter. The five parameters which were calibrated are:  $m$ , the parameter of the exponential transmissivity function or recession curve (units of depth, m),  $\ln(T_o)$ , the natural logarithm of the effective transmissivity of the soil when just saturated (units of  $m^2/h$ ),  $SRmax$ , the soil profile storage available for transpiration (units of depth, m),  $SRinit$ , the initial storage deficit in the root zone (units of depth, m), and  $ChVel$ , an effective surface routing velocity for scaling the distance/area or network width function (units of m/hr). TOPMODEL was calibrated using a grid cell size of 15 meters for the water year of 1995. The model was then validated using the water years 1996 and 1997. Hydrographs generated by TOPMODEL using the calibrated set of parameters for 1995, 1996, and 1997 water years are contained in Appendices E, F, and G, respectively. The calibrated model parameters from the 15-meter grid cell size were then used with grid cell sizes of 30, 60, 90, and 120 meters.

Initial values for the parameters were estimated from published values and from the Slapton Woods Catchment example files that were downloaded with TOPMODEL. Iorgulescu and Jordan (1994) published values for  $m$  which included an acceptable range of 0.001 to 0.050 m and more specifically 0.0221 and 0.031 m for two different catchments. The Slapton Woods Catchment example contains a value for  $m$  of 0.032 m. Published values for  $\ln(T_o)$  include 35 for a 60 m grid cell size (Franchini *et al.*, 1996) and

42 for a 20 m grid cell size (Saulnier *et al.*, 1997). The Slapton Woods Catchment example contains a value of 5 for  $\ln(T_o)$ . The Slapton Woods Catchment example contains values for  $SR_{max}$ ,  $Sr_{init}$ , and  $ChVel$  of 0.05m, 0.002m, and 3600m/h, respectively.

The  $ChVel$  parameter was adjusted until the rising side of the simulated hydrograph and the timing of the peak flows closely matched the observed. The  $m$ ,  $SR_{max}$ , and  $\ln(T_o)$  parameters were adjusted simultaneously until the peak flow, recession tail, and runoff volume of the simulated hydrograph best matched that of the observed hydrograph. The  $SR_{init}$  parameter was set at 0 to allow TOPMODEL to perform initialization without the influence of the user. An optimum set of parameters was obtained using the preceding procedure for each 2500 hour simulation interval in 1995. An average set of parameters was then determined taking into consideration the magnitude of the rainfall events in each interval. The parameters values which simulate well the larger storms were given more weight.

#### 4.4 Analysis Techniques

Both visual comparison and a series of statistics were used to evaluate model performance for HEC-1 and TOPMODEL. In addition to the visual comparison, the hydrographs produced by each model were evaluated based on relative error, bias, standard error, and mean arithmetic relative error (MARE) of the peak flows, times to peak, and flow volume.

The relative error is calculated using the following formula:

$$\text{Relative Error} = \frac{q_s - q_o}{q_o} \quad (6)$$

where:

- $q_s$  = Simulated value of flow, time to peak, or flow volume.
- $q_o$  = Observed value of flow, time to peak, or flow volume.

The bias is calculated using the following formula:

$$\text{Bias} = \sum_{i=1}^n \left( \frac{q_s - q_o}{q_o} \right) \quad (7)$$

where:

$$n = \text{Number of events.}$$

The mean arithmetic relative error, MARE, is calculated using the following formula:

$$\text{MARE} = \frac{1}{n} \cdot \sum_{i=1}^n \left( \frac{q_s - q_o}{q_o} \right) \quad (8)$$

The standard error is calculated using the following formula:

$$\text{Standard Error} = \sqrt{\frac{1}{n} \cdot \sum_{i=1}^n \left( \frac{q_s - q_o}{q_o} \right)^2} \quad (9)$$

The TOPMODEL topographic index distributions were evaluated based on their mean, variance, and standard deviation. The following formulae were used to calculate these statistics (Walpole and Myers, 1993).

The mean,  $\mu$ , of the topographic index distribution is calculated using the following formula:

$$\mu = \sum_x x \cdot f(x) \quad (10)$$

where:

$$x = \text{Representative value of the topographic index for an interval.}$$

$f(x)$  = Decimal fraction of the total grid cells in the topographic index interval.

The variance,  $\sigma^2$ , of the topographic index distribution is calculated using the following formula:

$$\sigma^2 = \sum_x (x - \mu)^2 \cdot f(x) \quad (11)$$

The standard deviation,  $\sigma$ , of the topographic index distribution is calculated using the following formula:

$$\sigma = \sqrt{\sum_x (x - \mu)^2 \cdot f(x)} \quad (12)$$

# 5 Results and Discussion

## 5.1 TOPMODEL

### 5.1.1 Relationship between Topographic Index and Grid Cell Size

The topographic index for each grid cell size is plotted as a frequency distribution in Figure 13 and as a cumulative frequency distribution in Figure 14. These graphs show that grid cell size significantly affects the distribution of the topographic index. An increase in the grid cell size shifts the distribution toward higher values of  $\ln(a / \tan \beta)$ . Conversely, a decrease in the grid cell size shifts the distribution toward lower values of  $\ln(a / \tan \beta)$ .

Table 1 contains the statistics of the topographic index for each grid cell size. These statistics, calculated using methods from Walpole and Myers (1993), also show a shift toward higher values of the topographic index with increasing grid cell size. The mean and standard deviation of the topographic index increase with grid cell size. The mean of the topographic index increases from 5.70 for a 15 m grid cell size to 8.09 m for a 120 meter grid cell size. Figure 15 graphically displays the relationship between grid cell size and mean of the topographic index. Both Zhang and Montgomery (1994) and Wolock and Price (1994) reported similar relationships between the mean of the topographic index and grid cell size.

### 5.1.2 Effect of the $m$ Parameter on Simulated Hydrograph

The  $m$  parameter characterizes the decrease in hydraulic conductivity with depth. The simulated hydrograph generated by TOPMODEL is very sensitive to changes in the  $m$  parameter. Figures 16 (a) - (g) show the effect of the simulated hydrograph as the value of the  $m$  parameter increases from 0.001 to 0.020 m. (Note the changes in the scale on the y-axis.) The value of  $m$  for each execution of TOPMODEL is displayed in the output window on the left above the hydrograph and rain data. A six hour period of rain, with constant rate of 1.524 mm/hr, began at 200 hours. This rainfall pattern is somewhat

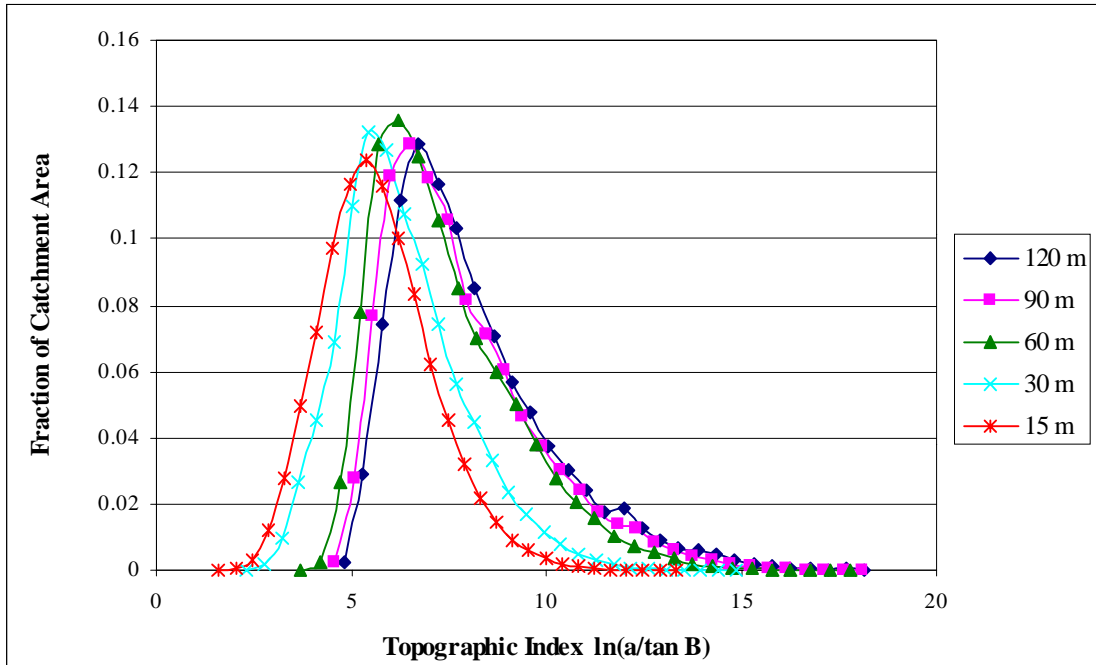


Figure 13. Frequency distribution of the topographic index for varying grid cell sizes.

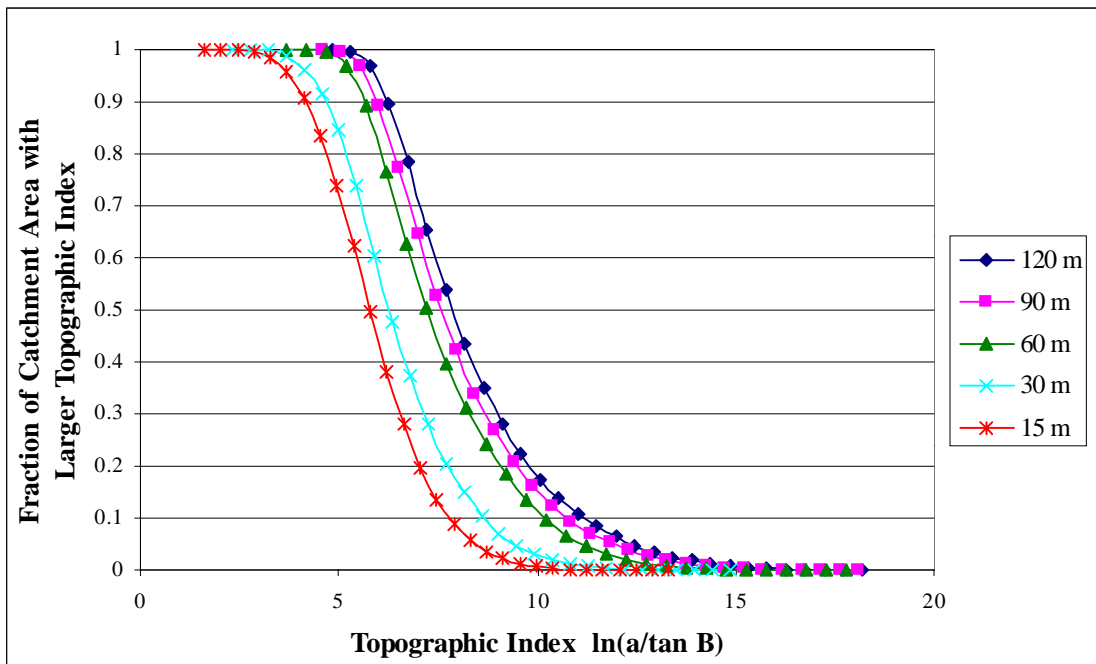


Figure 14. Cumulative frequency distribution of the topographic index for varying grid cell sizes.

Table 1. Topographic index statistics for varying grid cell sizes.

<b>Grid Cell Size (m)</b>	<b>Mean Topographic Index</b>	<b>Variance</b>	<b>Standard Deviation</b>
120	8.09	4.02	2.01
90	7.79	3.74	1.93
60	7.38	3.30	1.82
30	6.28	2.47	1.57
15	5.70	2.03	1.42

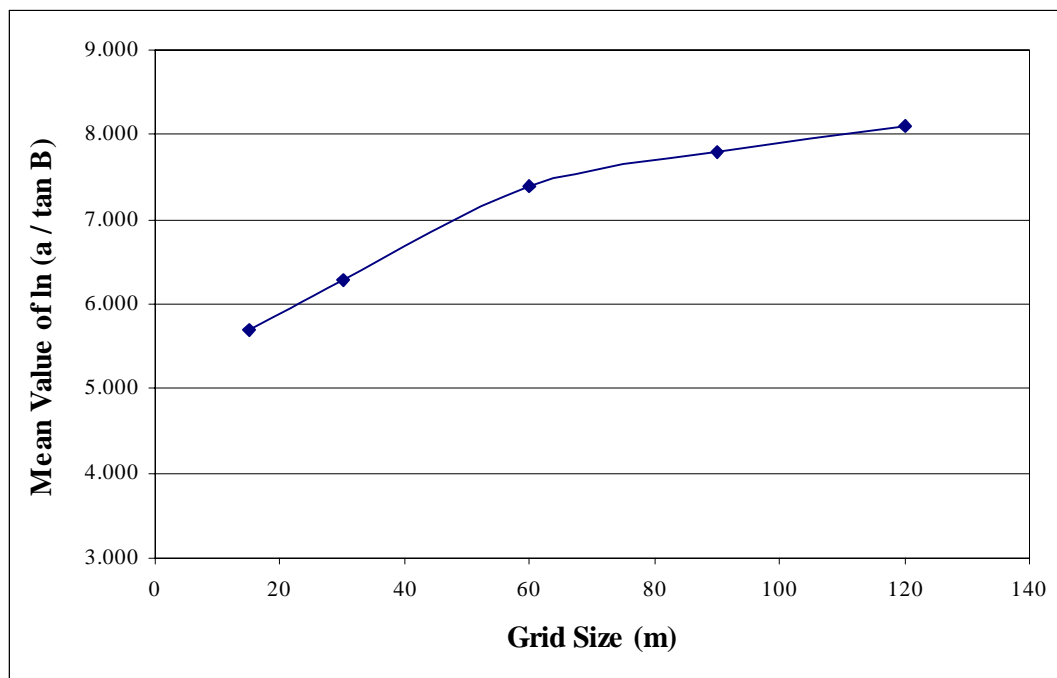


Figure 15. Plot of mean value of topographic index for each grid cell size.

unrealistic and more “normal” rainfall patterns would typically result in less “flashy” (meaning it rises and falls very quickly) hydrographs. TOPMODEL requires observed flow data in order to run a simulation. TOPMODEL uses this observed flow to initialize the baseflow. A constant observed flow of 0.02 mm/hr was used; this gives a good point of reference with which the simulated hydrograph can be compared.

As can be seen in Figures 16 (a) - (g), both the shape of the hydrograph and the peak flow change quite dramatically with the  $m$  parameter. For lower values of  $m$  (i.e.

0.001 and 0.002 m), the peak flow is much larger, the hydrograph appears to be “flashy”, and the flow returns to 0.02 mm/hr quickly, within 60 to 100 hours. As the  $m$  parameter increases to intermediate values (i.e. 0.003, 0.004, and 0.006 m), the hydrograph begins to take the shape of more traditional observed hydrographs. With these increased  $m$  values the simulated hydrograph responds slower, thus the peak drops and the recession becomes more gradual. The peak flow drops slowly with increases in  $m$  and seems to level off at 0.09 mm/hr. For higher values of  $m$  (i.e. 0.010 and 0.020 m), the peak flow remains constant at 0.09 mm/hr, the hydrograph again appears to be somewhat “flashy”, but the flow returns to 0.02 mm/hr very slowly, after almost 250 hours.

To better understand the effect of the  $m$  parameter on the simulated hydrograph, the two components of a hydrograph generated by TOPMODEL, surface and subsurface, must be examined. For large values of  $m$ , the proportion of rainfall that reaches the outlet via a surface route is decreased. This occurs because large values of  $m$  indicate a deeper effective soil (see Section 3.3.2.6.2) allowing more rainfall to infiltrate the soil. For small values of  $m$ , the proportion of rainfall that reaches the outlet via a surface route is increased. This occurs because small values of  $m$  indicate a more shallow effective soil allowing less rainfall to infiltrate the soil.

The  $m$  parameter also has a significant impact on the subsurface portion of the runoff. For small values of  $m$ , the amount of subsurface flow decreases and moves toward the outlet very quickly, in fact, it arrives at the outlet almost coincident with the surface flow. This results in large peak flows and very little contribution to baseflow after the rainfall has ended. This phenomenon can be attributed to the shallow effective soil associated with small values of  $m$ . For large values of  $m$ , the amount of subsurface flow increases and moves toward the outlet very slowly, arriving at the outlet over a long time span. This results in smaller peaks flows, which consist almost entirely of surface flow, and large contributions to baseflow from subsurface flow after the rainfall event. This phenomenon can be attributed to the deeper effective soil associated with large values of  $m$ .

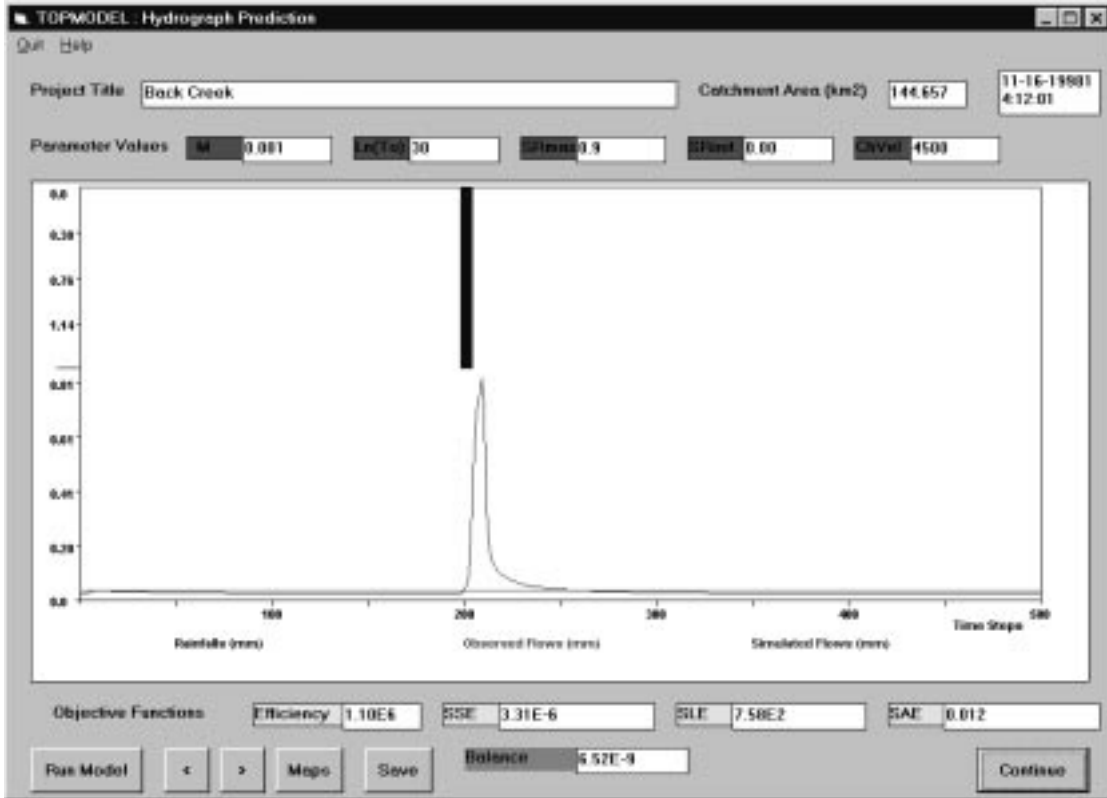


Figure 16 (a).  $m = 0.001m$ .

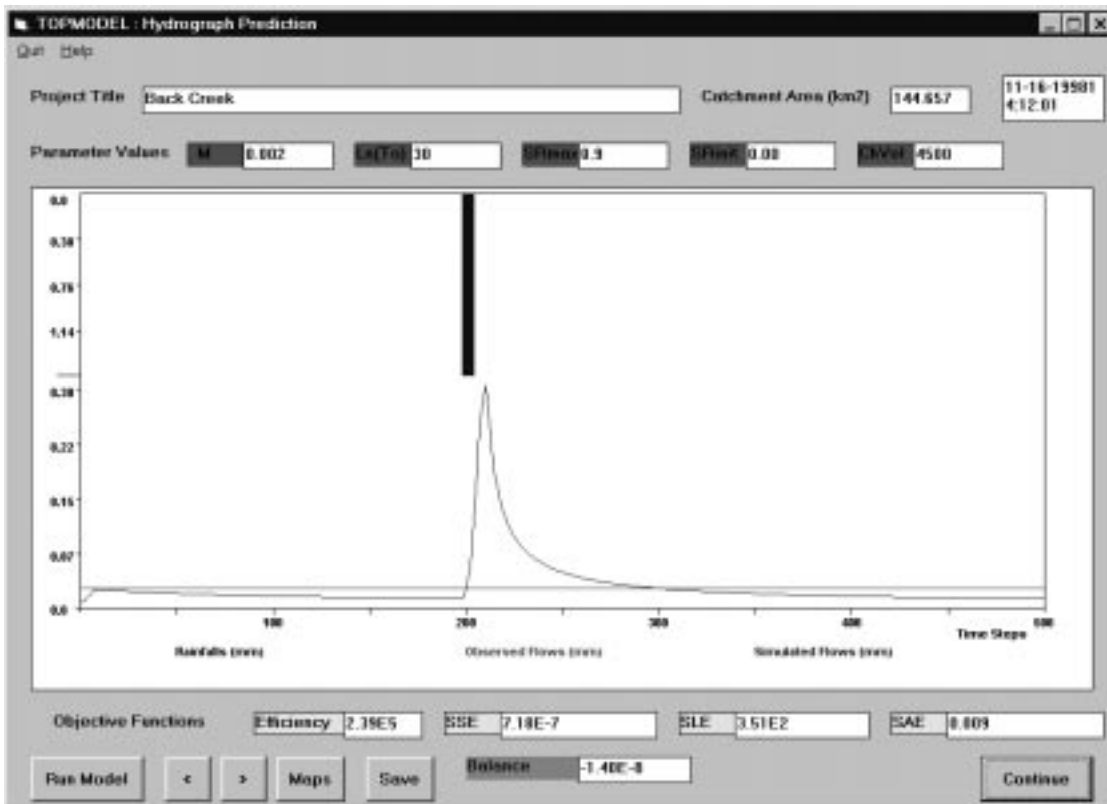


Figure 16 (b).  $m = 0.002m$ .

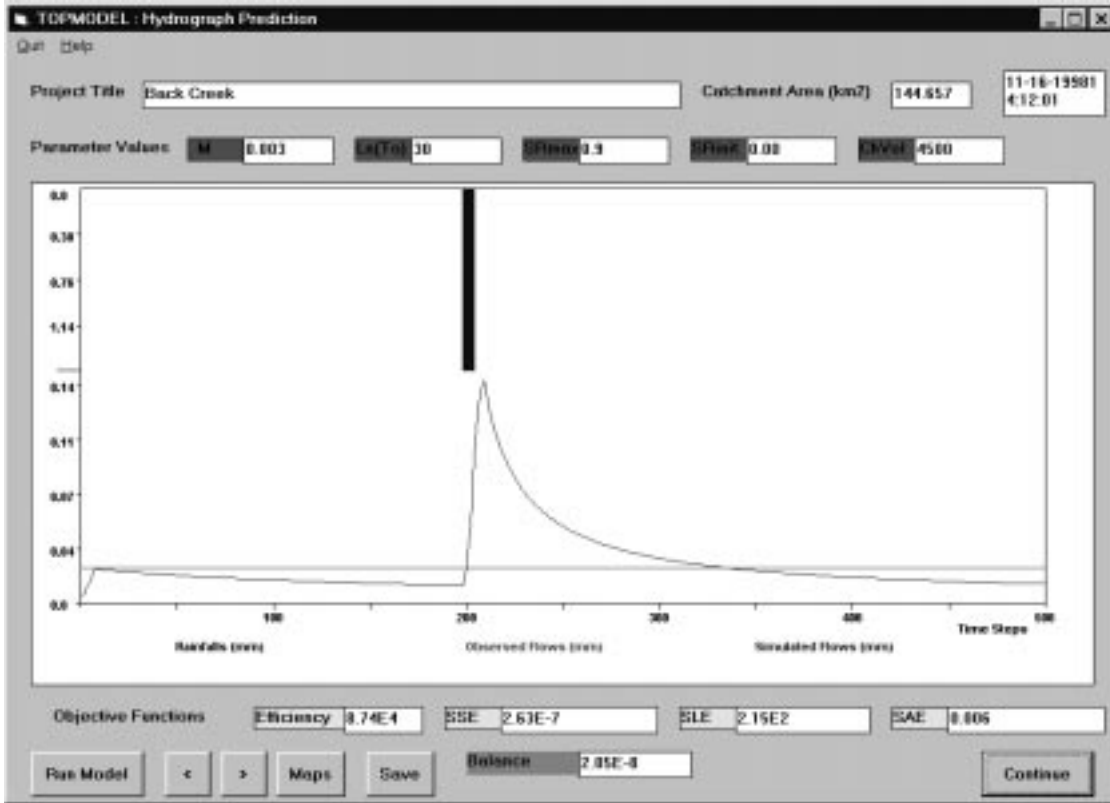


Figure 16 (c).  $m = 0.003m$ .

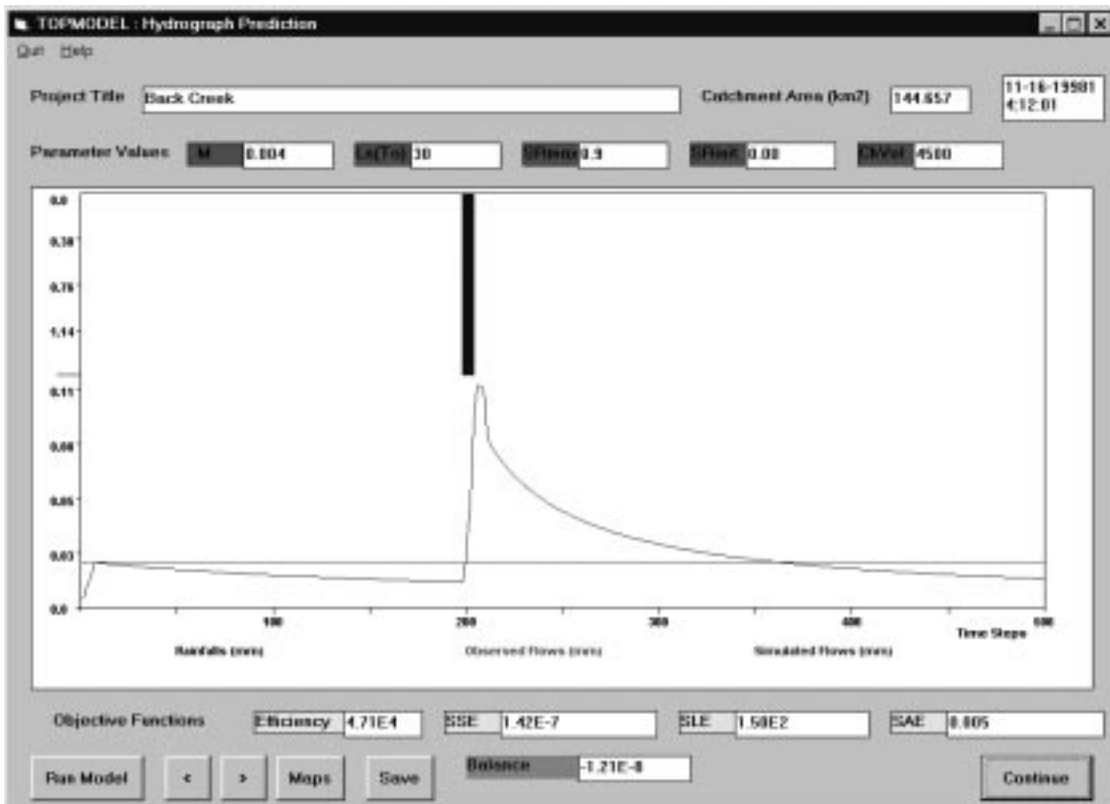


Figure 16 (d).  $m = 0.004m$ .

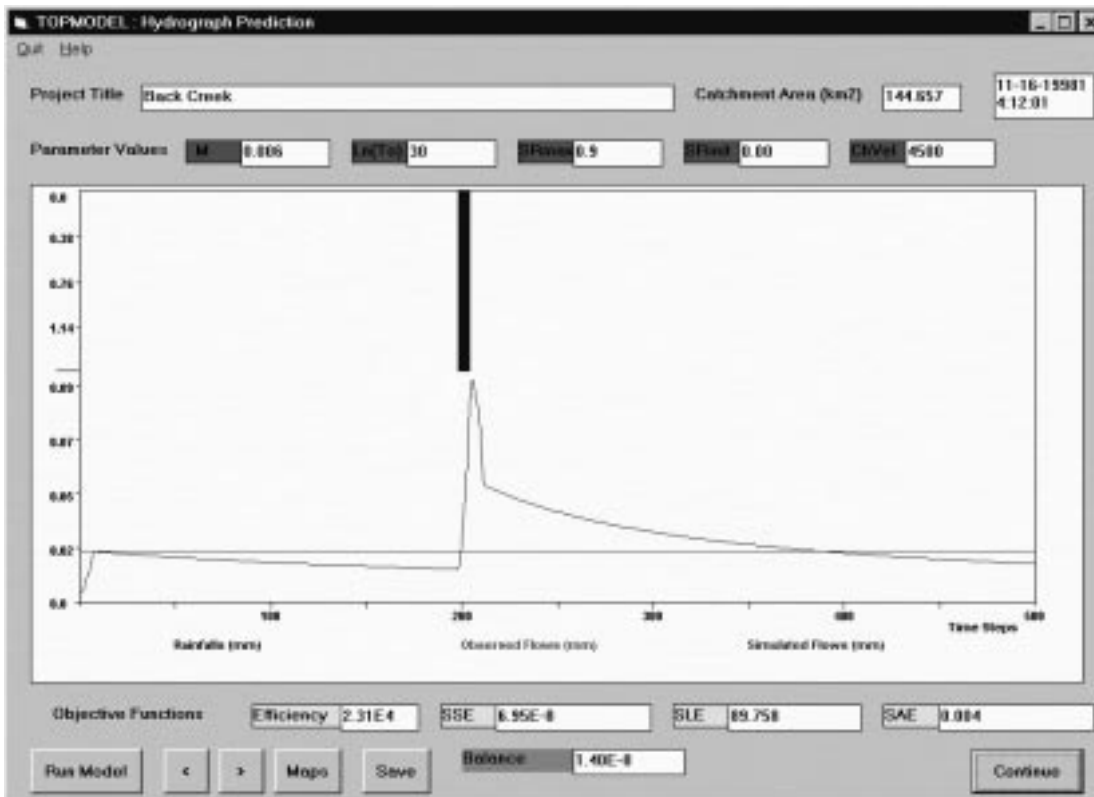


Figure 16 (e).  $m = 0.006m$ .

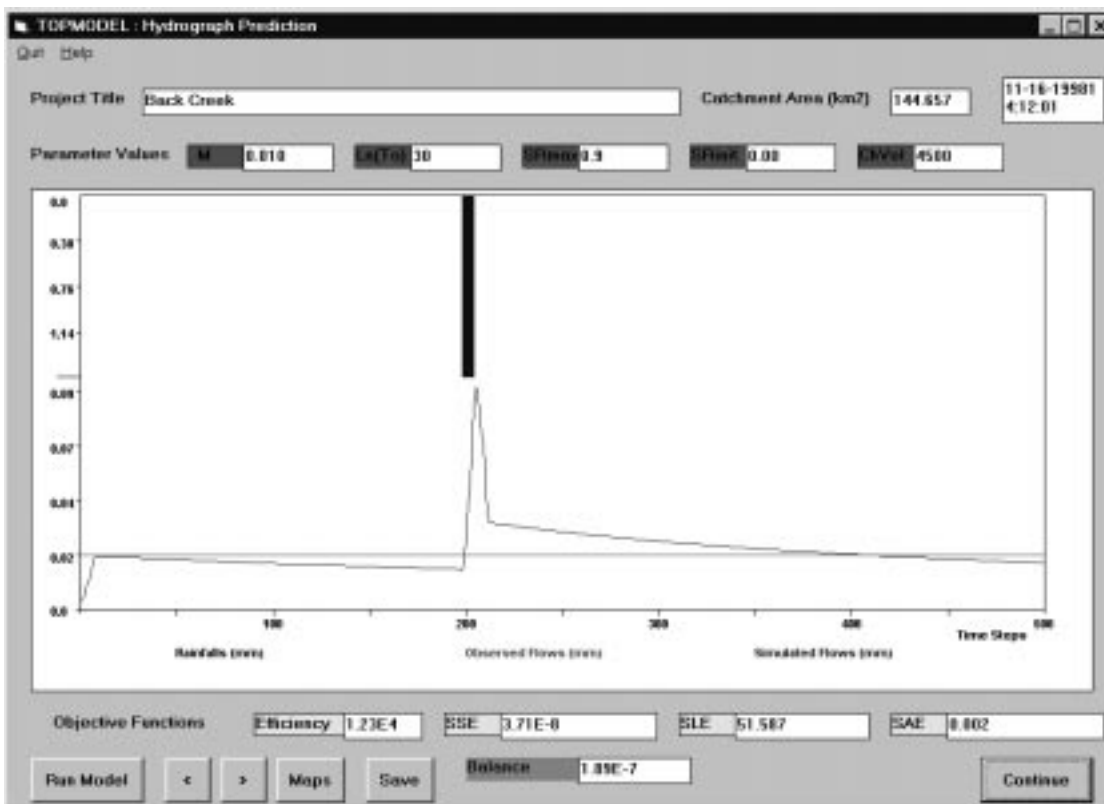


Figure 16 (f).  $m = 0.010m$ .

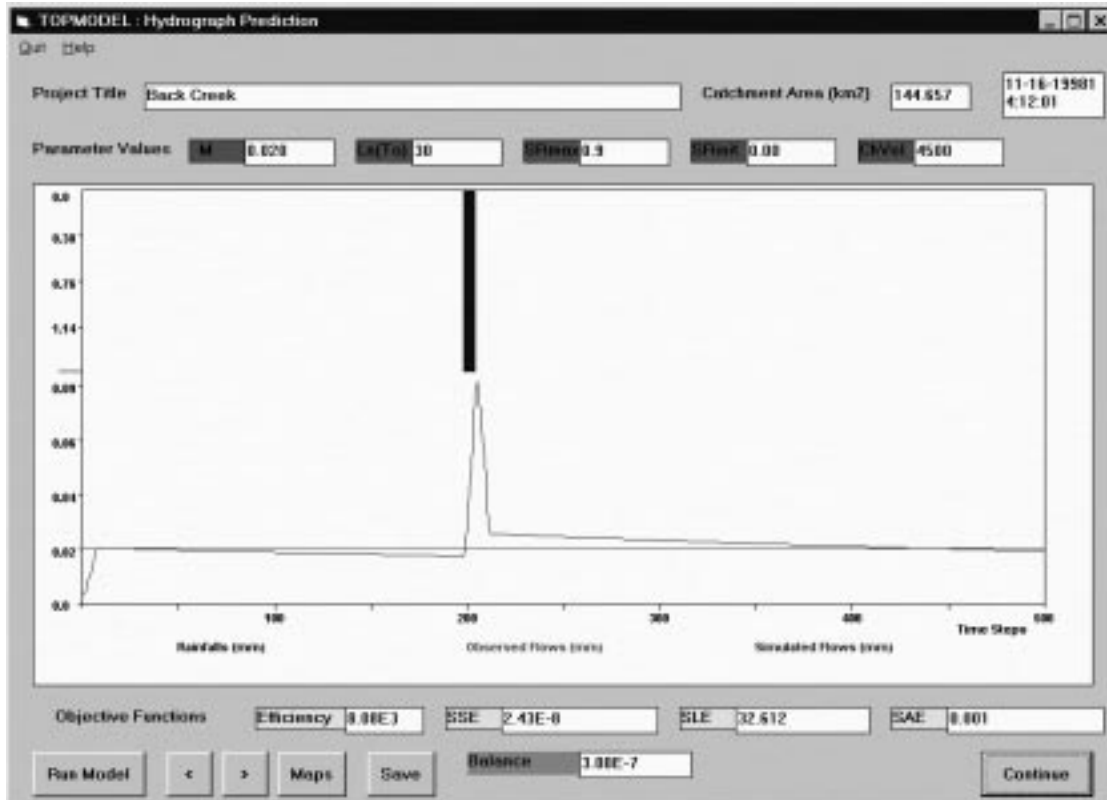


Figure 16 (g).  $m = 0.020m$ .

### 5.1.3 Effect of the $\ln(T_o)$ Parameter on Simulated Hydrograph

The  $\ln(T_o)$  parameter is the natural logarithm of the effective transmissivity of the soil when just saturated. The simulated hydrograph generated by TOPMODEL is sensitive to changes in the  $\ln(T_o)$  parameter, although not as sensitive as to changes in the  $m$  parameter. Figures 17 (a) - (e) show the effect of the simulated hydrograph as the value of the  $\ln(T_o)$  parameter increases from 5 to 45  $\ln(m^2/h)$ . (Note the changes in the scale on the y-axis.) The value of  $\ln(T_o)$  for each execution of TOPMODEL is displayed in the output window just to the right of the  $m$  parameter. The same rainfall data and observed flow data were used as in the  $m$  parameter analysis.

As can be seen in Figures 17 (a) - (e), both the shape of the hydrograph and the peak flow change quite dramatically with the  $\ln(T_o)$  parameter. For lower values of  $\ln(T_o)$  (i.e. 5, 15 and 25), the peak flow is larger, and the hydrograph appears to be “flashy” (meaning it rises and falls very quickly). As the  $\ln(T_o)$  parameter increases to higher

values (i.e. 35 and 45), the hydrograph takes the shape of more traditional observed hydrographs. These larger values of  $\ln(T_o)$  result in slower simulated hydrograph response, thus lowering the peak flow. The peak flow drops with increases in  $\ln(T_o)$  and seems to level off at 0.09 mm/hr.

To better understand the effect of the  $\ln(T_o)$  parameter on the simulated hydrograph, the two components, surface and subsurface, of a hydrograph generated by TOPMODEL must be examined again. The  $\ln(T_o)$  parameter does not seem to significantly impact the recession tail of the hydrograph or baseflow which is dominated by subsurface flow. With each value of  $\ln(T_o)$ , the recession seems to begin at a flow of 0.07 to 0.08 mm/hr at approximately the same time. At first glance, this doesn't appear to be true because the hydrographs have dissimilar shapes, but closer examination, taking into account the changing y axis, reveals the recession tails are almost identical. In addition, the hydrograph for each value of  $\ln(T_o)$  returns to the datum value of 0.02 mm/hr at approximately 350 to 360 hours. The  $\ln(T_o)$  parameter does, however, have a large impact on the surface portion of the runoff. For small values of  $\ln(T_o)$ , the peak flow resulting from surface flow is almost 300% larger than the 0.09mm/hr resulting from larger values of  $\ln(T_o)$ . However, the magnitude of the peak flow seems to have little impact on the recession tail of the hydrograph or the baseflow after the rainfall event.

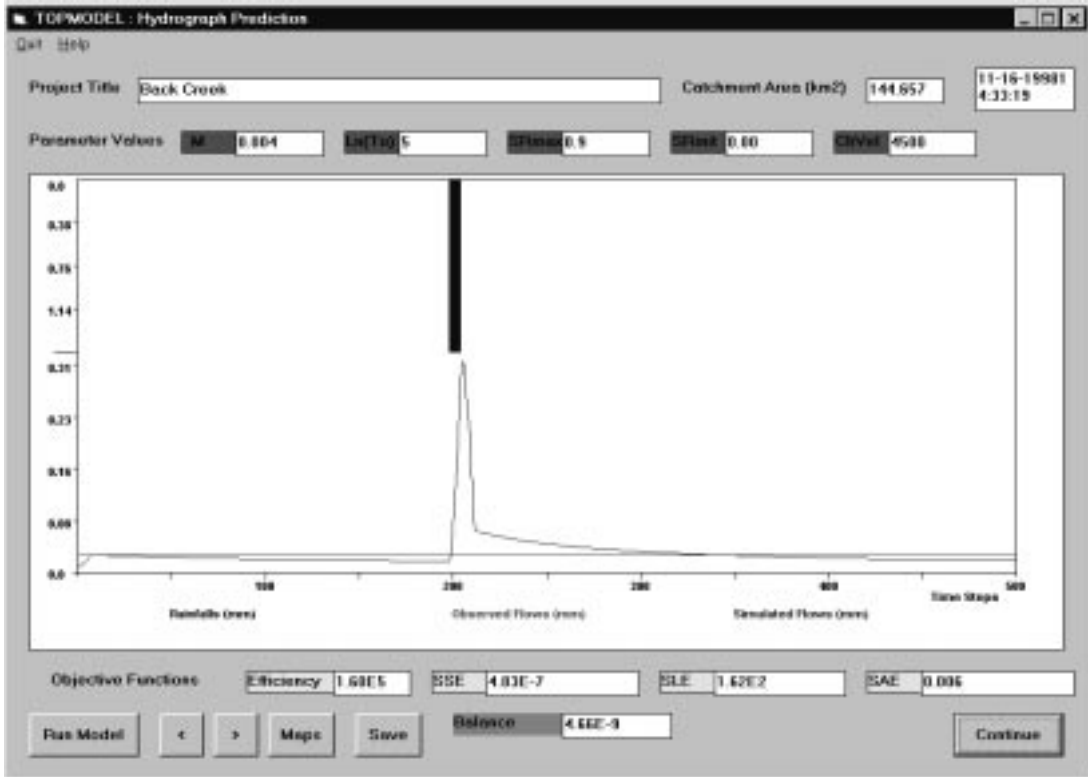


Figure 17 (a).  $\ln(T_o) = 5$ .

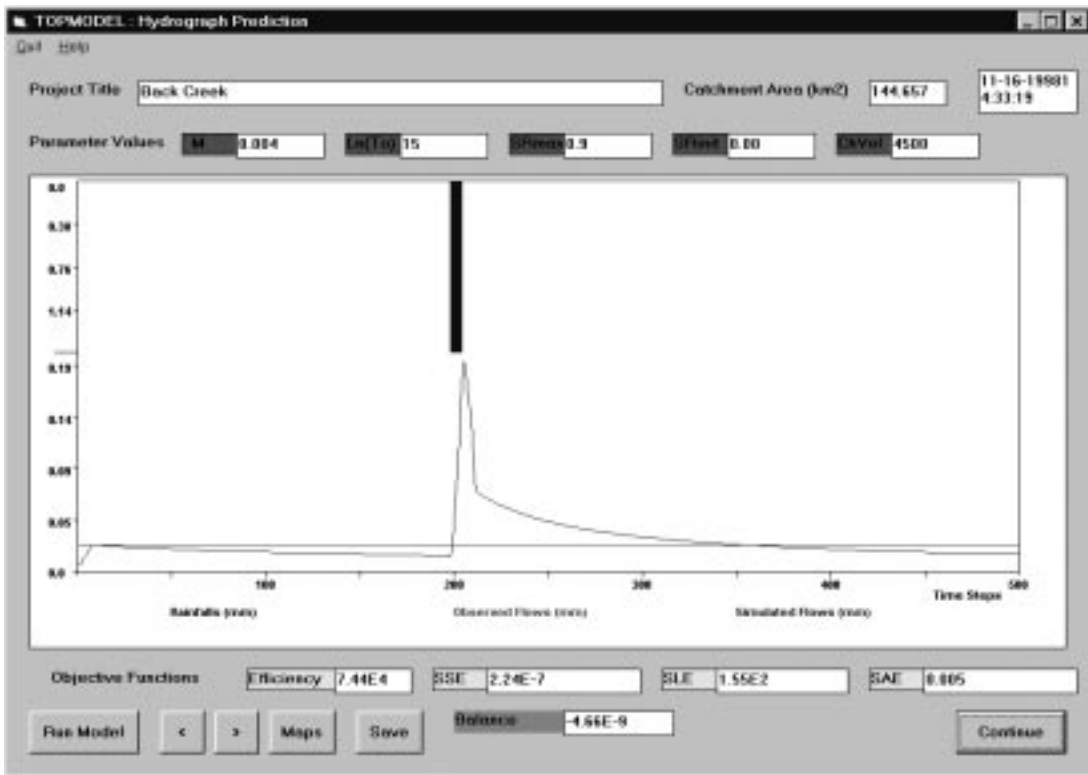


Figure 17 (b).  $\ln(T_o) = 15$ .

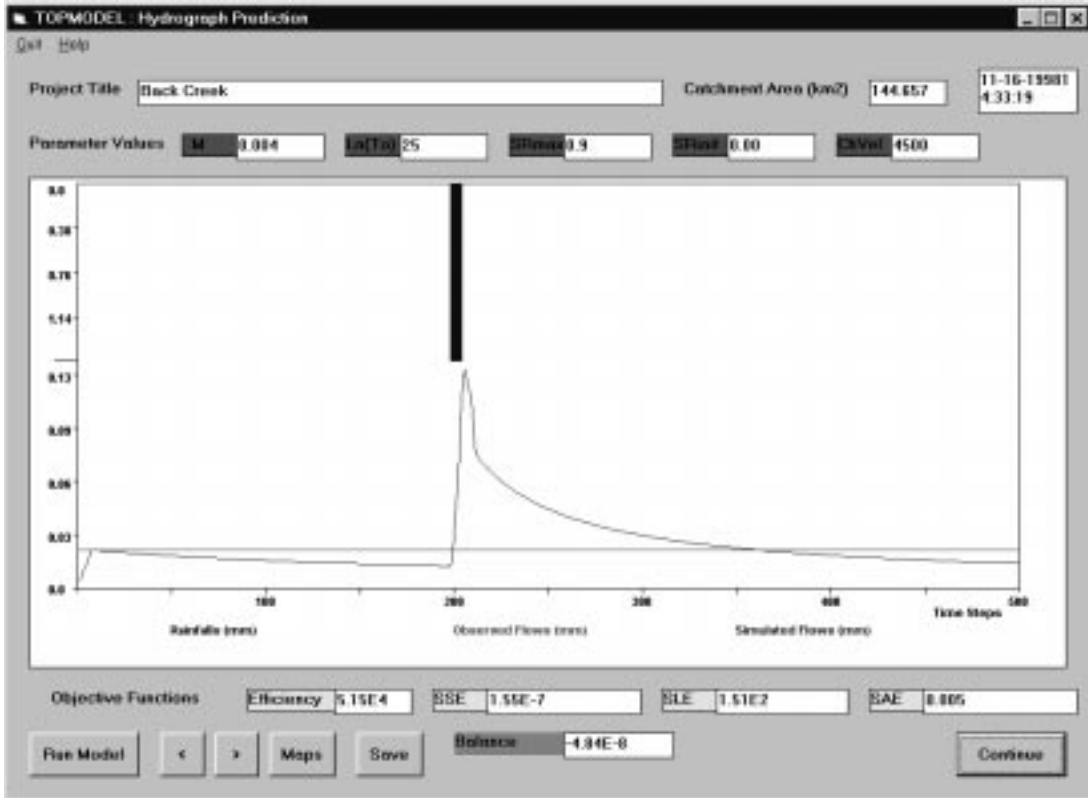


Figure 17 (c).  $\ln(T_o) = 25$ .

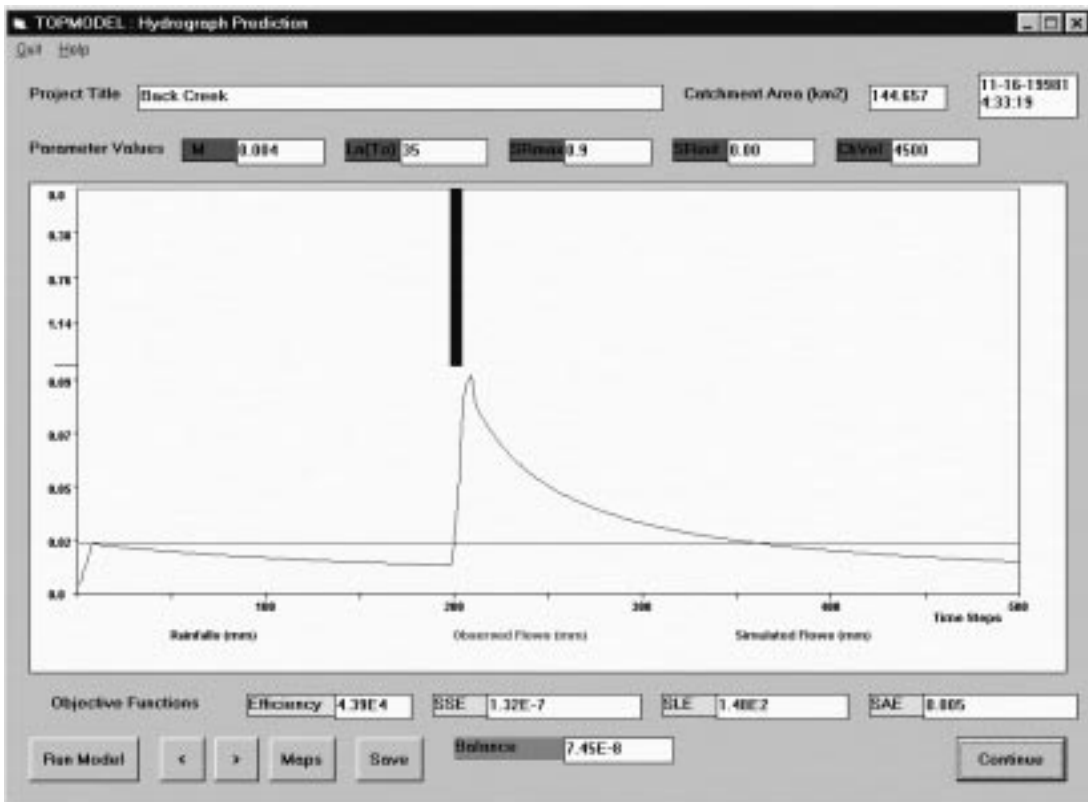


Figure 17 (d).  $\ln(T_o) = 35$ .

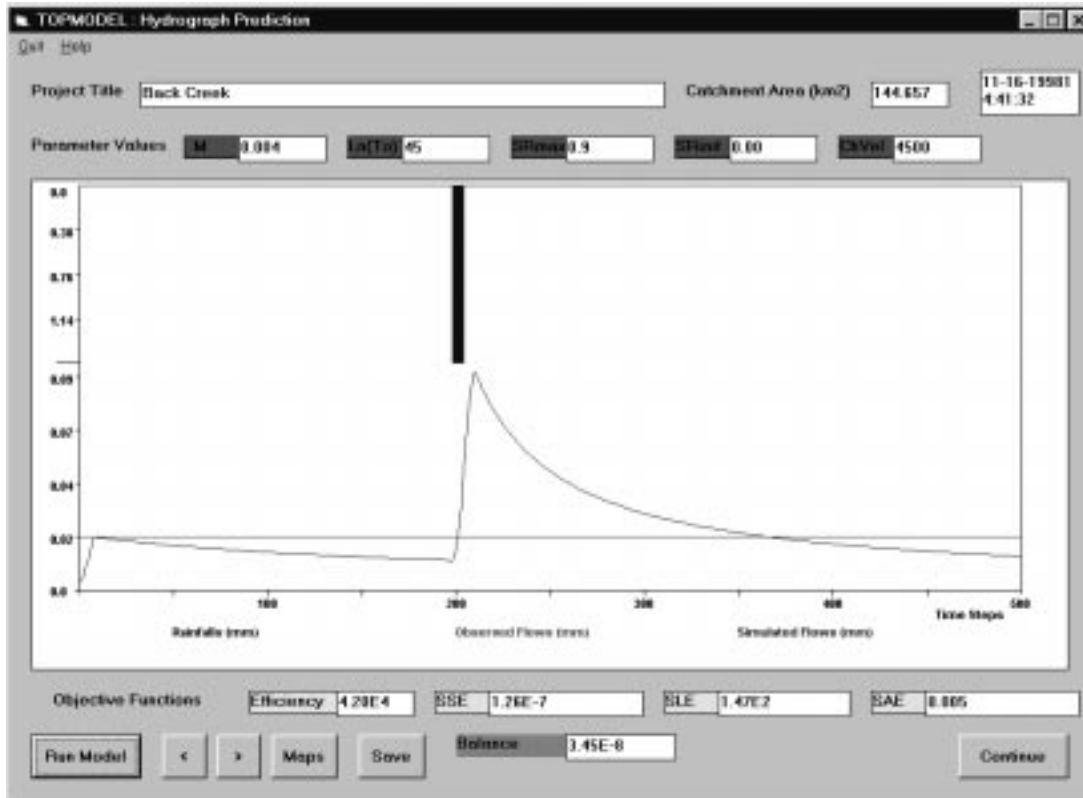


Figure 17 (e).  $\ln(T_o) = 45$ .

#### 5.1.4 Effect of the *ChVel* Parameter on Simulated Hydrograph

The *ChVel* parameter is the effective surface routing velocity for scaling the distance/area routing procedure. Linear routing is assumed and the units are meters per hour. The rising side of a simulated hydrograph generated by TOPMODEL is sensitive to changes in the *ChVel* parameter. Figures 18 (a) - (c) show the effect of the simulated hydrograph as the value of the *ChVel* parameter increases from 750 to 4500 (m/hr). (Note the changes in the scale on the y-axis.) The value of *ChVel* for each execution of TOPMODEL is displayed in the output window on the right above the hydrograph and rain data. The same rainfall data and observed flow data were used as in the *m* and  $\ln(T_o)$  parameter analyses.

As can be seen in Figures 18 (a) - (c), the shape of the hydrograph, the time to peak, and the peak flow all change with the *ChVel* parameter. As the value of *ChVel* increases from 750 to 1500 to 4500 m/hr, the peak flow increases slightly, but more

importantly, the time to peak decreases significantly, from about 35 hours to only about 8 hours.

The *ChVel* parameter does not seem to affect the shape of the recession tail of the hydrograph, but it does affect the recession tail by delaying the beginning of the recession by about the same length of time as the peak is delayed. For each value of *ChVel*, the recession seems to begin at a flow of 0.07 to 0.08 mm/hr. For *ChVel* equal to 750 m/hr, the hydrograph returns to the datum value of 0.02 mm/hr at approximately 380 hours. For *ChVel* equal to 1500 m/hr, the hydrograph returns to the datum value of 0.02 mm/hr at approximately 370 hours. Finally, for *ChVel* equal to 4500, the hydrograph returns to the datum value of 0.02 mm/hr at approximately 360 hours.

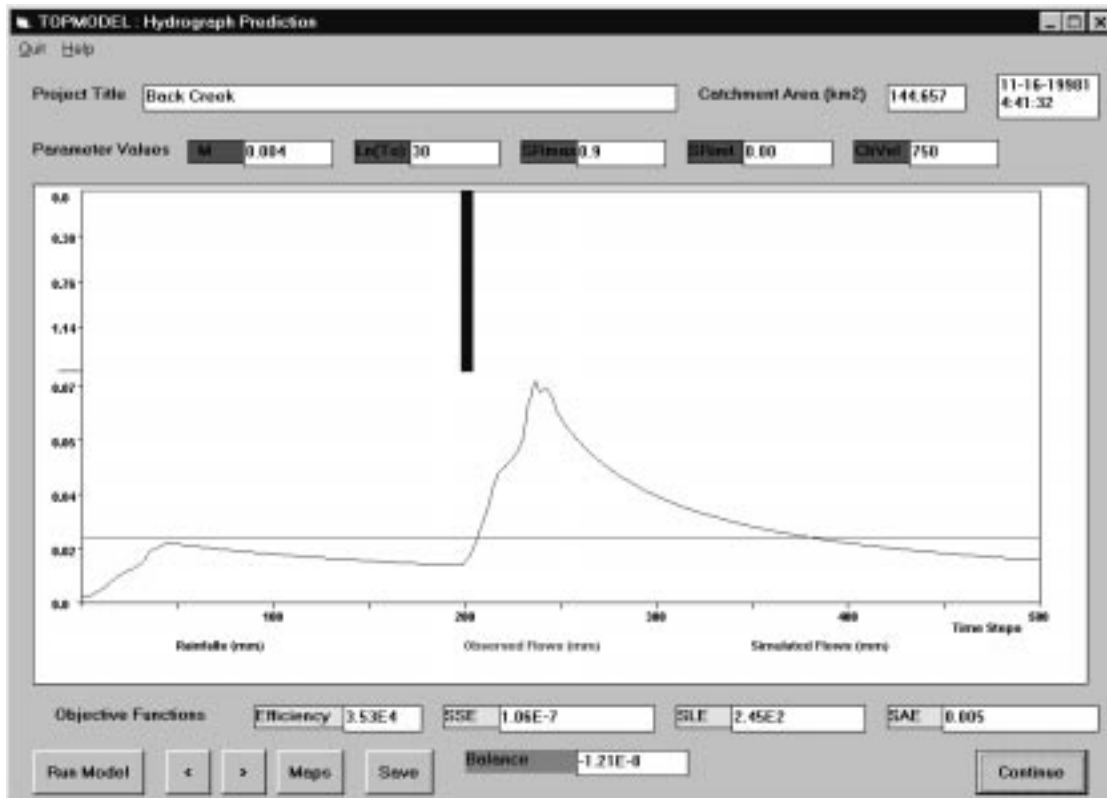


Figure 18 (a). *ChVel* = 750 m/hr.

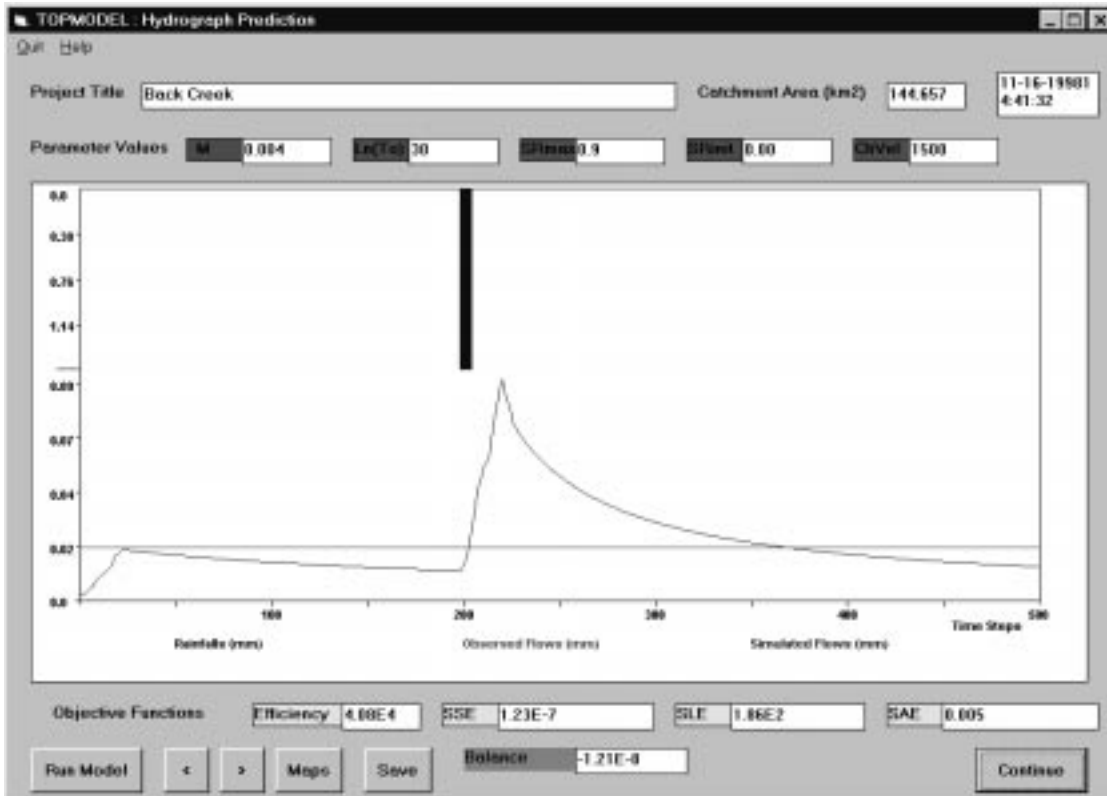


Figure 18 (b).  $ChVel = 1500$  m/hr.

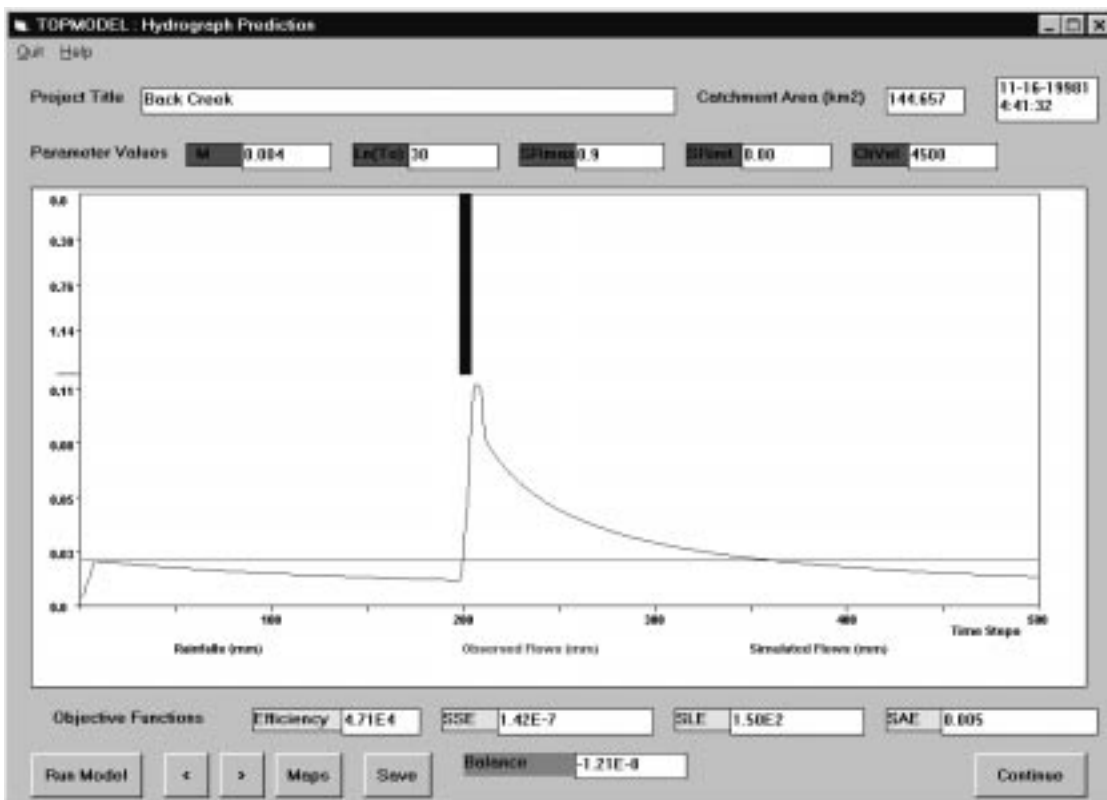


Figure 18 (c).  $ChVel = 4500$  m/hr.

### 5.1.5 Effect of Antecedent Moisture on Simulated Hydrograph

A major advantage of using a continuous model, such as TOPMODEL, is its ability to account for the amount of moisture in the soil column between rainfall events. In TOPMODEL, the simulated response to a rainfall event is very sensitive to the amount of moisture present in the soil column. This moisture in the soil column is controlled by the  $m$  and  $\ln(T_o)$  parameters, the magnitude of the previous rainfall event, and length of time since the previous rainfall event. Intuitively, it makes sense that as time passes without precipitation, moisture in the soil column decreases via evapotranspiration and drainage toward the catchment outlet. This decrease in soil moisture affects the hydrologic response during the next rainfall event by allowing more space for water to infiltrate the soil thus decreasing the amount of surface runoff.

Poor hydrograph simulation can occur if an insufficient length of modeling time precedes the rainfall event. This would be the case if a rainfall event falls near the beginning of a 2500 hour simulation interval. TOPMODEL may not have enough time to accurately predict the amount of water in the soil column. Consider the case when a rainfall event occurs at the beginning of a 2500 hour simulation interval and is preceded by a long dry antecedent period. The soil will actually be drier than TOPMODEL predicts. Therefore, TOPMODEL will underestimate the amount of water that will infiltrate the soil. The result is that TOPMODEL will tend to overpredict the runoff hydrograph. Now consider the case when a rainfall event falls at the beginning of a 2500 hour simulation interval and is preceded by a large rainfall event that occurs just before the beginning of the 2500 hour simulation interval. The soil will actually contain more moisture than TOPMODEL predicts. Therefore, TOPMODEL will overestimate the amount of water that will infiltrate the soil. The result is that TOPMODEL will tend to underpredict the runoff hydrograph.

Figure 19 (a) shows a rainfall event that occurs near the middle of a 2500 hour simulation interval. The model has had sufficient time to account for soil moisture prior to the precipitation event. Figure 19 (b) shows the same rainfall event that now occurs at the beginning of a 2500 hour simulation interval. The model has not had sufficient time

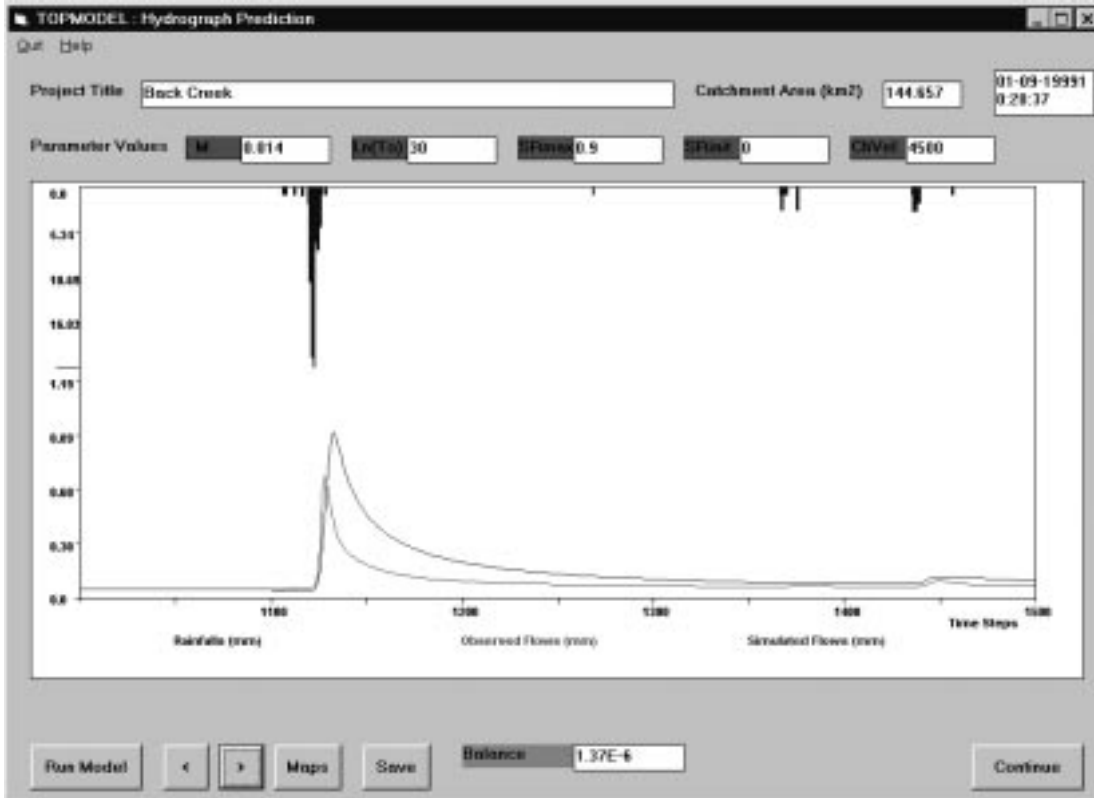


Figure 19 (a). November 1996 storm occurring at the end of a simulation period.

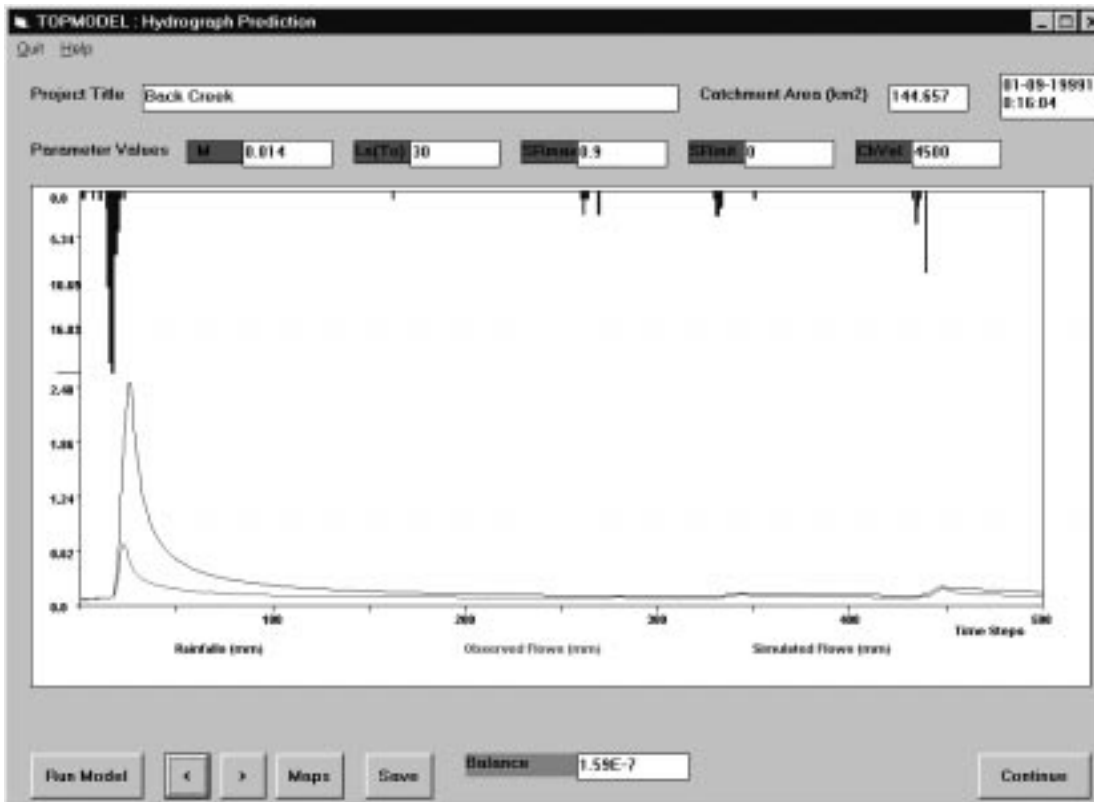


Figure 19 (b). November 1996 event occurring at the beginning of a simulation period.

to account for soil moisture prior to the precipitation event. A relatively dry period precedes the precipitation event, therefore, the model overpredicts the event hydrograph. (Note the changes in scale on the y-axis.)

#### **5.1.6 Effect of Grid Cell Size on TOPMODEL Simulated Hydrograph**

As discussed previously in Section 5.1.1, this study demonstrates that increasing the grid cell size from 15 up to 120 meters causes the distribution of the topographic index to shift to higher values. The basic equations and assumptions of TOPMODEL indicate that an increase in the topographic index would result in an increase in the saturated area and, therefore, in runoff discharge. However, this phenomenon was not observed in this study. Figures 20 (a) & (b) show the simulated hydrographs with grid cell sizes of 15 and 120 m, respectively. As can be seen, changing the grid cell size does not produce an observable effect on the discharge from the watershed. This was confirmed by comparing the model output developed using each grid cell size for the water year of 1995; no variations in the simulated hydrographs were observed. In a study performed by Franchini *et al.* (1996), similar results were obtained and the same insensitivity to the topographic index distribution was recorded. He writes, “TOPMODEL is surprisingly insensitive to the basin’s actual index curve, to such a degree... that the index curve can be replaced with” another basin’s curve “without significantly altering the set of discharge quantities generated.”

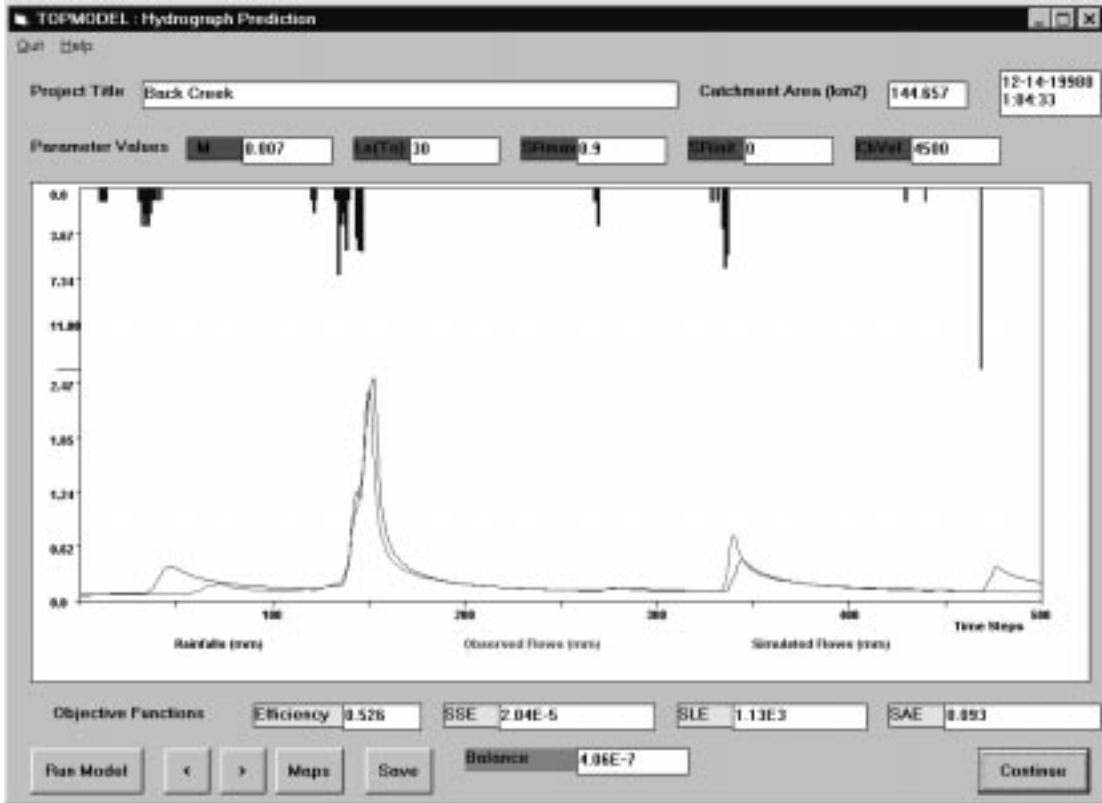


Figure 20 (a). January 1996 event modeled with a 15 meter grid cell size.

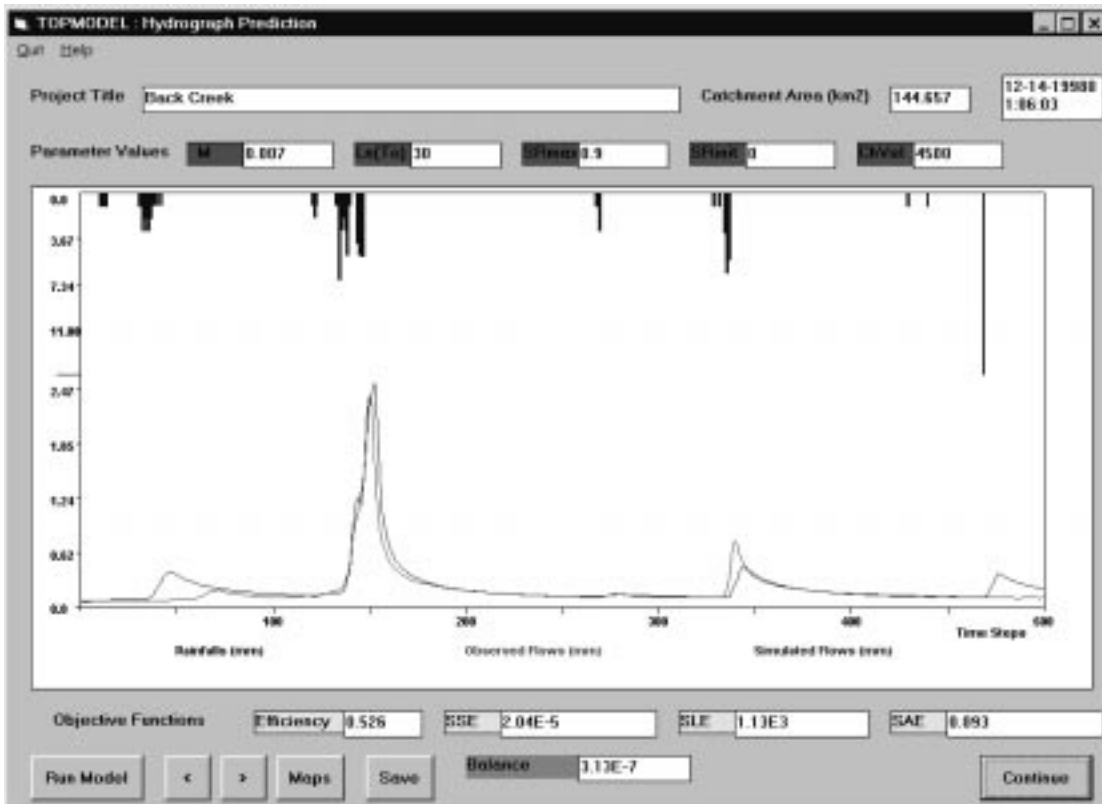


Figure 20 (b). January 1996 event modeled with a 120 meter grid cell size.

The topographic distributions shown in Figures 21 (a) & (b) were artificially generated. One goal of this exercise was to determine how large a shift in the distribution must take place in order to produce a change in the simulated hydrograph (see Figure 21 (a)). Using the 15 meter distribution as a starting point, it was found that a positive shift of about 30 in the distribution of the topographic index was required to produce an observable change in the model hydrograph response. Figures 22 (a) & (b) show, respectively, the simulated hydrograph using the original topographic index distribution and the slightly changed simulated hydrograph using the distribution increased by 30. Another goal was to determine if simply changing the shape without shifting the entire distribution would impact the model response (see Figure 21 (b)). This produced no observable change in the simulated hydrograph.

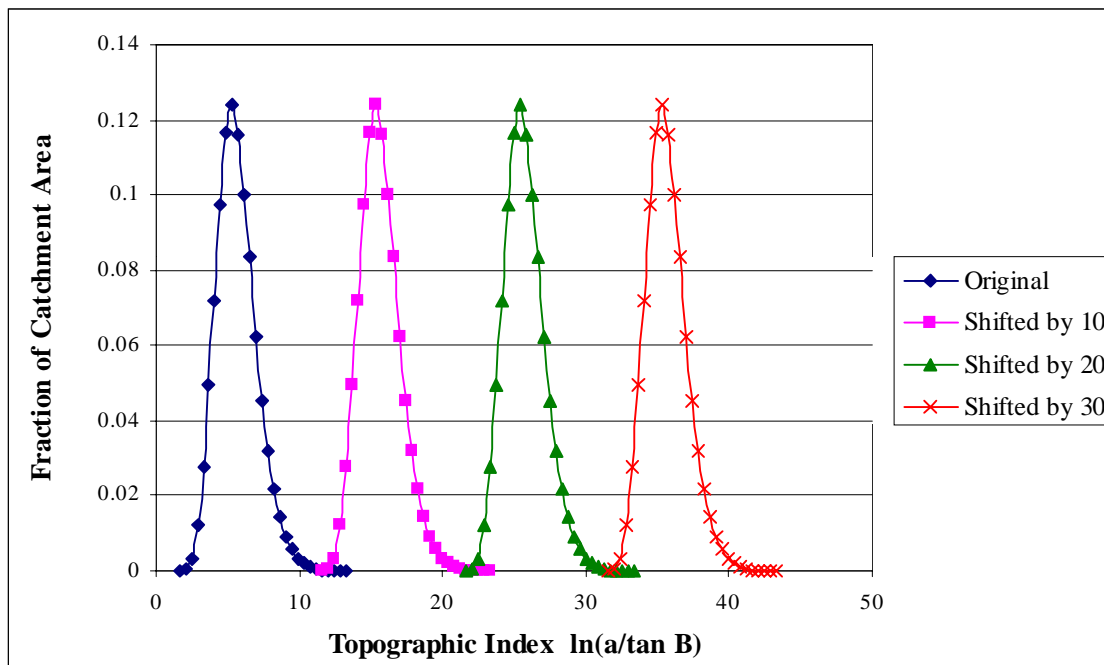


Figure 21 (a). Original 15 meter topographic distribution and synthetic distributions shifted by increments of 10.

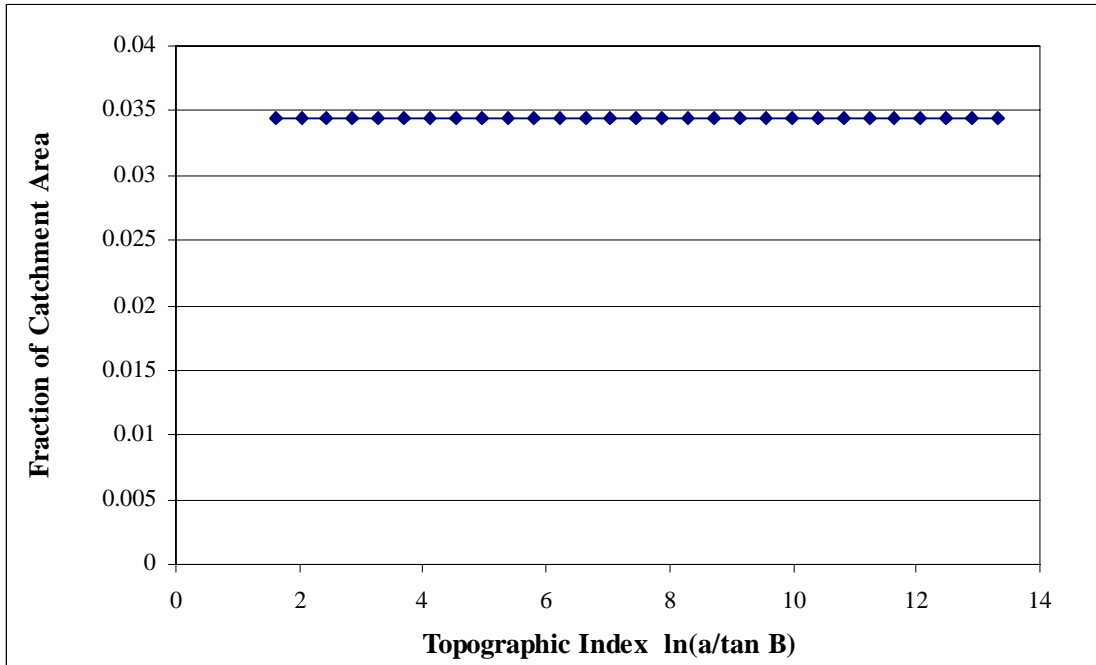


Figure 21 (b). Uniform topographic index distribution covering the same interval as the 15 meter distribution.

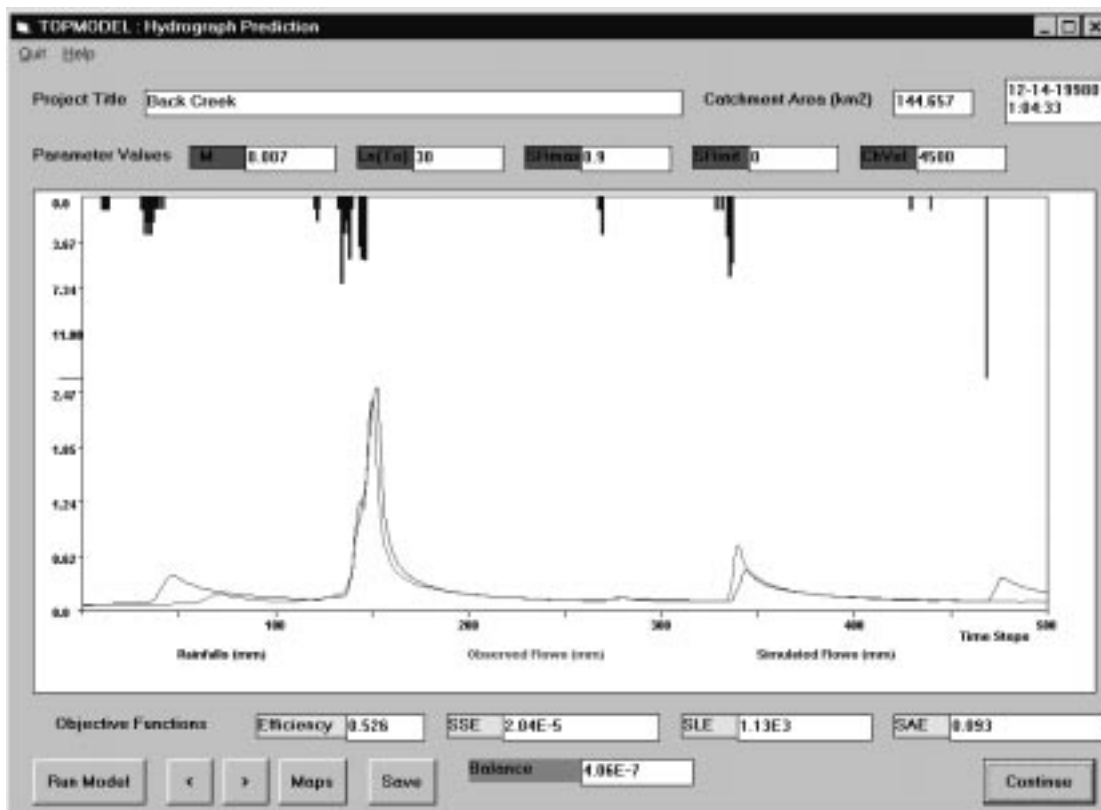


Figure 22 (a). January 1996 event modeled with original 15 meter distribution.

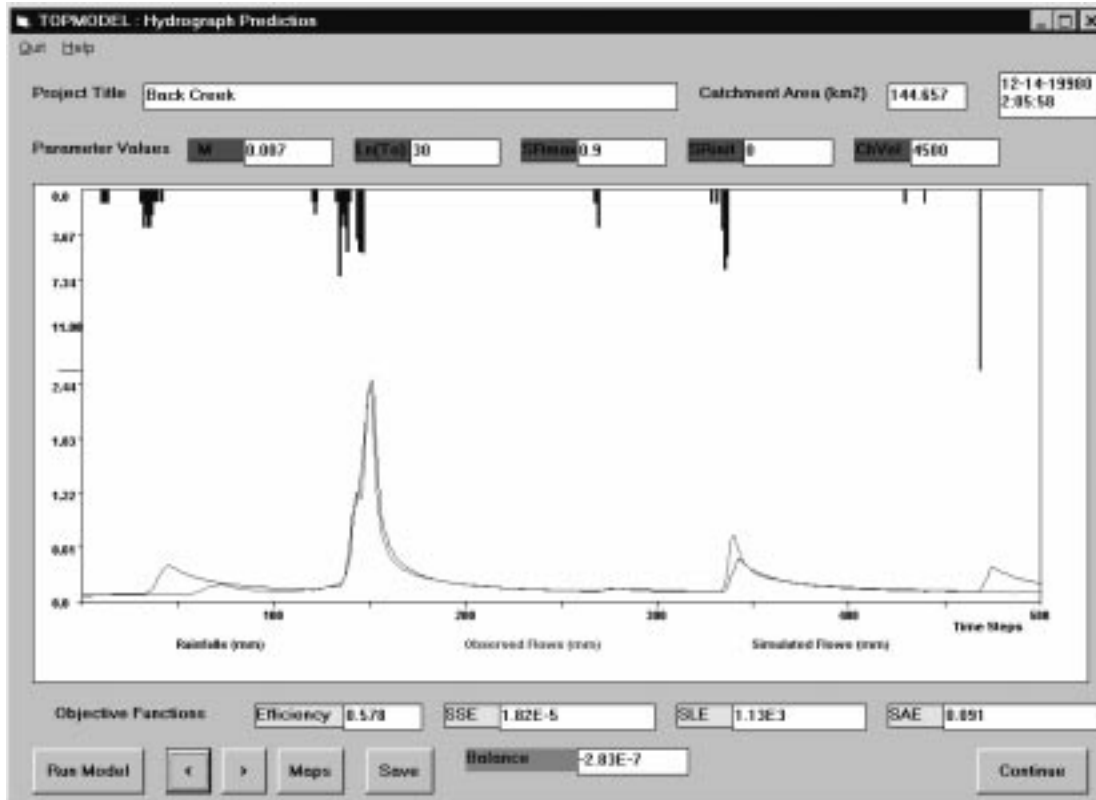


Figure 22 (b). January 1996 event modeled with synthetic distribution shifted by 30.

## 5.2 HEC-1

### 5.2.1 Effect of Spatial Scale on Simulated Hydrograph

Figure 23 shows one representative storm which was simulated using both 81 and 20 subareas. Appendix H consists of a set of figures containing simulated hydrographs from each of the storms modeled using HEC-1. Visual comparison of the hydrographs produced using 81 and 20 subareas reveals that there are slight differences in the two hydrographs. However, the differences do not seem to be significant. Generally, the peak flows and times to peak are quite similar.

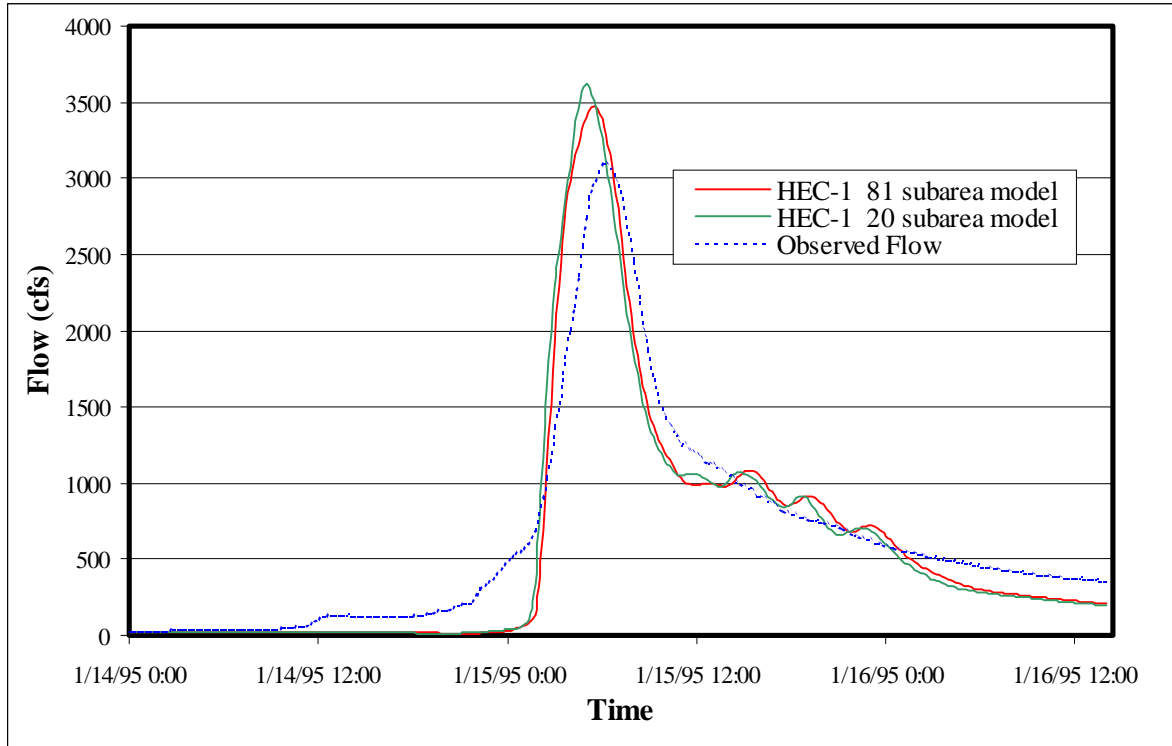


Figure 23. January 1995 event simulated using 20 subarea and 81 subarea HEC-1 models.

Tables 2, 3, & 4 contain statistics comparing the peak flows, times to peak, and storm volumes (see Section 4.4 for statistical equations used). These tables show that there is not a large difference between any of the statistics calculated from the 81 subarea model and the 20 subarea model. Analyzing the peak flow statistics in Table 2, reveals that the relative error is slightly nearer zero for the 81 subarea model for six of the eight storms. The MARE is larger for the 81 subarea model, whereas the standard error is larger for the 20 subarea model. The mean arithmetic relative error (MARE) is not as meaningful a statistic as standard error because events with large positive and large negative relative errors can essentially cancel each other out resulting in a small MARE. The standard error statistic does not have this flaw because the relative error is squared, thus eliminating negative values.

Table 2. Comparison of HEC-1 peak flows generated by 81 and 20 subarea models.

Event	81 Subareas (cfs)	20 Subareas (cfs)	Observed (cfs)	Relative Error 81 Subareas	Relative Error <sup>2</sup> 81 Subareas	Relative Error 20 Subareas	Relative Error <sup>2</sup> 20 Subareas
Apr-92	7645	7450	8460	-0.096	0.009	-0.119	0.014
Jan-95	3477	3618	3102	0.121	0.015	0.166	0.028
Jun-95	3850	3636	6390	-0.397	0.158	-0.431	0.186
Aug-96	9767	9866	1166	7.377	54.413	7.461	55.673
Sep-96	6814	6938	3892	0.751	0.564	0.783	0.613
Nov-96	1231	1220	921	0.337	0.113	0.325	0.105
Jun-97	416	381	1327	-0.687	0.471	-0.713	0.508
Jan-98	2186	1969	1883	0.161	0.026	0.046	0.002
<b>Bias *</b>				<b>0.189</b>		<b>0.056</b>	
<b>Standard Error *</b>					<b>1.164</b>		<b>1.207</b>
<b>Mean Arithmetic Relative Error *</b>				<b>0.027</b>		<b>0.008</b>	

\* Calculations exclude August 1996 storm.

Table 3 displays the statistics for times to peak. The time to peak for a given hydrograph (i.e. *Sep-96, 20 subarea model*) was determined by calculating the time from the initial rise in the *observed* hydrograph to the peak of the *Sep-96, 20 subarea model* hydrograph. The relative error for the 81 subarea model is closer to zero for four of the six events. The MARE and standard error were both slightly smaller for the 81 subarea model. The June 1997 and January 1998 events were excluded due to their difficult to define times to peak. The June 1997 event had extremely different rainfall data between the four rain gauges which made modeling performance very poor. The January 1998 observed hydrograph began to rise slowly approximately 12 hours before the rapid increase in flow. This very gradual increase in flow was not modeled by HEC-1, and, therefore, makes determining and comparing times to peak for observed versus simulated hydrographs difficult. The timing of all three peaks (observed, 81 subarea model, and 20 subarea model) for the January 1998 event is very good, all occur within fifteen minutes of the others.

Table 3. Comparison of HEC-1 times to peak generated by 81 and 20 subarea models.

Event	81 Subareas (hrs)	20 Subareas (hrs)	Observed (hrs)	Relative Error 81 Subareas	Relative Error <sup>2</sup> 81 Subareas	Relative Error 20 Subareas	Relative Error <sup>2</sup> 20 Subareas
Apr-92	11.75	12	11.75	0.000	0.000	0.021	0.000
Jan-95	11.25	10.75	11.75	-0.043	0.002	-0.085	0.007
Jun-95	1.75	1.75	2.50	-0.300	0.090	-0.300	0.090
Aug-96	3.50	3.00	5.25	-0.333	0.111	-0.429	0.184
Sep-96	6.75	6.50	8.00	-0.156	0.024	-0.188	0.035
Nov-96	4.25	4.50	5.00	-0.150	0.023	-0.100	0.010
Jun-97	n/a	n/a	n/a	n/a	n/a	n/a	n/a
Jan-98	n/a	n/a	n/a	n/a	n/a	n/a	n/a
<b>Bias **</b>				<b>-0.982</b>		<b>-1.080</b>	
<b>Standard Error **</b>					<b>0.500</b>		<b>0.571</b>
<b>Mean Arithmetic Relative Error **</b>				<b>0.164</b>		<b>0.180</b>	

\*\* Calculations exclude June 1997 and January 1998 storms.

Table 4 displays the statistics for flow volumes. These flow volumes include both the base flow and surface runoff components. The analysis was performed using both components for four reasons: (a) separating base flow from surface runoff is somewhat arbitrary (it has been referred to as more of an art than a science), (b) HEC-1 generally performs reasonably well when modeling base flow in the short term, and, therefore, would not significantly bias the total volumes, (c) the volume of base flow when compared to the volume of surface runoff is very small, and (d) using a constant length of time for the calculations of flow volume adds consistency to the method. The statistics shown in Table 4 reveal that the relative error for the 81 subarea model is smaller for six of the eight events. In addition, the standard error and MARE for the 81 subarea model are also slightly smaller.

Table 4. Comparison of HEC-1 flow volumes generated by 81 and 20 subarea models.

Event	81 Subareas (cfs hrs)	20 Subareas (cfs hrs)	Observed (cfs hrs)	Relative Error 81 Subareas	Relative Error <sup>2</sup> 81 Subareas	Relative Error 20 Subareas	Relative Error <sup>2</sup> 20 Subareas
Apr-92	6594	6494	6828	-0.034	0.001	-0.049	0.002
Jan-95	3074	3058	3378	-0.090	0.008	-0.095	0.009
Jun-95	4223	4141	4375	-0.035	0.001	-0.053	0.003
Aug-96	6955	6947	1021	5.812	33.779	5.804	33.688
Sep-96	4964	4913	3585	0.385	0.148	0.370	0.137
Nov-96	1029	1025	1245	-0.173	0.030	-0.177	0.031
Jun-97	1098	1075	1470	-0.253	0.064	-0.269	0.072
Jan-98	1742	1672	2121	-0.179	0.032	-0.212	0.045
<b>Bias *</b>				<b>-0.380</b>		<b>-0.484</b>	
<b>Standard Error *</b>					<b>0.533</b>		<b>0.547</b>
<b>Mean Arithmetic Relative Error *</b>				<b>0.054</b>		<b>0.069</b>	

\* Calculations exclude August 1996 storm.

## 5.3 Comparison of HEC-1 and TOPMODEL

### 5.3.1 Large storm modeling accuracy compared for TOPMODEL and HEC-1

In this study, the comparison of TOPMODEL and HEC-1 is limited in that the models can only be compared for the limited number of large storms that were modeled in both HEC-1 and TOPMODEL for the water years of 1995, 1996, and 1997. The output from both models for the events used in this comparison can be found in Appendices H and I. This portion of the study focuses on the large storm simulation performance of each model. These storms are listed in Tables 5 and 6 and indicated on the annual hydrographs in Appendix J. The hydrographs generated by the two models were analyzed based on: (a) peak flows, (b) times to peak, and (c) visual comparison.

Table 5 contains the peak flow statistics for HEC-1 and TOPMODEL. Analyzing these peak flow statistics reveals that the relative error is nearer zero for both models for three of the six storms. The MARE is slightly smaller for HEC-1, but the standard error is larger. See Section 5.2.1 for comments on the MARE and standard error statistics.

Table 5. Comparison of HEC-1 and TOPMODEL peak flows.

Event	HEC-1 81 Subareas (cfs)	TOPMODE L (cfs) [mm/hr]	Observed (cfs)	Relative Error HEC-1	Relative Error <sup>2</sup> HEC-1	Relative Error TOPMODEL	Relative Error <sup>2</sup> TOPMODEL
Jan-95	3477	4285 [3.02]	3102	0.121	0.015	0.381	0.146
Jun-95	3850	5363 [3.78]	6390	-0.397	0.158	-0.161	0.026
Aug-96	9767	9436 [6.65]	1166	7.377	54.413	7.093	50.310
Sep-96	6814	4526 [3.19]	3892	0.751	0.564	0.163	0.027
Nov-96	1231	1262 [0.89]	921	0.337	0.113	0.371	0.138
Jun-97	416	116 [0.082]	1327	-0.687	0.471	-0.912	0.832
<b>Bias *</b>				<b>0.124</b>		<b>-0.157</b>	
<b>Standard Error *</b>					<b>1.149</b>		<b>1.081</b>
<b>Mean Arithmetic Relative Error *</b>				<b>0.018</b>		<b>0.022</b>	

\* Calculations exclude August 1996 storm.

Table 6 displays the statistics for times to peak. The time to peak for a given hydrograph (i.e. *Sep-96, HEC-1*) was determined by calculating the time from the initial rise in the *observed* hydrograph to the peak of the *Sep-96, HEC-1* hydrograph. The relative error for the HEC-1 model is closer to zero for four of the five events. The MARE and standard error are both significantly smaller for the HEC-1 model.

Table 6. Comparison of HEC-1 and TOPMODEL times to peak.

Event	HEC-1 81 Subareas (hrs)	TOPMODE L (hrs)	Observed (hrs)	Relative Error HEC-1	Relative Error <sup>2</sup> HEC-1	Relative Error TOPMODEL	Relative Error <sup>2</sup> TOPMODEL
Jan-95	11.25	14.15	11.75	-0.043	0.002	0.204	0.042
Jun-95	1.75	6.35	2.50	-0.300	0.090	1.540	2.372
Aug-96	3.50	4.10	5.25	-0.333	0.111	-0.219	0.048
Sep-96	6.75	10.15	8.00	-0.156	0.024	0.269	0.072
Nov-96	4.25	8.25	5.00	-0.150	0.023	0.650	0.423
Jun-97	n/a	n/a	n/a	n/a	n/a	n/a	n/a
<b>Bias **</b>				<b>-0.982</b>		<b>2.444</b>	
<b>Standard Error **</b>					<b>0.500</b>		<b>1.719</b>
<b>Mean Arithmetic Relative Error **</b>				<b>0.164</b>		<b>0.407</b>	

\*\* Calculations exclude June 1997 storm. See Section 5.2.1 for explanation.

A visual comparison of the two models makes apparent a few characteristics of both models. HEC-1 generally produces a hydrograph with a shape very similar to that of the observed hydrograph. The runoff volumes are relatively close to the observed volumes. The recession tail of the hydrograph is usually modeled quite well. HEC-1 usually models the rising side adequately, however, it is common for the model to neglect initial increases in flow before the more intense precipitation begins. This behavior can be seen in the following events: April 1992, January 1995, June 1997, and January 1998. This phenomenon is related to the default  $0.2 * S$  initial abstraction used by HEC-1. In the storms listed above, the depth of rainfall designated as initial abstraction by HEC-1 is larger than the amount of initial abstraction that actually occurs. Therefore, HEC-1 underpredicts the amount of runoff during the period before the initial abstraction is satisfied.

The shape of hydrographs produced by TOPMODEL are generally realistic. The major deficiencies in the hydrographs generated by TOPMODEL are overprediction of runoff volume and elongation of the recession tail. These problems could not be remedied by adjusting the parameters without sacrificing model performance. Unfortunately, statistical comparisons of flow volume could not be made between HEC-1 and TOPMODEL due to the exclusively graphical output of TOPMODEL. Limited by the small number of storms modeled, it is difficult to visually determine which model simulates observed hydrologic response better.

### **5.3.2 Continuous versus event based modeling**

A major advantage of using a continuous model, such as TOPMODEL, is its ability to account for the amount of moisture in the soil column between rainfall events. Section 5.1.5 discussed the sensitivity of TOPMODEL hydrograph prediction to the length of modeling time prior to a rainfall event. This modeling time prior to an event allows TOPMODEL to account for soil moisture. Without sufficient time prior to an event, TOPMODEL becomes more of an event based model than a continuous model. TOPMODEL can also be intentionally used as an event based model by beginning the simulation shortly before a rainfall event and ending the simulation shortly after the event.

Because using TOPMODEL this way does not allow sufficient time for the model to accurately predict soil moisture, the model must rely on a value of  $SR_{init}$ , the initial storage deficit in the root zone, which is input by the user.

The August 1996 event was modeled using HEC-1, an event based model, and TOPMODEL as both an event based and a continuous model. Figures 24 (a), (b), and (c) contain the resulting hydrographs and Table 7 compares the peak flows from each simulation. As evident from Figures 24 (a), (b), and (c) and from Table 7, there is quite a difference between the continuous and event based simulations. The continuous model simulation is somewhat better than the event based simulations. Because of the long dry period prior to the event, the event based simulations greatly overpredict the peak flow. It is interesting that both event based simulations predict about the same peak flow. The dry period prior to the event is so long that the continuous simulation underpredicts the peak flow, in fact, the model barely shows any hydrograph response to the precipitation.

The August 1996 event was modeled using HEC-1, an event based model, and TOPMODEL as both an event based and a continuous model. Figures 24 (a), (b), and (c) contain the resulting hydrographs, and Table 7 compares the peak flows from each simulation. As evident from Figures 24 (a), (b), and (c) and from Table 7, there is quite a difference between the continuous and event based simulations. The continuous model simulation is arguably better than the event based simulations. Because of the long dry period prior to the event, the event based simulations greatly overpredict the peak flow. It is interesting that both event based simulations predict about the same peak flow. The dry period prior to the event is so long that the continuous simulation underpredicts the peak flow, in fact, the model barely shows any hydrograph response to the precipitation.

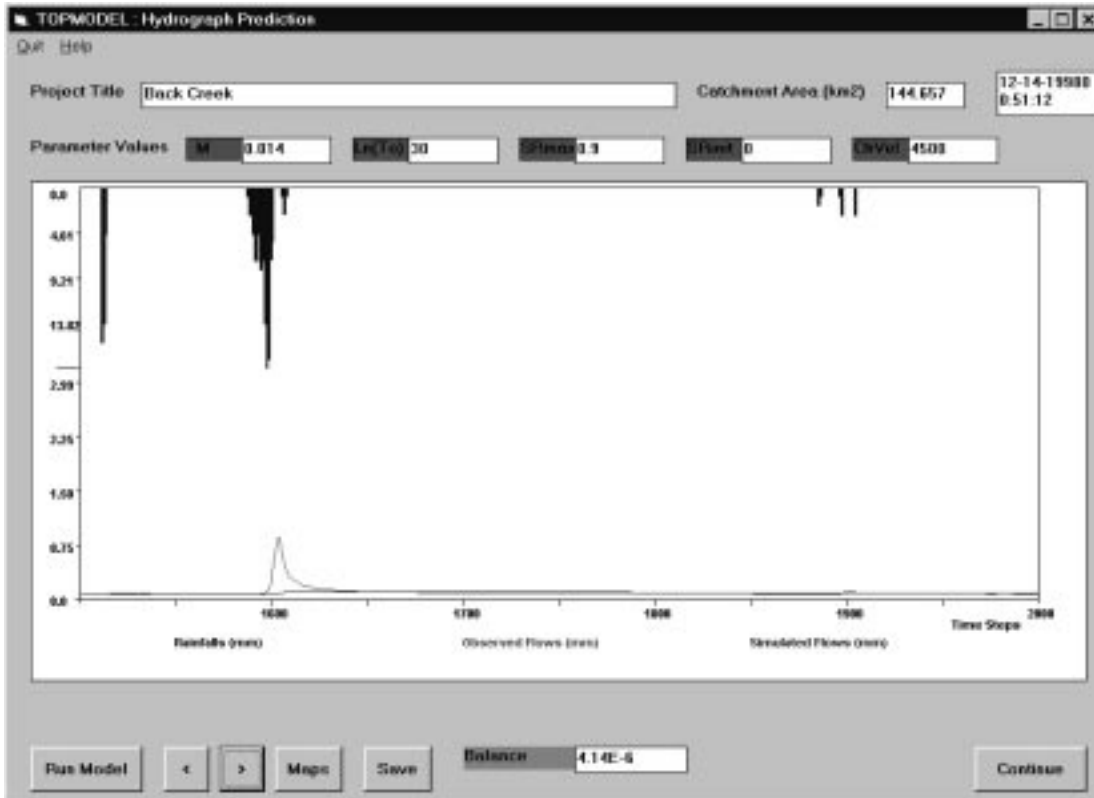


Figure 24 (a). August 1996 event; TOPMODEL continuous simulation.

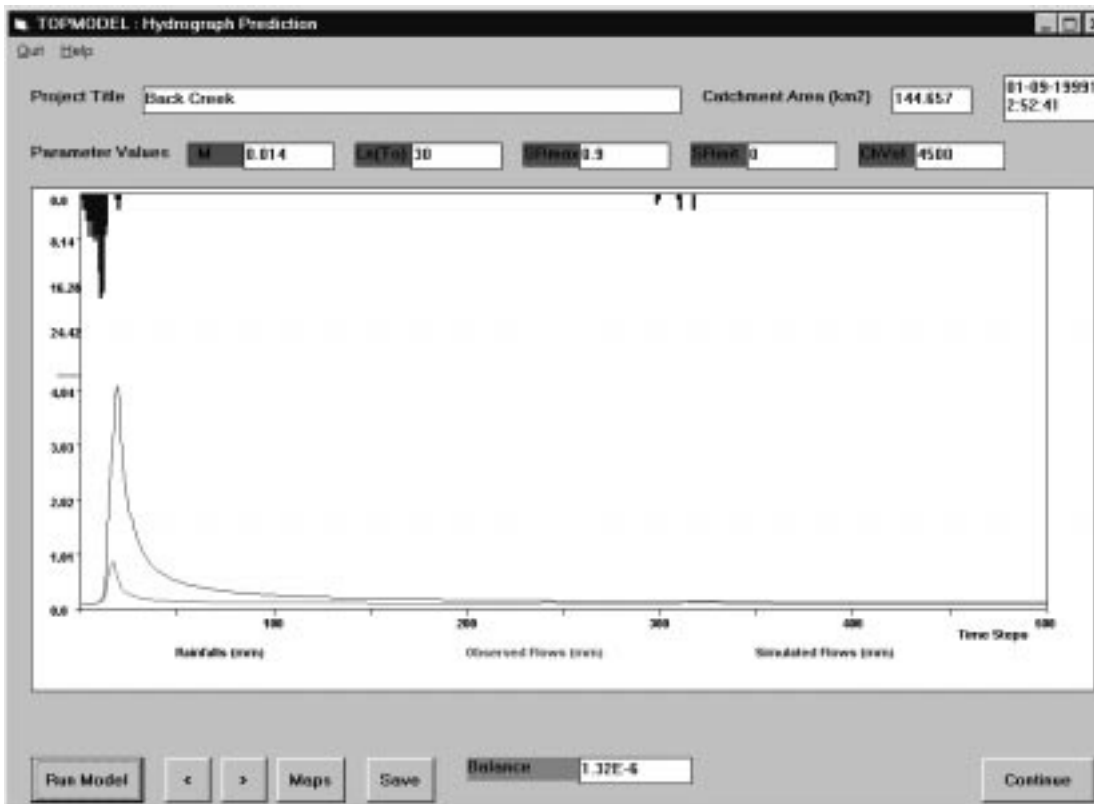


Figure 24 (b). August 1996 event; TOPMODEL event based simulation.

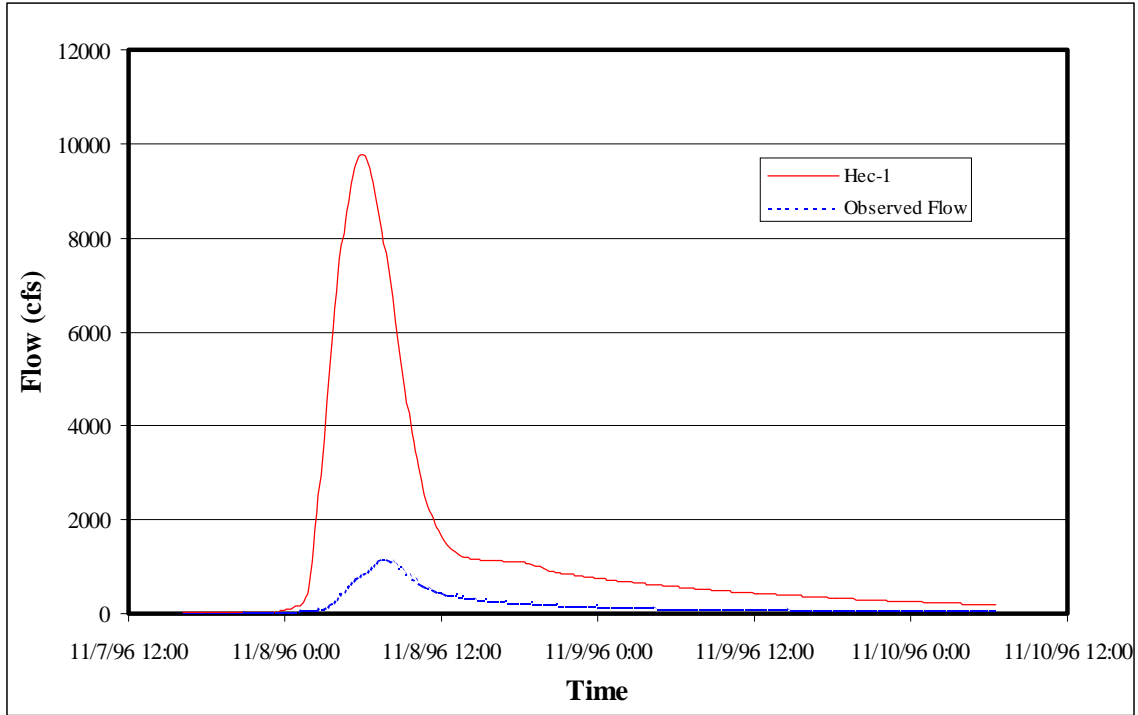


Figure 24 (c). August 1996 event; HEC-1 event based simulation.

Table 7. Comparison of continuous and event based simulation peak flows.

Event	HEC-1 Event Based (cfs)	TOPMODEL Event Based (cfs) [mm/hr]	TOPMODE L Continuous (cfs) [mm/hr]	Observed (cfs)	Relative Error HEC-1	Relative Error TOPMODE L Event Based	Relative Error TOPMODE L Continuous
Aug-96	9767	5817 [4.10]	270 [0.19]	1166	7.377	3.989	-0.768
Nov-96	1231	3575 [2.52]	1262 [0.89]	921	0.337	2.882	0.371

As mentioned previously in Section 5.1.5, the November 1996 event was also modeled by TOPMODEL using both a continuous and an event based simulation. Figures 25 (a), (b), and (c) contain the resulting hydrographs generated by TOPMODEL and HEC-1, and Table 7 compares the peak flows from each simulation. The dry period prior to the November event was not as long as that prior to the August event, and as a result, the peak flows for the event based and continuous simulations are not as vastly different.

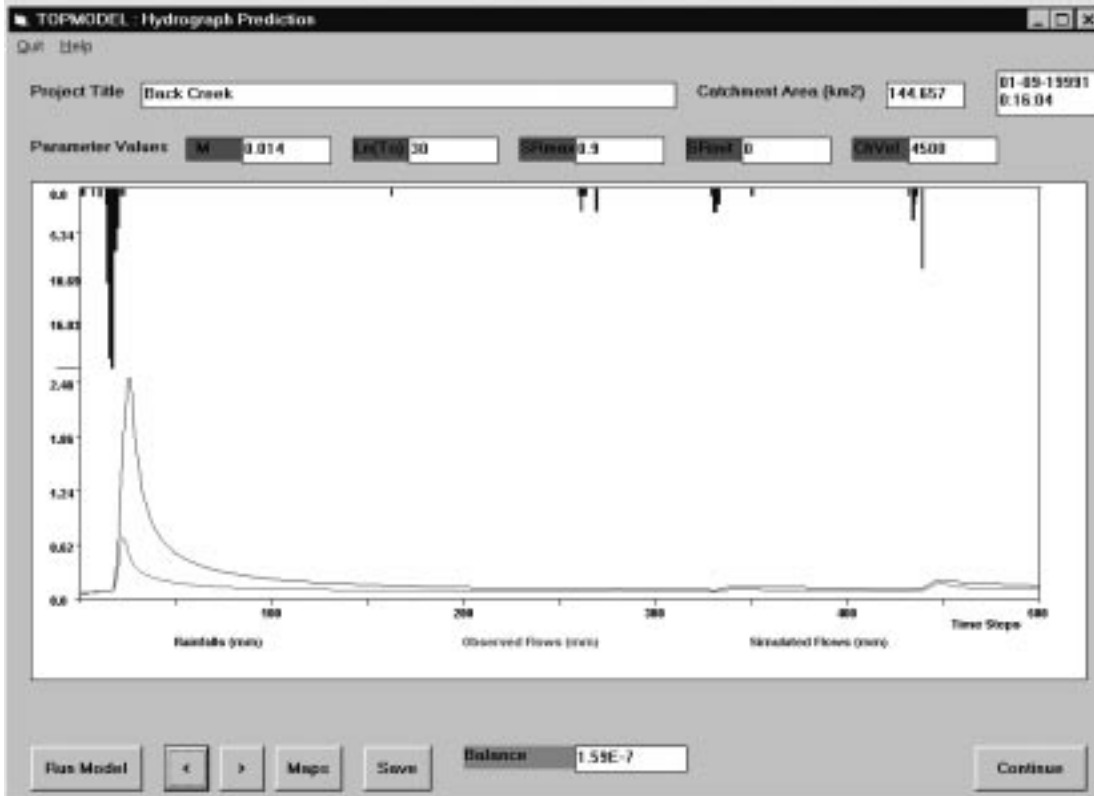


Figure 25 (a). November 1996 event; TOPMODEL event based simulation.

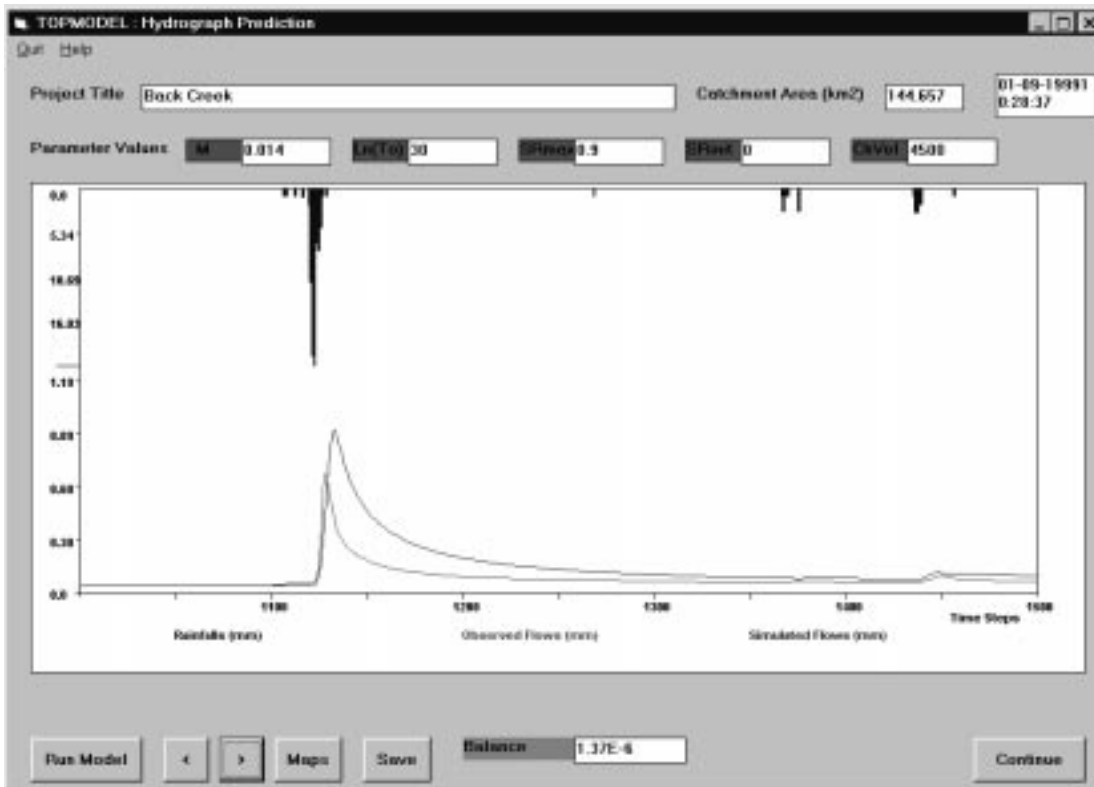


Figure 25 (b). November 1996 event; TOPMODEL continuous simulation.

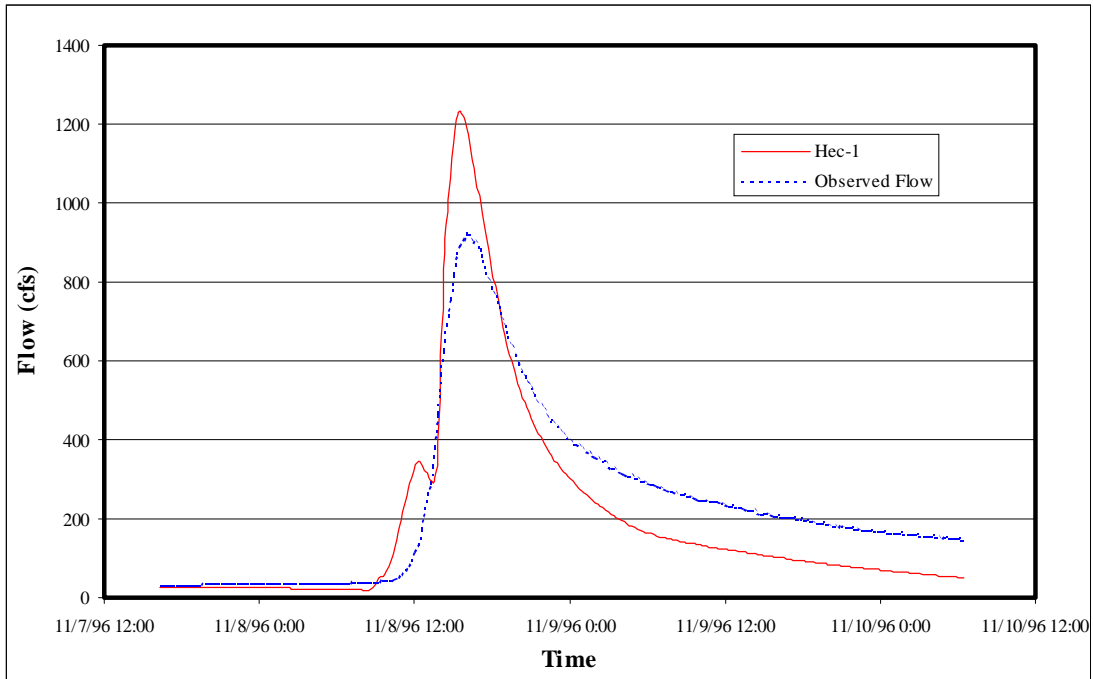


Figure 25 (c). November 1996 event; HEC-1 simulation.

# 6 Summary, Conclusions, and Future Research

## 6.1 Summary

In this study, two hydrologic models were applied to the Back Creek watershed. The two models were HEC-1, an event based lumped model, and TOPMODEL, a continuous semi-distributed model. These models were used to investigate (a) the issue of spatial scale in hydrologic modeling, and (b) two approaches to modeling, continuous versus event based.

To begin the investigation into the effect of spatial scale, two HEC-1 models were developed with a different number of subareas in each. The hydrographs generated by each HEC-1 model for a number of large rainfall events were analyzed visually and statistically.

Then, TOPMODEL was applied to the same watershed using a series of different size grid cells. The first step in applying TOPMODEL to a watershed involves GIS analysis. ArcView was used to manipulate and prepare DEMs for use in the GRIDATB program which calculates the topographic index distribution for TOPMODEL. The GRIDATB program, as downloaded from the TOPMODEL web site, is written to accommodate only small watersheds (hillslope scale). The program was edited in order to accommodate larger watersheds with relatively small grid cell sizes. The hydrographs generated by TOPMODEL with each grid cell size were compared in order to assess the sensitivity of hydrographs produced by TOPMODEL to grid cell size. Analyses were also performed to determine the sensitivity of TOPMODEL hydrographs to several model parameters. Observations were made on what effects changing each parameter had on the shape of the simulated hydrograph, peak flow, runoff volume, and time to peak.

The modeling performances of the event based HEC-1 and the continuous TOPMODEL were analyzed and compared visually and statistically for the large storms modeled by HEC-1. TOPMODEL was also executed as an event based model for two single events and the resulting hydrographs were compared to the HEC-1 and continuous TOPMODEL results.

A significant original contribution of this study was the application of TOPMODEL to a catchment larger than the program was designed to model. Another contribution was to develop a procedure for delineating watersheds from USGS DEMs using ArcView. An investigation was also performed to determine the effect of each TOPMODEL parameter on the simulated hydrograph. Finally, the dependence of TOPMODEL parameters and hydrograph simulation on grid cell size was determined.

## 6.2 Conclusions

No observable improvement resulted from increasing the number of subareas in the HEC-1 models from 20 to 81. Slight differences exist in the hydrographs produced from the two HEC-1 models, but generally, the models performed similarly.

An increase in grid cell size from 15 to 120 meters resulted in increased values of the mean of the topographic index. However, hydrographs generated by TOPMODEL were completely unaffected by this increase in the topographic index. TOPMODEL is very insensitive to the shape of the topographic index distribution as well as to positive shifts in the distribution. In fact, a positive shift of about 30 in the distribution of the topographic index was required to produce an observable change in the model hydrograph response. This seems to render useless the process of obtaining and manipulating DEMs and generating the topographic index distribution using GRIDATB. This could be an advantage for TOPMODEL users in that watersheds could be modeled with only knowledge of the total watershed area, the required routing table, initial values for the five parameters, and a topographic index distribution from another watershed. Of course, evapotranspiration, rainfall data, and observed streamflow data would still have to be provided by the user.

It was determined that the parameters that had the greatest effect on hydrographs generated by TOPMODEL were the  $m$  and  $\ln(T_o)$  parameters. Optimal values for these parameters were difficult to determine and were somewhat different for most storms. The  $ChVel$  parameters also had a large effect on the simulated hydrographs, but an optimal value was quickly determined by matching the rising limb of the observed and simulated hydrographs. The routing procedure (discussed in Section 5.1.4) lumps overland and

channel flow together and uses this *ChVel* parameter to route this surface runoff to the outlet. The *SRmax* and *SRinit* parameters had less significant effects on the simulated hydrographs. Because varying grid cell size from 15 to 120 meters had no effect on the simulated hydrograph, the five parameters mentioned above need not be adjusted as grid cell size changes. Therefore, it can be said that the model parameters are independent of grid cell size.

The limited number of storms used to compare HEC-1 and TOPMODEL makes it difficult to determine definitively which model simulates large storms better. It does appear that perhaps HEC-1 is slightly superior in that regard. It can be stated more definitively that both HEC-1 and TOPMODEL, when used as a continuous model, simulate large storms better than TOPMODEL, when used as an event based model.

TOPMODEL was developed for use on small, hillslope scale catchments. It is evident from this study that some assumptions and procedures in TOPMODEL which may be appropriate for small catchments may not be appropriate for the Back Creek watershed. Rainfall data was available for four rain gages in the proximity of Back Creek; however, TOPMODEL is capable of receiving data from only one gage. In addition, TOPMODEL uses a simple linear surface routing equation as opposed to a raster grid based method to route rainfall excess. The linear routing method may perform adequately for small catchments, but a more sophisticated method is appropriate for larger catchments such as the Back Creek watershed.

### **6.3 Future Research**

A major limitation of TOPMODEL, especially when applied to watersheds larger than about 10 square miles, is its inability to use spatially varied rainfall distributions for a single watershed. Precipitation distributions and totals vary a great deal spatially as well as temporally. A version of TOPMODEL which utilizes gridded precipitation or unique precipitation for each subcatchment could improve simulation accuracy. Further simulation improvement could result from incorporating a raster based routing method to route rainfall excess through a catchment, grid cell by grid cell. Such a routing procedure

could route runoff as either overland or channel flow based on the flow accumulation at each grid cell.

The above changes to TOPMODEL would require the program to adopt a distributed, raster based structure as opposed to the lumped structure currently employed. This raster based structure would make it possible for individual grid cells to contain unique values for soil characteristics such as  $m$  and  $\ln(T_o)$ . A raster based structure would enable TOPMODEL to be used on very large basins with complex routing, diverse soil conditions, and spatially variable rainfall.

# References

- Anderson, M.G. and Burt, T.P. 1985. Modelling strategies. In *Hydrological Forecasting*. eds. Anderson, M.G. and Burt, T.P. New York: John Wiley & Sons.
- Bedient, P.B. and Huber, W.C. 1992. *Hydrology and Floodplain Analysis*. 2<sup>nd</sup> edition. New York: Addison-Wesley Publishing Company.
- Beven, K. *TOPMODEL Users Notes. Windows Version 97.01*.
- Beven, K. *TOPMODEL. Windows Version 97.01*. Computer software.
- Beven, K. 1989. Changing ideas in hydrology—The case of physically-based models. *Journal of Hydrology*. 105: 157-172.
- Beven, K. and Kirkby, M.J. 1979. A physically-based variable contributing area model of basin hydrology. *Hydrological Sciences Bulletin*. 24: 43-69.
- Beven, K.J., Kirkby, M.J., Schofield, N., and Tagg, A.F. 1984. Testing a physically-based flood forecasting model (TOPMODEL) for three U.K. catchments. *Journal of Hydrology*. 69: 119-143.
- Beven, K.J., Lamb, R., Quinn, P., Romanowicz, R., and Freer, J. 1995. TOPMODEL. In *Computer Models of Watershed Hydrology*, ed. Vijay P. Singh. Colorado: Water Resources Publications. pp. 627-668.
- Beven, K., Quinn, P., Romanowicz, R., Freer, J., Fisher, J., and Lamb, R. TOPMODEL and GRIDATB, A users guide to the distribution versions (95.02). CRES Technical Report TR110 (2nd Edition).
- Bloschl, G. and Sivapalan, M. 1995. Scale issues in hydrological modelling: A review. In *Scale Issues in Hydrological Modelling*. eds. Kalma, J.D. and Sivapalan, M. Chichester: John Wiley & Sons. pp. 9-48.
- Burges, S.J. 1997. Streamflow Prediction -- Capabilities, Opportunities, and Challenges. *Water Science and Technology Board Colloquium on Hydrologic Sciences*. National Academy of Sciences, Washington DC.
- Crawford, N.H. and Lindsey, R.K. 1966. *Digital Simulation in Hydrology, Stanford Watershed Model IV*. Technical Report 39, Civil Engineering Department, Stanford University, California.
- Dewberry and Davis. 1998. *Dewberry and Davis Stormwater Management Project*.

- Dooge, J.C.I. 1977. Problems and methods of rainfall-runoff modelling. In *Mathematical Methods for Surface Water Hydrology*. eds. Ciriani, T.A., Maione, U., and Wallis, J.R. Chichester: Wiley. pp. 71-108.
- ESRI, Environmental Systems Research Institute, Inc. 1996a. *Arcview GIS, Version 3.1*. Computer software. California.
- ESRI, Environmental Systems Research Institute, Inc. 1996b. *Arcview Spatial Analyst, Version 1.1*. Computer software. California.
- Finnerty, B.D., Smith, M.B., Seo, D.J., Koren, V., and Moglen, G.E. 1997. Space-time scale sensitivity of the Sacramento model to radar-gage precipitation inputs. *Journal of Hydrology*. 203: 21-38.
- Franchini, M., Wendling, J., Obled, C., and Todini, E. 1996. Physical interpretation and sensitivity analysis of the TOPMODEL. *Journal of Hydrology*. 175: 293-338.
- Gupta, V.K., Rodriguez-Iturbe, I., and Wood, E.F. 1986. Preface. In *Scale Problems in Hydrology*. Dordrecht: D. Reidel Publishing Company. pp. vii-viii.
- Holko, L. and Lepisto, A. 1997. Modelling the hydrological behaviour of a mountain catchment using TOPMODEL. *Journal of Hydrology*. 196: 316-377.
- Iorgulescu, I. and Jordan, J.P. 1994. Validation of TOPMODEL on a small Swiss catchment. *Journal of Hydrology*. 159: 255-273.
- Kilgore, J. 1997. *Development and Evaluation of a GIS-Based Spatially Distributed Unit Hydrograph Model*. MS BSE Thesis.
- Kirkby, M.J. 1976. Hydrograph modelling strategies. *Processes in Physical and Human Geography*. Edited by R. Peel, M. Chrisholm, and P. Haggett. London: Academic.
- Klemes, V. 1983. Conceptualisation and scale in hydrology. *Journal of Hydrology*. 65:1-23.
- Maidment, D.R. 1993. GIS and hydrologic modeling. In *Environmental Modeling with GIS*. eds. Goodchild, M.F., Parks, B.O., Steyaert, L. New York: Oxford University Press.
- McDonnell, R.A. 1996. Including the spatial dimension: Using geographical information systems in hydrology. *Prog. Physical Geography*. 20(2): 159-177.
- Mulvaney, T.J. 1851. On the use of self-registering rain and flood gauges in making observations of the relations of rainfall and of flood discharges in a given catchment. *Transactions of the Institution of Civil Engineers, Ireland*. 4(2): 18.

- Nash, J.E. and Sutcliffe, J.V. 1970. River flow forecasting through conceptual models, 1, A discussion of principles. *Journal of Hydrology*. 10: 282-290.
- O'Connell, P.E. 1991. A historical perspective. In *Recent Advances in the Modeling of Hydrologic Systems*. Kluwer, Dordrecht. pp. 3-30.
- Pilgrim, D.H., Cordery, I., and Baron, B.C. 1982. Effects of catchment size on runoff relationship. *Journal of Hydrology*. 58: 205-221.
- Quinn, P.F., Beven, K.J., and Lamb, R. 1995. The  $\ln(a/\tan\beta)$  index: How to calculate it and how to use it within the TOPMODEL framework. *Hydrological Processes*. 9: 161-182.
- Roberson, J.A. and Cowe, C.T. 1995. *Engineering Fluid Mechanics*. 5<sup>th</sup> Edition. New York: John Wiley & Sons, Inc.
- Robson, A.J., Whitehead, P.G., and Johnson, R.C. 1993. An application of a physically based semi-distributed model to the Balquhider catchments. *Journal of Hydrology*. 145: 357-370.
- Saulnier, G. and Beven, K., and Obled, C. 1997. Digital elevation analysis for distributed hydrological modeling: Reducing scale dependence in effective hydraulic conductivity values. *Water Resources Research*. 33(9): 2097-2101.
- Sherman, L. K. 1932. Streamflow from rainfall by unit-graph method. *Engineering News Record*. 108: 501-505.
- Singh, V.P. 1995. Watershed Modeling. In *Computer Models of Watershed Hydrology*. ed. Singh, V.P. Colorado: Water Resources Publications. pp. 1-22.
- Sivapalan, M. and Kalma, J.D. 1995. Scale problems in hydrology: Contributions of the Robertson Workshop. In *Scale Issues in Hydrological Modelling*. eds. Kalma, J.D. and Sivapalan, M. Chichester: John Wiley & Sons. pp. 1-8.
- Soil Conservation Service. 1986. *Urban Hydrology for Small Watersheds*. 2<sup>nd</sup> edition. Technical Release No. 55. Washington D.C. U.S. Department of Agriculture.
- Sorooshian, S. and Gupta, V.K. 1983. Automatic calibration of conceptual rainfall-runoff models: The question of parameter observability and uniqueness. *Water Resources Research*. 19:260-268.
- Sorooshian, S. and Gupta, V.K. 1995. Model Calibration. In *Computer Models of Watershed Hydrology*, ed. Vijay P. Singh. Colorado: Water Resources Publications. pp. 23-68.

- Todini, E. 1988. Rainfall-runoff modelling—past, present, and future. *Journal of Hydrology*. 100: 341- 352.
- US Army Corps of Engineers, Hydrologic Engineering Center. 1990. *HEC-1 Flood Hydrograph Package, Users Manual*.
- Walpole, R.E. and Myers, R.H. 1993. *Probability and Statistics for Engineers and Scientists. Fifth Edition*. New York: Macmillan Publishing Company. pp. 84 - 93.
- Wilson, J.P., GIS-based Land Surface/Subsurface Modeling: New Potential for New Models. [http://www.ncgia.ucsb.edu/conf/SANTA\\_FE\\_CD-ROM/sf\\_papers/wilson\\_john/wilson.html](http://www.ncgia.ucsb.edu/conf/SANTA_FE_CD-ROM/sf_papers/wilson_john/wilson.html)
- Wolock, D.M. 1995. Effects of subbasin size on topographic characteristics and simulated flow paths in Sleepers River watershed, Vermont. *Water Resources Research*. 31(8): 1989-1997.
- Wolock, D.M. and Price, C.V. 1994. Effects of digital elevation model map scale and data resolution on a topography-based watershed model. *Water Resources Research*. 30(11): 3041-3052.
- Zhang, W. and Montgomery, D.R. 1994. Digital elevation model grid size, landscape representation, and hydrological simulations. *Water Resources Research*. 30(4): 1019-1028.

# Appendix A

## TOPMODEL Instructions

This appendix contains sample files and instructions on how to use TOPMODEL. Several preparatory procedures must be performed before executing the TOPMODEL program. Digital Elevation Models (DEMs) must be obtained and then manipulated in a GIS program such as ArcView. Instructions on how to use ArcView are contained in Appendix D. The raster file output by ArcView is used as input to the GRIDATB file which calculates the topographic index for each grid cell. GRIDATB, which can be downloaded from the TOPMODEL web site, then divides all of the topographic index values from every grid cell in the watershed into 29 regular intervals. This tabular distribution of the decimal fraction of the total area in each topographic index interval is the only topographic input to TOPMODEL. GRIDATB generates two output files. Examples and descriptions of these files can be found in Appendix B.

Four input files must be constructed before the TOPMODEL program will execute. The first file is called the Project file which must be constructed for each catchment to be modeled. This file contains only the four following lines:

1. Text description of application (i.e. Back Creek).
2. Catchment Data filename (i.e. \$catparm.dat).
3. Hydrological Input Data filename (i.e. \$inpt.dat).
4. Topographic Index Map filename (i.e. \$map.dat ) (may be left blank, but line must exist).

A sample of a Project file, *back.prj*, appears in italics below:

*Back Creek*  
*\$catparm.dat*  
*\$inpt.dat*  
*\$map.dat*

A Catchment Data file contains a tabular distribution of the percent of total area contained in each topographic index interval. This information is generated by the GRIDATB program and can be copied directly from the output file. See Appendix B for more detail. The file also includes a table containing the percent of the total catchment area downstream of the corresponding distance from the catchment outlet along the main channel. At the end of the file is a value for each of the five parameters and a range of values for each parameter to be used in the Parameter Sensitivity Analysis. An example of a Catchment Data file, *\$catparm.dat*, appears in italics below:

<i>Back Creek Catchment</i>	Descriptive Title
<i>29 144.657</i>	No. of topographic index intervals. Total watershed area.
<i>.00000 13.32344</i>	
<i>.00002 12.90506</i>	
<i>.00004 12.48667</i>	
<i>.00010 12.06829</i>	
<i>.00023 11.64991</i>	
<i>.00048 11.23153</i>	
<i>.00101 10.81315</i>	
<i>.00189 10.39477</i>	
<i>.00339 9.97639</i>	
<i>.00576 9.55801</i>	
<i>.00924 9.13963</i>	
<i>.01424 8.72125</i>	
<i>.02181 8.30287</i>	
<i>.03213 7.88449</i>	Tabular distribution of the topographic index.
<i>.04523 7.46611</i>	
<i>.06231 7.04773</i>	
<i>.08356 6.62935</i>	
<i>.10001 6.21097</i>	
<i>.11585 5.79258</i>	
<i>.12396 5.37420</i>	
<i>.11647 4.95582</i>	

<i>.09730</i>	<i>4.53744</i>		
<i>.07191</i>	<i>4.11906</i>		
<i>.04957</i>	<i>3.70068</i>		
<i>.02787</i>	<i>3.28230</i>		
<i>.01222</i>	<i>2.86392</i>		
<i>.00297</i>	<i>2.44554</i>		
<i>.00040</i>	<i>2.02716</i>		
<i>.00002</i>	<i>1.60878</i>		
9			No. of routing intervals.
<i>0.0</i>	<i>0.0</i>		Routing data.
<i>0.143497</i>	<i>6014.</i>		
<i>0.196014</i>	<i>9551.</i>		
<i>0.328499</i>	<i>12677.</i>		
<i>0.462917</i>	<i>17724.</i>		
<i>0.526787</i>	<i>20656.</i>		
<i>0.6527</i>	<i>24542.</i>		
<i>0.802589</i>	<i>25963.</i>		
<i>1.0</i>	<i>33192.</i>		
<i>0.014</i>	<i>0.002</i>	<i>0.05</i>	m parameter
<i>30.0</i>	<i>10.0</i>	<i>40.0</i>	ln(To) parameter
<i>0.90</i>	<i>0.01</i>	<i>0.1</i>	SRmax parameter
<i>0.00</i>	<i>0.0</i>	<i>0.1</i>	SRinit parameter
<i>4500.</i>	<i>500.</i>	<i>5000.</i>	ChVel parameter

The Hydrological Input Data file contains the number of time steps and the duration of a time step in the first line of the file. The file also contains three columns of data. The columns from left to right are: incremental rain, evapotranspiration, and discharge rate per unit area. The units of each column are meters per hour. An example of a Catchment Data file, *\$catparm.dat*, appears in italics below:




<i>20</i>	<i>1</i>		
<i>0.00000000</i>	<i>0.00045705</i>	<i>0.00000839</i>	
<i>0.00000000</i>	<i>0.00043386</i>	<i>0.00000839</i>	
<i>0.00000000</i>	<i>0.00038605</i>	<i>0.00000839</i>	
<i>0.00000000</i>	<i>0.00031631</i>	<i>0.00000839</i>	
<i>0.00000000</i>	<i>0.00022862</i>	<i>0.00000839</i>	
<i>0.00000000</i>	<i>0.00012794</i>	<i>0.00000839</i>	
<i>0.00000000</i>	<i>0.00000000</i>	<i>0.00000839</i>	
<i>0.00000000</i>	<i>0.00000000</i>	<i>0.00000787</i>	
<i>0.00000000</i>	<i>0.00000000</i>	<i>0.00000787</i>	
<i>0.00000000</i>	<i>0.00000000</i>	<i>0.00000787</i>	
<i>0.00000000</i>	<i>0.00000000</i>	<i>0.00000787</i>	



<i>0.01582357</i>	<i>0.00000000</i>	<i>0.00000787</i>
<i>0.01385107</i>	<i>0.00000000</i>	<i>0.00001042</i>
<i>0.00469032</i>	<i>0.00000000</i>	<i>0.00001314</i>
<i>0.00000000</i>	<i>0.00000000</i>	<i>0.00001427</i>
<i>0.00000000</i>	<i>0.00000000</i>	<i>0.00001874</i>
<i>0.00000000</i>	<i>0.00000000</i>	<i>0.00002259</i>
<i>0.00000000</i>	<i>0.00001083</i>	<i>0.00002755</i>
<i>0.00000000</i>	<i>0.00010269</i>	<i>0.00002755</i>
<i>0.00000000</i>	<i>0.00020566</i>	<i>0.00002786</i>



The format of the Topographic Index Map file is identical to the input file and output map file for the GRIDATB program except that it is limited to a grid size of 100 by 100 cells. A program named GRIDREDU, which can be downloaded with TOPMODEL, can reduce the size of the grid by a reducing factor, N, specified by the user. The program selects every N<sup>th</sup> cell in the matrix in both the x and y directions and creates a new, smaller file with these selected topographic index values. This file is used only for display purposes, so using the GRIDREDU program has no effect on the model simulation. An example of a Topographic Index Map file, *\$map.dat*, appears in italics below:

*The Creek, 15 meter grid cell size*

<i>8</i>	<i>5</i>	<i>15.0</i>						
<i>9999.0</i>	<i>9999.0</i>	<i>9999.0</i>	<i>4.3170</i>	<i>5.0098</i>	<i>9999.0</i>	<i>9999.0</i>	<i>9999.0</i>	<i>9999.0</i>
<i>9999.0</i>	<i>4.8281</i>	<i>5.3282</i>	<i>5.7823</i>	<i>6.2066</i>	<i>6.7918</i>	<i>6.5069</i>	<i>9999.0</i>	<i>9999.0</i>
<i>4.7226</i>	<i>6.1201</i>	<i>6.7986</i>	<i>7.2200</i>	<i>7.5275</i>	<i>8.7725</i>	<i>9.0801</i>	<i>7.6257</i>	
<i>9999.0</i>	<i>4.0939</i>	<i>4.5060</i>	<i>4.1991</i>	<i>4.5391</i>	<i>5.3408</i>	<i>9999.0</i>	<i>9999.0</i>	<i>9999.0</i>
<i>9999.0</i>	<i>9999.0</i>	<i>9999.0</i>	<i>4.1625</i>	<i>9999.0</i>	<i>9999.0</i>	<i>9999.0</i>	<i>9999.0</i>	<i>9999.0</i>

Once the three files above have been generated, the TOPMODEL program may be started by executing the *Topmodel.exe* file. From the first window, select *Load Project*. Double click on the name of the project file (i.e. *back.prj*), ensure that the names of the other input files are correct, and click on . Select *Hydrograph Simulation* and click on . To run the model, click on . The parameters can be adjusted by changing their values displayed above the hydrograph and precipitation window. TOPMODEL can perform simulations with up to 2500 time steps,

but can only displays 500 time steps at a time. To scroll between 500 time step intervals, click on the  and  buttons.

To utilize TOPMODEL's parameter sensitivity capability, select  to exit the *Hydrograph Prediction* window. Select *Parameter Sensitivity Plots* and click on . Check the box beside each parameter to be investigated. These parameters require three values which must be provided by the user, a *Current Value* (this value is used when generating sensitivity plots for other parameters) and a *Minimum Value* and a *Maximum Value* for the sensitivity plot. The output is a plot of model efficiency versus parameter value. This analysis option can be used to aid in determining optimum parameter values for model calibration.

# Appendix B

## Sample GRIDATB Files

This appendix contains a small example grid file which is used as input to GRIDATB. The example file below in italics can be generated by ArcView with slight modifications (see Appendix D). The first line is a descriptive title. The second line contains the number of columns, the number of rows, and the grid cell size. The elevation corresponding to each grid cell in the matrix begins on the third line. GRIDATB uses a default elevation of 9999, this indicates that the grid cell is not in the watershed of interest.

*The Creek, 15 meter grid cell size*

```

8 5 15
9999 9999 9999 1008 1006 9999 9999 9999
9999 1010 1008 1006 1004 1002 1001 9999
1012 1009 1007 1005 1003 1001 1000 999
9999 1012 1010 1009 1006 1003 9999 9999
9999 9999 9999 1012 9999 9999 9999 9999

```

The *ditn* file created by GRIDATB for the above example is shown in italics below. The file contains a list of sinks or boundary cells and a tabular distribution of the topographic index. The first column in the table is the percent of the total area within the interval boundaries listed in the right column.

*The Creek, 15 meter grid cell size*

```

SINK OR BOUNDARY NODE AT 8 3

NUMBER OF ITERATIONS REQUIRED FOR A/TANB CALCS 3
NUMBER OF SINK NODES 1
29
.00 9.08015
.04545 8.90207

```

.04545	8.72399
.00	8.54591
.00	8.36782
.00	8.18974
.00	8.01166
.00	7.83358
.00	7.65550
.09091	7.47742
.00	7.29934
.04545	7.12125
.00	6.94317
.09091	6.76509
.00	6.58701
.04545	6.40893
.00	6.23085
.09091	6.05277
.00	5.87469
.04545	5.69660
.00	5.51852
.04545	5.34044
.04545	5.16236
.04545	4.98428
.04545	4.80620
.04545	4.62812
.09091	4.45004
.04545	4.27195
.13636	4.09387

The map file created by GRIDATB for the above example is shown in italics below. The file is a raster grid of the topographic index value in each grid cell.

*The Creek, 15 meter grid cell size*

8	5	15.0					
9999.0	9999.0	9999.0	4.3170	5.0098	9999.0	9999.0	9999.0
9999.0	4.8281	5.3282	5.7823	6.2066	6.7918	6.5069	9999.0
4.7226	6.1201	6.7986	7.2200	7.5275	8.7725	9.0801	7.6257
9999.0	4.0939	4.5060	4.1991	4.5391	5.3408	9999.0	9999.0
9999.0	9999.0	9999.0	4.1625	9999.0	9999.0	9999.0	9999.0

# Appendix C

## GRIDATB Source FORTRAN Code

```
C*****
C GRIDATB
C PROGRAM TO CALCULATE A/TANB VALUES FROM GRIDDED ELEVATION DATA
C
C VERSION 95.01
C for MS-DOS PC with EGA graphics and maths co-processor
C
C Compiled using Lahey Fortran77 and Grafmatic Graphics
C
C
C Originally written by Keith Beven 1983, revised for distribution
C 1993,1995
C*****
C This program is distributed freely with only two conditions.
C
C 1. In any use for commercial or paid consultancy purposes a
C suitable royalty agreement must be negotiated with Lancaster
C University (Contact Keith Beven)
C
C 2. In any publication arising from use for research purposes the
C source of the program should be properly acknowledged and a
C pre-print of the publication sent to Keith Beven at the address
C below.
C
C All rights retained 1993
C Keith Beven
C Centre for Research on Environmental Systems and Statistics
C Institute of Environmental and Biological Sciences
C Lancaster University, Lancaster LA1 4YQ, UK
C
C Tel: (+44) 1524 593892 Fax: (+44) 1524 593985
C Email: K.Beven@UK.AC.LANCASTER
C
C This program was modified by Ryan Fedak, rfedak@vt.edu
C*****
*
*
CHARACTER ELEVFILE*10,ATBFILE*10,MAPFILE*10
CHARACTER*80 TITLE
COMMON/MAP/NX,NY,E(1710,1710),ATB(1710,1710),A(1710,1710)
DIMENSION AC(30),ST(30),Y(30)
*
Write(6,1002)
1002 Format(////,1x,'GRIDATB Version: 95.01'////////
1 1x,'Centre for Research on Environmental Systems and Statistics'/
```

```

2 1x,'Lancaster University, Lancaster LA1 4YQ, UK'/////
  Write(6,602)
602  format(/1x,'          Press return to continue'/)
  Read(5,*)
* Read in and open data files
  WRITE(6,*)('The data in the elevation file should be in meters.')
  WRITE(6,*)('Type single quotes around all file names.')
  WRITE(6,610)
610  Format(1x,'Input name of raw elevation file : ')
  READ (5,*) ELEVFILE
  write(*,*) elevfile
  WRITE(6,611)
611  Format(1x,'Input name of output ln(a/tanB) map file : ')
  READ(5,*)MAPFILE
  WRITE(6,612)
612  Format(1x,'Input name of output and ln(a/tanB) ditn file : ')
  READ(5,*)ATBFILE
  OPEN(4,file=elevfile,status='old',err = 499)
  OPEN(7,file=mapfile)
  OPEN(8,file=atbfile)
*
* READ IN ELEVATION DATA
  READ(4,"(A)")TITLE
  READ(4,*)Nx,Ny,DX
  DX=DX*0.00000001
  Write(7,700)title
  Write(8,700)title
700  format(A)
  Write(7,701)Nx,Ny,Dx
701  format(2i6,f6.1)

  DO 9 J=1,NY
*
* READS ELEVATIONS BY ROWS STARTING FROM BOTTOM LEFT HAND CORNER
  READ(4,*)(E(I,J),I=1,NX)
  9  CONTINUE
* 400 FORMAT(2I6,F6.1)
* 401 FORMAT(8F10.1)
*
* SET ALL NON-CATCHMENT A/TANB VALUES TO 99999 (elevation) AND ALL
* CATCHMENT VALUES TO -9.9. SET ALL A VALUES TO DX*DX
  NATB=0
  DO 10 I=1,Nx
  DO 10 J=1,Ny
  A(I,J)=DX*DX
  IF(E(I,J).GE.9999.)THEN
    NATB=NATB+1
    ATB(I,J)=E(I,J)
  ELSE
    ATB(I,J)=-9.9
  ENDIF
10  CONTINUE
*

```

```

*
* CALCULATE A/TANB VALUES FOR CATCHMENT GRID SQUARES
  CALL ATANB(DX,NATB)
*
* Calculate ATANB histogram for use in TOPMODEL
  NAC = 29
* find limits
  atbmax = 0.
  atbmin = 9999.

  do 20 i=1,nx
  do 20 j=1,ny
  if(atb(i,j).lt.9999.)then
    if(atb(i,j).gt.atbmax)atbmax = atb(i,j)
    if(atb(i,j).lt.atbmin)atbmin = atb(i,j)
  endif
  20 continue
c
  datb = (atbmax-atbmin)/(NAC-1)
c
c Initialise histogram count
  do 15 i = 1,NAC
  15 y(i) = 0.
c
  total = 0.
  do 30 i=1,nx
  do 30 j=1,ny
  if(atb(i,j).lt.9999.)then
    index = int((atb(i,j)-atbmin)/datb)+1
    if(index.gt.nac-1)index=nac-1
    y(index)=y(index)+1
    total = total + 1
  endif
  30 continue
*
  ac(1)=0.
  st(1)=atbmax
  do 40 i=2,nac
  ac(i)= y(nac-i+1)/total
  st(i)=atbmax-(i-1)*datb
  40 continue
  write(8,800)nac
  800 format(i6)
  Write(8,801)(AC(i),ST(i),i=1,NAC)
  801 format(2f10.5)
*
  STOP
  499 write(6,604)
  604 format(1x'*****'/
  1 1x,'Input Elevation File does not exist -'/
  2 1x,' Failing gracefully!'/
  3 1x,'*****'/)

```

```

STOP
END
*
*
SUBROUTINE ATANB(DX,NATB)
COMMON/MAP/NX,NY,E(1710,1710),ATB(1710,1710),A(1710,1710)
DIMENSION ROUTE(9),TANB(9)
*
DX2=1/(1.414*DX)
DX1=1/DX
NSINK=0
ITER=0
Write(6,698)
698 Format(1x,'Subroutine ATB - counting iterations.....')
*
50 CONTINUE
ITER=ITER+1
Write(6,699)iter
699 format(i8)
*
* LOOP THROUGH GRID SQUARES...CHECK IF THERE IS AN UPSLOPE ELEMENT THAT
* DOES NOT HAVE AN ATANB VALUE.....IF SO, THEN CANNOT CARRY OUT ELEMENT
* CALCULATIONS. CONTINUE ITERATIONS UNTIL NATB=NX*NY
*
DO 10 I=1,NX
DO 10 J=1,NY
*
*
* SKIP NON-CATCHMENT GRID SQUARES
IF(E(I,J).GE.9999.)GO TO 10
*
* SKIP SQUARES ALREADY DONE
Write(6,*)ATB
IF(ATB(I,J).GT.-9.)GO TO 10
*
* CHECK THE 8 POSSIBLE FLOW DIRECTIONS FOR UPSLOPE ELEMENTS WITHOUT
* AN ATANB VALUE
Write (6,*)('c')
IF(I-1.GE.1)THEN
IF(J-1.GE.1)THEN
IF(E(I-1,J-1).GT.E(I,J).AND.ATB(I-1,J-1).LT.0.)GO TO 10
ENDIF
IF(E(I-1,J).GT.E(I,J).AND.ATB(I-1,J).LT.0.)GO TO 10
IF(J+1.LE.NY)THEN
IF(E(I-1,J+1).GT.E(I,J).AND.ATB(I-1,J+1).LT.0.)GO TO 10
ENDIF
ENDIF
IF(J-1.GE.1.)THEN
IF(E(I,J-1).GT.E(I,J).AND.ATB(I,J-1).LT.0.)GO TO 10
ENDIF
IF(J+1.LE.NY)THEN
IF(E(I,J+1).GT.E(I,J).AND.ATB(I,J+1).LT.0.)GO TO 10
ENDIF
ENDIF
IF(I+1.LE.NX)THEN

```

```

IF(J-1.GE.1)THEN
  IF(E(I+1,J-1).GT.E(I,J).AND.ATB(I+1,J-1).LT.0.)GO TO 10
ENDIF
IF(E(I+1,J).GT.E(I,J).AND.ATB(I+1,J).LT.0.)GO TO 10
IF(J+1.LE.NY)THEN
  IF(E(I+1,J+1).GT.E(I,J).AND.ATB(I+1,J+1).LT.0.)GO TO 10
ENDIF
ENDIF
*
* THERE ARE NO UPSLOPE ELEMENTS WITHOUT AN A/TANB VALUE.....START
* CALCULATIONS USING CURRENT VALUE OF A
*
* FIND THE OUTFLOW DIRECTIONS AND CALCULATE THE SUM OF WEIGHTS USING
* (TANB *CONTOUR LENGTH) WHERE CONTOUR LENGTH IS 0.5*DX FOR CARDINAL
* DIRECTIONS AND 0.354*DX FOR DIAGONAL DIRECTIONS
*
SUM=0.
DO 12 K=1,9
12 ROUTE(K)=0.
NROUT=0
IF(I-1.GE.1)THEN
  IF(J-1.GE.1)THEN
    IF(E(I-1,J-1).LT.E(I,J))THEN
      TANB(1)=(E(I,J)-E(I-1,J-1))*DX2
      ROUTE(1)=0.354*DX*TANB(1)
      SUM=SUM+ROUTE(1)
      NROUT=NROUT+1
    ENDIF
  ENDIF
  IF(E(I-1,J).LT.E(I,J))THEN
    TANB(2)=(E(I,J)-E(I-1,J))*DX1
    ROUTE(2)=0.5*DX*TANB(2)
    SUM=SUM+ROUTE(2)
    NROUT=NROUT+1
  ENDIF
  IF(J+1.LE.NY)THEN
    IF(E(I-1,J+1).LT.E(I,J))THEN
      TANB(3)=(E(I,J)-E(I-1,J+1))*DX2
      ROUTE(3)=0.354*DX*TANB(3)
      SUM=SUM+ROUTE(3)
      NROUT=NROUT+1
    ENDIF
  ENDIF
ENDIF
IF(J-1.GE.1)THEN
  IF(E(I,J-1).LT.E(I,J))THEN
    TANB(4)=(E(I,J)-E(I,J-1))*DX1
    ROUTE(4)=0.5*DX*TANB(4)
    SUM=SUM+ROUTE(4)
    NROUT=NROUT+1
  ENDIF
ENDIF
IF(J+1.LE.NY)THEN
  IF(E(I,J+1).LT.E(I,J))THEN

```

```

        TANB(6)=(E(I,J)-E(I,J+1))*DX1
        ROUTE(6)=0.5*DX*TANB(6)
        SUM=SUM+ROUTE(6)
        NROUT=NROUT+1
    ENDIF
ENDIF
IF(I+1.LE.NX)THEN
    IF(J-1.GE.1)THEN
        IF(E(I+1,J-1).LT.E(I,J))THEN
            TANB(7)=(E(I,J)-E(I+1,J-1))*DX2
            ROUTE(7)=0.354*DX*TANB(7)
            SUM=SUM+ROUTE(7)
            NROUT=NROUT+1
        ENDIF
    ENDIF
    IF(E(I+1,J).LT.E(I,J))THEN
        TANB(8)=(E(I,J)-E(I+1,J))*DX1
        ROUTE(8)=0.5*DX*TANB(8)
        SUM=SUM+ROUTE(8)
        NROUT=NROUT+1
    ENDIF
    IF(J+1.LE.NY)THEN
        IF(E(I+1,J+1).LT.E(I,J))THEN
            TANB(9)=(E(I,J)-E(I+1,J+1))*DX2
            ROUTE(9)=0.354*DX*TANB(9)
            SUM=SUM+ROUTE(9)
            NROUT=NROUT+1
        ENDIF
    ENDIF
ENDIF
IF(NROUT.EQ.0)THEN
*
* NO DOWNSLOPE DIRECTION MUST BE AN INTERNAL SINK OR AN OUTFLOW NODE ON
* THE BOUNDARY
    WRITE(8,601)I,J
601  FORMAT(1X,'SINK OR BOUNDARY NODE AT',2I6)
    NSINK=NSINK+1
C
* ASSUME THAT THERE IS A CHANNEL OF LENGTH DX RUNNING MIDWAY THROUGH
* THE SINK OR BOUNDARY NODE. TAKE AVERAGE INFLOW SLOPE ANGLE TO REPRES
* TANB AND A/(2DX) TO REPRESENT a.
    SUMTB=0.
    NSLP=0.
    IF(I-1.GE.1)THEN
        IF(J-1.GE.1)THEN
            IF(E(I-1,J-1).LT.9999.)THEN
                SUMTB=SUMTB+(E(I-1,J-1)-E(I,J))*DX2
                NSLP=NSLP+1
            ENDIF
        ENDIF
        IF(E(I-1,J).LT.9999.)THEN
            SUMTB=SUMTB+(E(I-1,J)-E(I,J))*DX1
            NSLP=NSLP+1
        ENDIF
    ENDIF

```

```

IF(J+1.LE.NY)THEN
  IF(E(I-1,J+1).LT.9999.)THEN
    SUMTB=SUMTB+(E(I-1,J+1)-E(I,J))*DX2
    NSLP=NSLP+1
  ENDIF
ENDIF
ENDIF
IF(J-1.GE.1)THEN
  IF(E(I,J-1).LT.9999.)THEN
    SUMTB=SUMTB+(E(I,J-1)-E(I,J))*DX1
    NSLP=NSLP+1
  ENDIF
ENDIF
IF(J+1.LE.NY)THEN
  IF(E(I,J+1).LT.9999.)THEN
    SUMTB=SUMTB+(E(I,J+1)-E(I,J))*DX1
    NSLP=NSLP+1
  ENDIF
ENDIF
IF(I+1.LE.NX)THEN
  IF(J-1.GE.1)THEN
    IF(E(I+1,J-1).LT.9999.)THEN
      SUMTB=SUMTB+(E(I+1,J-1)-E(I,J))*DX2
      NSLP=NSLP+1
    ENDIF
  ENDIF
  IF(E(I+1,J).LT.9999.)THEN
    SUMTB=SUMTB+(E(I+1,J)-E(I,J))*DX1
    NSLP=NSLP+1
  ENDIF
  IF(J+1.LE.NY)THEN
    IF(E(I+1,J+1).LT.9999.)THEN
      SUMTB=SUMTB+(E(I+1,J+1)-E(I,J))*DX2
      NSLP=NSLP+1
    ENDIF
  ENDIF
ENDIF
*
* CALCULATE AVERAGE INFLOW SLOPE ANGLE
SUMTB=SUMTB/NSLP
IF(SUMTB.GT.0.000001)THEN
  ATB(I,J)=A(I,J)/(2*DX*SUMTB)
  ATB(I,J)=ALOG(ATB(I,J)) + ALOG(10000000000000000.)
ELSE
  ATB(I,J)=9999.9
ENDIF
NATB=NATB+1
* THESE NODES ARE IGNORED IN ATANB CALCULATIONS
GO TO 10
ENDIF
*
* CALCULATE WEIGHTED AVERAGE A/TANB VALUE
*

```

```

* NB. This formulation uses contour length distance weights for the
* cardinal directions of 0.5 and for the diagonal directions of
* 0.354. The upslope flow area is distributed in the downslope
* flow directions proportionally to tanb(i)*cld(i) where cld is
* the contour length distance, so that:
*   A = A1 + A2 + A3 ....downslope directions only
*   = C * ( tanb(1)*cld(1) + tanb(2)*cld(2) ....)
* or C = A / sum of (tanb(i)*cld(i))
* and A1 = A * C * tanb(1) * cld(1)
*   A2 = A * C * tanb(2) * cld(2) etc
* To calculate a/tanb for this grid square a value of tanb is
* calculated based on the same distance weights so that
* tanb = sum of (tanb(i)*cld(i)) / sum of (cld(i))
*   (...downslope directions only...)
* then the value of a/tanb for this square will be
* ATB = A / (sum of (cld(i)) * tanb)
*   = A / (sum of (tanb(i)*cld(i))
*   = C
*   C=(A(I,J)/SUM)
*   ATB(I,J)=ALOG(C) + ALOG(100000000000000000.)
*   NATB=NATB+1
*   IF(I-1.GE.1)THEN
*     IF(J-1.GE.1)A(I-1,J-1)=A(I-1,J-1)+C*ROUTE(1)
*     A(I-1,J)=A(I-1,J)+C*ROUTE(2)
*     IF(J+1.LE.NY)A(I-1,J+1)=A(I-1,J+1)+C*ROUTE(3)
*   ENDIF
*   IF(J-1.GE.1)A(I,J-1)=A(I,J-1)+C*ROUTE(4)
*   IF(J+1.LE.NY)A(I,J+1)=A(I,J+1)+C*ROUTE(6)
*   IF(I+1.LE.NX)THEN
*     IF(J-1.GE.1)A(I+1,J-1)=A(I+1,J-1)+C*ROUTE(7)
*     A(I+1,J)=A(I+1,J)+C*ROUTE(8)
*     IF(J+1.LE.NY)A(I+1,J+1)=A(I+1,J+1)+C*ROUTE(9)
*   ENDIF
10  CONTINUE
    IF(NATB.LT.NX*NY)GO TO 50
    DO 20 J=1,NY
      WRITE(7,701)(ATB(I,J),I=1,NX)
20  CONTINUE
701  FORMAT(8F10.4)
      WRITE(8,602)ITER,NSINK
602  FORMAT(///1X,'NUMBER OF ITERATIONS REQUIRED FOR A/TANB CALCS',I6/
1  1X,'NUMBER OF SINK NODES',I6)
      RETURN
      END

```

# Appendix D

## ArcView Instructions

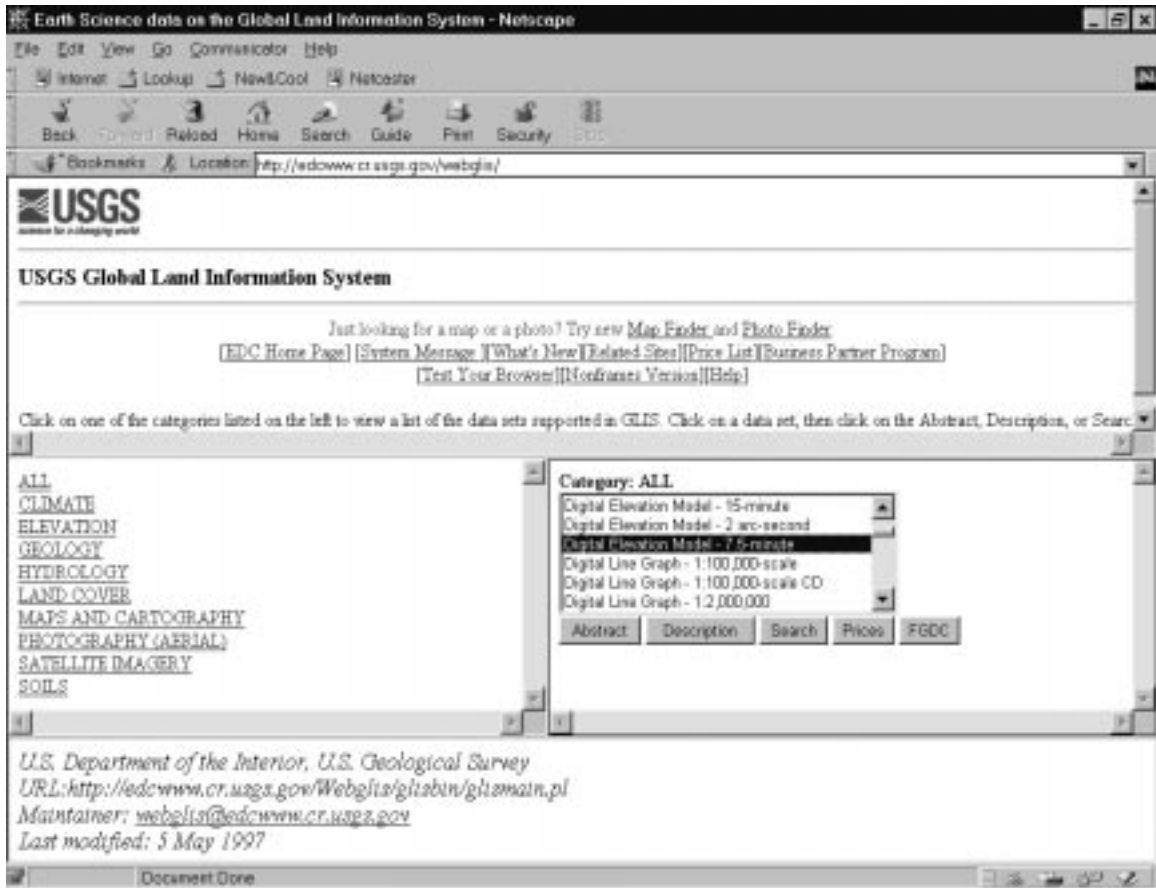
The following set of instructions should enable the reader to duplicate the work performed in ArcView for this study. The instructions could also be used to import and manipulate other DEMs. The ArcView windows shown in this appendix were taken from the computer program referenced by ESRI (1996).

### Table of Contents

1. Basic ArcView Terms Defined .....	100
2. Downloading a SDTS/DEM file from the USGS home page .....	100
3. Unzipping a SDTS/DEM file.....	102
4. Converting from SDTS/DEM format to DEM format.....	103
5. Adding Extensions to ArcView .....	104
6. Activating the Extensions in ArcView .....	104
7. Importing a DEM file into ArcView .....	106
8. Viewing a theme .....	107
9. Editing or customizing a legend.....	107
10. Converting dimensions of DEMs from feet to meters .....	107
11. Combining several DEMs using the Mosaic function.....	108
12. Delineating a watershed.....	110
13. Creating a theme containing only the watershed.....	119
14. Extracting a rectangle containing the watershed.....	122
15. Changing the value of grid cells outside the watershed from 9999 to <i>No data</i> .....	124
16. Changing grid cell size.....	126
17. Exporting data for use in TOPMODEL.....	127

## 1. **Basic ArcView Terms Defined**

- 1.1 **Theme-** A layer of data, such as a Digital Elevation Model (DEM) or a network of streams which can be manipulated and viewed independently.
  - 1.2 **Shape Theme-** An abstract class that defines the behavior of a geometric shape. Subclasses of shape define specific geometry. All shape geometry is planar, not spherical.
  - 1.3 **Grid Themes-** The GRID format is a proprietary ESRI format that supports 32-bit integer and 32-bit floating-point raster grids. Grids are especially suited to representing geographic phenomena that vary continuously over space, and for performing spatial modeling and analysis of flows, trends, and surfaces such as hydrology. DEMs are imported as grid themes which have a grid cell size specified in the DEM (usually 30 meters). Each grid cell contains one integer value which represents the elevation in that grid cell. Most DEMs will have a portion of a border of grid cells that contain no data; this results from small errors when the USGS generated the DEMs.
2. Downloading a SDTS/DEM file from the USGS home page (the USGS sometimes refers to a Digital Elevation Model, DEM, as a SDTS/DEM file or simply a SDTS file).
    - 2.1 Go to: <http://edcwww.cr.usgs.gov/webglis/> shown below.



- 2.2 Scroll down through the *Category: ALL* box and highlight *Digital Elevation Model – 7½ -minute*. Click on the *Search* button.
- 2.3 Click on *State Name*.
- 2.4 Click on *Virginia*.
- 2.5 Click on the name of the 7.5-minute Digital Elevation Model you want to download. The four DEMs containing a portion of the Back Creek Watershed are Bent Mountain, Elliston, Garden City, and Hardy.
- 2.6 Click on the file name (i.e. 30.1.1.1119778.tar.gz). If there is more than one file, select the most recent file.
- 2.7 Select *Save it to disk* and click on *OK*.
- 2.8 Select the directory in which you want to save the file. It may be advantageous to create a separate directory for each SDTS/DEM file being downloaded.
- 2.9 Click on *Save*.

2.10 Exit the internet and open a browser program, usually *File Manager* or *Windows Explorer*.

3. Unzipping a SDTS/DEM file.

3.1 Go to the directory where the SDTS/DEM file is saved.

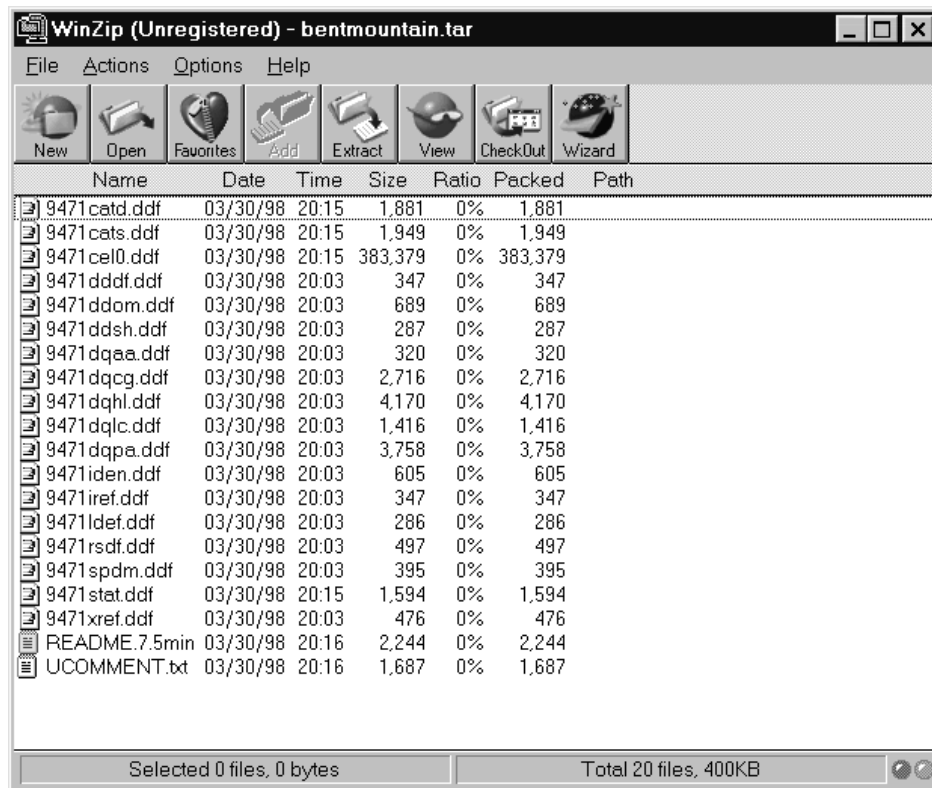
3.2 The SDTS/DEM file is compressed with a utility called *gzip* which creates a file with a *.gz* extension. Depending on how your web browser is configured you might have to uncompress the file yourself.

3.3 If more than one file (the names should contain eight characters including a mixture of numbers and letters) appears in your browser window, your browser was probably able to unzip the file automatically.

3.4 If only one file (with a *.gz* extension) appears in your browser, unzip the file.

3.4.1 To use *Winzip*, first change the file name to an eight character name with the extension *.tgz* (i.e. *Bentmoun.tgz*).

3.4.2 Double click on the file name, click on *Yes* if a dialogue box asks if you would like to decompress the file. *Winzip* should display several files with the *.ddf* extension, shown below.



3.4.3 Click on the *Extract* icon. Select the same directory in which you downloaded the SDTS/DEM file. Click on *Extract*. Close *Winzip*.

3.4.4 There should now be several *.ddf* files in the same directory in which you downloaded the SDTS/DEM file.

#### 4. Converting from SDTS/DEM format to DEM format.

4.1 Download *sdt2dem.exe* (a program that converts *.ddf* files to *.dem* files) from <ftp://www.blm.gov/pub/gis/sdts/dem/>

4.2 Copy the file *sdt2dem.exe* to the directory containing the unzipped *.ddf* files.

4.3 Execute *sdt2dem.exe* by double clicking on it.

4.4 Follow the instructions in the program. (Note: The cell file is the largest file.

The characters in the 7 and 8 positions are probably “10”, that the lower case letter “L” and zero.)

4.5 When the program has completed, there should be a file with the extension *.dem* that can be imported into ArcView.

5. Adding Extensions to ArcView.

5.1 The *Spatial Analyst 1.1* extension is required to perform watershed delineation and many other necessary functions. This extension may be purchased from the ESRI home page. Install *Spatial Analyst 1.1* on your computer following the instructions during setup and the instructions in the *Readme.txt* file. When you have finished, there should be a file named *Spatial.avx* in the directory

`\Esri\Av_gis30\ArcView\Ext32`.

5.2 Go to <http://andes.esri.com/arcscripts/beginsearch.cfm?psw=ArcView+3%2Ex>.

5.3 Download the extension named *Spatial Tools* into the directory

`\Esri\Av_gis30\ArcView\Ext32`.

5.4 Unzip the file *spatialtools.zip* and export the unzipped file *spatialtools.avx* into the same directory.

5.5 Obtain the Watershed Delineator extension from the TNRCC, Texas Natural Resource Conservation Commission, web site (<http://www.tnrcc.texas.gov/>) or request it via email from either Dr. Dean Djokic <ddjokic@esri.com> at ESRI or Dr. Randy Dymond <dymond@vt.edu>. Copy the *WshdDel.avx* file into the directory `\Esri\Av_gis30\ArcView\Ext32`.

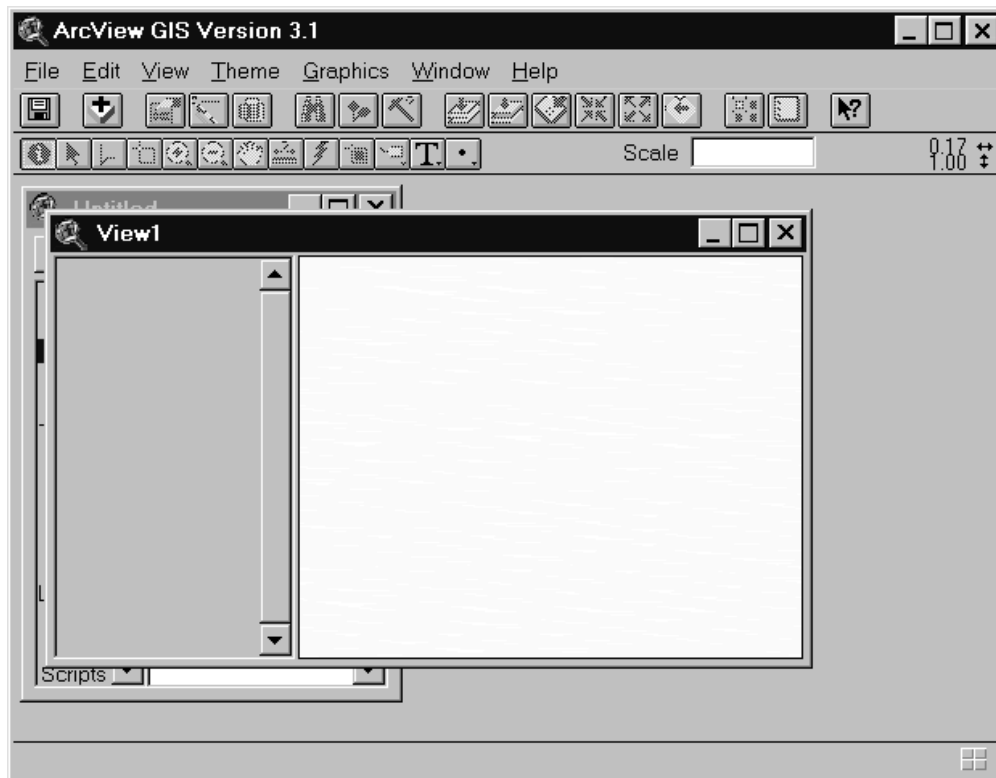
6. Activating the Extensions in ArcView.

6.1 Start *ArcView*.

6.2 Select *as a blank project* to begin a new project (as shown below).



- 6.3 Highlight the *Views* icon and click on *New* just above the icon. A *View 1* window should open up (as shown below).

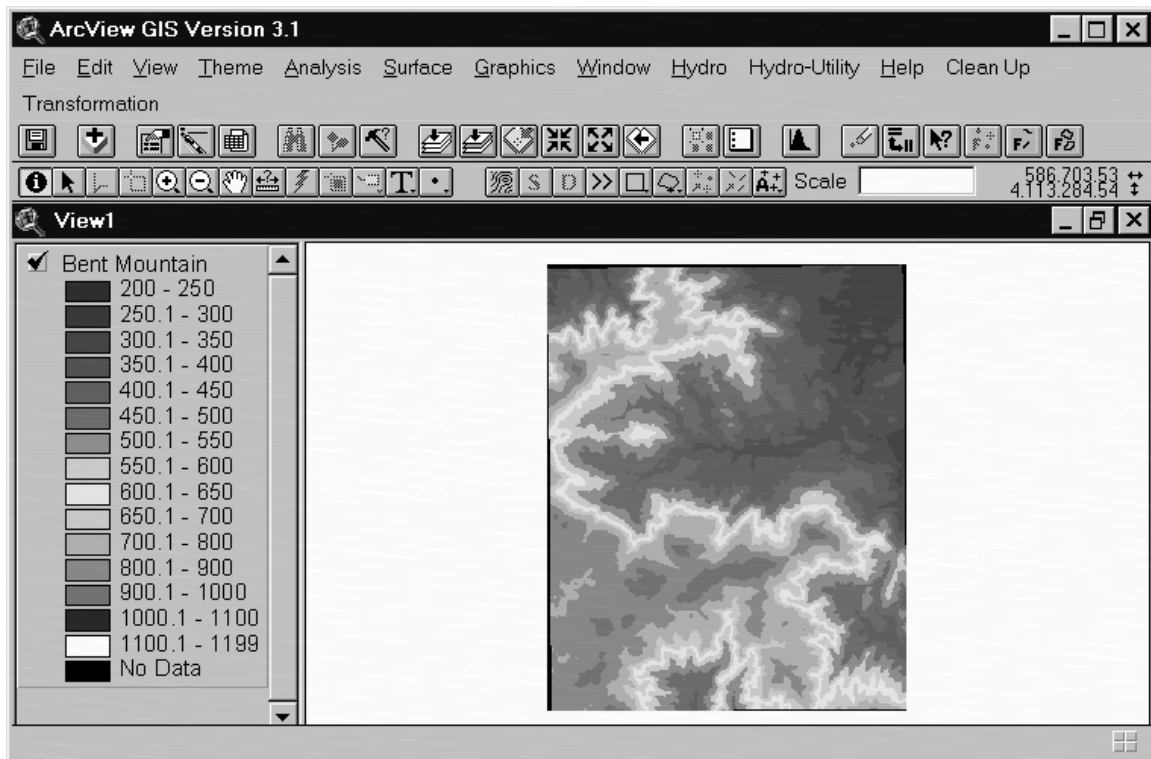


- 6.4 Under the *File* menu select *Set Working Directory*. Type in the path of the directory in which to store data. It may be advantageous to use a directory (which you may have to create) with the path  
`\Esri\Av_gis30\ArcView\Work\Tmp`. Caution: after working for a while in ArcView, this directory may accumulate a large amount of stored data (perhaps 100 megabytes or more). Ensure that you have sufficient hard drive space on your computer.
- 6.5 To activate the extensions, go to the *File* menu and select *Extensions*. Click in the boxes beside *Spatial Analyst*, *Spatial Tools*, and *Watershed Delineator*. Click on *OK*. Additional menus should now be available.

7. Importing a DEM file into ArcView.

7.1 To begin to import a DEM file, go to the *File* menu and select *Import Data Source*.

7.2 Select *USGS DEM* and click *OK*. Go to the directory where the DEM file was downloaded from the USGS. Select the desired DEM file and click *OK*. Ensure that the highlighted directory is the correct directory for data storage. Change the *Grid Name* to a meaningful name. Click on *OK*. Click on *Yes* when asked *Add grid as theme to the View?* ArcView will add a theme to the current view containing the data from the DEM. (A theme is a set of geographic features in a view. A theme represents a source of geographic data such as USGS DEMs.) To view the imported DEM as shown below, click in the box next to the theme name (i.e. Bent Mountain).

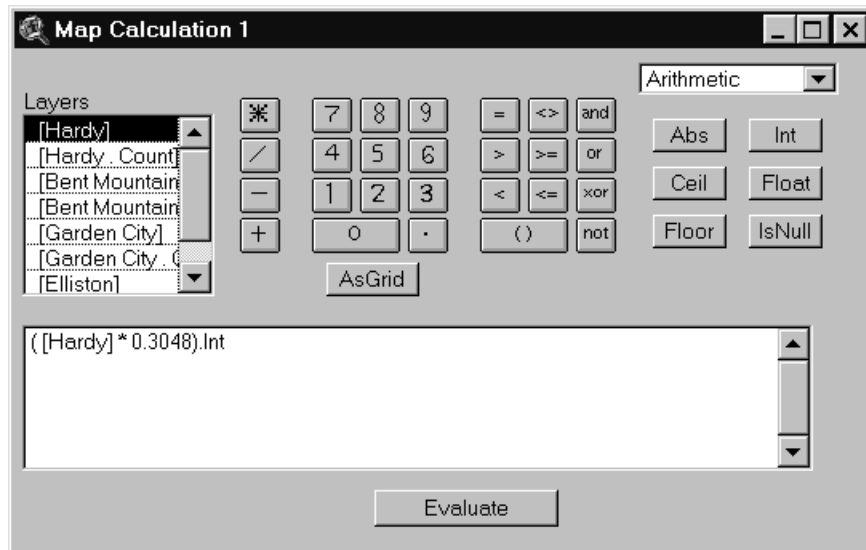


7.3 To import another DEM file into ArcView, repeat the steps: *Downloading a SDTS/DEM file from the USGS home page, Unzipping a SDTS/DEM file,*

*Converting from SDTS/DEM format to DEM format, and Importing a DEM into ARCVIEW.* A new theme is created for each DEM imported. A DEM file contains information which enables ArcView to accurately position a DEM relative to other DEMs. If the watershed of interest spans more than one DEM, import each DEM file containing a portion of the watershed. The four DEMs will be positioned in a horizontal row.

8. To view a theme, click in the box next to the theme name. To zoom in or out or to view the full extent of all of the themes, go to the *View* menu and select the appropriate option.
9. Editing or customizing a legend.
  - 9.1 Under the *Themes* select *Edit Legend*.
  - 9.2 To change a color, double click on the colored box in the *Symbol* column and select or create a new color.
  - 9.3 To change the range of values which correspond to a color, click on the range to be change in the *Value* column and type in the new range.
  - 9.4 Once a legend has been constructed that provides a good view of the themes, save the legend by clicking on save and entering a name for the file.
10. Converting the dimensions of DEMs from feet to meters. The USGS may have the Hardy DEM only in feet. The majority of the DEMs are in meters, and all DEMs must be in the same units.
  - 10.1 After importing the Hardy DEM into ArcView, it must be converted to meters.
  - 10.2 Under the *Analysis* menu, select *Map Calculator*.
    - 10.2.1 Find the window labeled *Layers*. Double click on the Hardy DEM layer.

The title of the Hardy DEM theme will appear in the lower calculation box.
    - 10.2.2 Click on the “\*” button and on the “0.3048” buttons. Push the right arrow key on the keyboard to get outside the parentheses.
    - 10.2.3 Go to the box in the top right corner and change the setting from *Logarithms* to *Arithmetic*. Click on the *Int* button. See window below.
    - 10.2.4 Click *Evaluate* and close the *Map Calculator* window. This will output a grid labeled *Map Calculation 1* with dimensions in meters as integers.



10.3 Highlight the theme labeled *Map Calculation 1* by clicking on the name of the theme.

10.4 Under the *Theme* menu, select *Convert to Grid*. Enter a name for the output theme (i.e. Hardyinmeters). This will change the status of the theme from temporary to permanent.

11. To combine several DEMs, use the Mosaic function.

11.1 Because the Back Creek Watershed spans more than one DEM theme, it is necessary to mosaic the themes together into one theme. Before proceeding, ensure that all of the required DEMs are imported into the ArcView.

11.2 To mosaic themes, go to the *Transformation* menu and select *Mosaic*. Select one of the themes to be mosaiced as the first grid theme. For this study, the four themes that need to be mosaiced together are Bent Mountain, Elliston, Garden City, and the Hardy theme that has been changed to meters. (It doesn't matter which theme is selected.) Click *OK*. Follow the instructions to select the rest of the themes to be mosaiced.

11.3 Often the borders of no data around the grid cells are too large to be filled in by the mosaic routine. Several individual cells of no data may exist where the seams between the themes used to be. To fill in these cells of no data, the *Boundary*

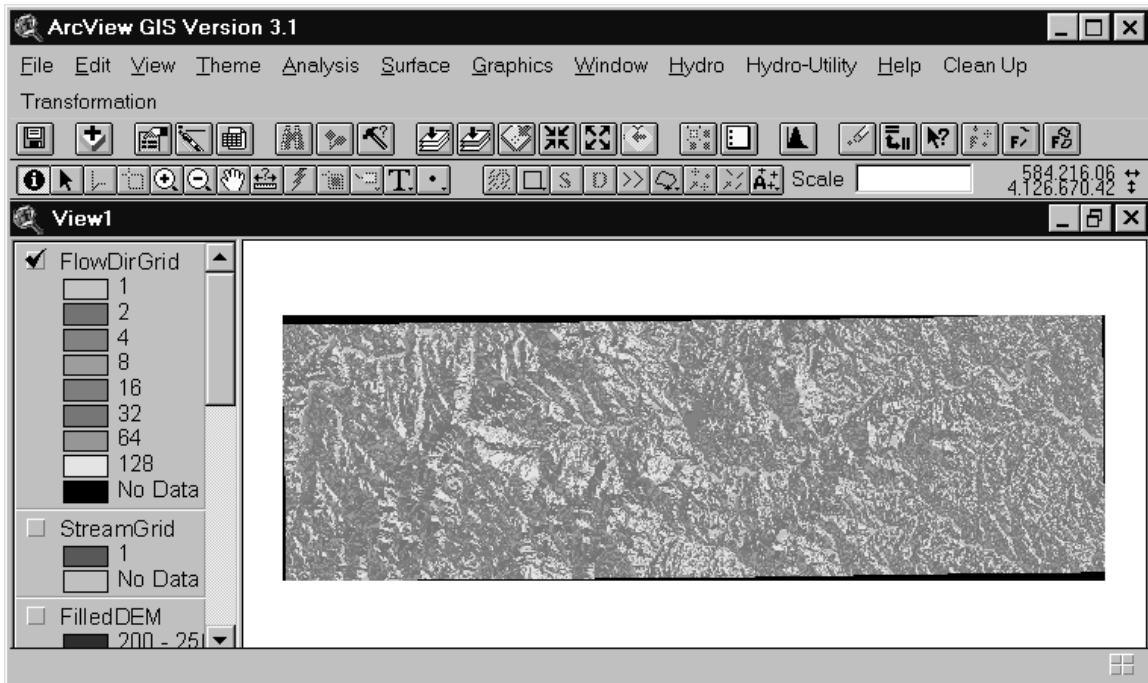
*Clean* routine must be performed. Highlight the theme entitled *Mosaiced grids of...* Under the *Clean Up* menu, select *Boundary Clean*. Click on the *OK* button in the next two windows.

11.4 Highlight the output theme from the *Boundary Clean* function. It should be the top theme in the menu and should be named *Grid#*. Under the *Theme* menu, select *Properties*. The top row in the window contains the *Theme Name*. Change the theme name to *RawDEM*.

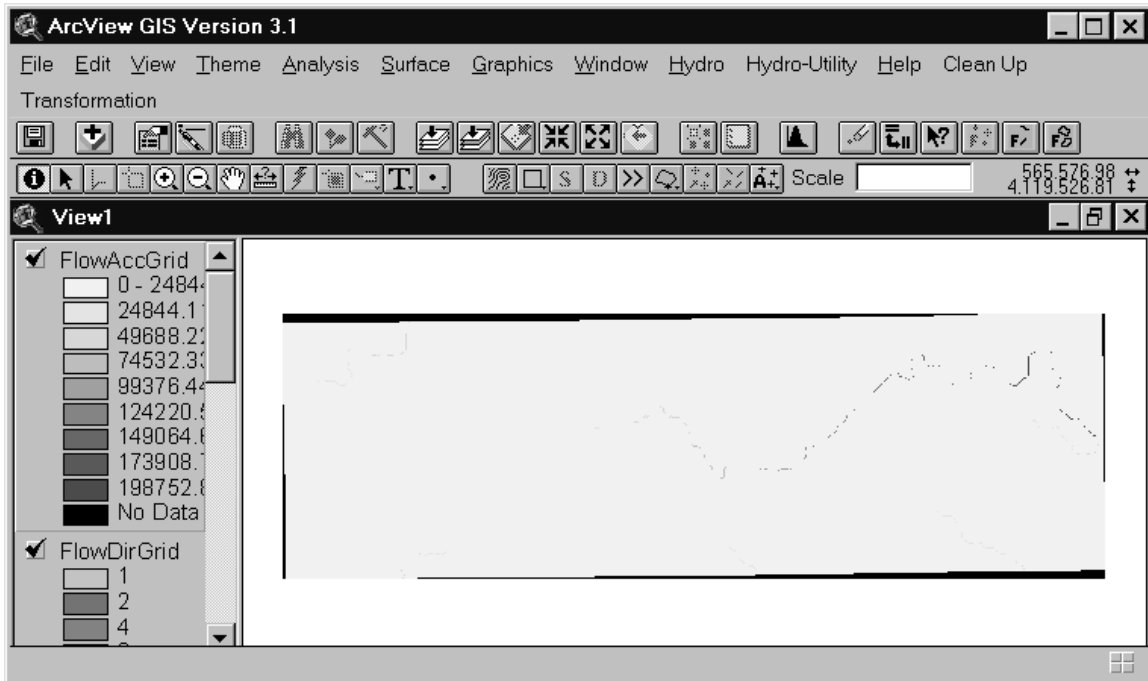
12. Delineate a watershed. Several preliminary functions must be performed before a watershed can be delineated.

12.1 Under the *Hydro* menu, select *Fill Sinks*. Enter the input theme, *RawDEM* and the output theme, *FilledDEM*. Click on *OK*. This will fill in any low spots in the DEM in which water would collect and have no where to flow.

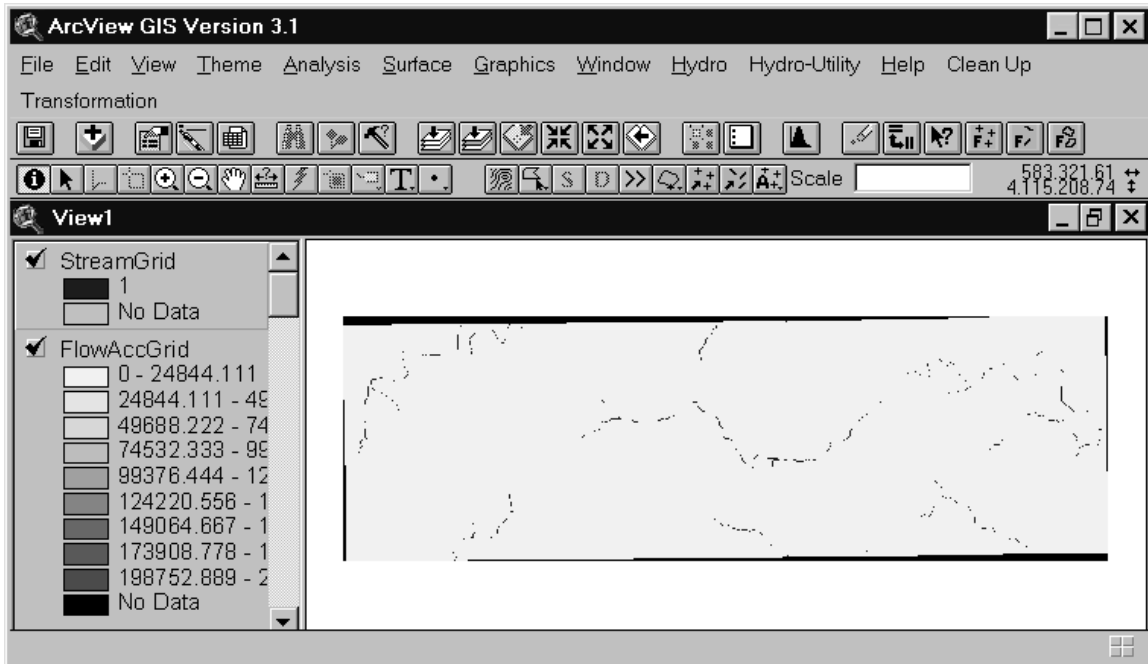
12.2 Under the *Hydro* menu, select *Flow Direction*. Enter the input theme, *FilledDEM* and the output theme, *FlowDirGrid*. Click on *OK*. Click on *OK* to accept *10000*. Click in the box beside the *FlowDirGrid* theme to activate the theme. As shown below, this grid contains information about which direction water will flow across the land surface.



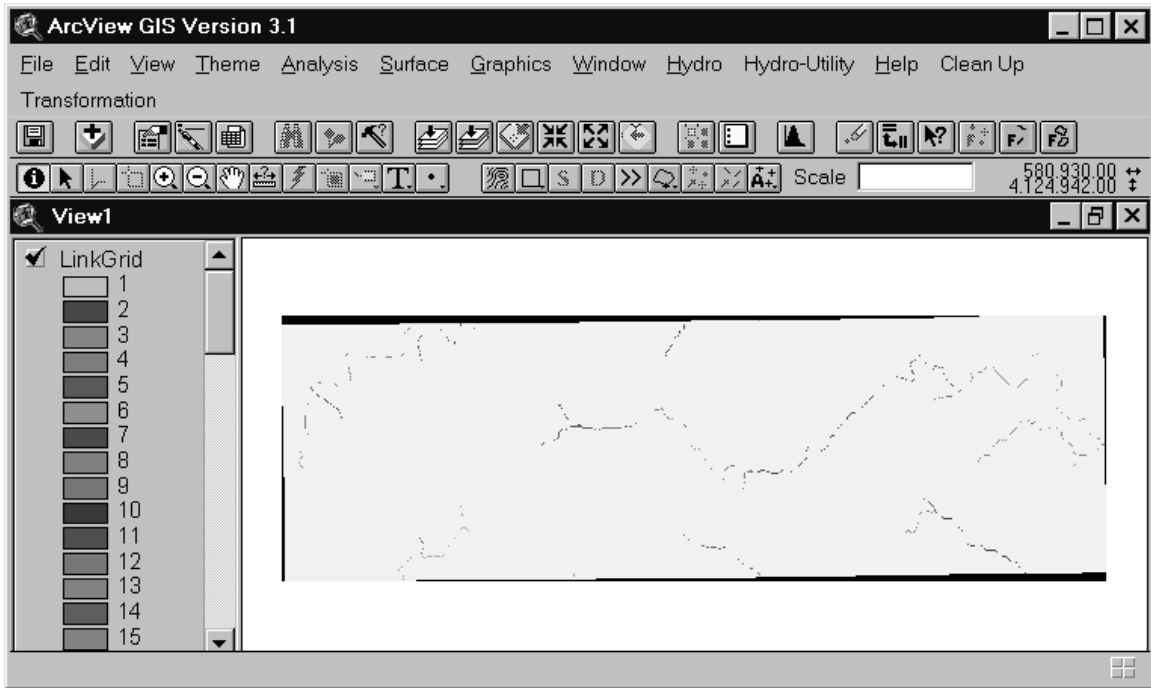
12.3 Under the *Hydro* menu, select *Flow Accumulation*. Enter the input theme, *FlowDirGrid* and the output theme, *FlowAccGrid*. Click on *OK*. Click on *OK*. Click in the box beside the *FlowAccGrid* theme to activate the theme as shown below.



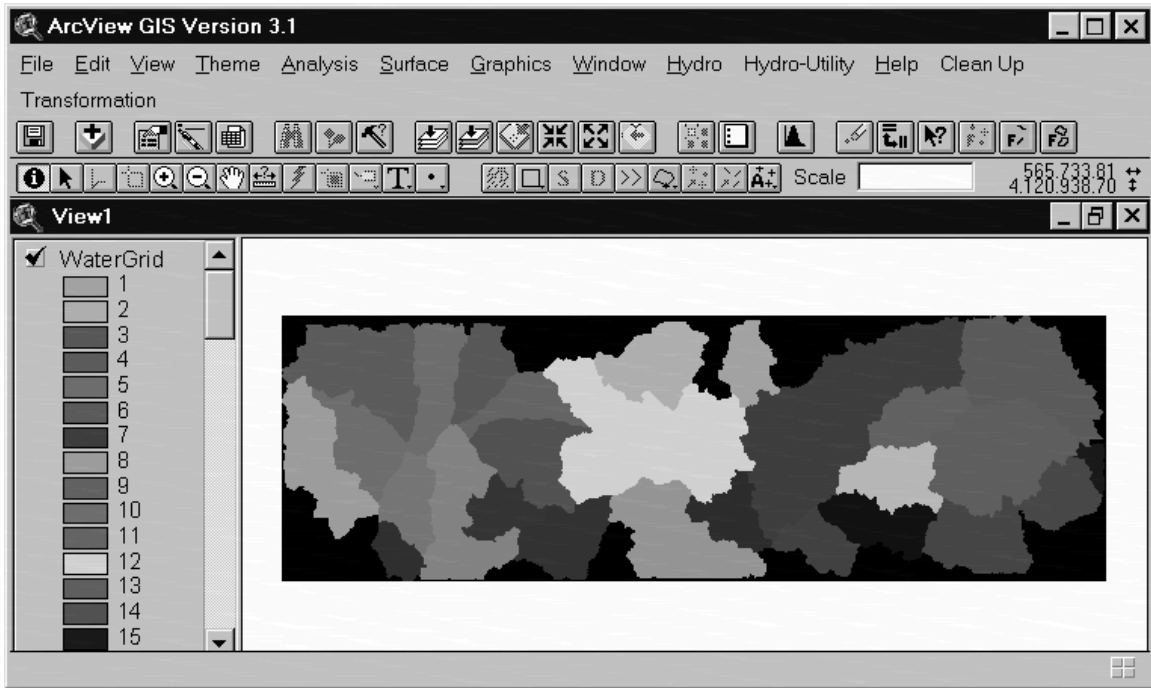
12.4 Under the *Hydro* menu, select *Stream Definition*. Enter the input theme, *FlowAccGrid* and the output theme, *StreamGrid*. Click on *OK*. Click on *OK*. Click in the box beside the *StreamGrid* theme to activate the theme as shown below.



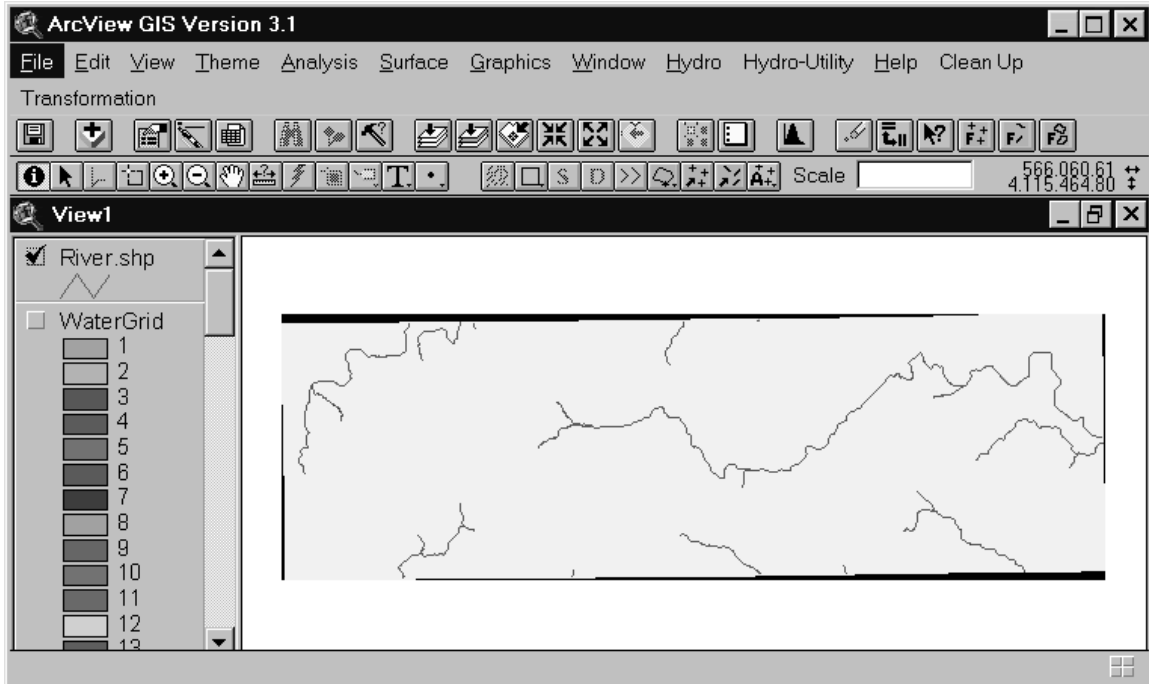
12.5 Under the *Hydro* menu, select *Stream Segmentation*. Enter the input theme 1, *FlowDirGrid*, the input theme 2, *StreamGrid* and the output theme, *LinkGrid*. Click on *OK*. Click on *OK*. Click in the box beside the *LinkGrid* theme to activate the theme as shown below.



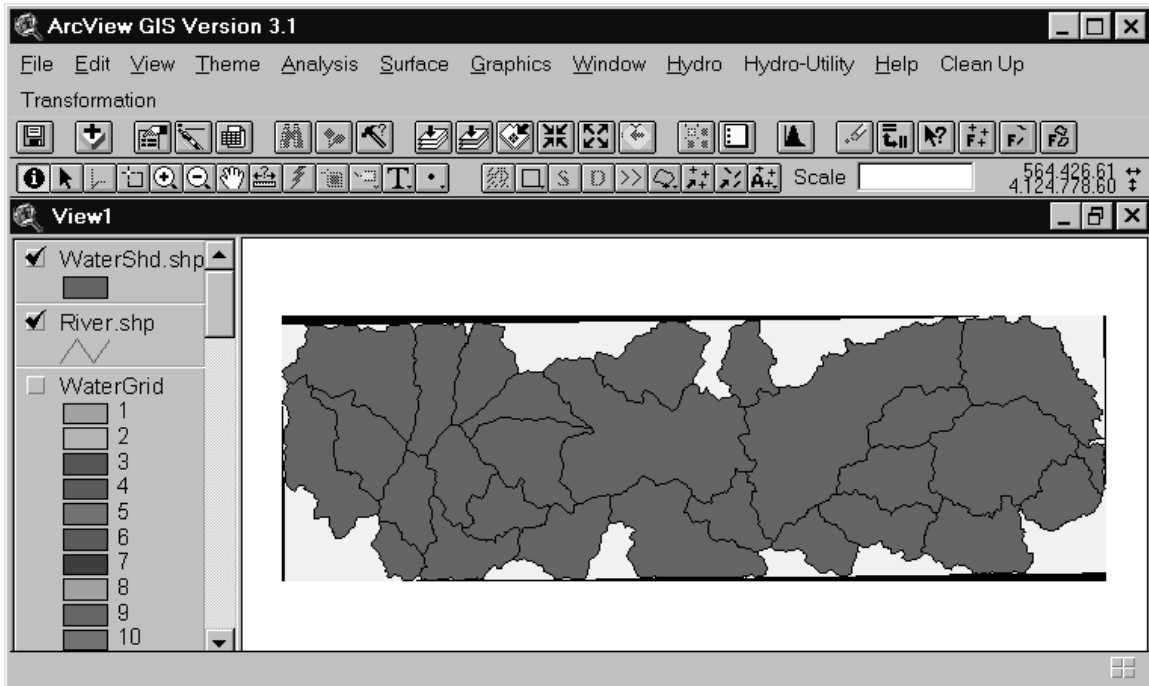
12.6 Under the *Hydro* menu, select *Watershed Subdelineation*. Enter the input theme 1, *FlowDirGrid*, the input theme 2, *LinkGrid* and the output theme, *WaterGrid*. Click on *OK*. Click in the box beside the *WaterGrid* theme to activate the theme as shown below.



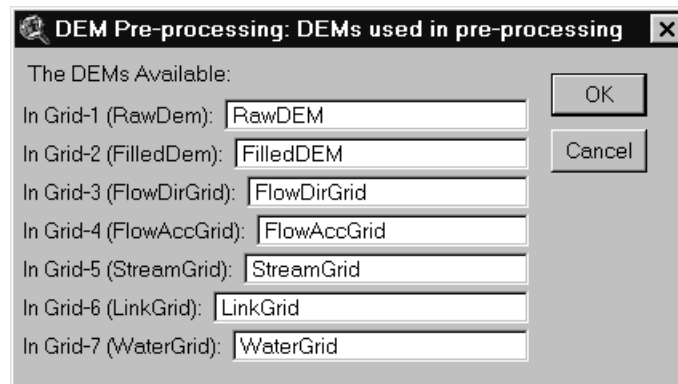
12.7 Under the *Hydro* menu, select *Line GRID to Shape*. Enter the input theme 1, *LinkGrid*, the input theme 2, *FlowDirGrid* and the output theme, *River*. Click on *OK*. Click in the box beside the *River* theme to activate the theme. To see the *River* theme better, deactivate the *WaterGrid* theme by clicking in the box beside the theme name as shown below.



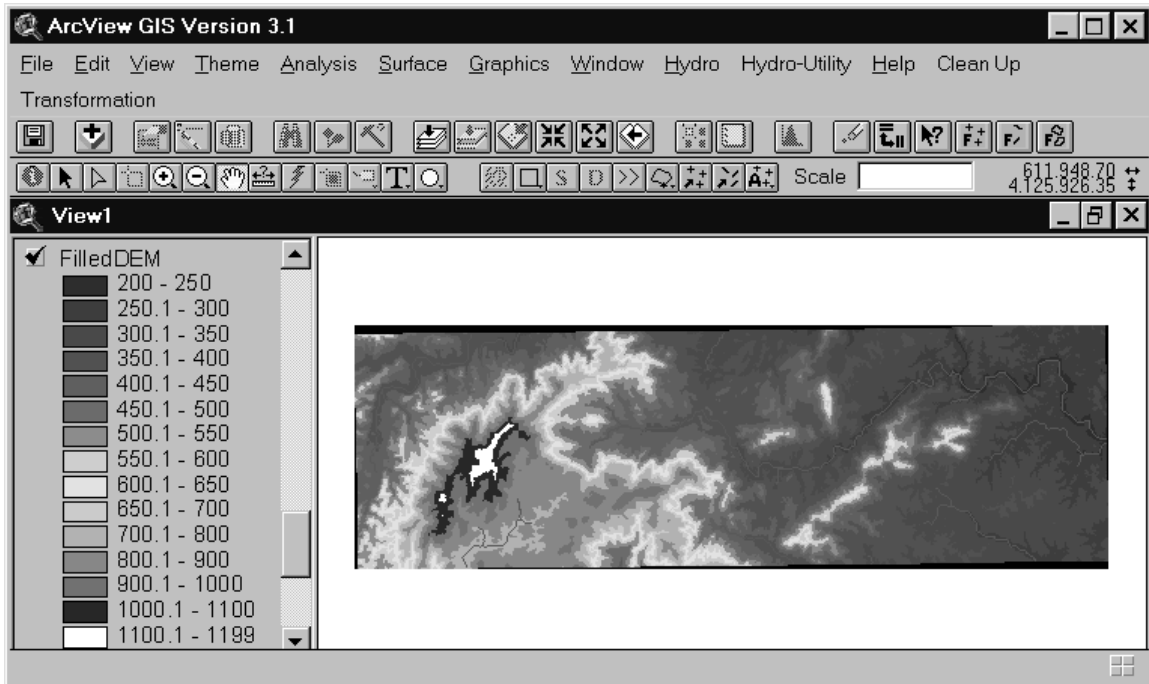
12.8 Under the *Hydro* menu, select *Poly GRID to Shape*. Enter the input theme, *WaterGrid* and the output theme, *WaterShd*. Click on *OK*. . Click in the box beside the *WaterShd* theme to activate the theme as shown below.




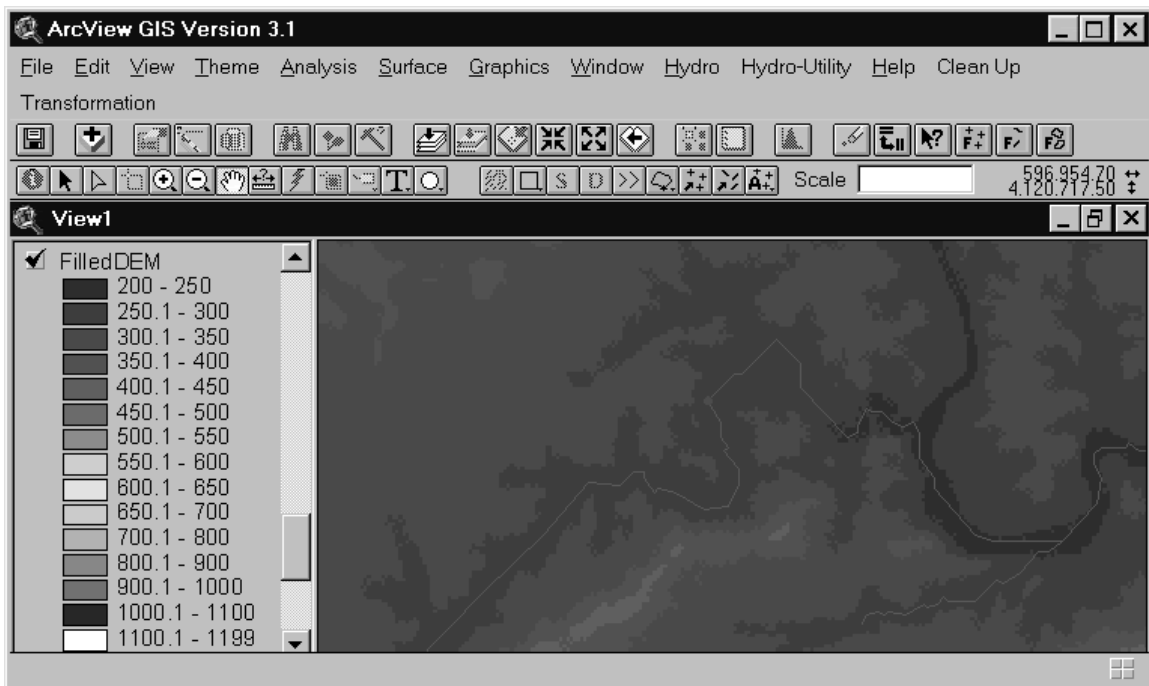
12.9 Under the *Hydro* menu, select *Delineation Files*. Ensure that the files are the same as shown below. Click *OK*.




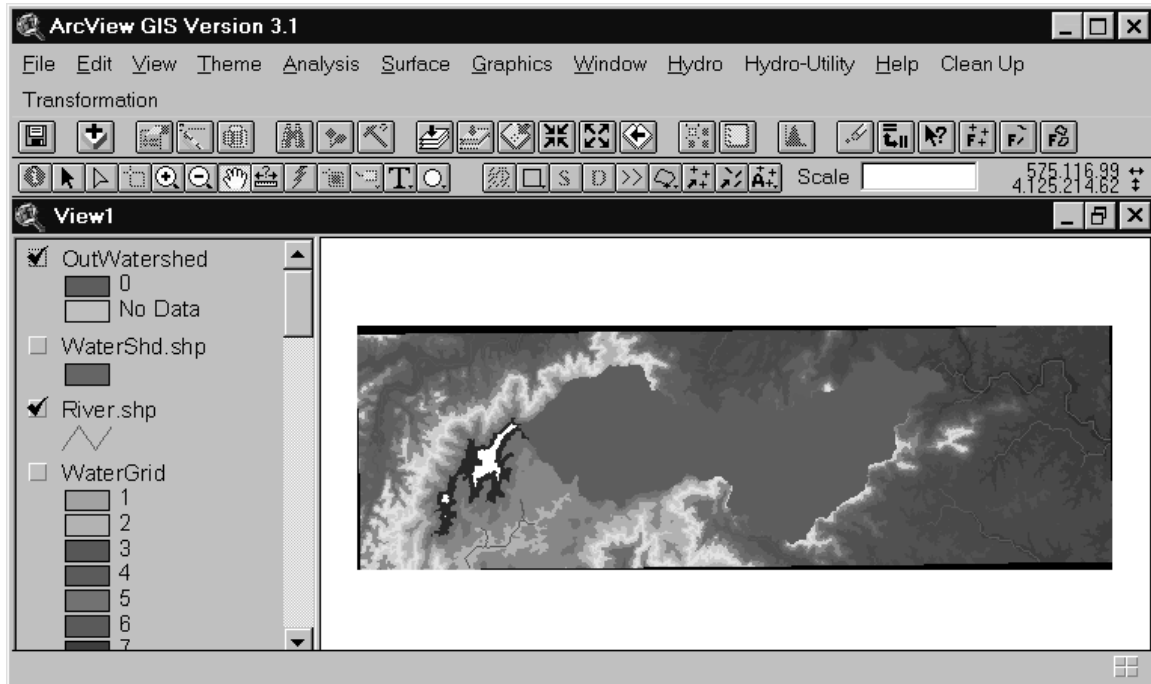
12.10 Under the *View* menu, select *Themes Off*. Scroll down through the themes and click in the box next to the *River.shp* and *FilledDEM* themes to activate the them as shown below.



12.11 Locate the outlet point for the watershed on the *FilledDEM* theme. If necessary, zoom to the area on the DEM where the outlet point is located. To zoom to an area, click on the  icon and draw a rectangle around the area to be enlarged. ArcView will zoom to that rectangle as shown below. The dot on the DEM below indicates the position of the outlet of the watershed which corresponds to the Dundee USGS stream gauge. This dot is solely for the purpose of these instructions and is not used by ArcView.



12.12 To delineate a watershed, click on the  icon . Indicate the position of the watershed outlet by clicking on the outlet point on the displayed DEM. ArcView will process for a few moments. A shape theme will be generated which represents the watershed. Click on the box next to the *Outwatershed* theme name to activate the theme as shown below.



13. Create a theme containing only the watershed.

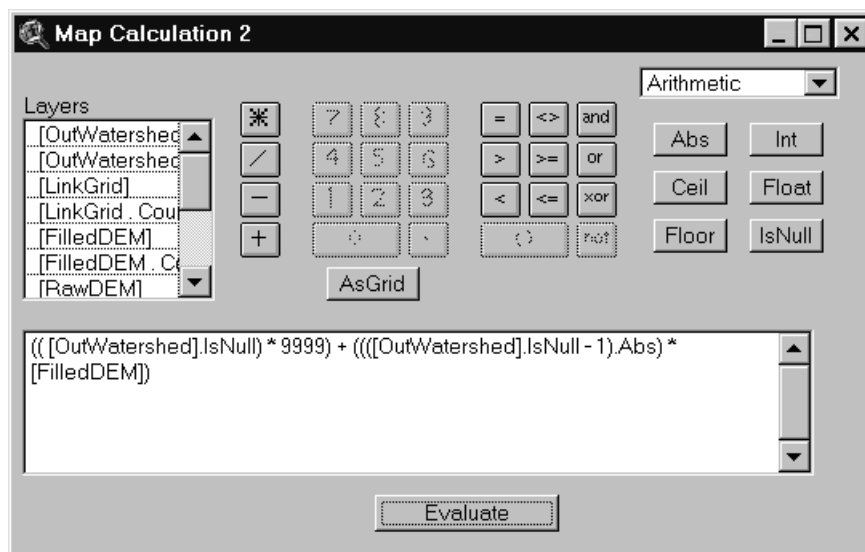
13.1 Under the *Analysis* menu, select *Map Calculator*. The window below shows the final equation after the following steps have been completed.

13.1.1 Find the window labeled *Layers*. Double click on the first *OutWatershed* layer. The *Outwatershed* theme name will appear in the lower calculation box..

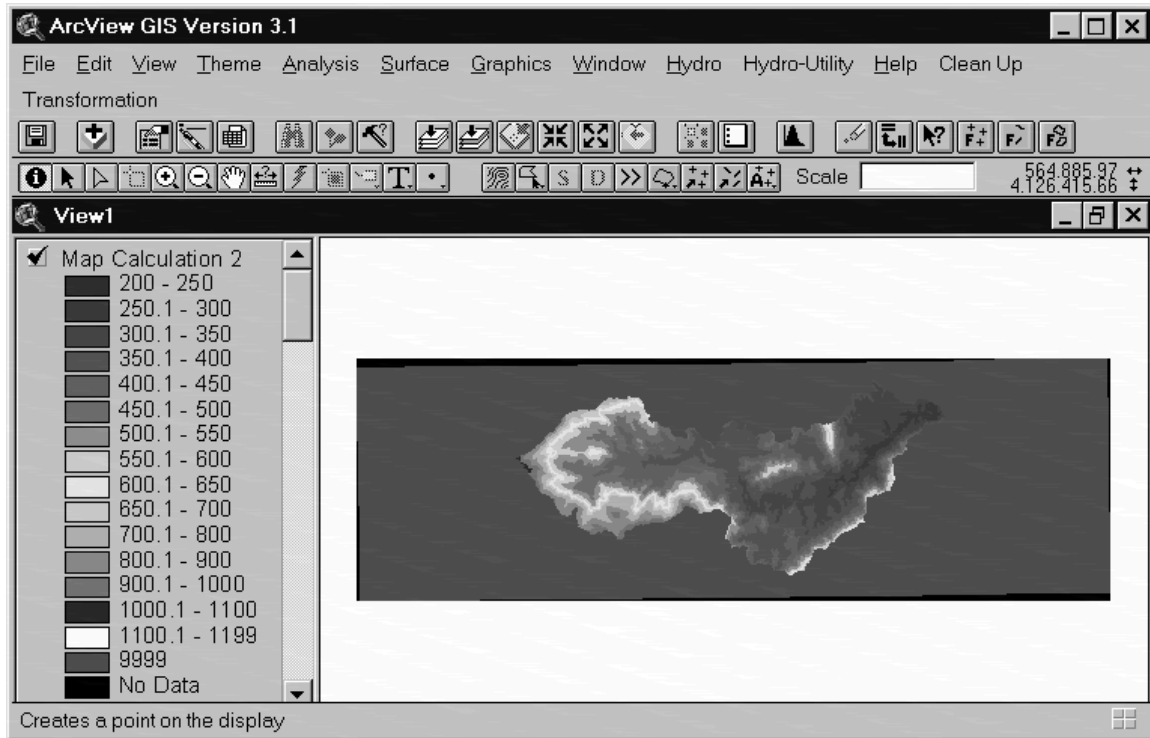
13.1.2 Go to the box in the top right corner and change the setting from *Logarithms* to *Arithmetic*. Click on the *IsNull* button.

13.1.3 Push the right arrow key on the keyboard once to get outside the parentheses.

- 13.1.4 Click on the “\*” button and four times on the “9” button. Click on the ( ) button. Click on the “+” button.
- 13.1.5 In the window labeled *Layers*, double click on the first *OutWatershed* layer. The *Outswatershed* theme name will appear in the lower calculation box.
- 13.1.6 Click on the ( ) button. Push the left arrow key on the keyboard once to get inside the parentheses. Click on the *IsNull* button.
- 13.1.7 Click on the “-” and “1” buttons.
- 13.1.8 Push the right arrow key on the keyboard once to get outside the parentheses. Click on the *Abs* button.
- 13.1.9 With the mouse, highlight the portion of the equation to the right of the “+” operator. Click on the ( ) button. Click on the “\*” button.
- 13.1.10 In the window labeled *Layers*, double click on the first *FilledDEM* layer. The *FilledDEM* theme name will appear in the lower calculation box.
- 13.1.11 Again, with the mouse, highlight the portion of the equation to the right of the “+” operator.
- 13.1.12 Click on the ( ) button. Click *Evaluate* and close the *Map Calculator* window. The output grid will be labeled *Map Calculation 2*.



13.2 This procedure will assign a value of 9999 to every grid cell outside the watershed. It will assign the elevation corresponding to that grid cell to every grid cell inside the watershed. The grid cells outside the watershed will later be changed to *No data* in order to change the size of the grid cells.

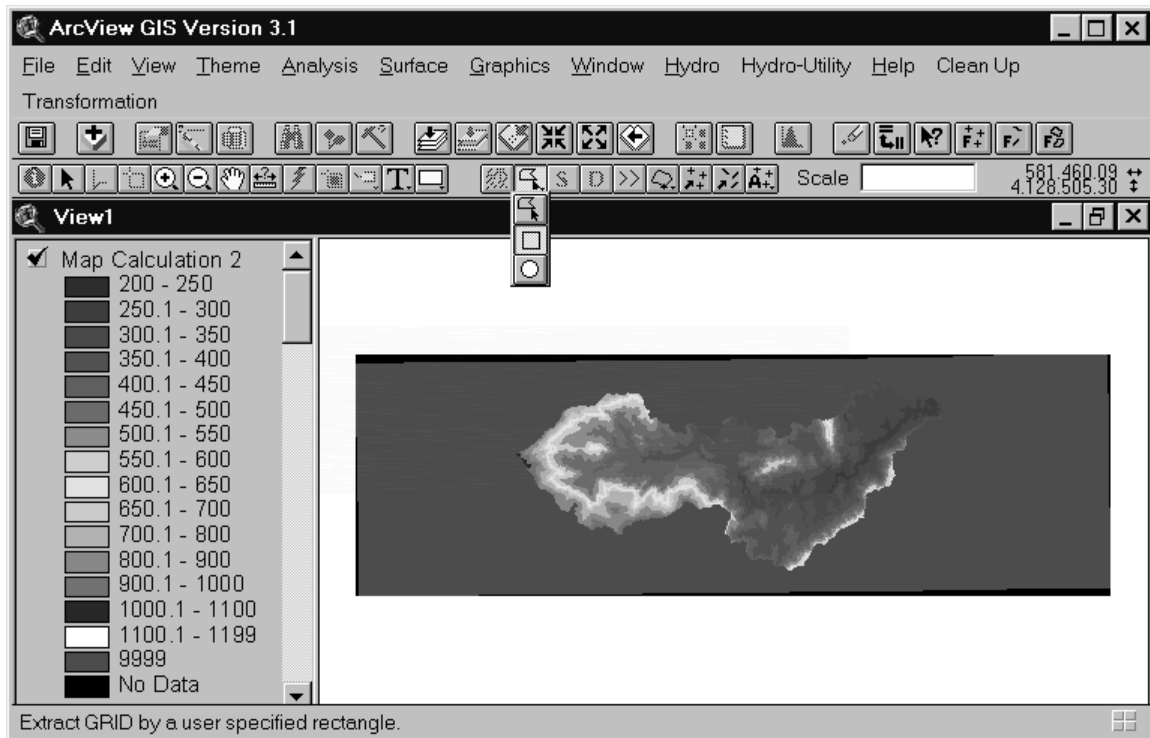


13.3 The legend will either have to be customized to view the new theme or a previously saved legend will have to be loaded by clicking on *Load* and selecting the appropriate file. To customize a legend, follow the instructions on *Editing or customizing a legend*. The legend below does not come with ArcView, rather the values and colors were manually altered. To view the theme, click in the box next to the *Map Calculation 2* theme name as shown above.

14. Extracting a rectangle containing the watershed. This will create a smaller grid theme and therefore a smaller file when it is exported.

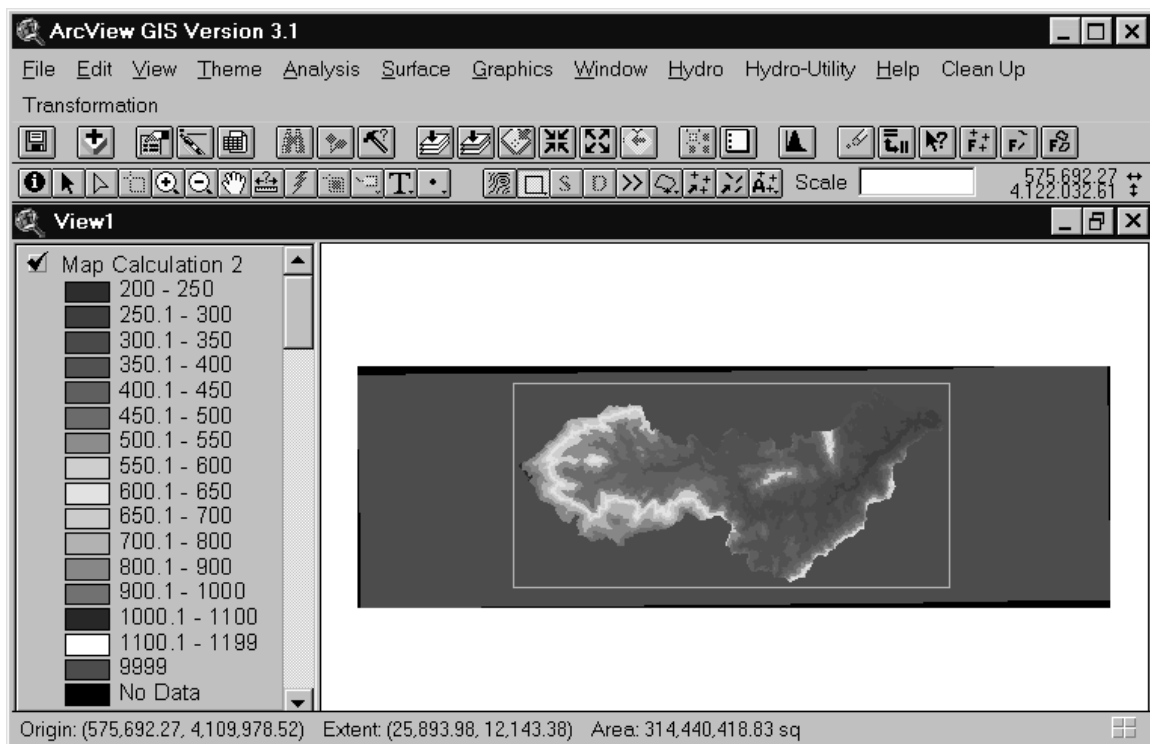
14.1 Under the *Analysis* menu, select *Properties*. Select the *Intersection of Inputs* as the *Analysis Extent*.

14.2 Click on the icon shown below and hold down the mouse button. Move the pointer down until it highlights the rectangle. Release the mouse button.



14.3 When the GRID Extraction window appears, select the theme containing the delineated watershed. In this study, it is *Map Calculation 2*.

14.4 Using the mouse, click and drag a rectangle around the watershed as shown below. The box should be close to the watershed boundaries, but the entire watershed must be contained within the rectangle. If a portion of the watershed lies outside the rectangle, click on *No* when asked to *Please Confirm*, otherwise click on *Yes*. A error *Segmentation Violation* may occur which will not effect the output theme, simply click on *Ok*.



14.5 Convert the output theme with the extension *.rct* to a permanent grid by highlighting the theme and selecting *Convert to Grid* under the *Theme* menu. Type in the name of the output grid (i.e. BackCreek). Click on *Yes* when asked to *Add grid as theme to the View*.

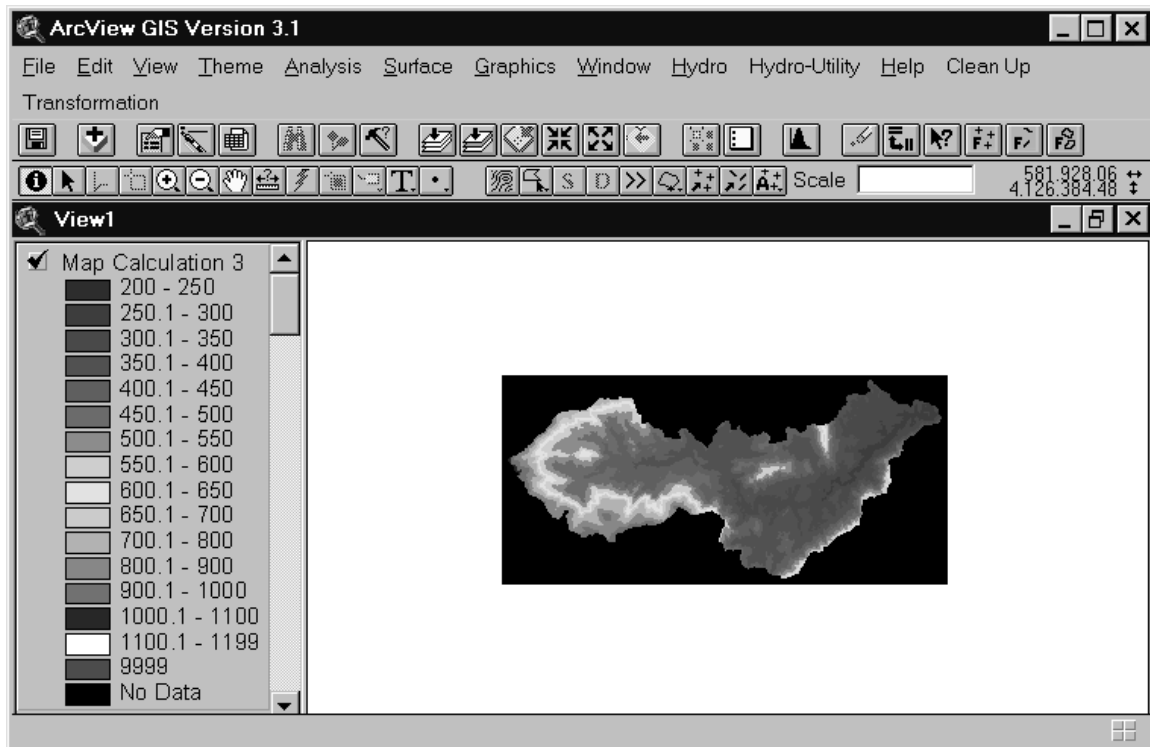
14.6 To view only the output theme, under the *View* menu select *Themes Off*. Click in the box beside the name (i.e. Back Creek).

14.7 The legend will either have to be customized to view the new theme or a previously saved legend will have to be loaded by clicking on *Load* and selecting

the appropriate file. To customize a legend, follow the instructions on *Editing or customizing a legend*.

15. Change the value of grid cells outside the watershed from 9999 to *No data*.
  - 15.1 Under the *Analysis* menu, select *Map Calculator*. The window below shows the final equation after the following steps have been completed.
    - 15.1.1 Find the window labeled *Layers*. Double click on the theme output by the extraction procedure (i.e. BackCreek). The title of the extracted DEM theme will appear in the lower calculation box.
    - 15.1.2 Click on the “< >” button. Click four times on the “9” button.
    - 15.1.3 Push the right arrow key on the keyboard once to get outside the parentheses.
    - 15.1.4 Click on the “\*” button, and double click on the theme output by the extraction procedure (i.e. BackCreek). The title of the extracted DEM theme will appear in the lower calculation box.
    - 15.1.5 Push the right arrow key on the keyboard once. Click on the ( ) button. Click on the “+” button.
    - 15.1.6 In the window labeled *Layers*, double click on the theme output by the extraction procedure (i.e. BackCreek). The title of the extracted DEM theme will appear in the lower calculation box.
    - 15.1.7 Click on the “=” button. Click four times on the “9” button.
    - 15.1.8 With the mouse, highlight the portion of the equation to the right of the “+” operator. Click on the ( ) button. Click on the “\*” button.
    - 15.1.9 In the window labeled *Layers*, double click on the first *OutWatershed* layer. The *OutWatershed* theme name will appear in the lower calculation box.





## 16. Changing grid cell size.

16.1 Highlight the theme containing the extracted watershed surrounded by *No data* as shown above (i.e. *Map Calculation 3*).

16.2 Under the *Analysis* menu, select *Resample*.

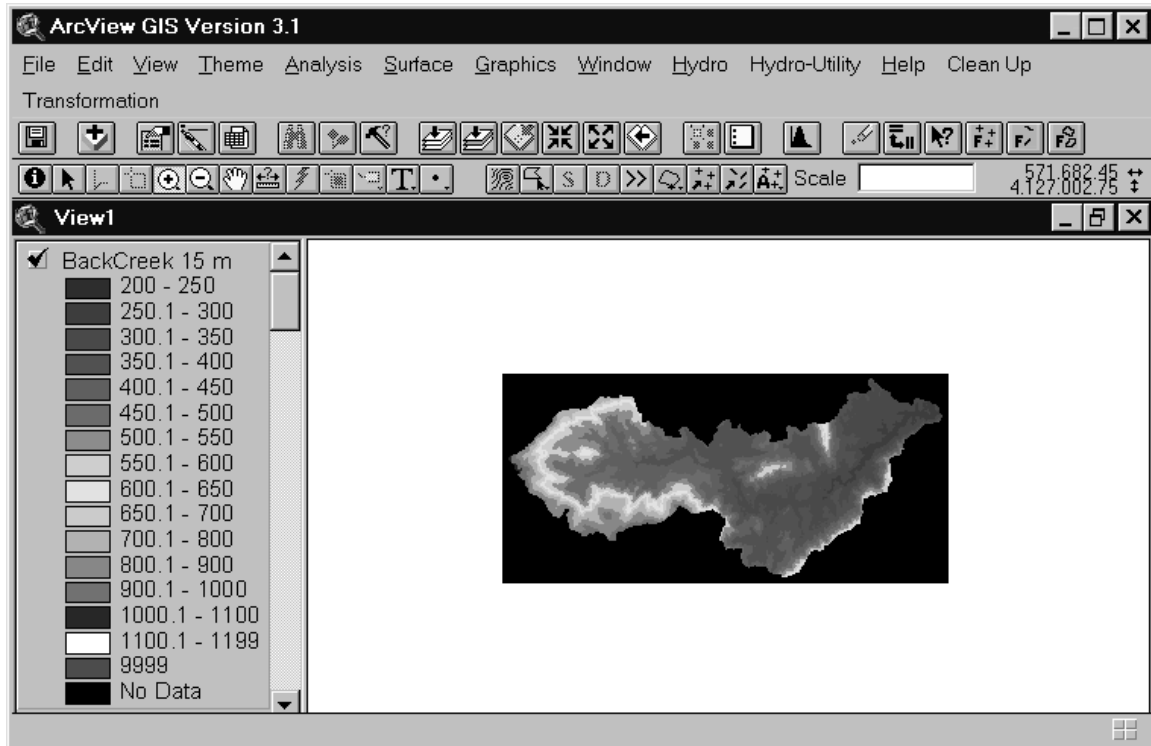
16.3 Enter the grid cell size for the output grid. Click *Ok*. For this study, DEMs with a grid cell size of 15, 60, 90 and 120 meters must be developed from the original 30 meter grid cell size DEMs.

16.3.1 When decreasing grid cell size, select *Cubic Convolution* as the *Resampling Method*.

16.3.2 When increasing grid cell size, select *Nearest Neighbor* as the *Resampling Method*.

16.4 To view the resampled theme, click in the box next to the theme name.

16.5 Rename the theme to help prevent confusion between the different resampled themes. To rename a theme, select *Properties* under the *Theme* menu. Change the *Theme Name* to a meaningful name (i.e BackCreek 15 m). The window shown below contains the 15 meter grid theme. The DEM is ready to be exported for use in TOPMODEL.



## 17. Exporting data for use in TOPMODEL.

17.1 Highlight the theme to be exported by clicking on the theme name. Under the *Theme* menu, select *Properties*. In the *Theme Properties* window, find the line labeled *Source*. The path and file name following *Source* indicates where the grid data is stored. Note the name of the file containing the grid data (probably *Grid#*).

17.2 Under the *File* menu, select *Export Data Source*.

17.3 Select *ASCII Raster* as *Export File Type*.

17.4 Select the name of the file containing the grid data and click *Ok*.

17.5 Enter a name for the export file (i.e. *Backcreek15.asc*).

17.6 The file must be edited in Wordpad before it can be read by the GRIDATB program which calculates the topographic index for TOPMODEL. The first six lines in the exported *.asc* file must be replaced with the two lines following the format below:

*Descriptive name of file*

*# of columns # of rows grid cell size in meters*

For example:

*Back Creek 15 meter grid*

*1726 810 15*

The file must be saved in text format and should have the *.grd* extension to distinguish it in from the ArcView exported file.

17.7 The *.grd* file can now be read by the GRIDATB program.

# Appendix E

## 1995 TOPMODEL Hydrographs

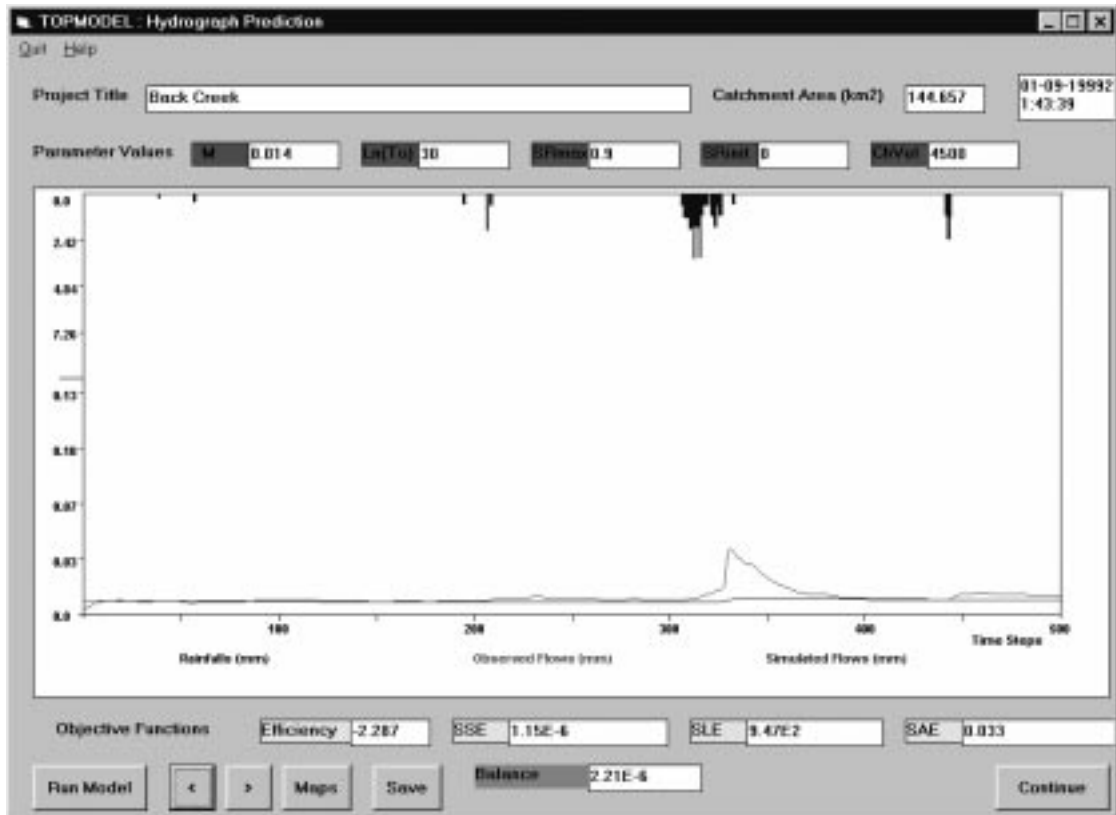


Figure E (1). 1995 water year, first 500 hour interval of first 2500 hour interval.

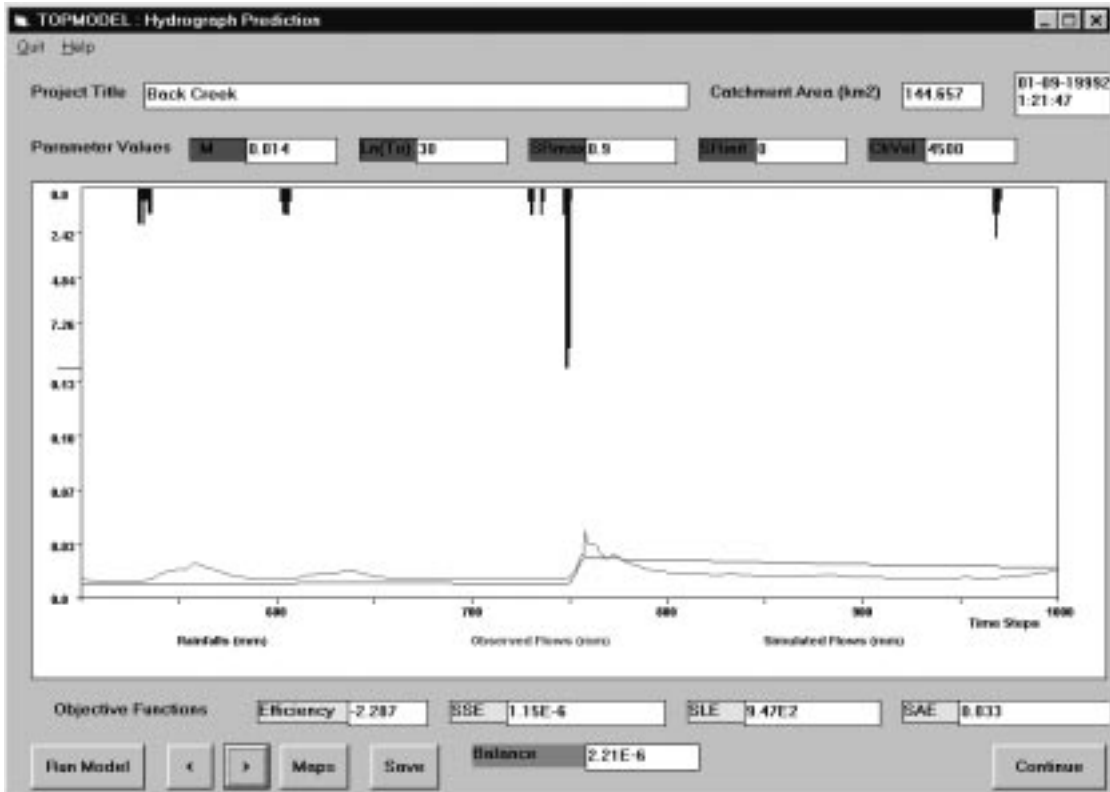


Figure E (2). 1995 water year, second 500 hour interval of first 2500 hour interval.

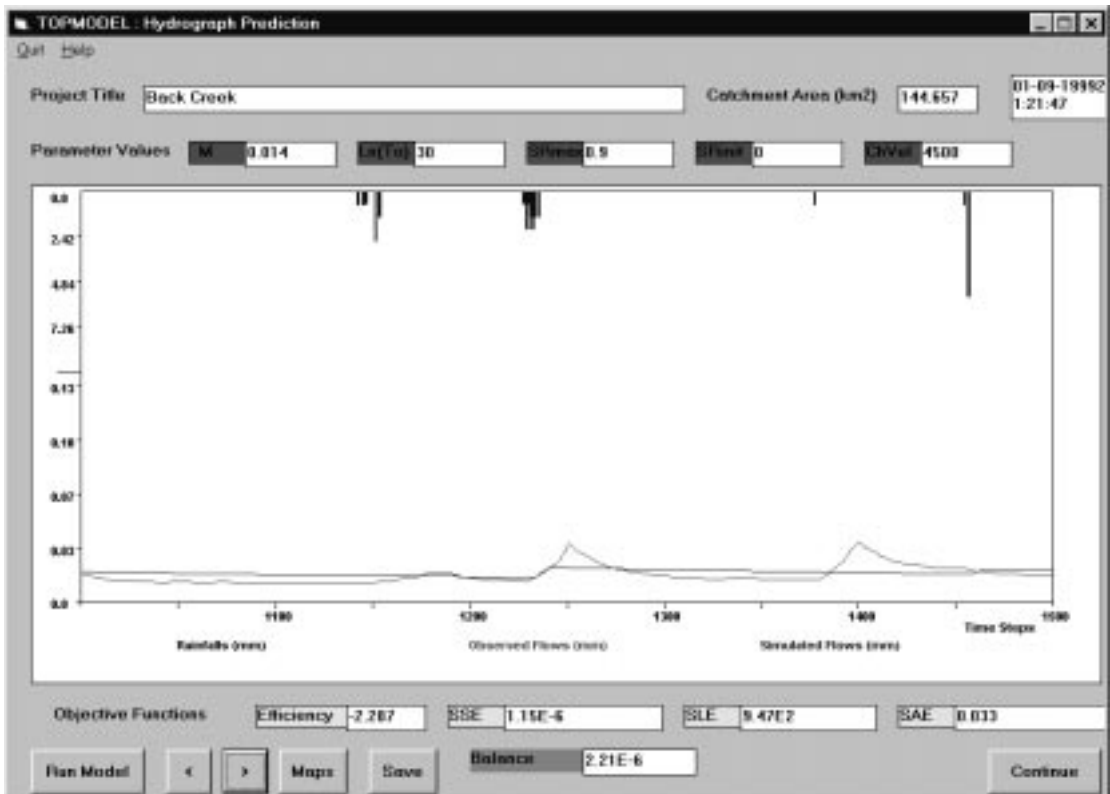


Figure E (3). 1995 water year, third 500 hour interval of first 2500 hour interval.

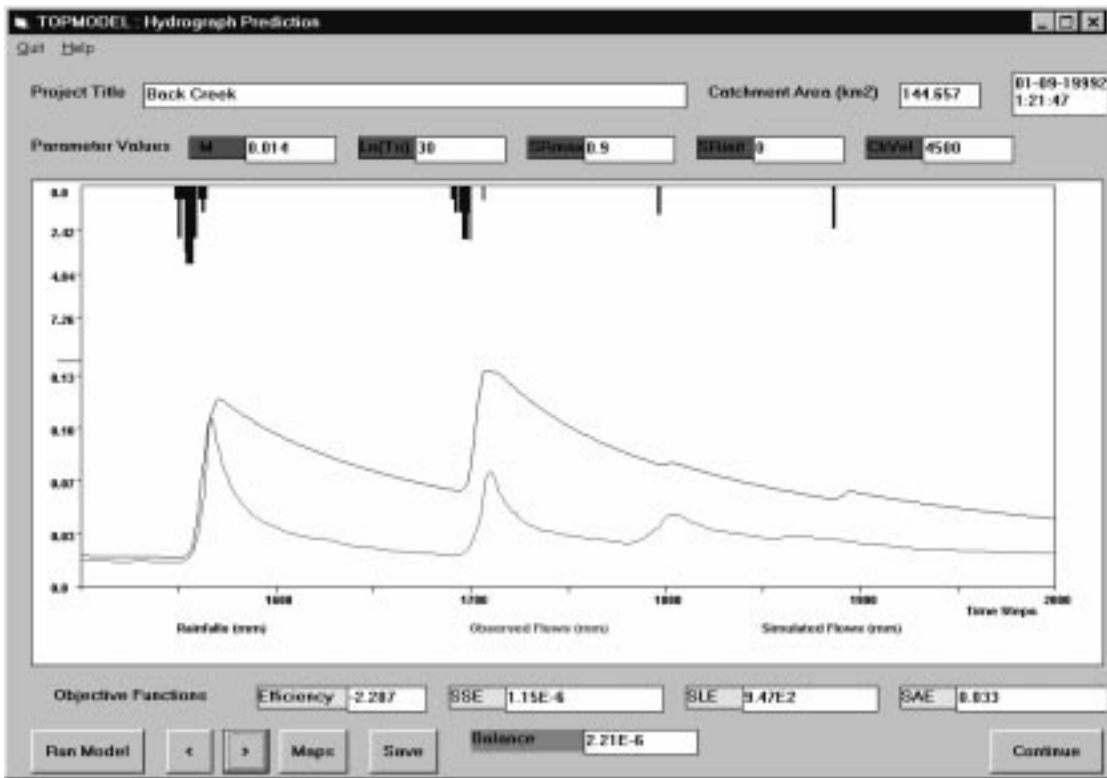


Figure E (4). 1995 water year, forth 500 hour interval of first 2500 hour interval.

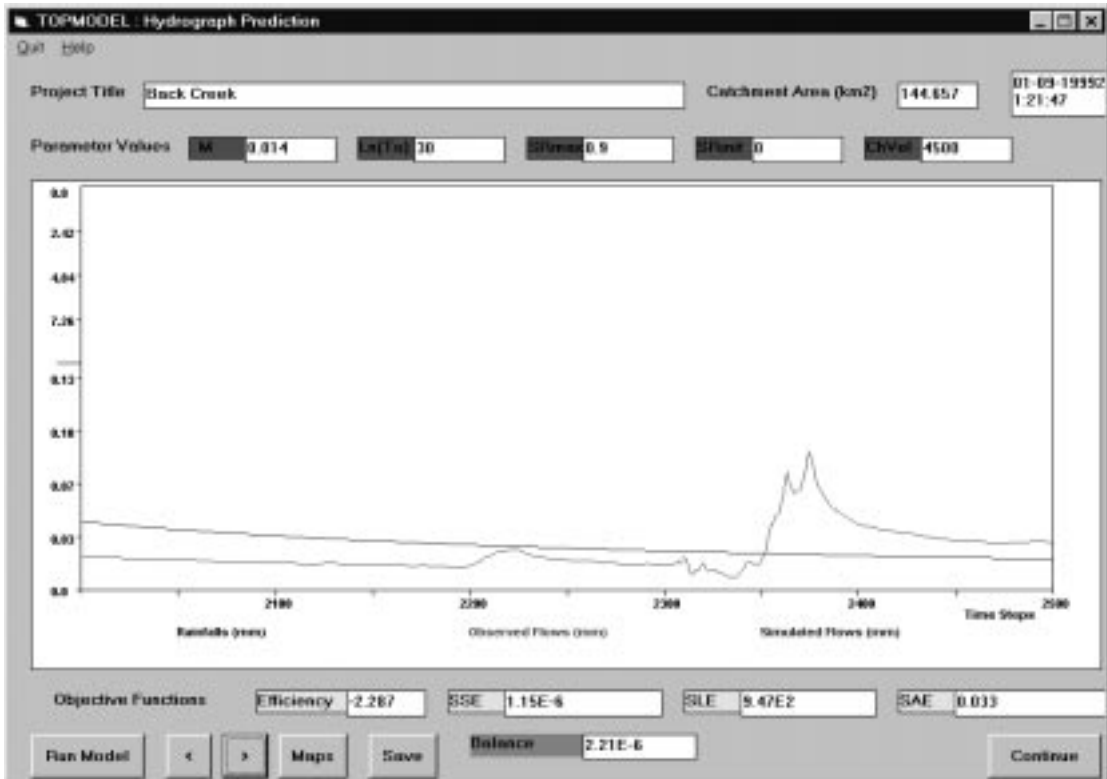


Figure E (5). 1995 water year, fifth 500 hour interval of first 2500 hour interval.

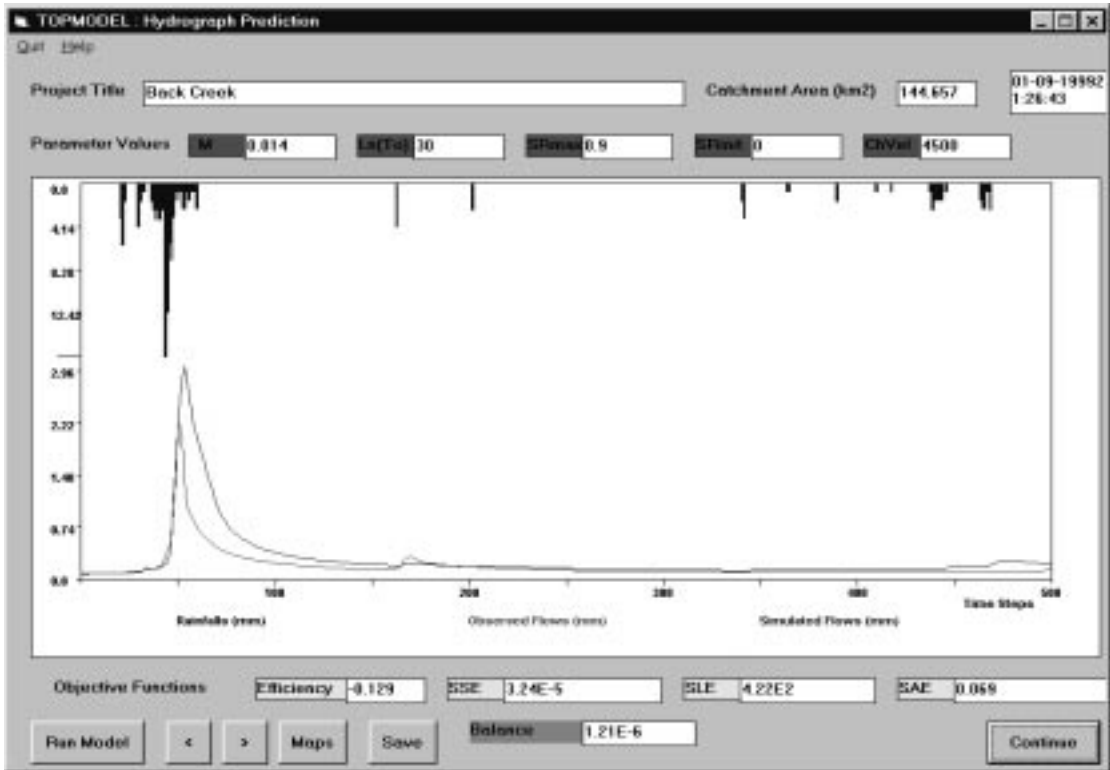


Figure E (6). 1995 water year, first 500 hour interval of second 2500 hour interval.

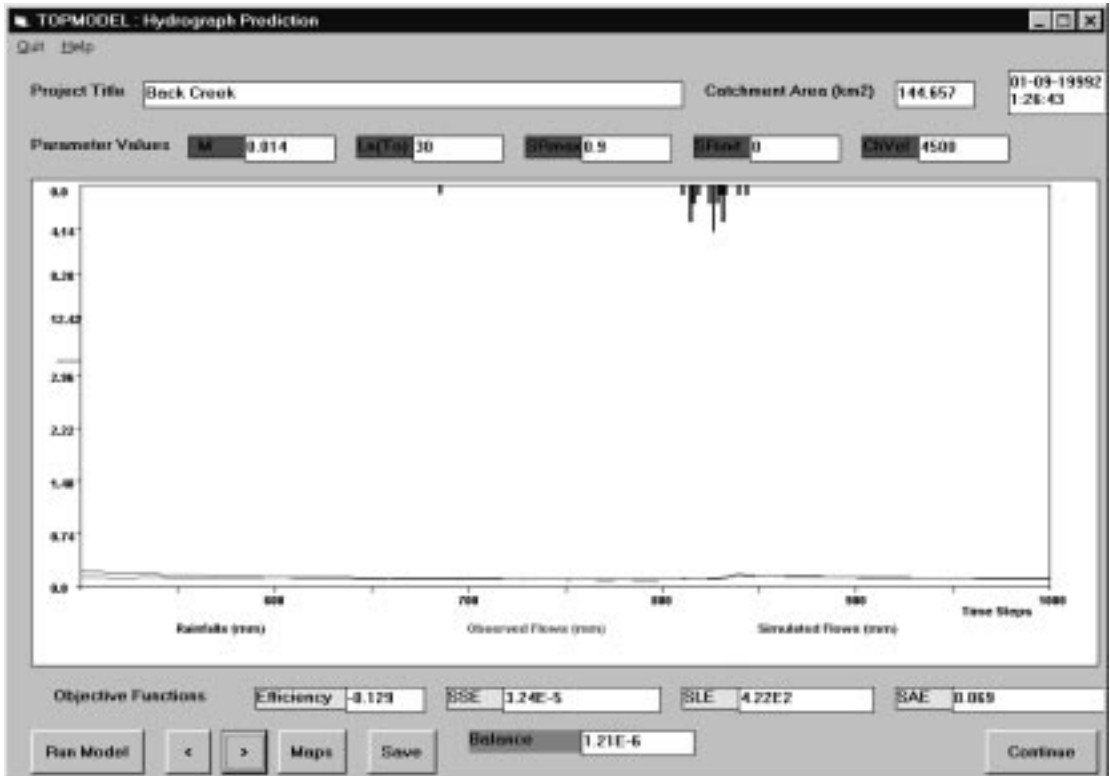


Figure E (7). 1995 water year, second 500 hour interval of second 2500 hour interval.

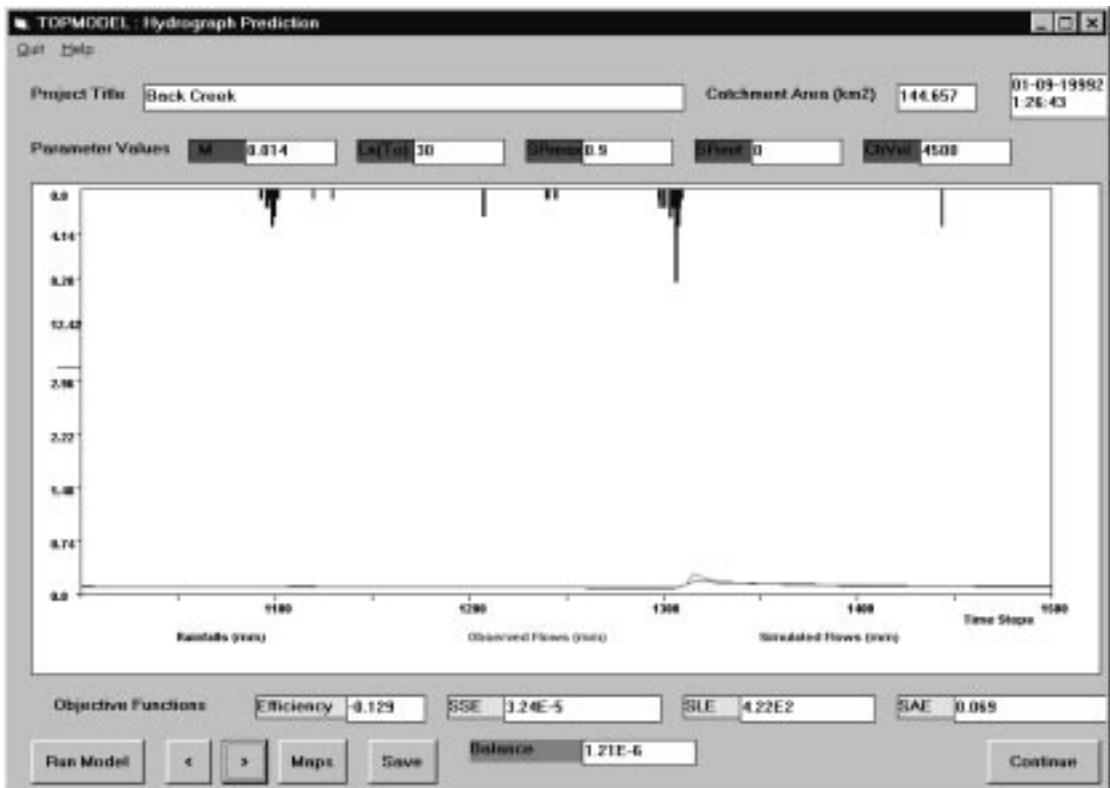


Figure E (8). 1995 water year, third 500 hour interval of second 2500 hour interval.

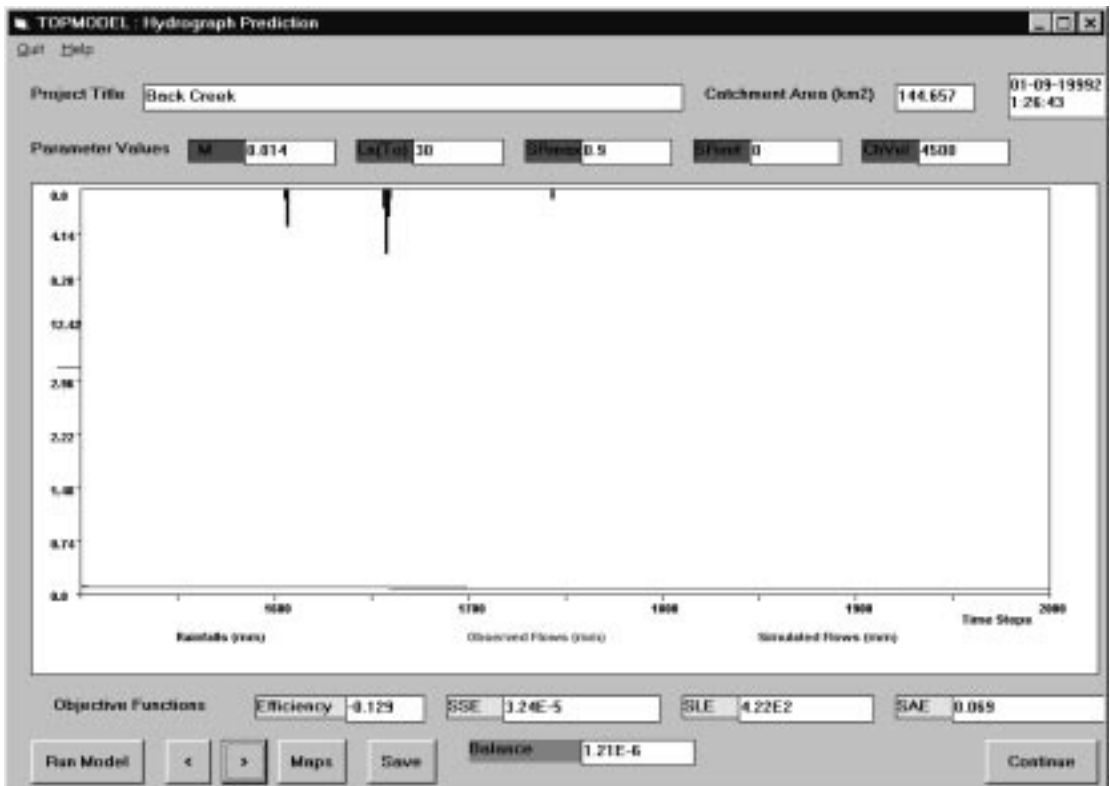


Figure E (9). 1995 water year, fourth 500 hour interval of second 2500 hour interval.

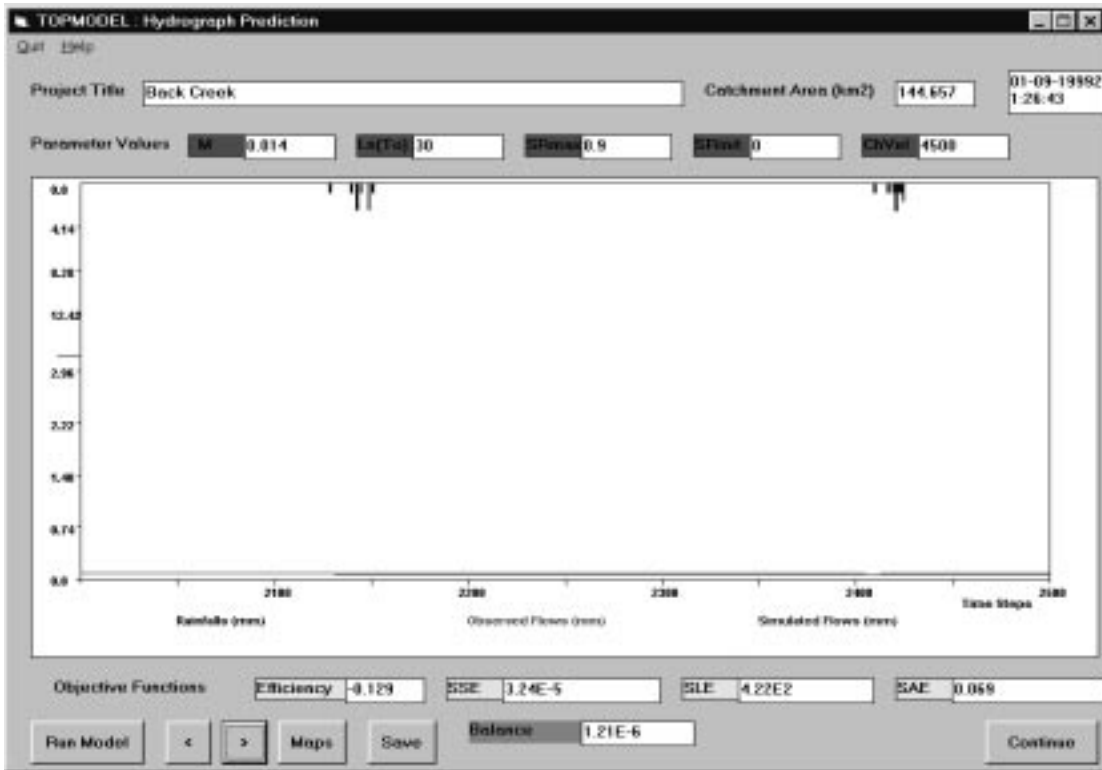


Figure E (10). 1995 water year, fifth 500 hour interval of second 2500 hour interval.

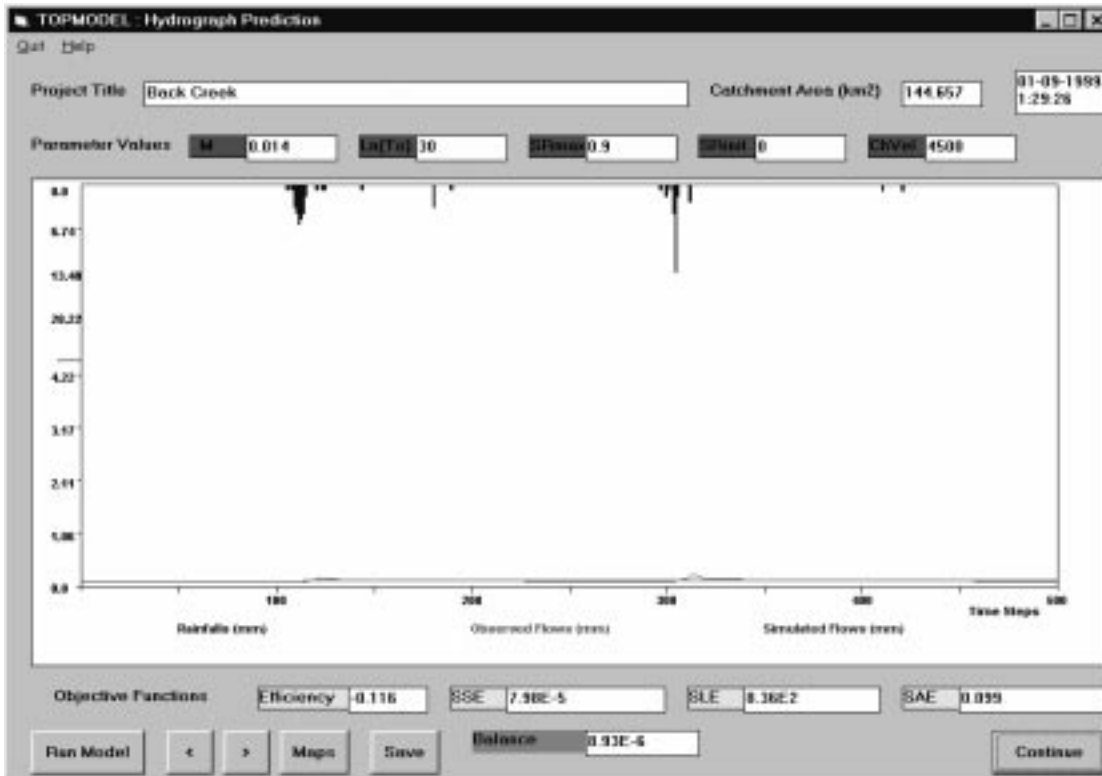


Figure E (11). 1995 water year, first 500 hour interval of third 2500 hour interval.

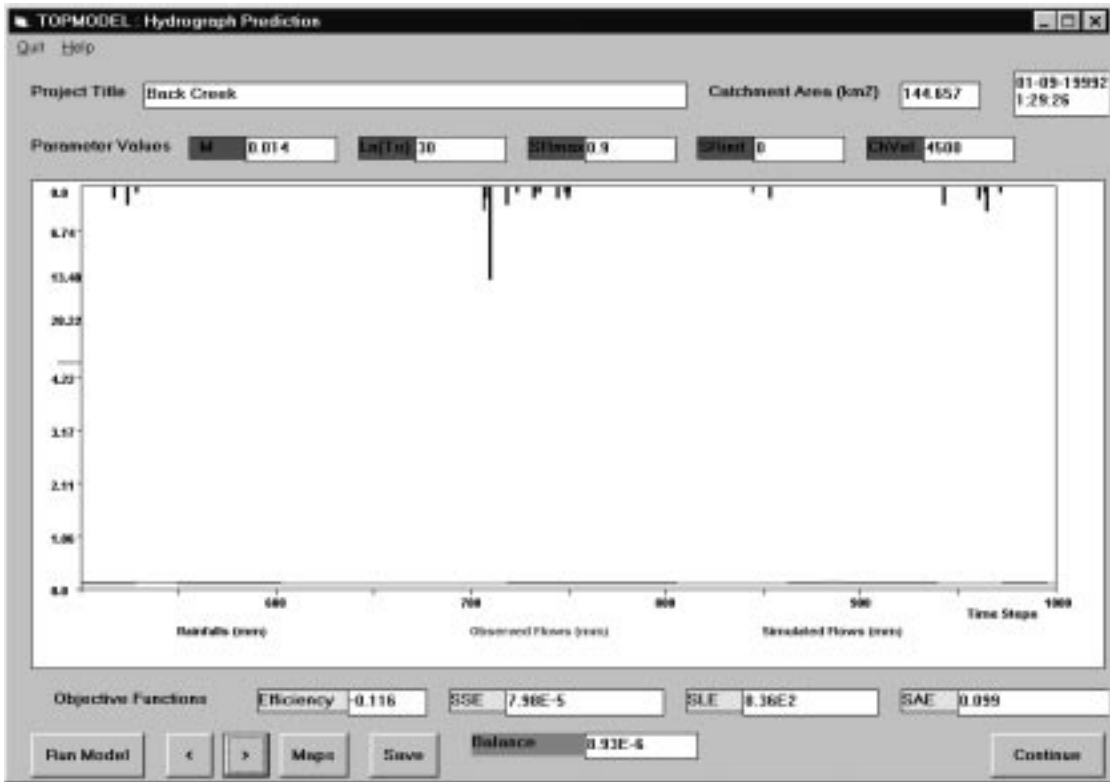


Figure E (12). 1995 water year, second 500 hour interval of third 2500 hour interval.

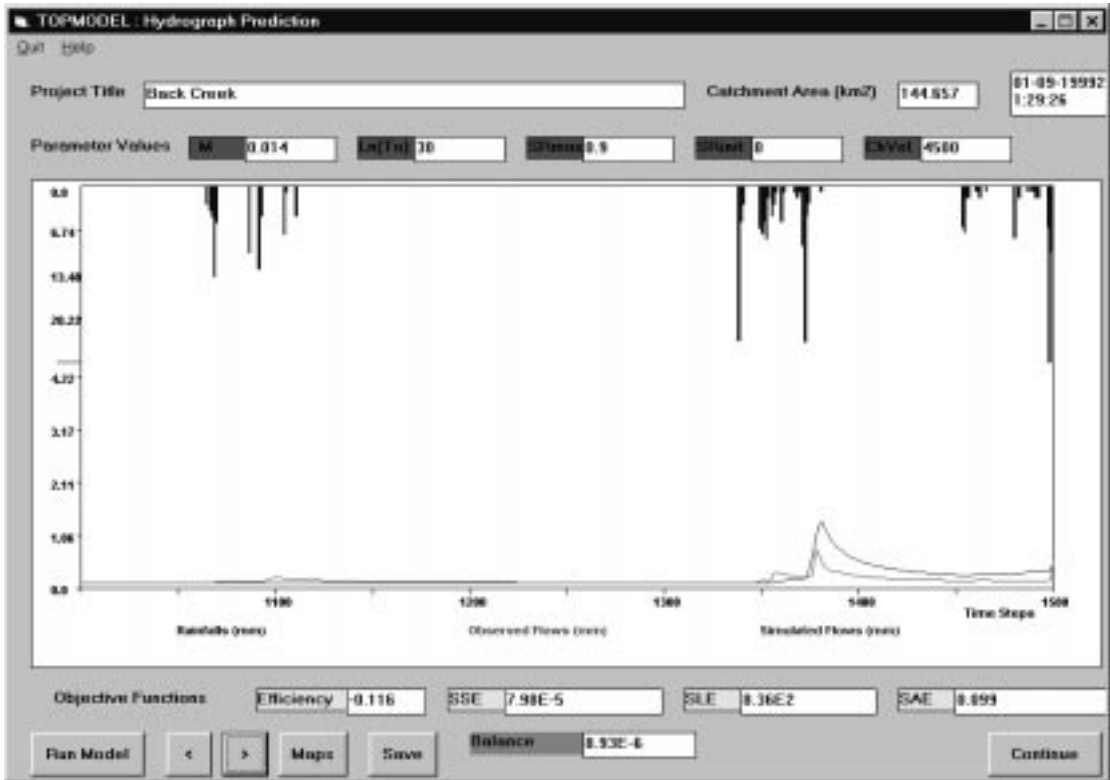


Figure E (13). 1995 water year, third 500 hour interval of third 2500 hour interval.

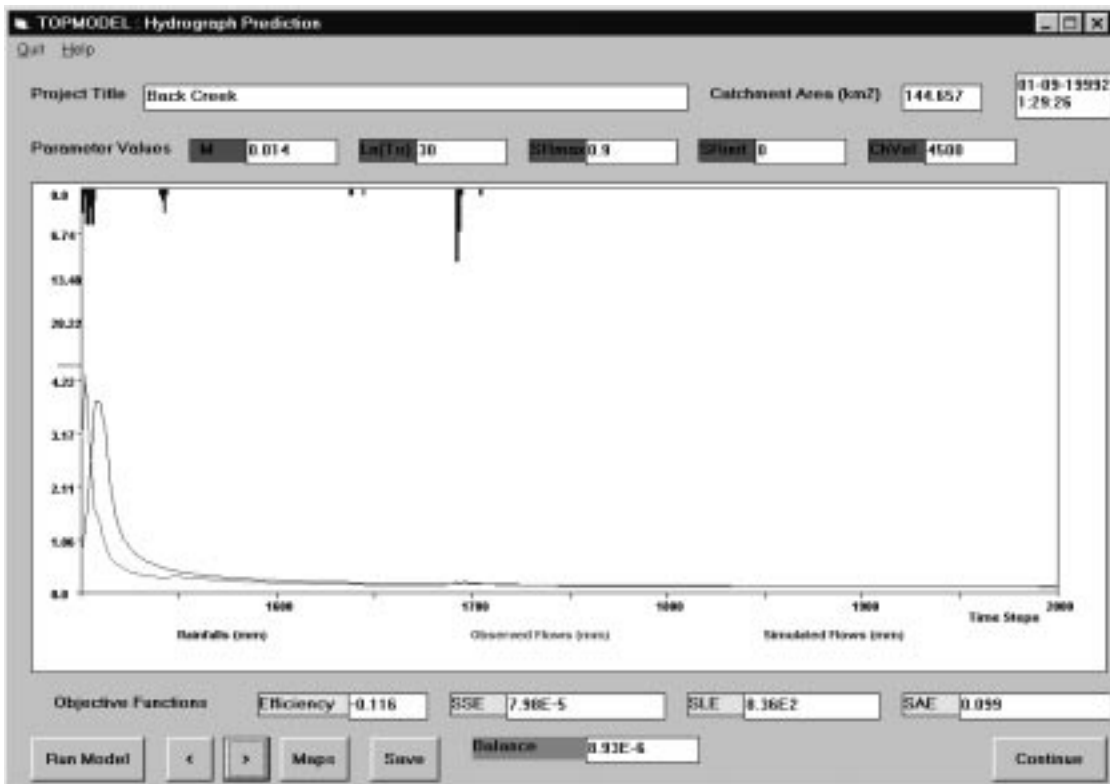


Figure E (14). 1995 water year, forth 500 hour interval of third 2500 hour interval.

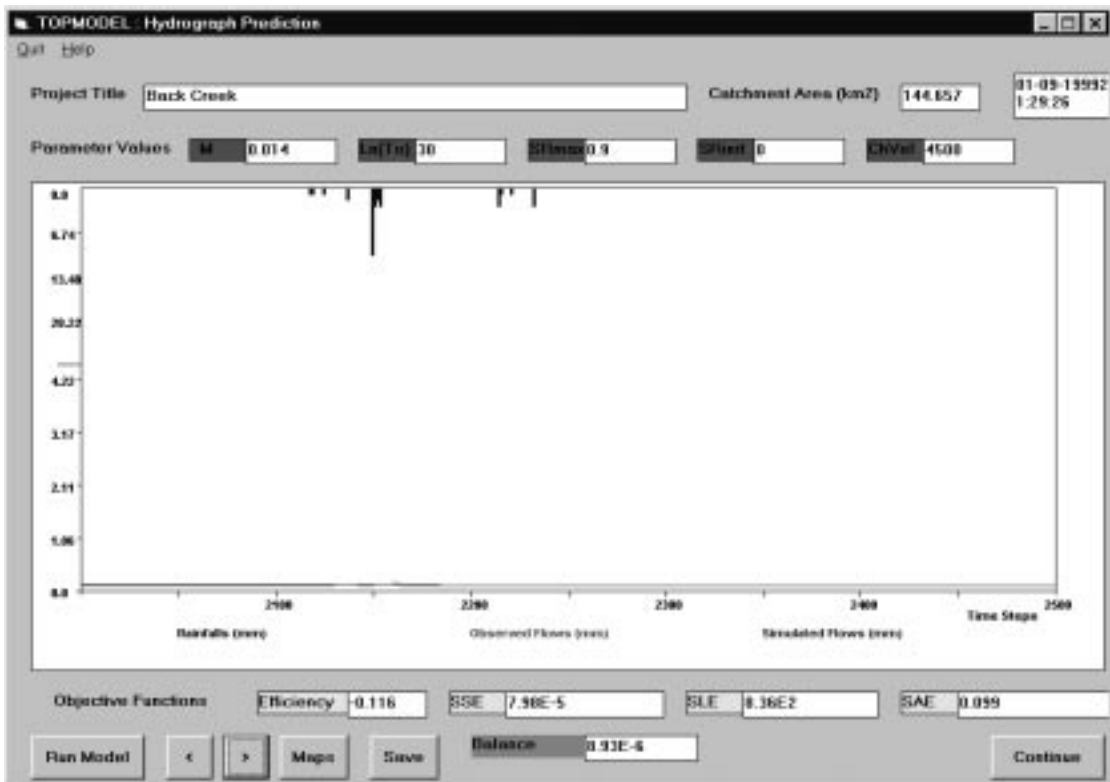


Figure E (15). 1995 water year, fifth 500 hour interval of third 2500 hour interval.

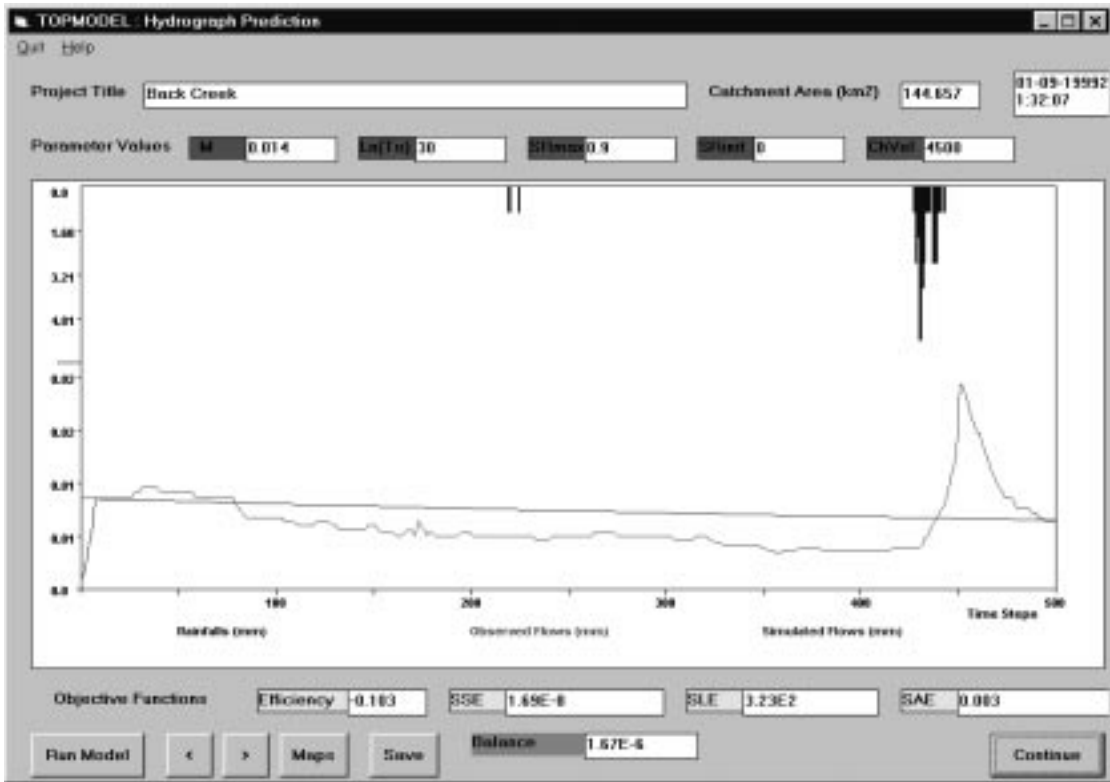


Figure E (16). 1995 water year, first 500 hour interval of forth 2500 hour interval.

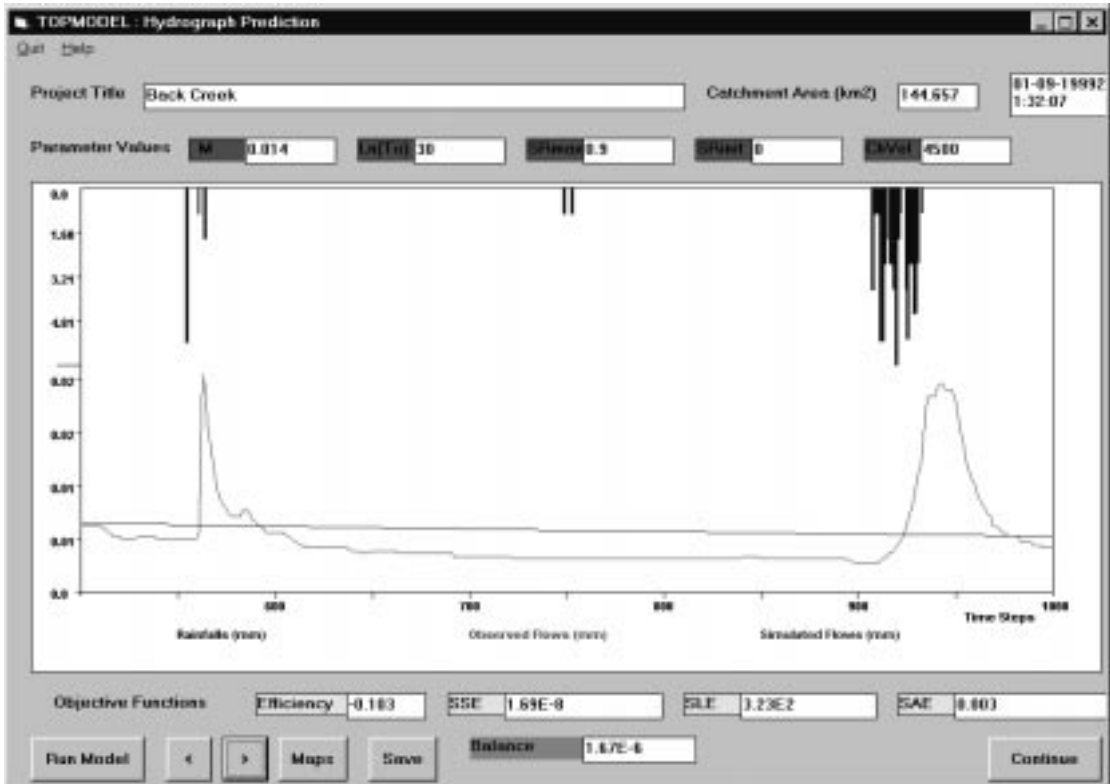


Figure E (17). 1995 water year, second 500 hour interval of forth 2500 hour interval.

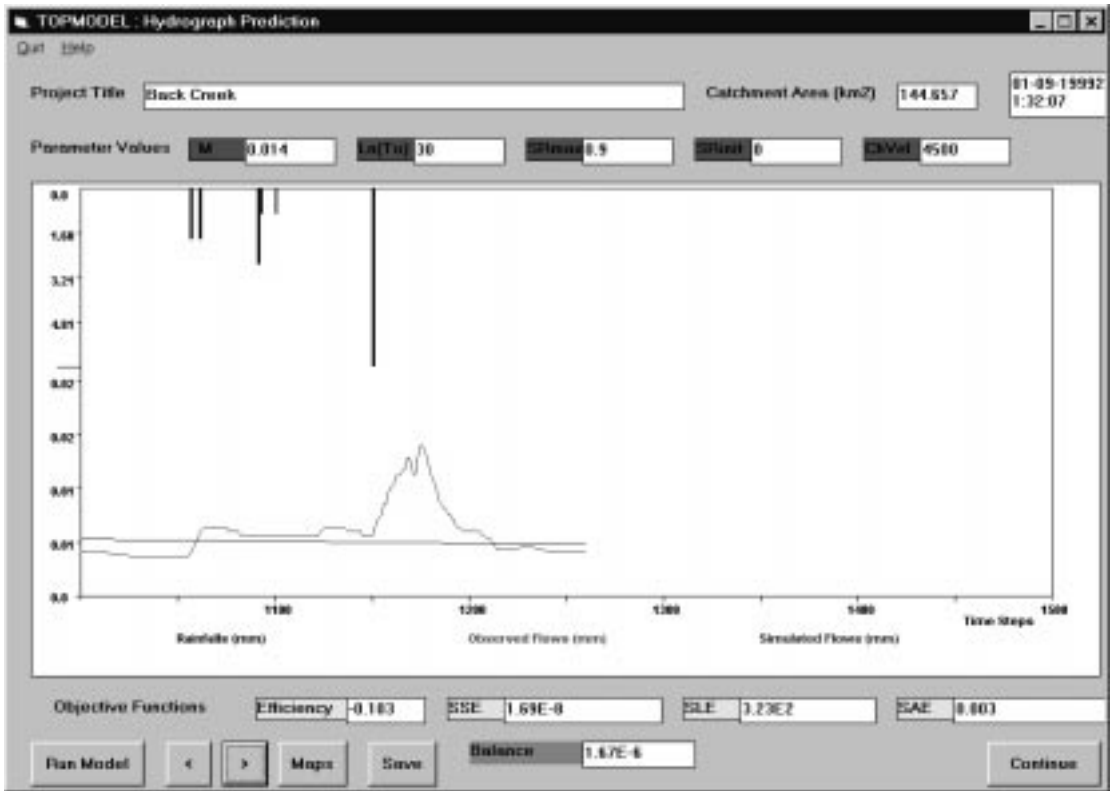


Figure E (18). 1995 water year, third 500 hour interval of forth 2500 hour interval.

# Appendix F

## 1996 TOPMODEL Hydrographs

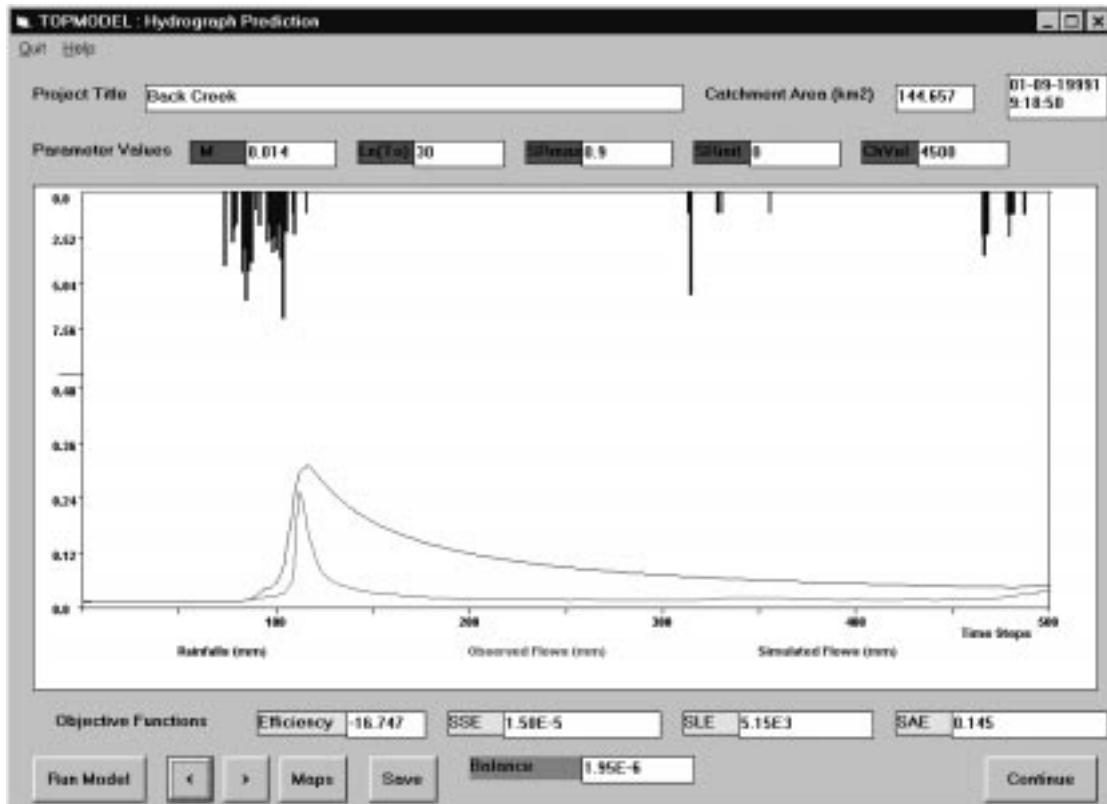


Figure F (1). 1996 water year, first 500 hour interval of first 2500 hour interval.

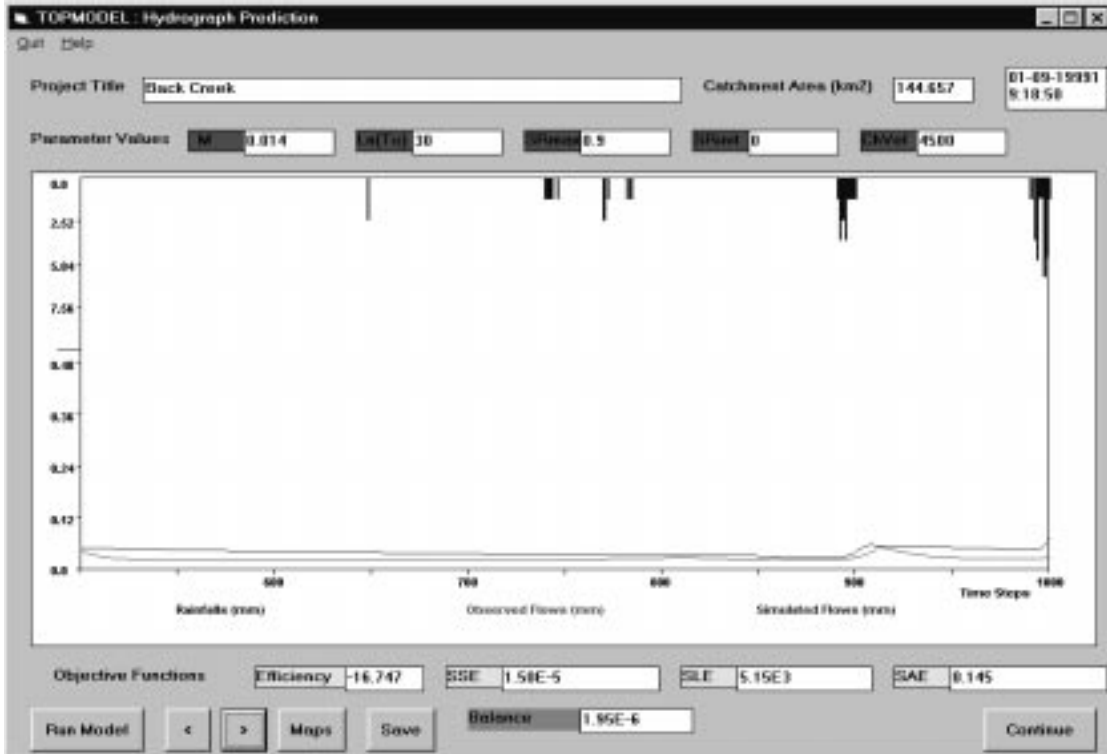


Figure F (2). 1996 water year, second 500 hour interval of first 2500 hour interval.

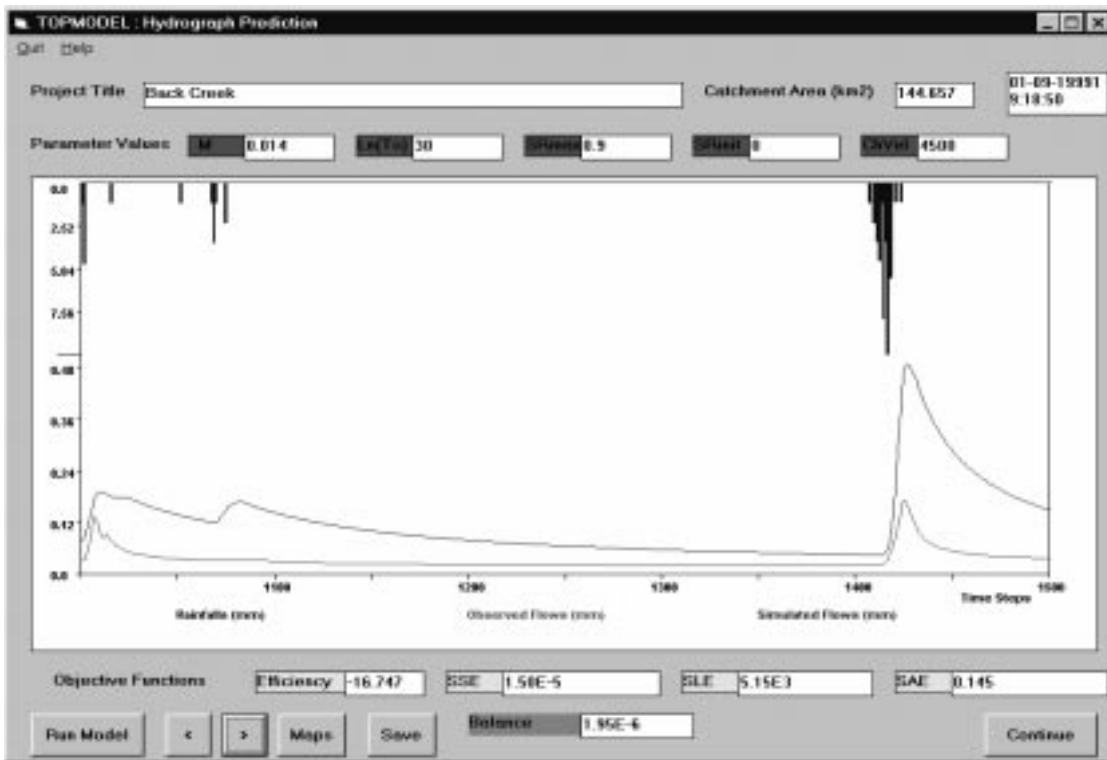


Figure F (3). 1996 water year, third 500 hour interval of first 2500 hour interval.

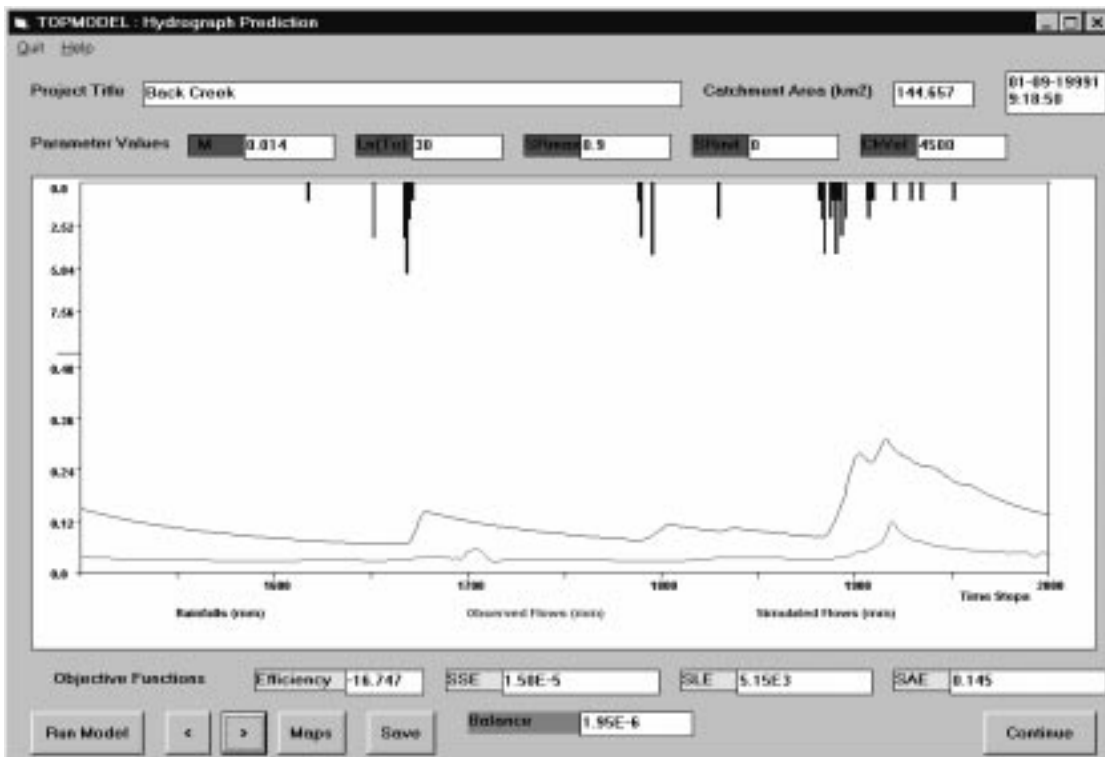


Figure F (4). 1996 water year, fourth 500 hour interval of first 2500 hour interval.

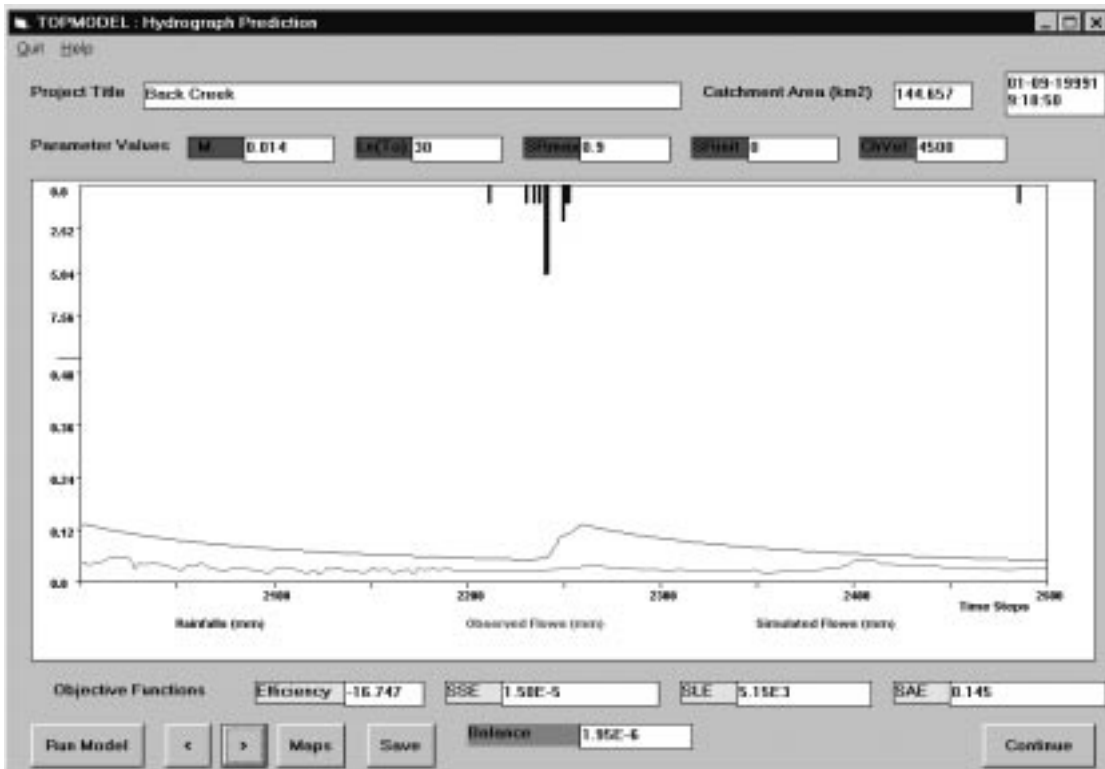


Figure F (5). 1996 water year, fifth 500 hour interval of first 2500 hour interval.

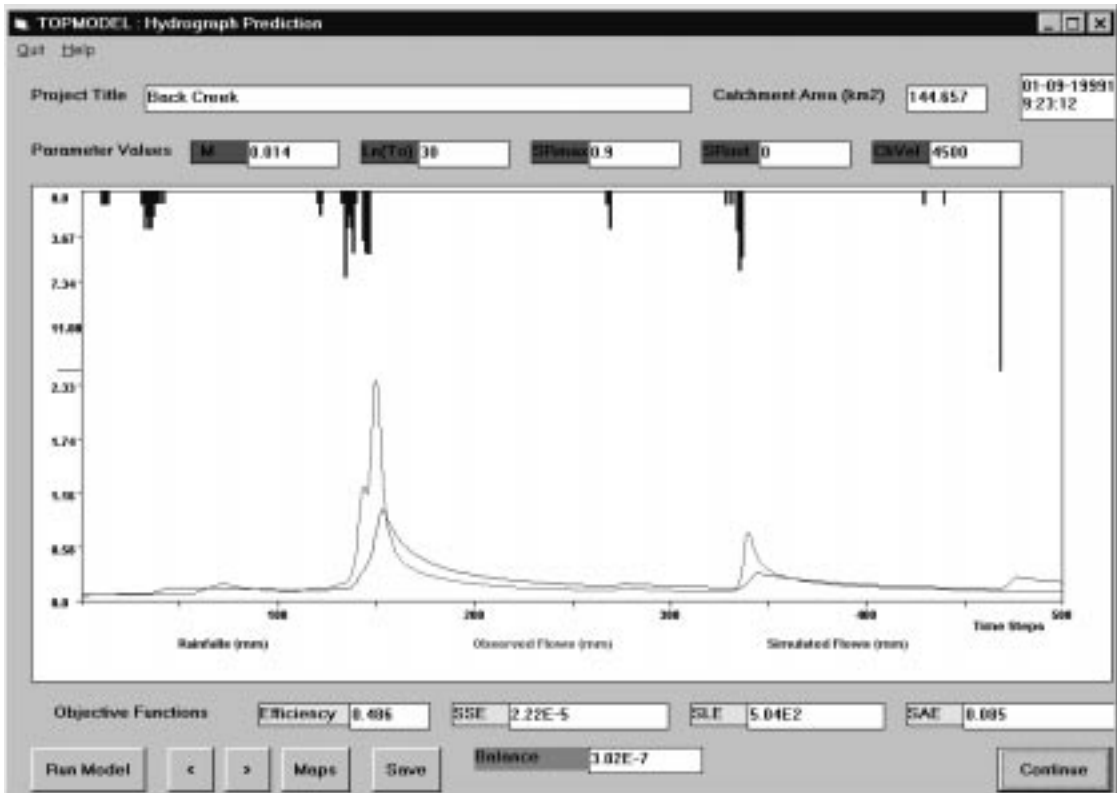


Figure F (6). 1996 water year, first 500 hour interval of second 2500 hour interval.

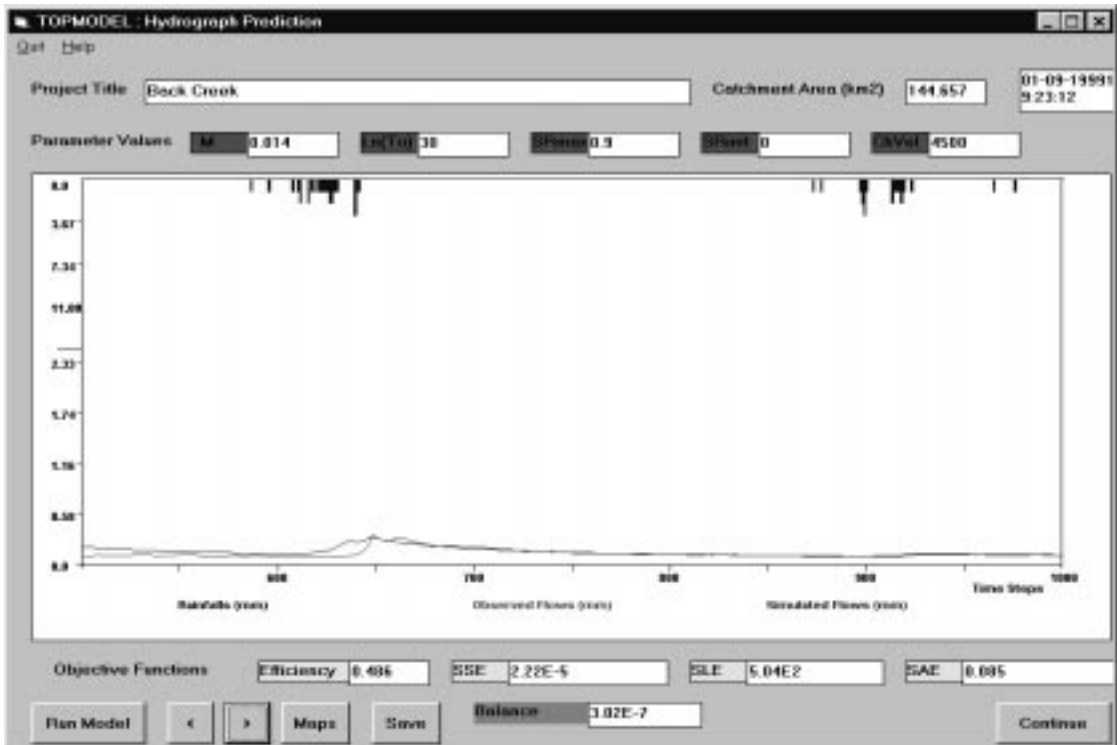


Figure F (7). 1996 water year, second 500 hour interval of second 2500 hour interval.

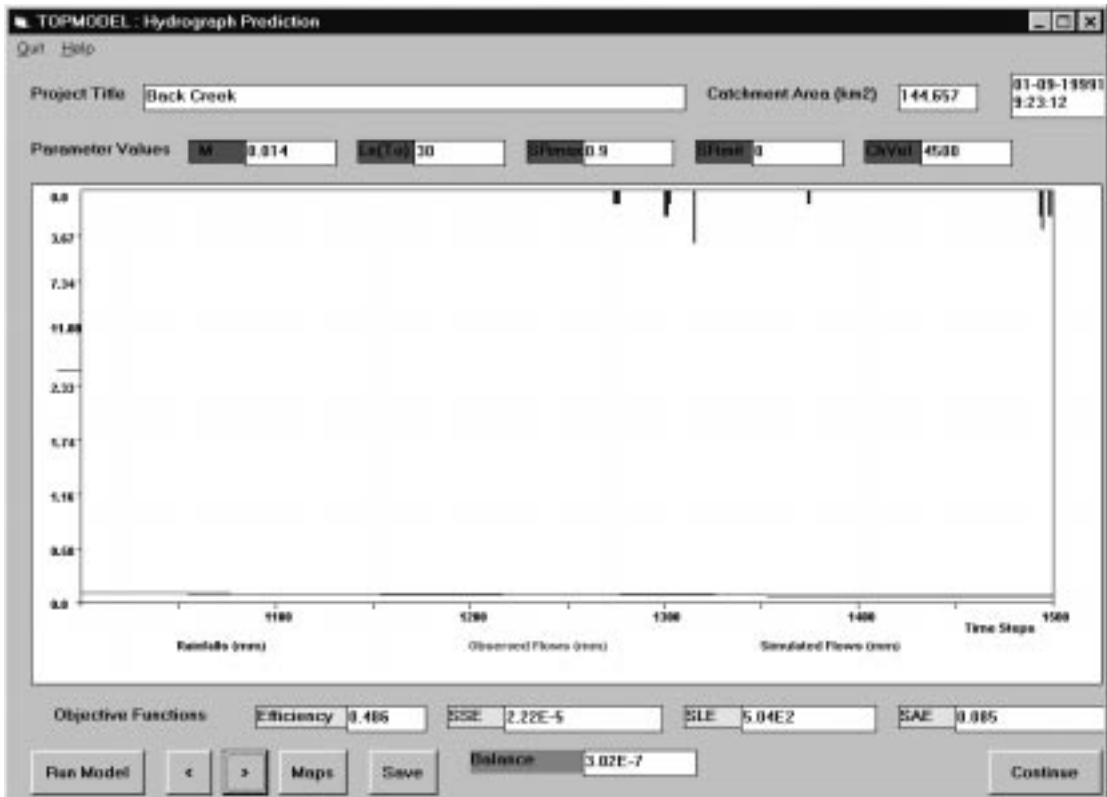


Figure F (8). 1996 water year, third 500 hour interval of second 2500 hour interval.

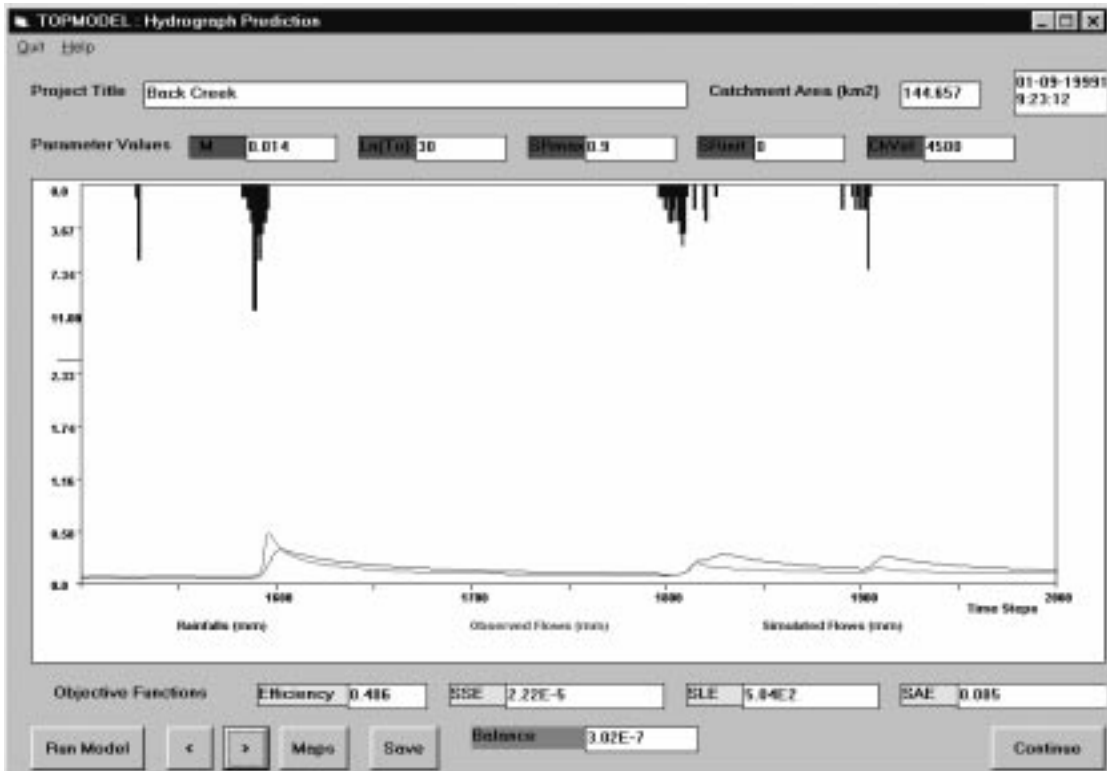


Figure F (9). 1996 water year, fourth 500 hour interval of second 2500 hour interval.

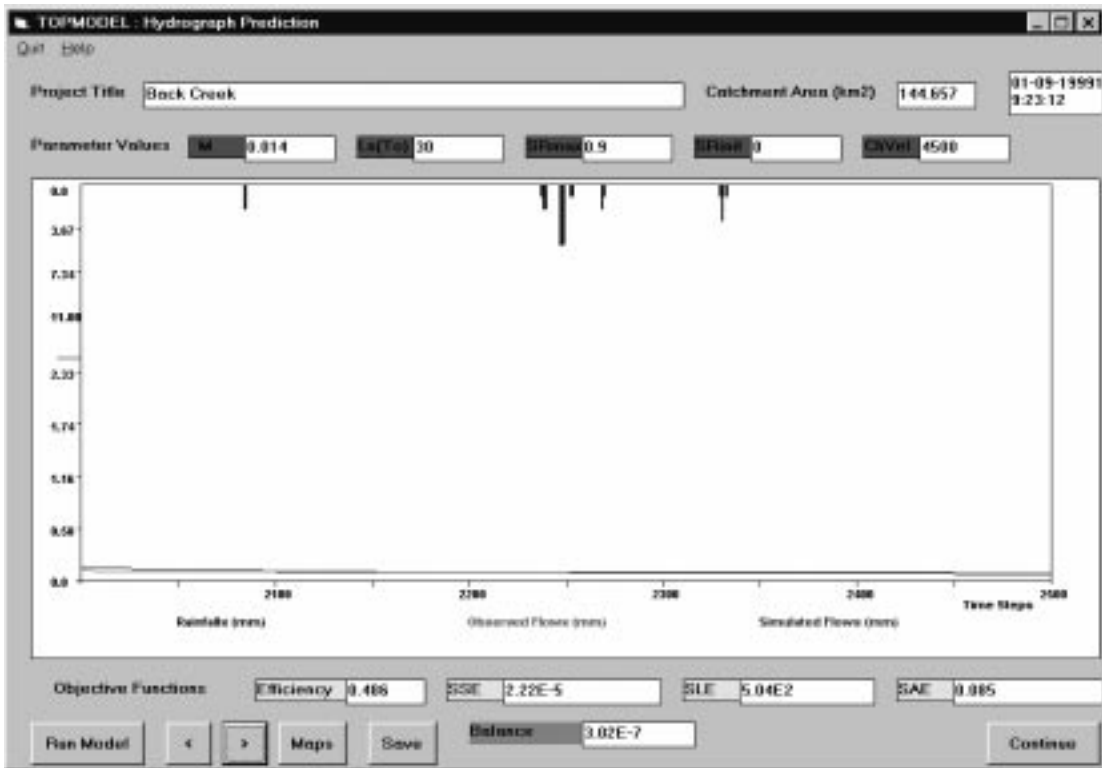


Figure F (10). 1996 water year, fifth 500 hour interval of second 2500 hour interval.

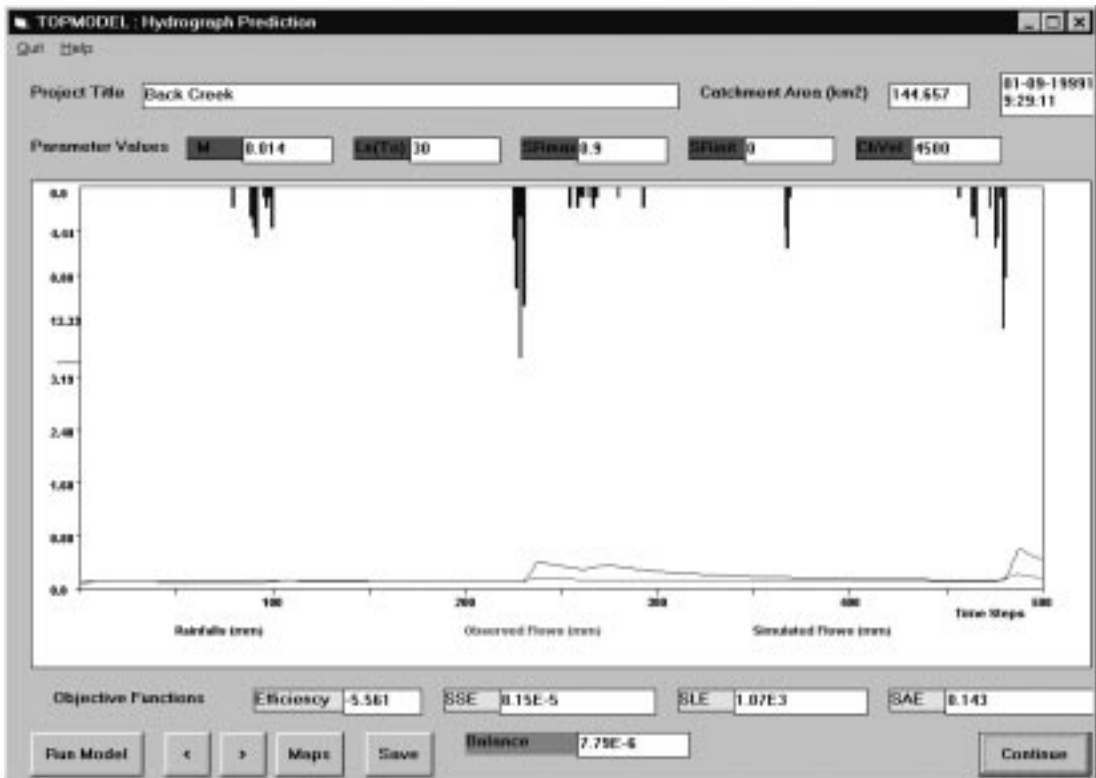


Figure F (11). 1996 water year, first 500 hour interval of third 2500 hour interval.

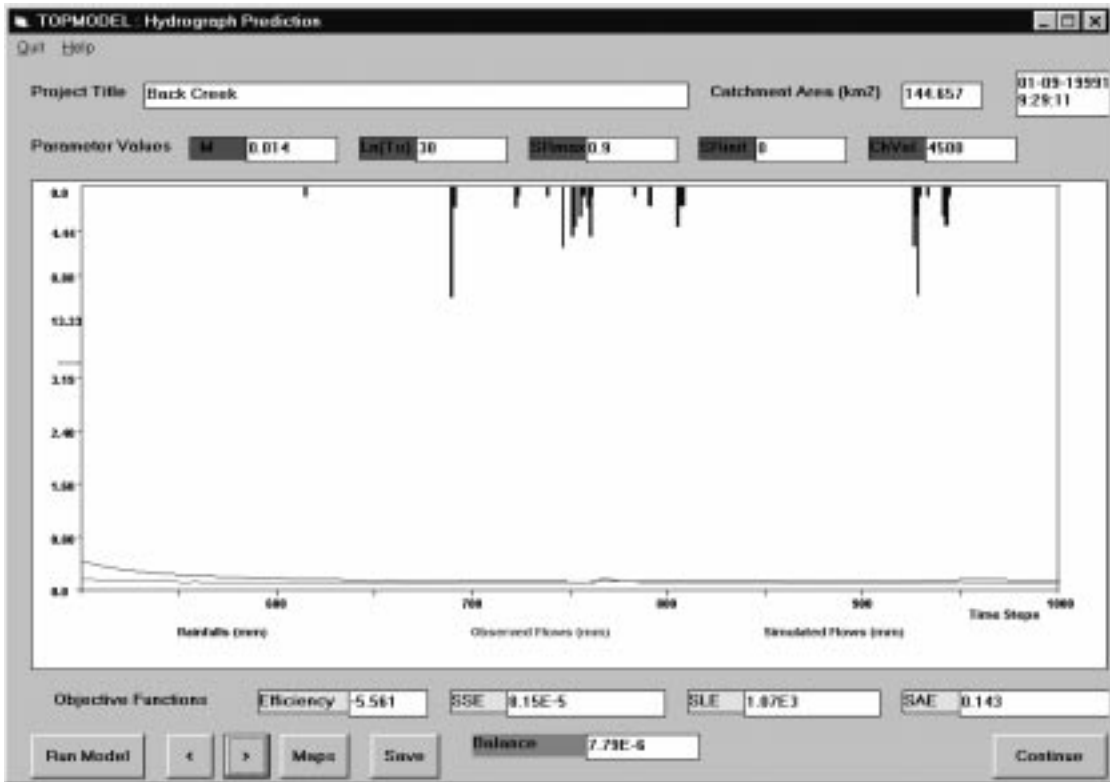


Figure F (12). 1996 water year, second 500 hour interval of third 2500 hour interval.

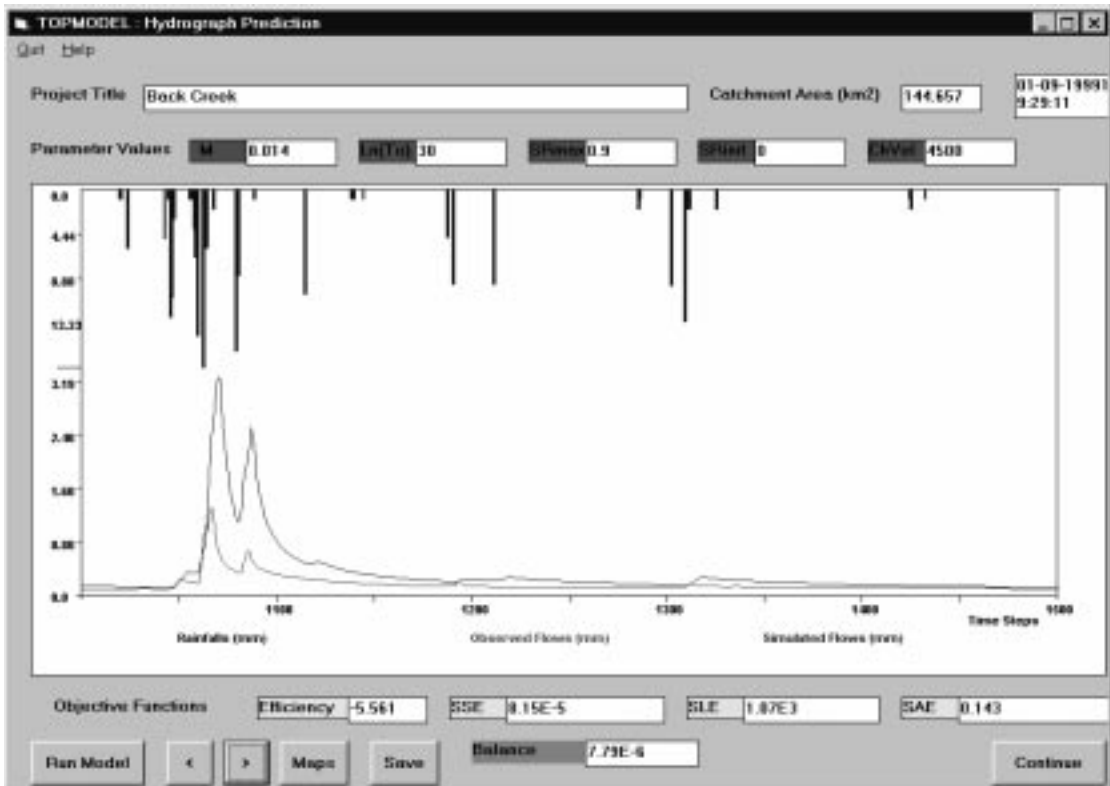


Figure F (13). 1996 water year, third 500 hour interval of third 2500 hour interval.

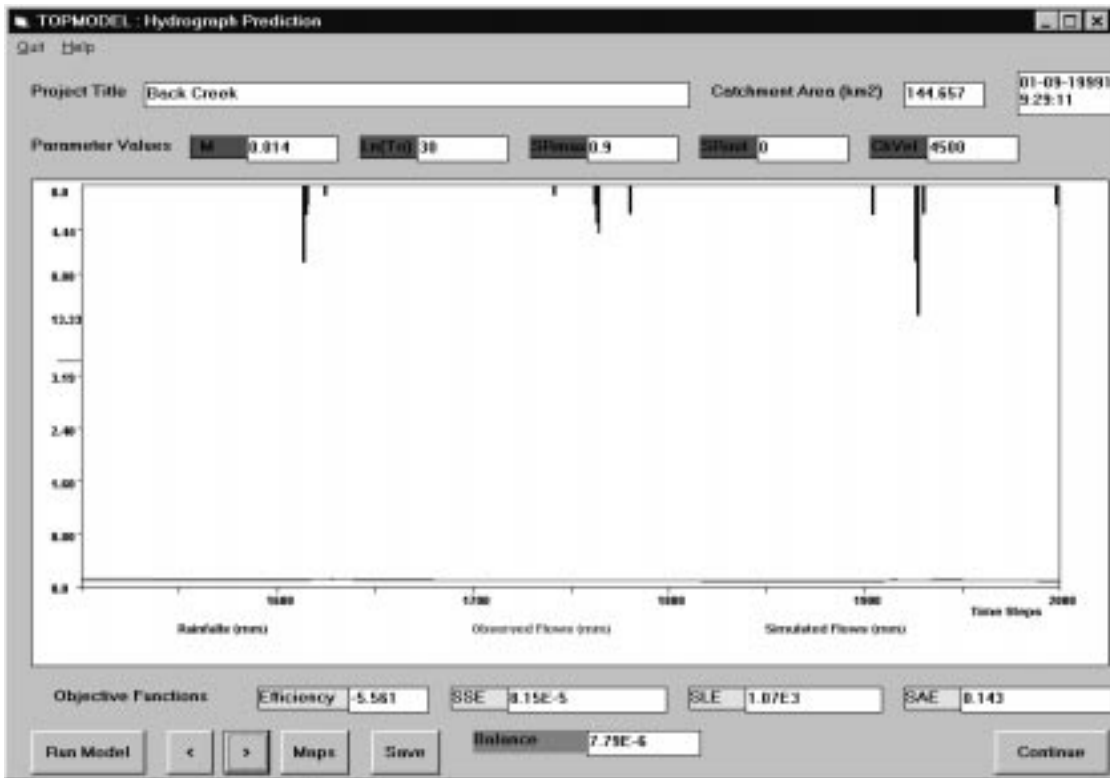


Figure F (14). 1996 water year, fourth 500 hour interval of third 2500 hour interval.

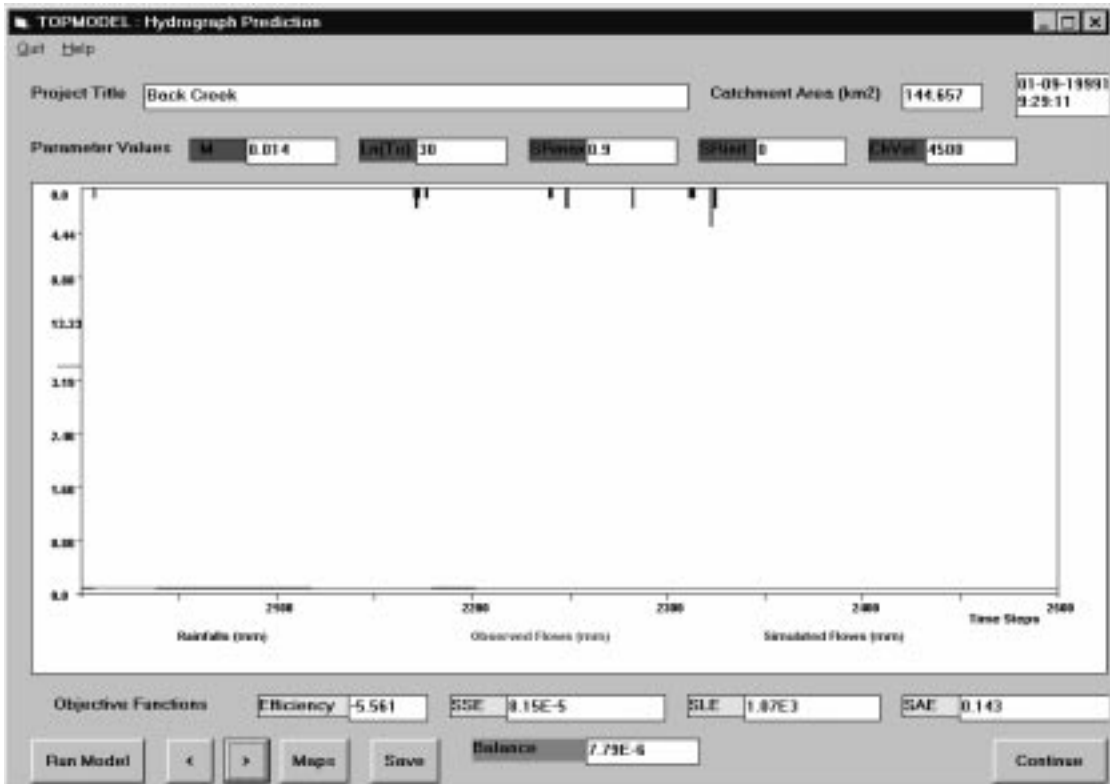


Figure F (15). 1996 water year, fifth 500 hour interval of third 2500 hour interval.

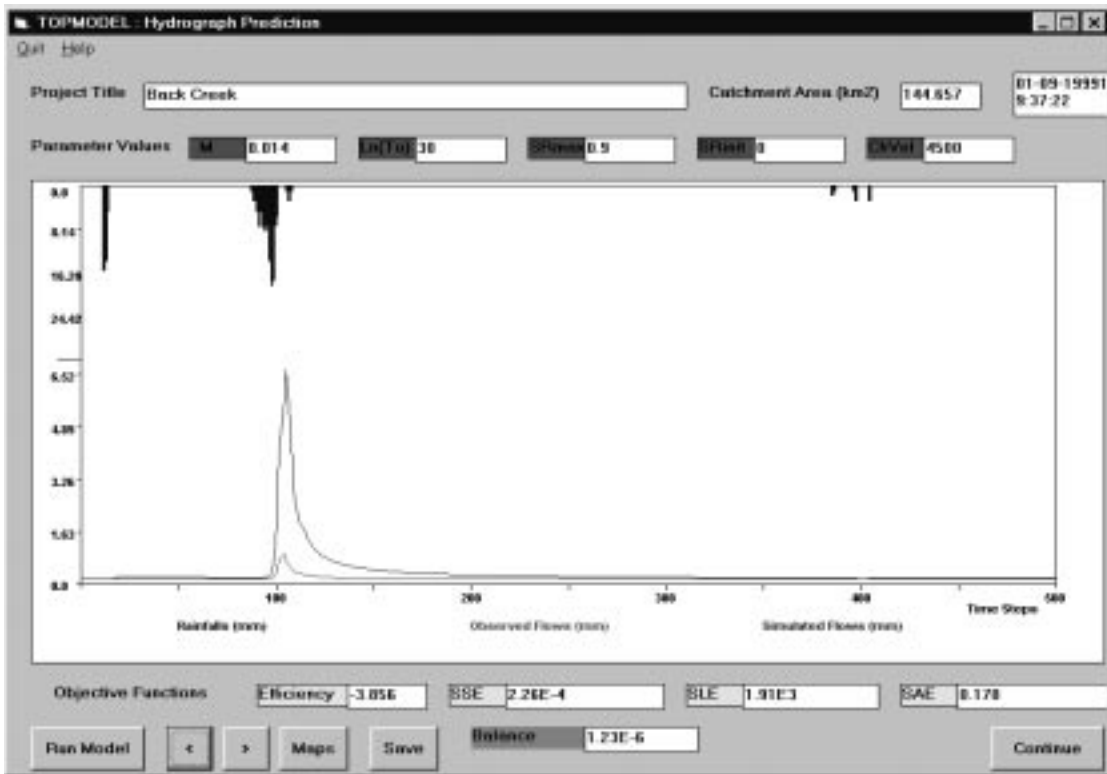


Figure F (16). 1996 water year, first 500 hour interval of forth 2500 hour interval.

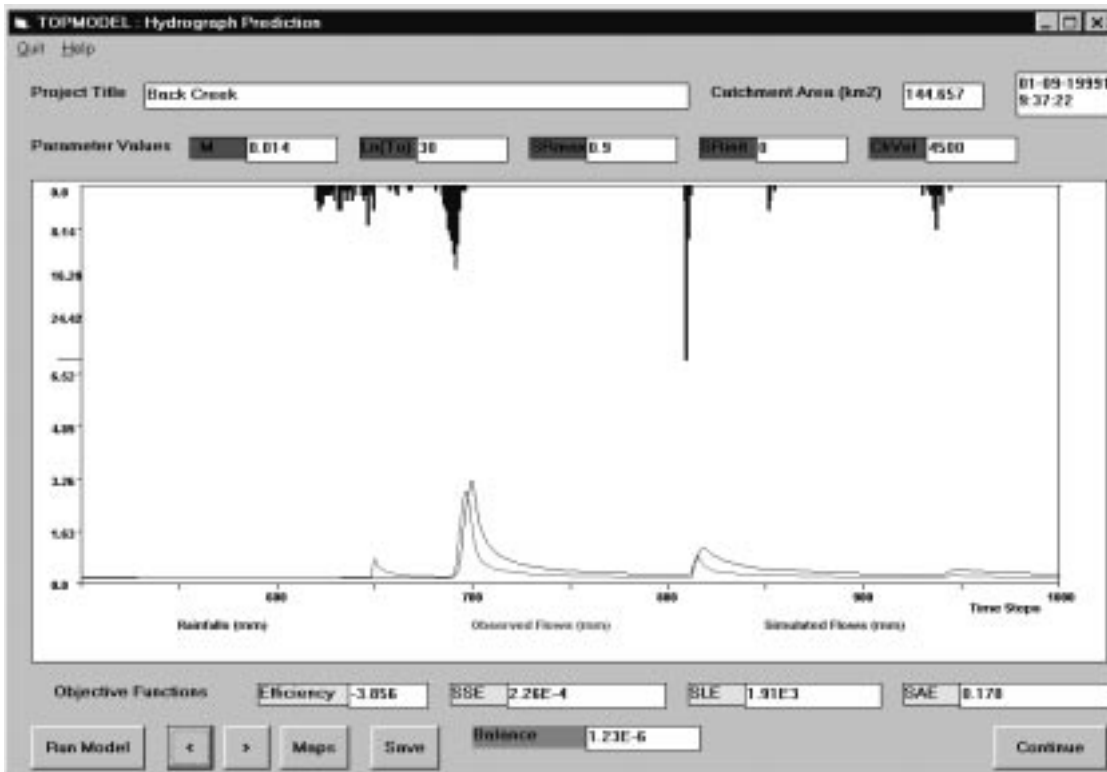


Figure F (17). 1996 water year, second 500 hour interval of forth 2500 hour interval.

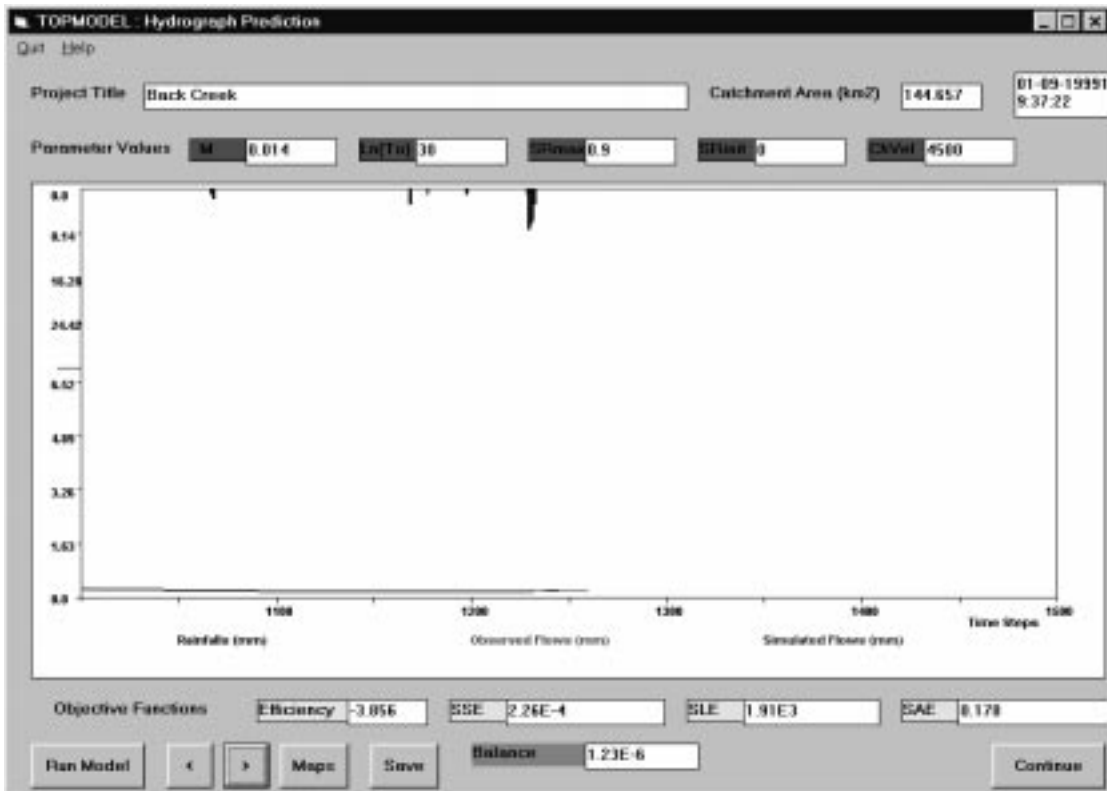


Figure F (18). 1996 water year, third 500 hour interval of forth 2500 hour interval.

# Appendix G

## 1997 TOPMODEL Hydrographs

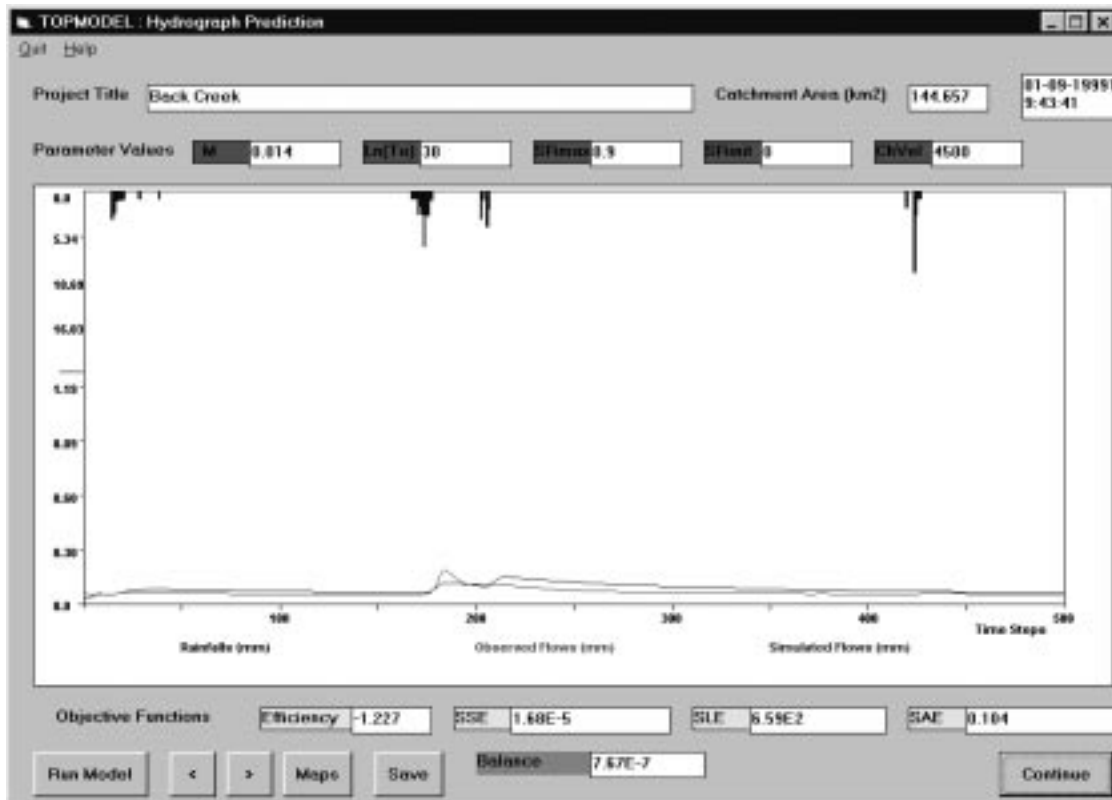


Figure G (1). 1997 water year, first 500 hour interval of first 2500 hour interval.

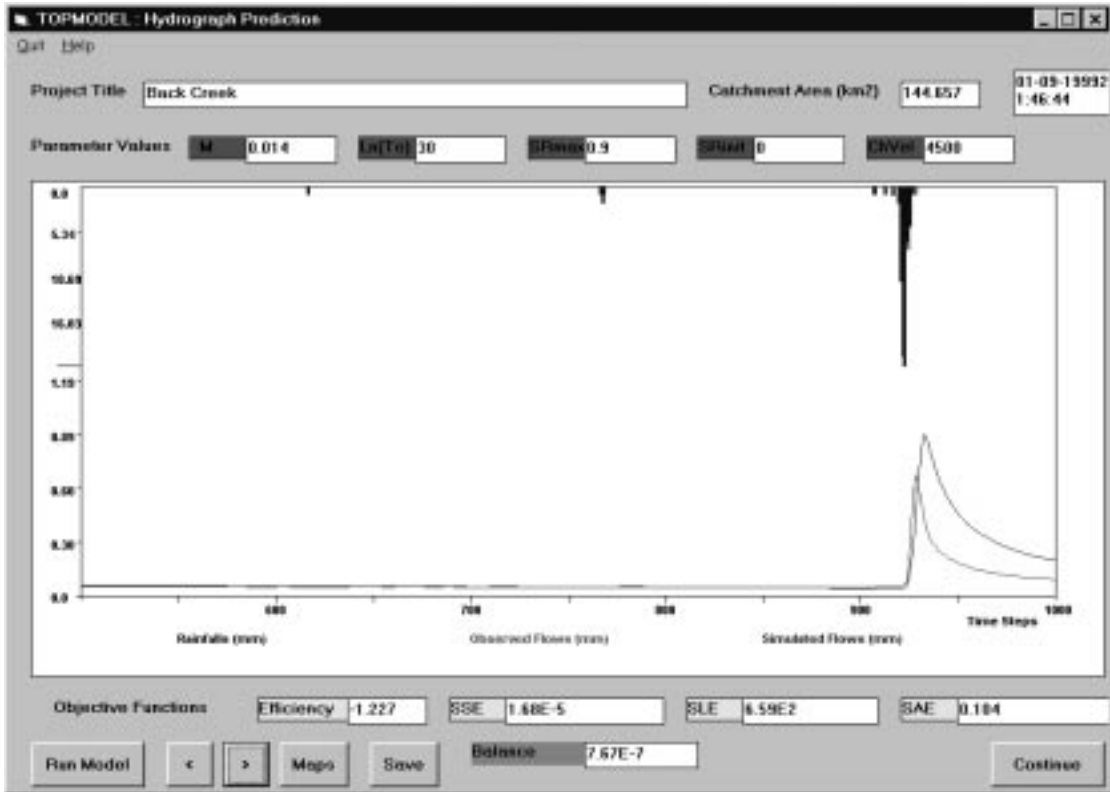


Figure G (2). 1997 water year, second 500 hour interval of first 2500 hour interval.

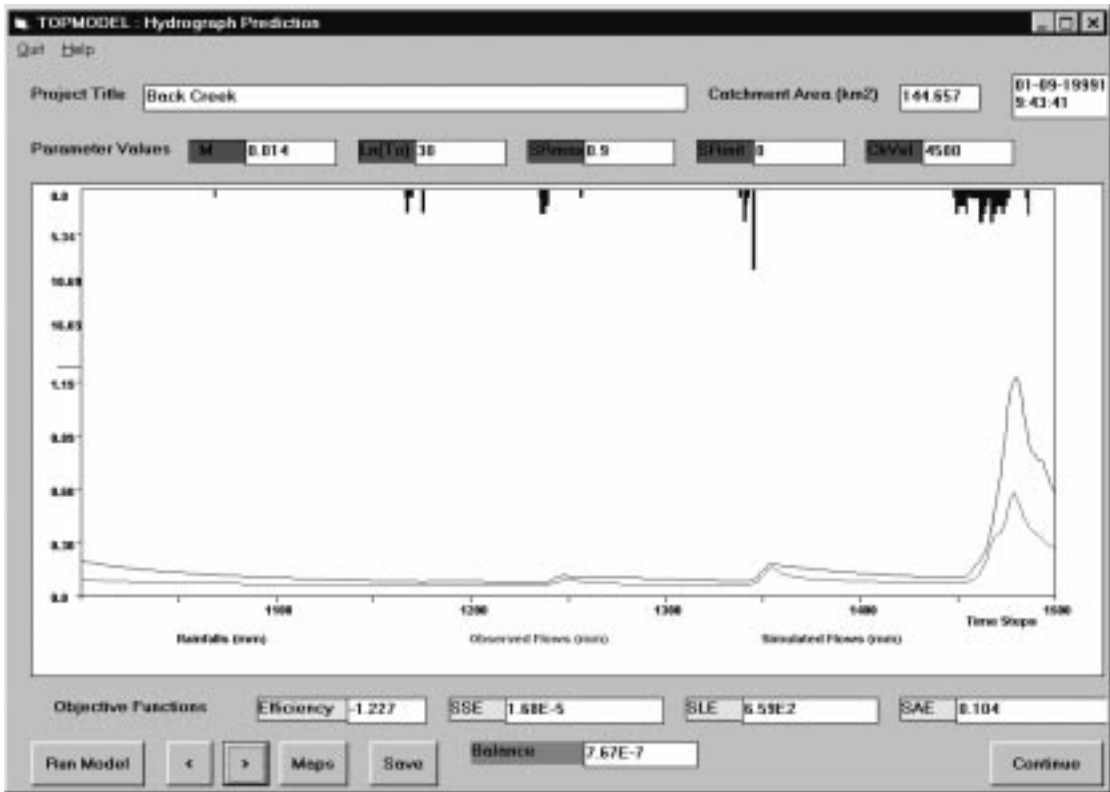


Figure G (3). 1997 water year, third 500 hour interval of first 2500 hour interval.

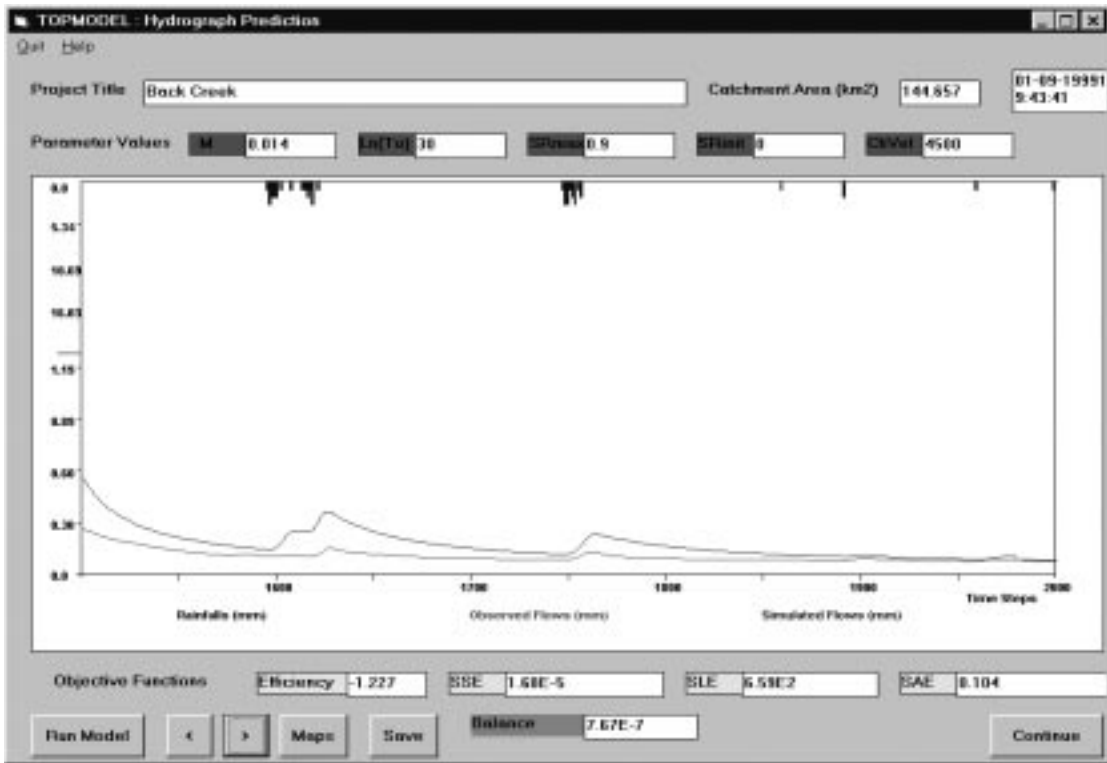


Figure G (4). 1997 water year, fourth 500 hour interval of first 2500 hour interval.

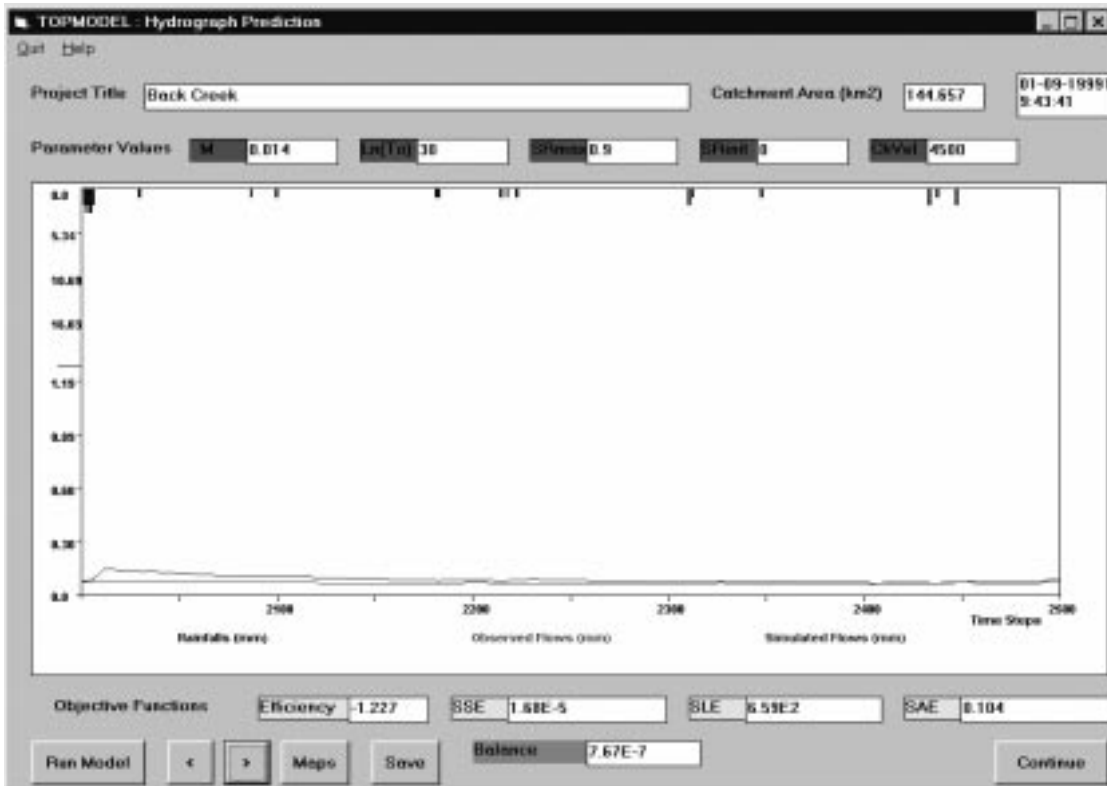


Figure G (5). 1997 water year, fifth 500 hour interval of first 2500 hour interval.

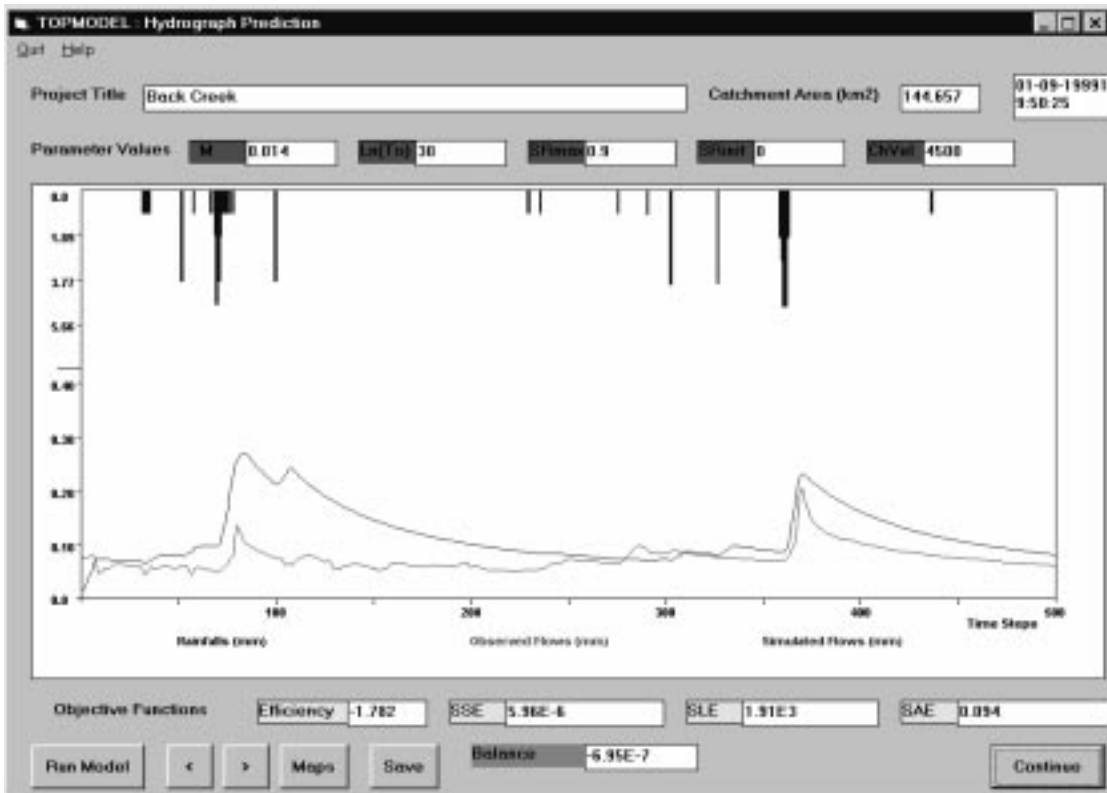


Figure G (6). 1997 water year, first 500 hour interval of second 2500 hour interval.

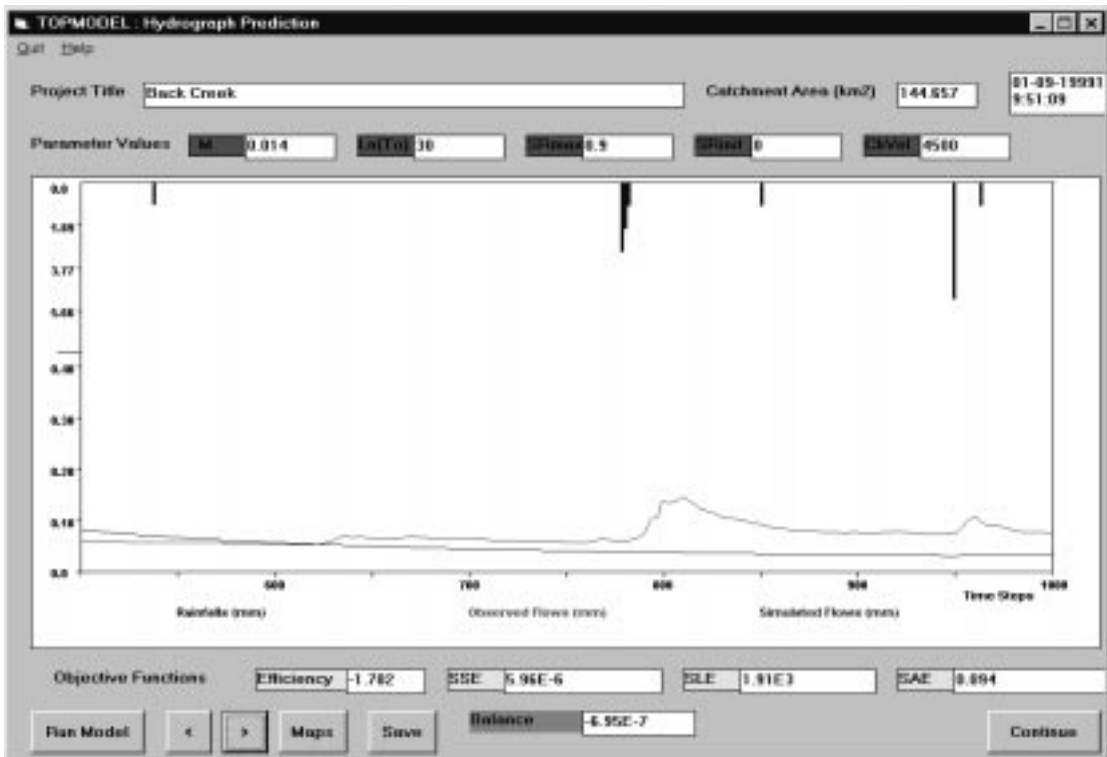


Figure G (7). 1997 water year, second 500 hour interval of second 2500 hour interval.

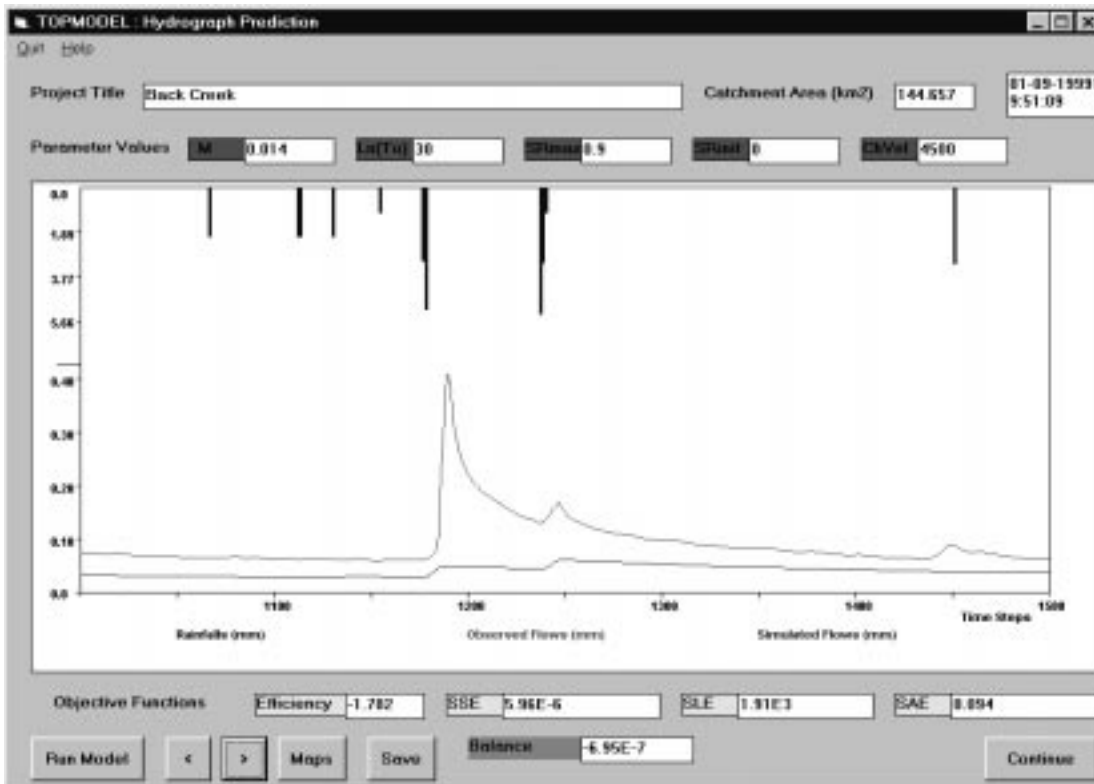


Figure G (8). 1997 water year, third 500 hour interval of second 2500 hour interval.

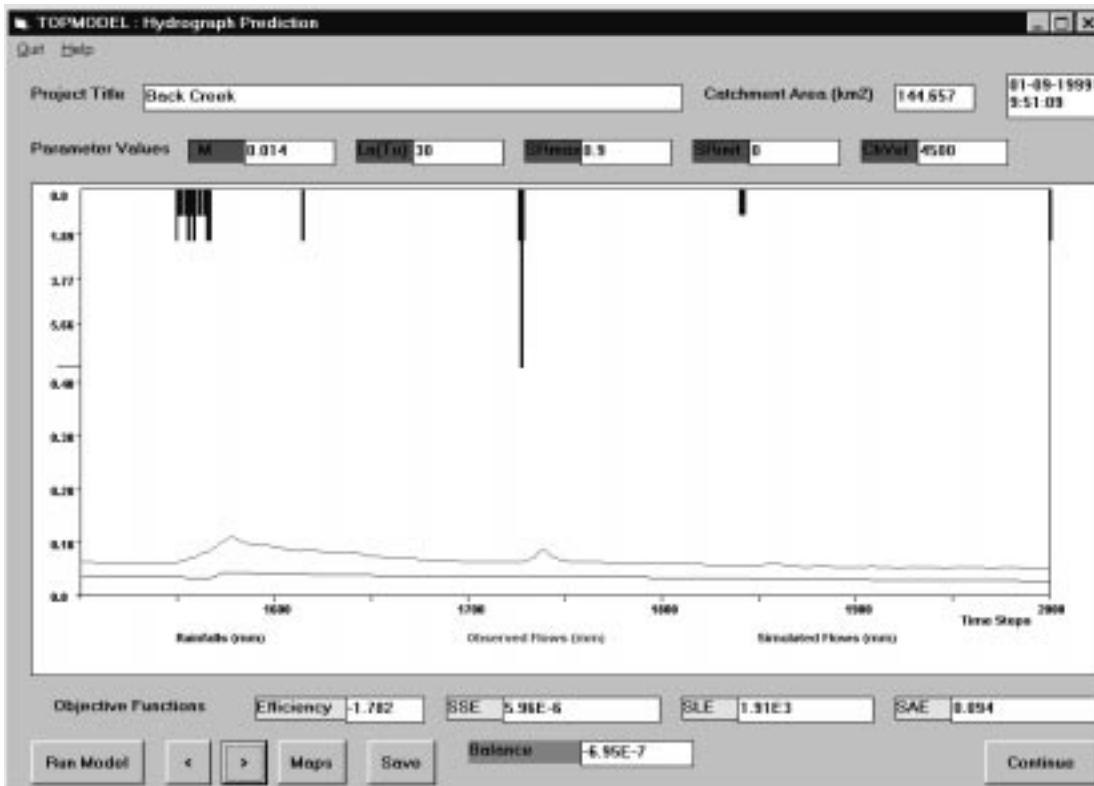


Figure G (9). 1997 water year, fourth 500 hour interval of second 2500 hour interval.

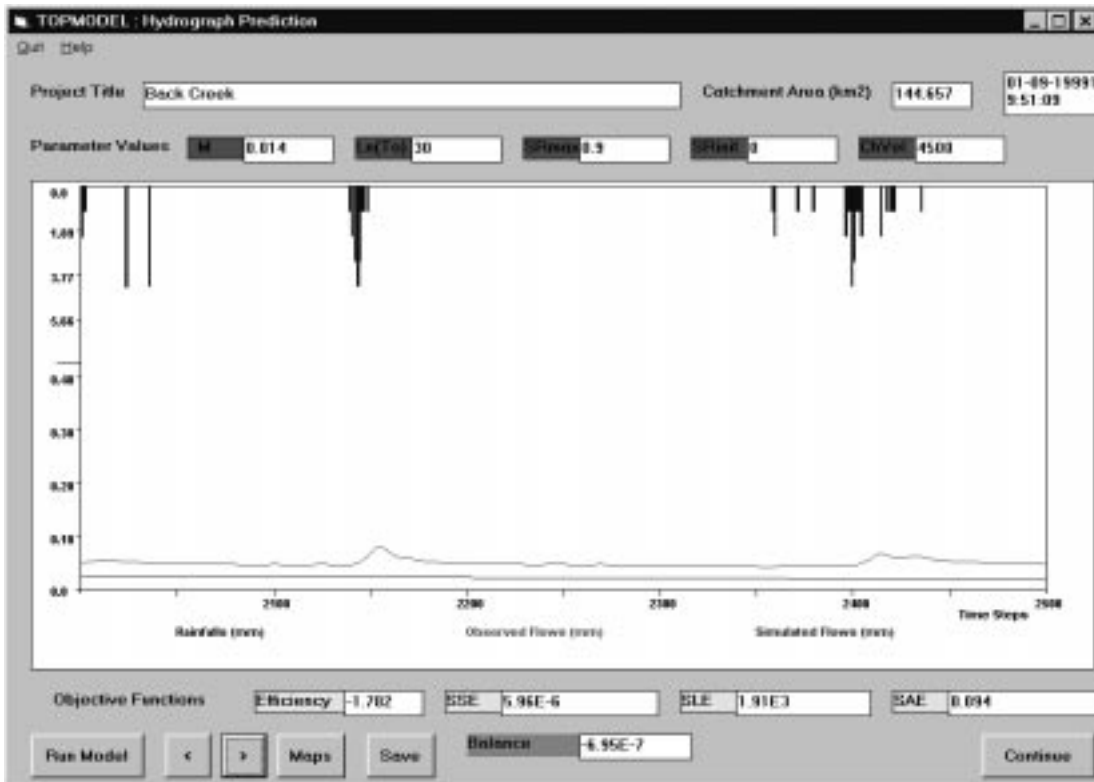


Figure G (10). 1997 water year, fifth 500 hour interval of second 2500 hour interval.

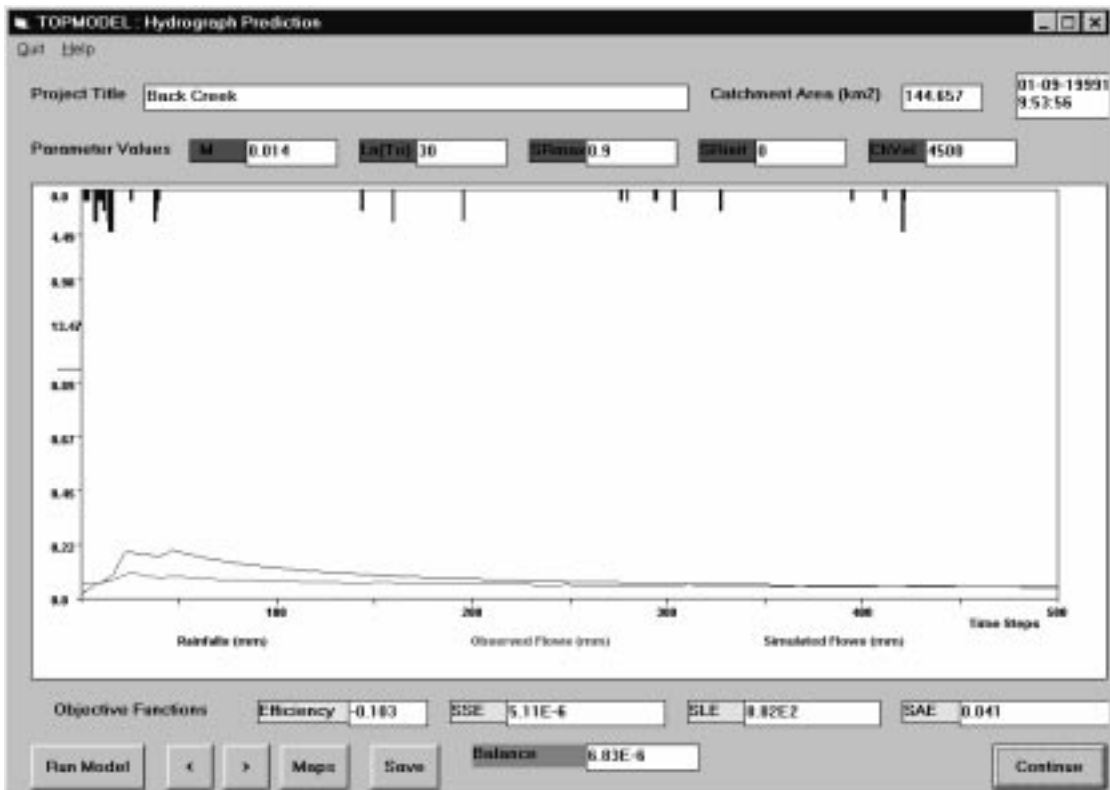


Figure G (11). 1997 water year, first 500 hour interval of third 2500 hour interval.

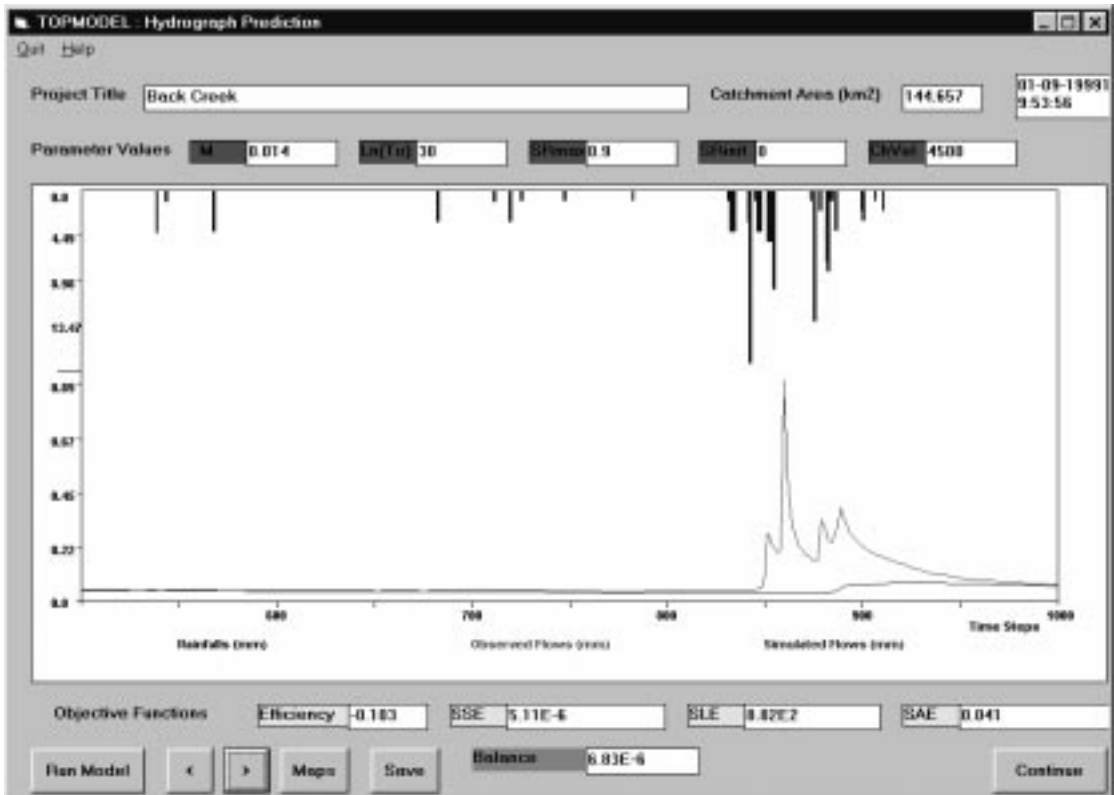


Figure G (12). 1997 water year, second 500 hour interval of third 2500 hour interval.

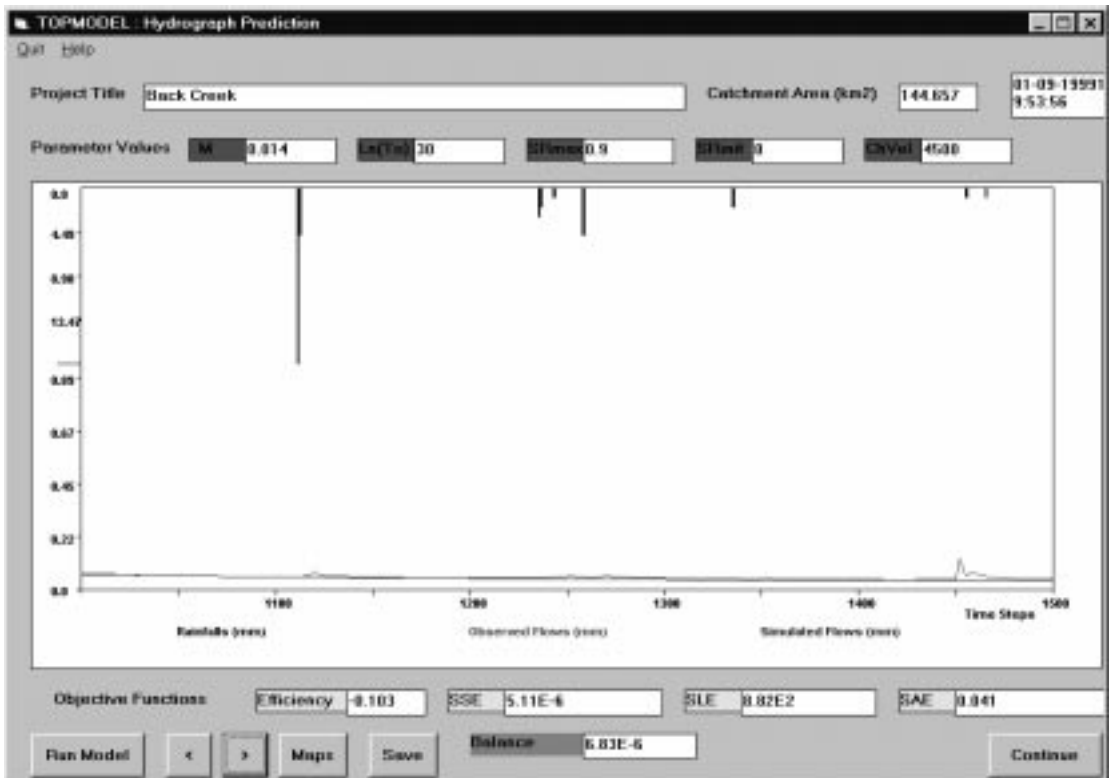


Figure G (13). 1997 water year, third 500 hour interval of third 2500 hour interval.

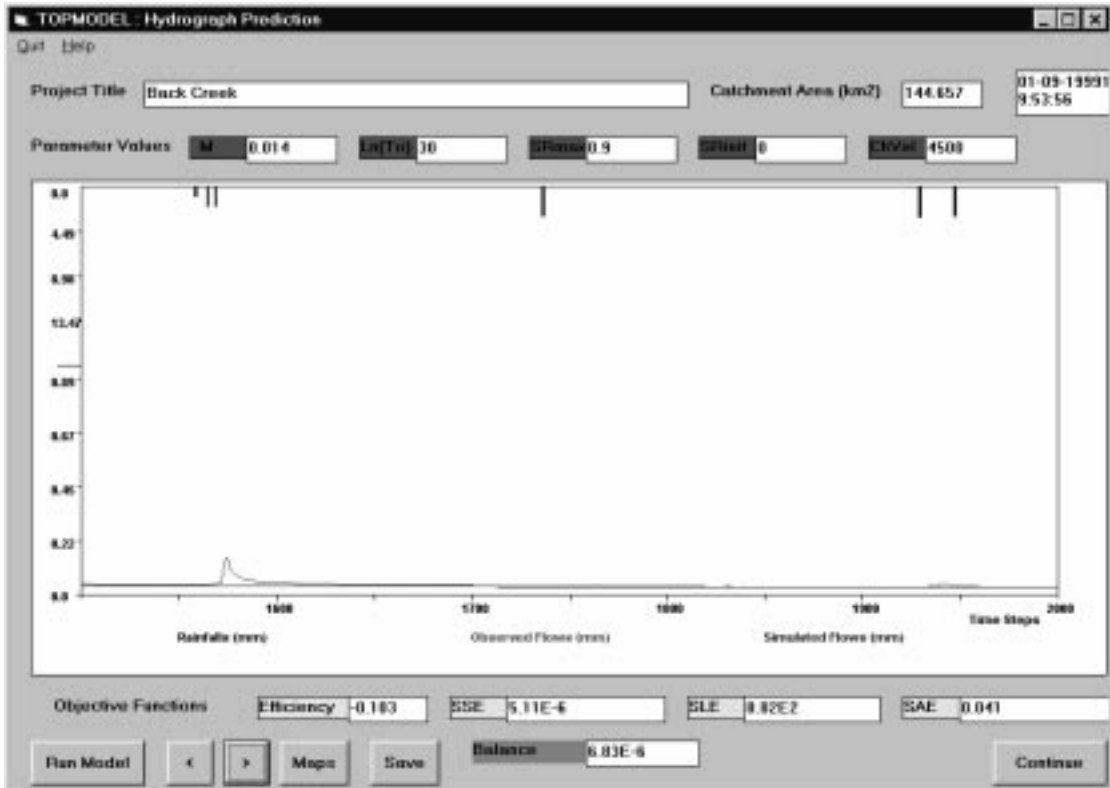


Figure G (14). 1997 water year, fourth 500 hour interval of third 2500 hour interval.

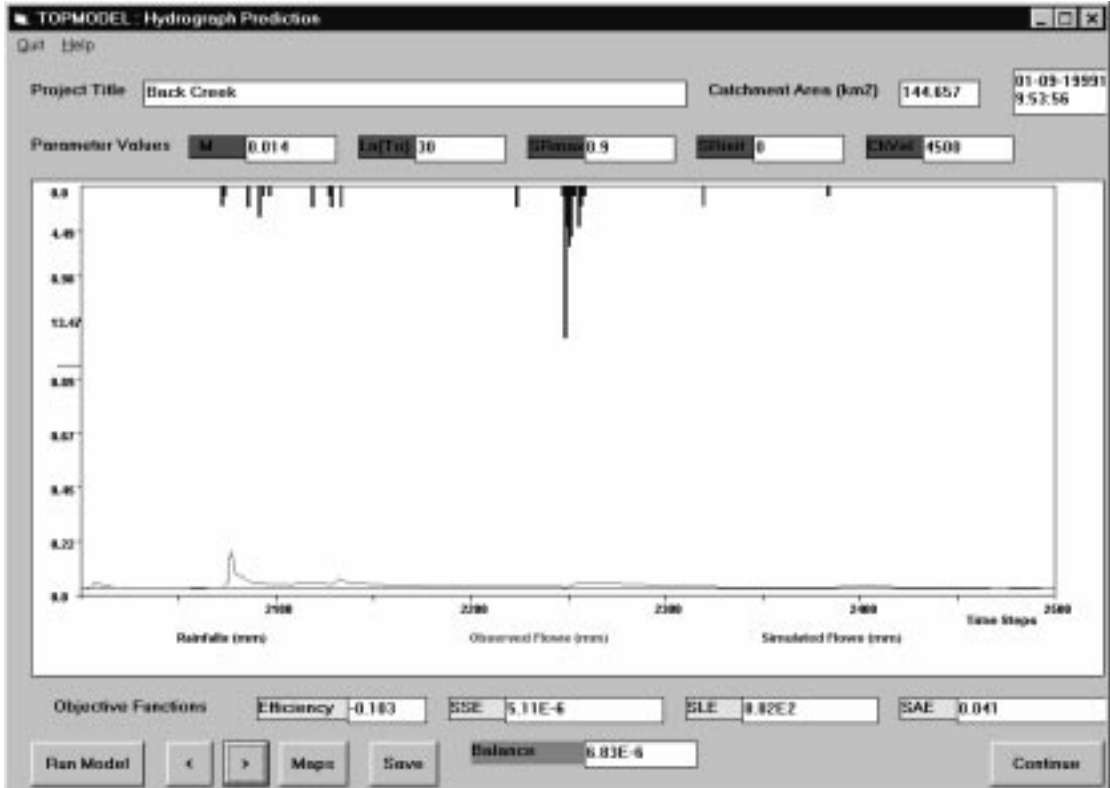


Figure G (15). 1997 water year, fifth 500 hour interval of third 2500 hour interval.

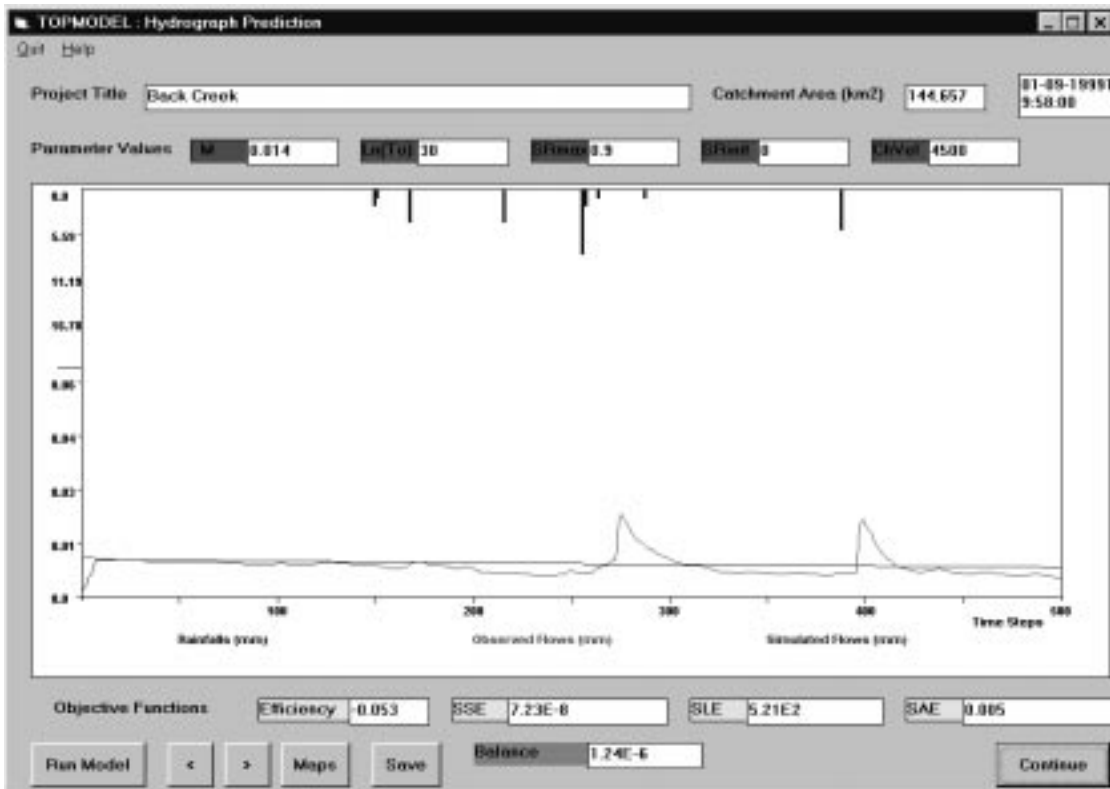


Figure G (16). 1997 water year, first 500 hour interval of forth 2500 hour interval.

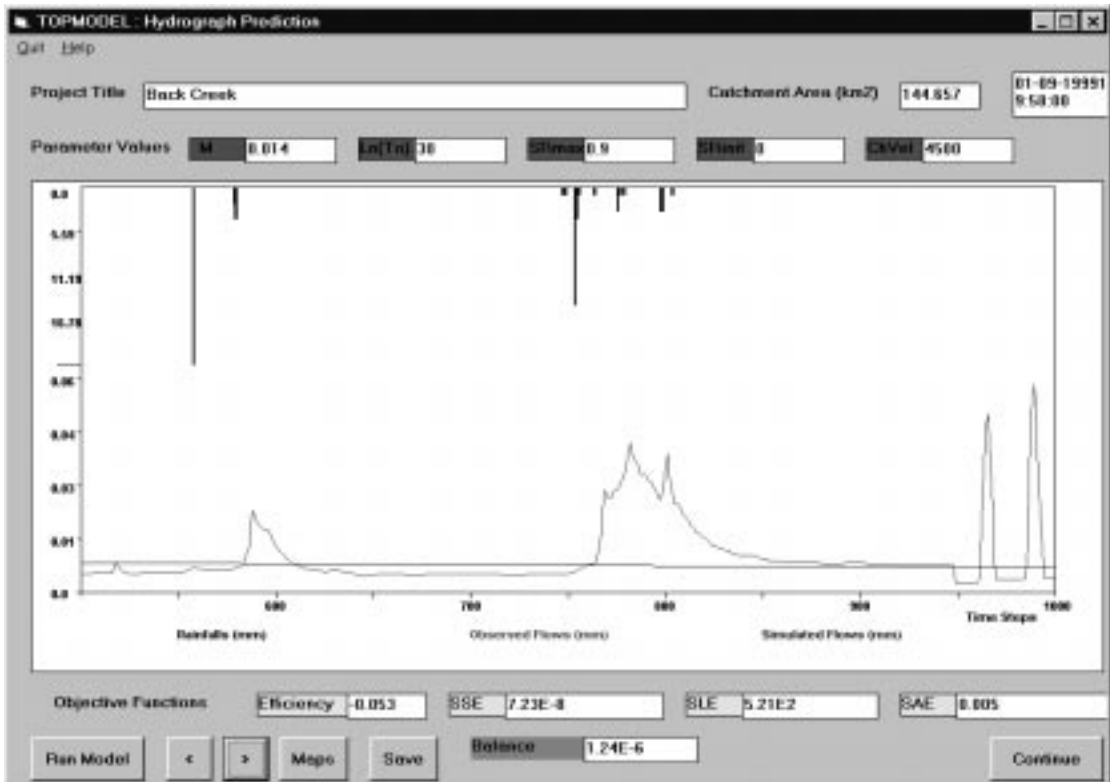


Figure G (17). 1997 water year, second 500 hour interval of forth 2500 hour interval.

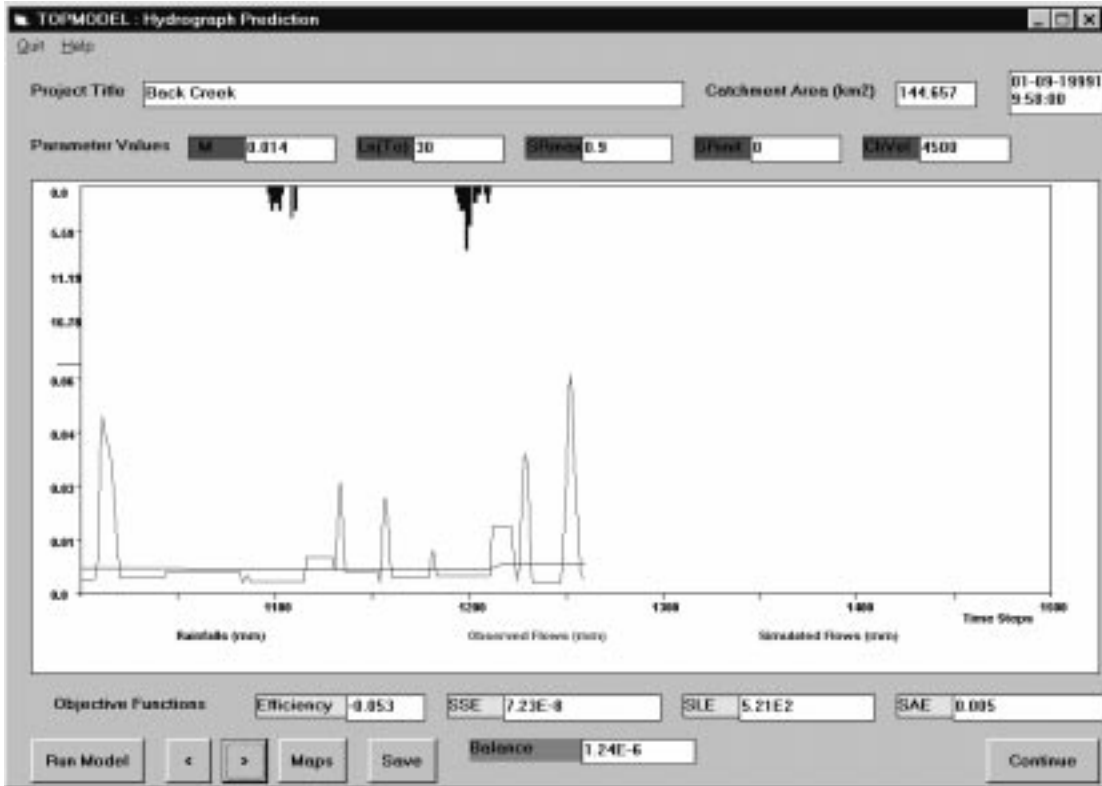


Figure G (18). 1997 water year, third 500 hour interval of forth 2500 hour interval.

# Appendix H

## HEC-1 Hydrographs

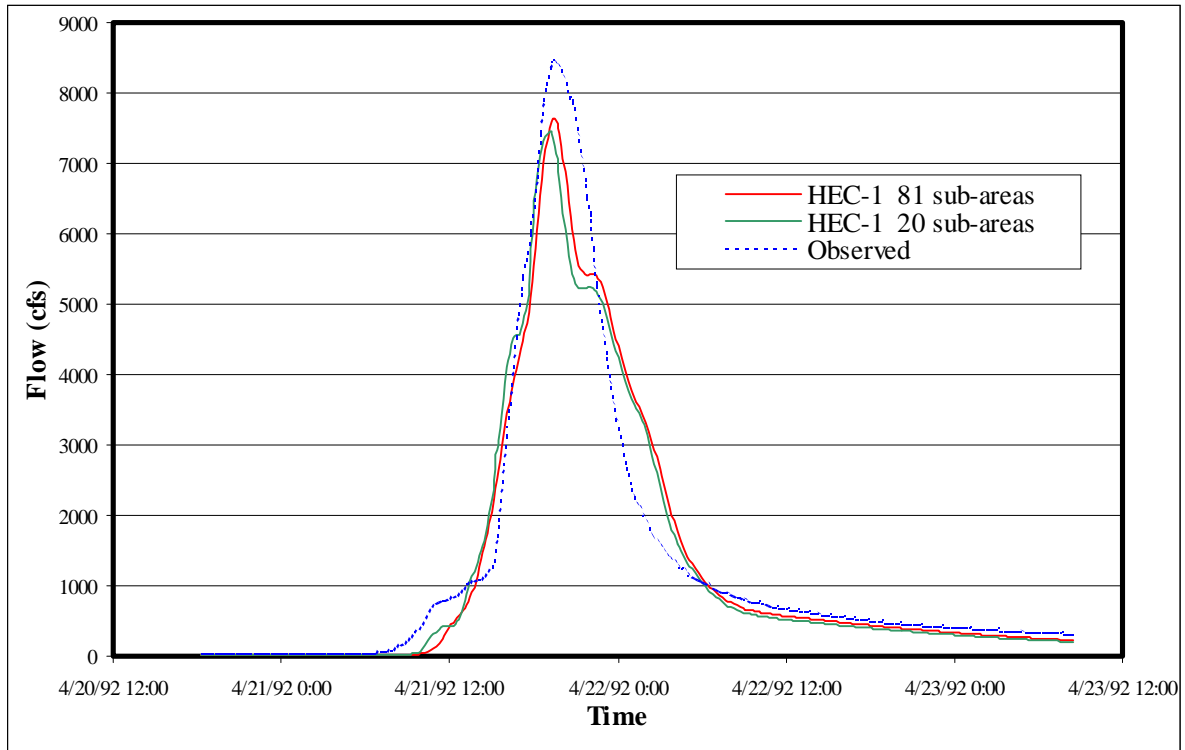


Figure H (1). April 1992 event; HEC-1 simulation.

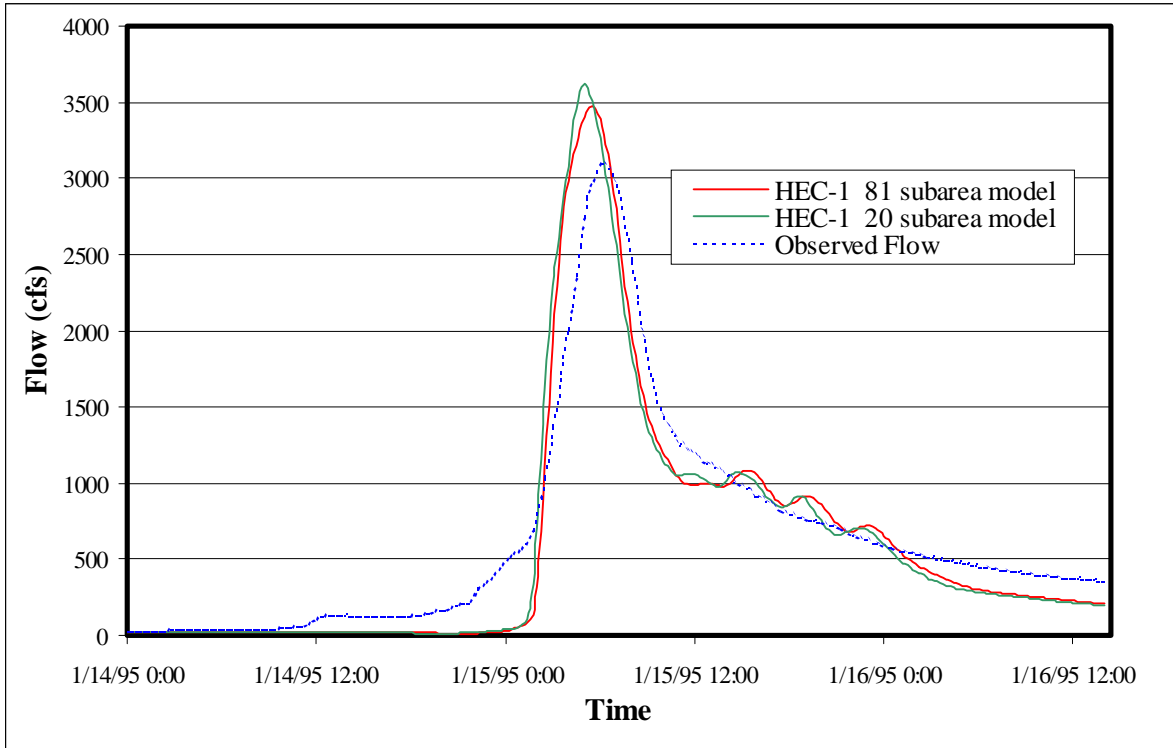


Figure H (2). January 1995 event; HEC-1 simulation.

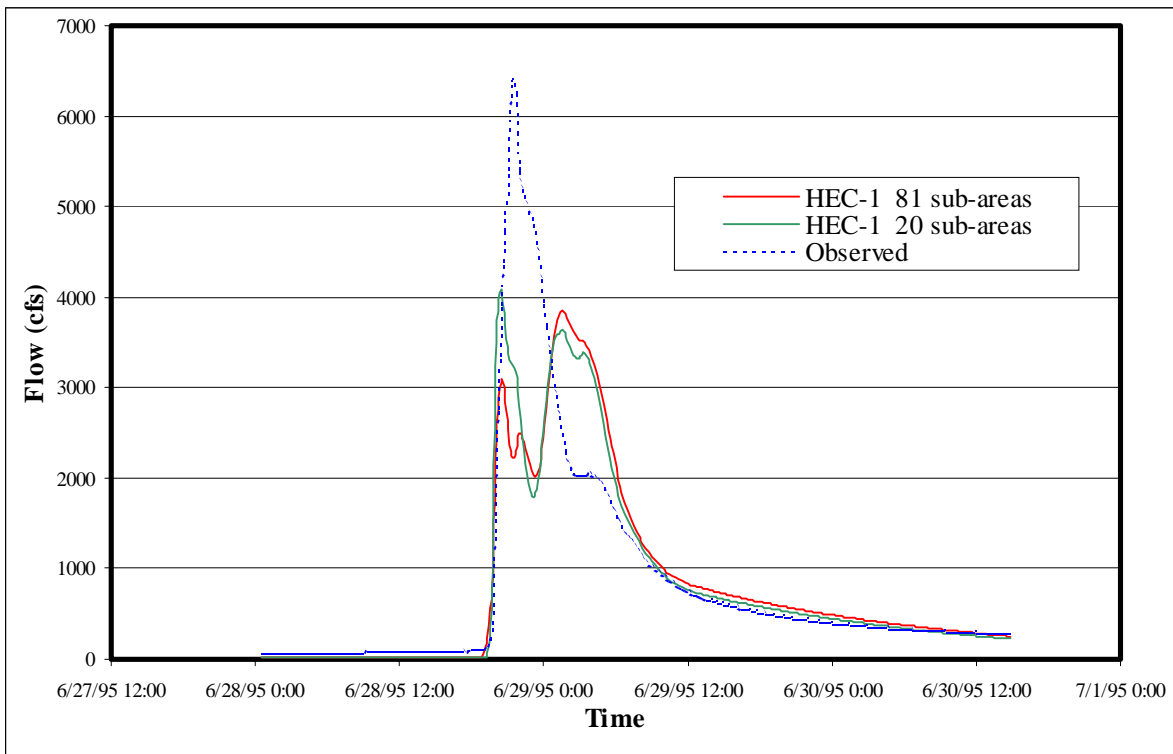


Figure H (3). June 1995 event; HEC-1 simulation.

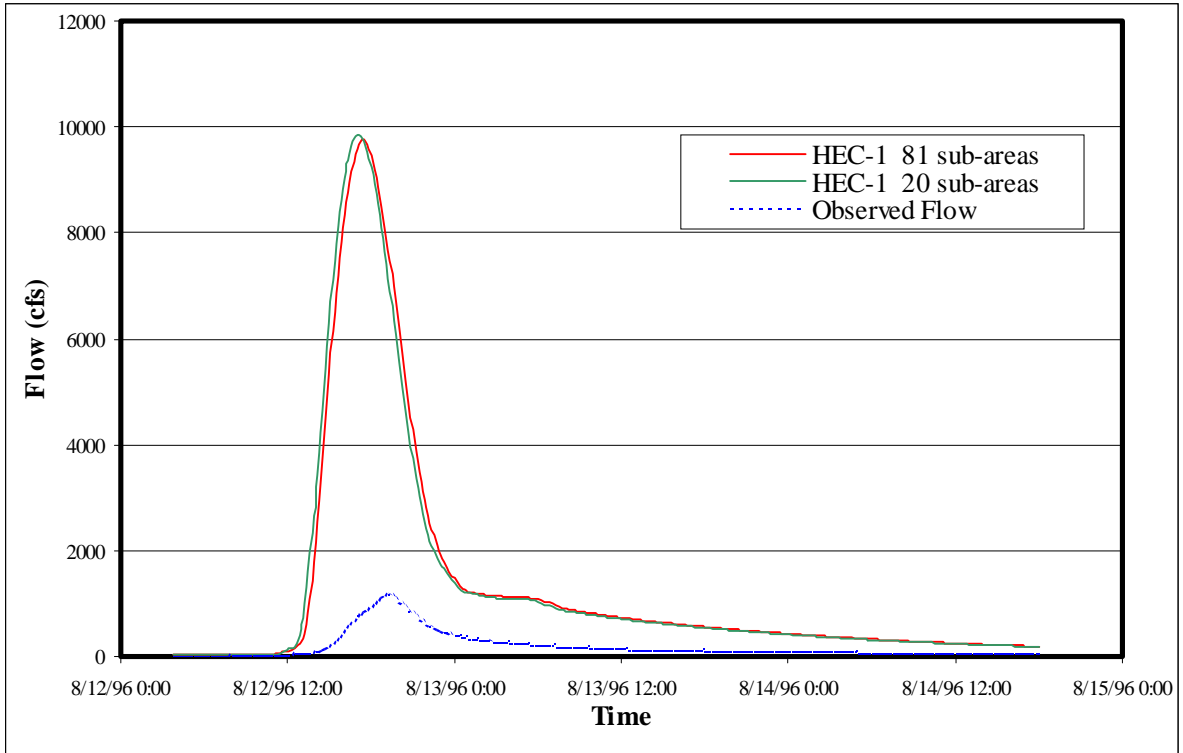


Figure H (4). August 1996 event; HEC-1 simulation.

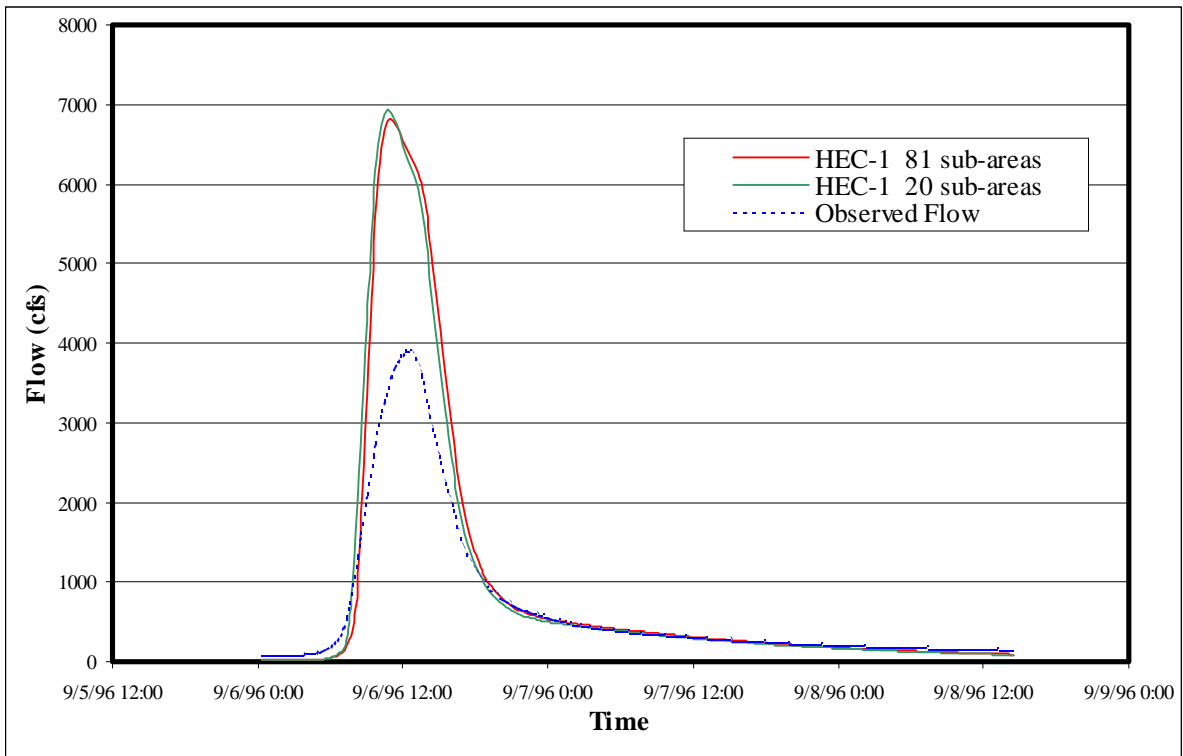


Figure H (5). September 1996 event; HEC-1 simulation.

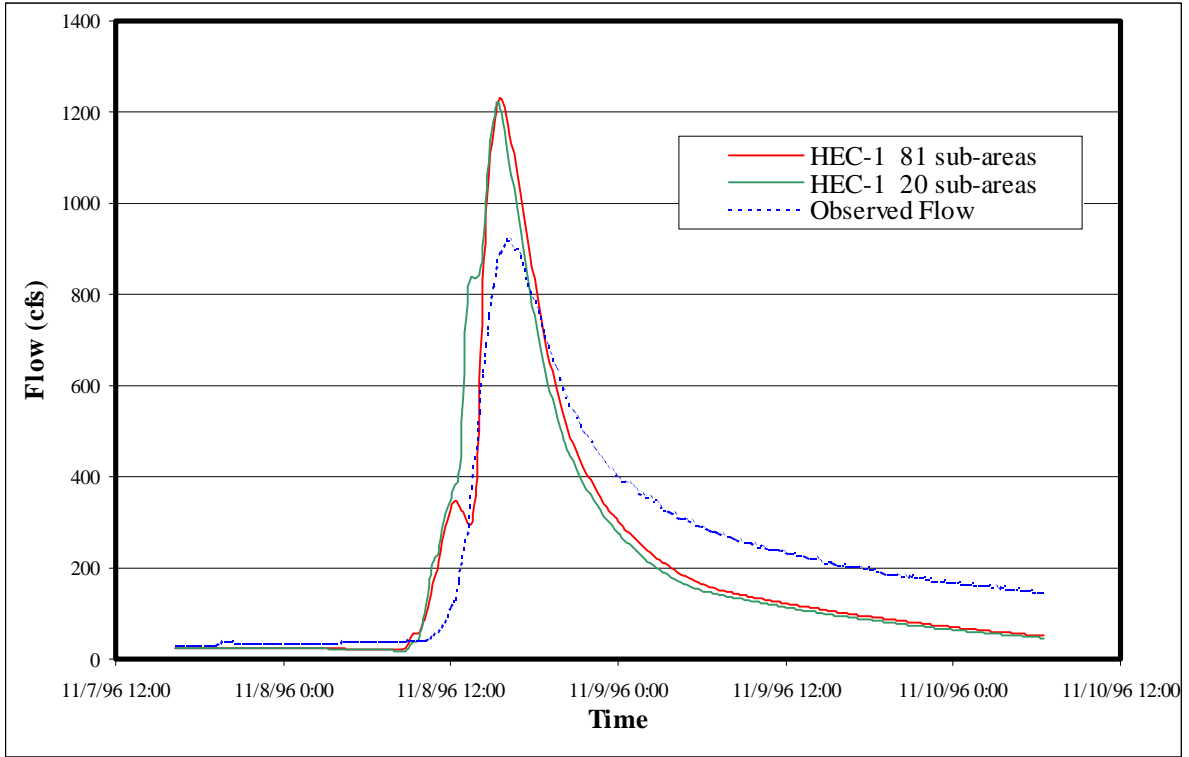


Figure H (6). November 1996 event; HEC-1 simulation.

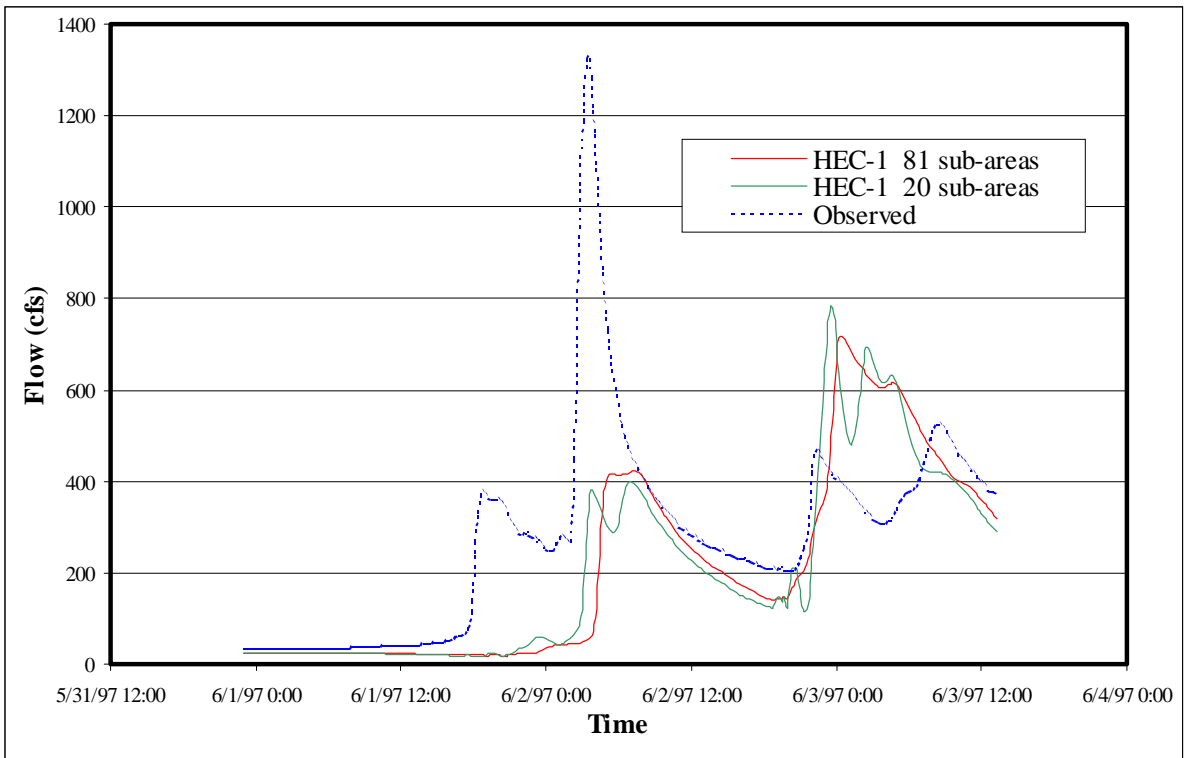


Figure H (7). June 1997 event; HEC-1 simulation.

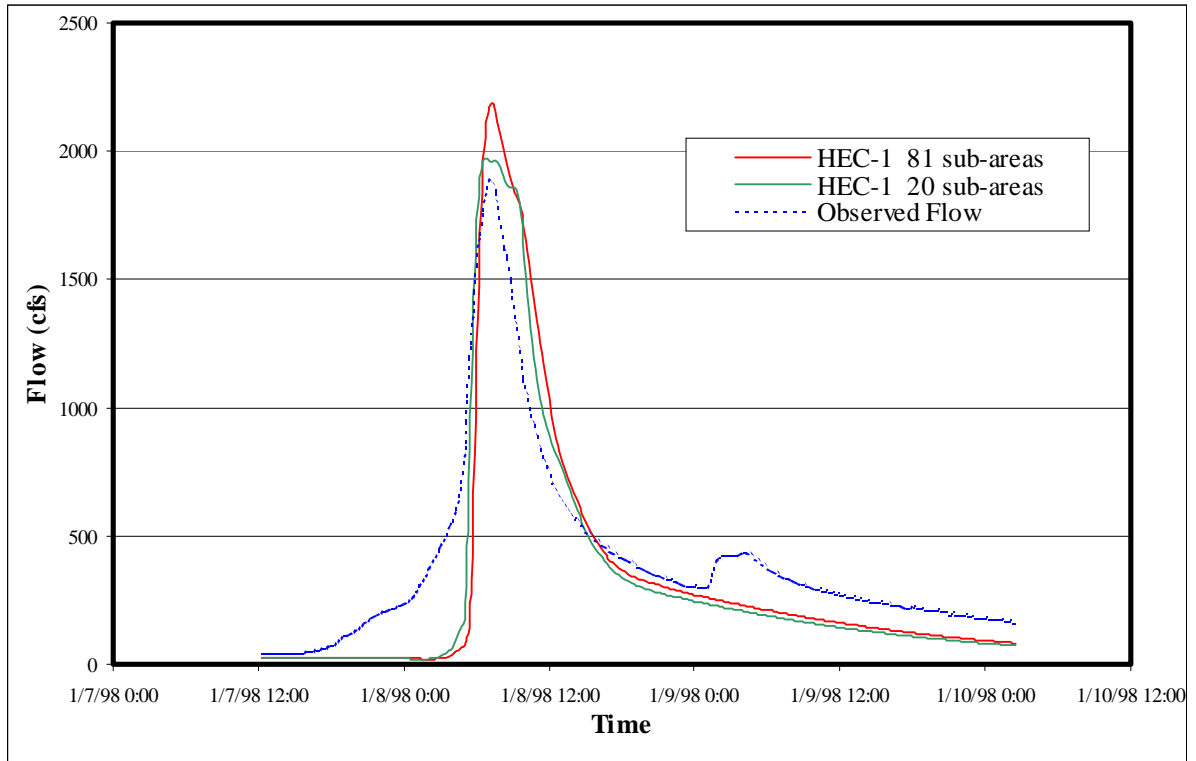


Figure H (8). January 1998 event; HEC-1 simulation.

# Appendix I

## TOPMODEL Hydrographs Used for Comparison with HEC-1

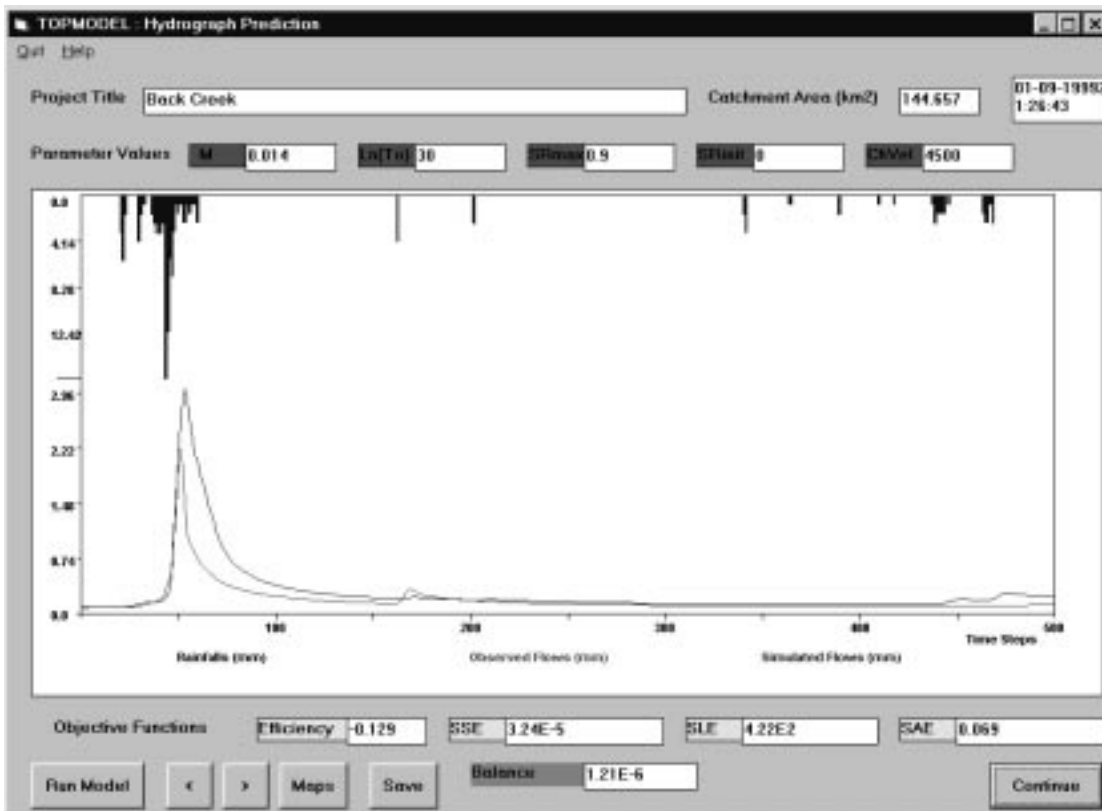


Figure A (1). January 1995 event; continuous TOPMODEL simulation.

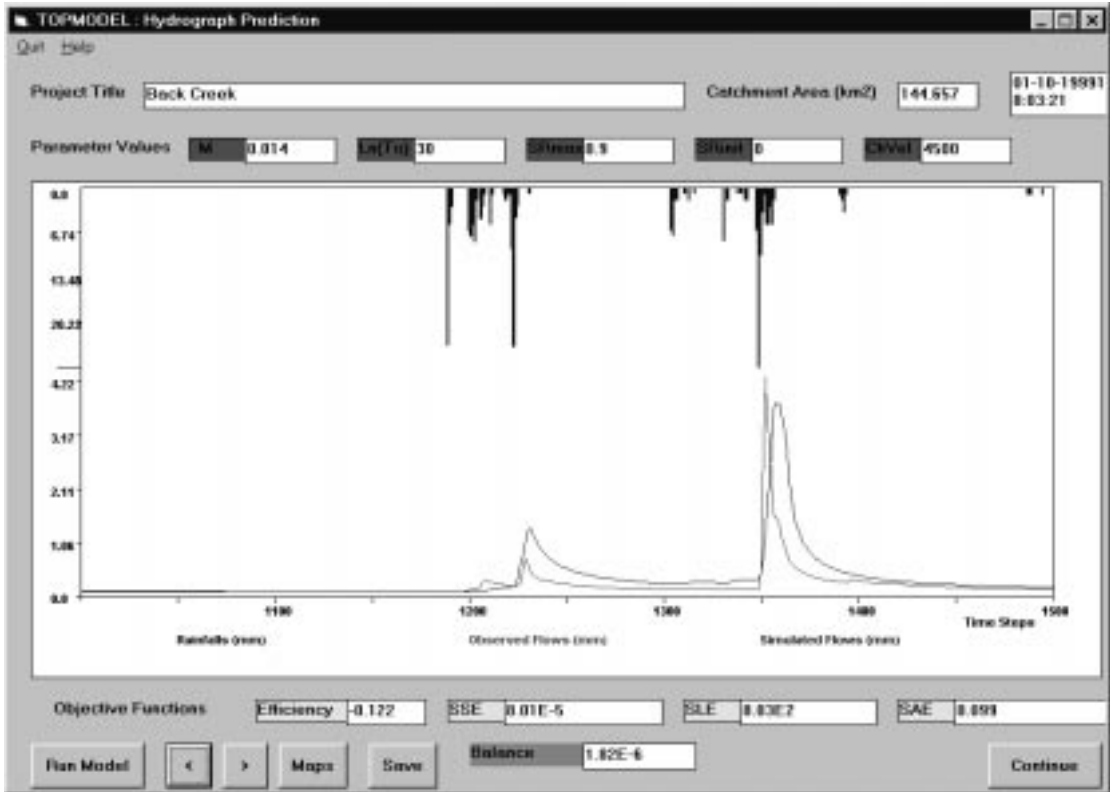


Figure I (2). June 1995 event; continuous TOPMODEL simulation.

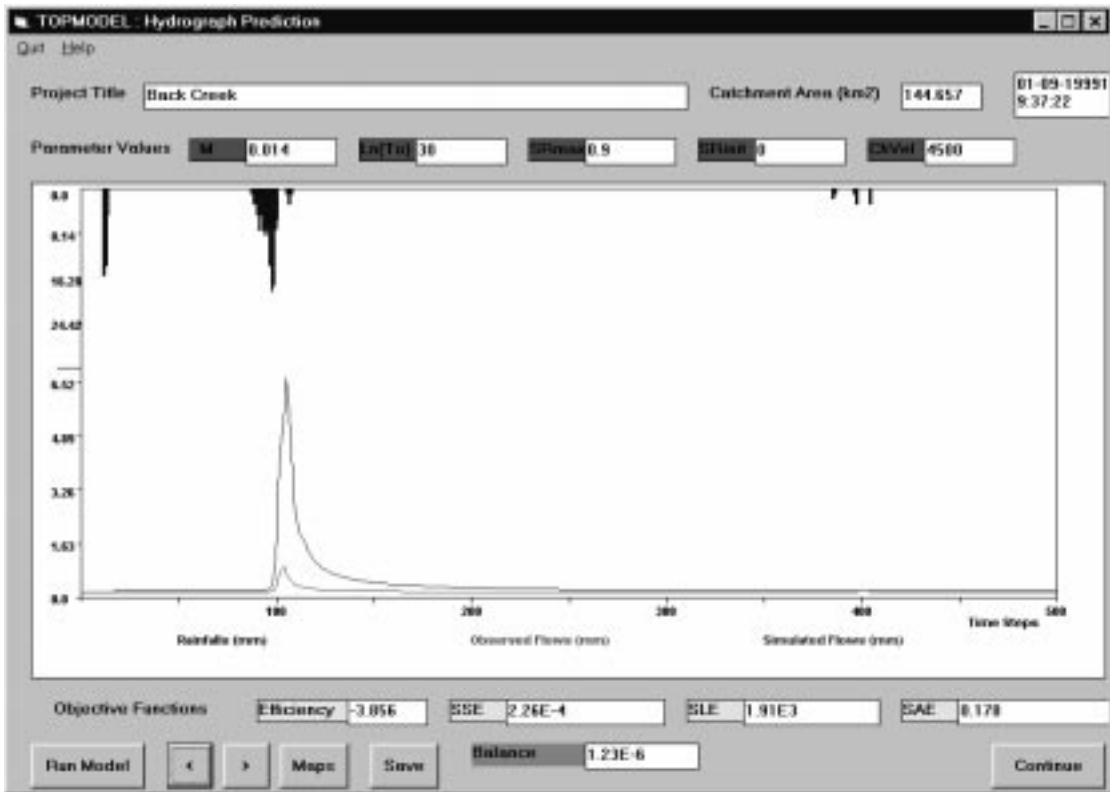


Figure I (3). August 1996 event; continuous TOPMODEL simulation.

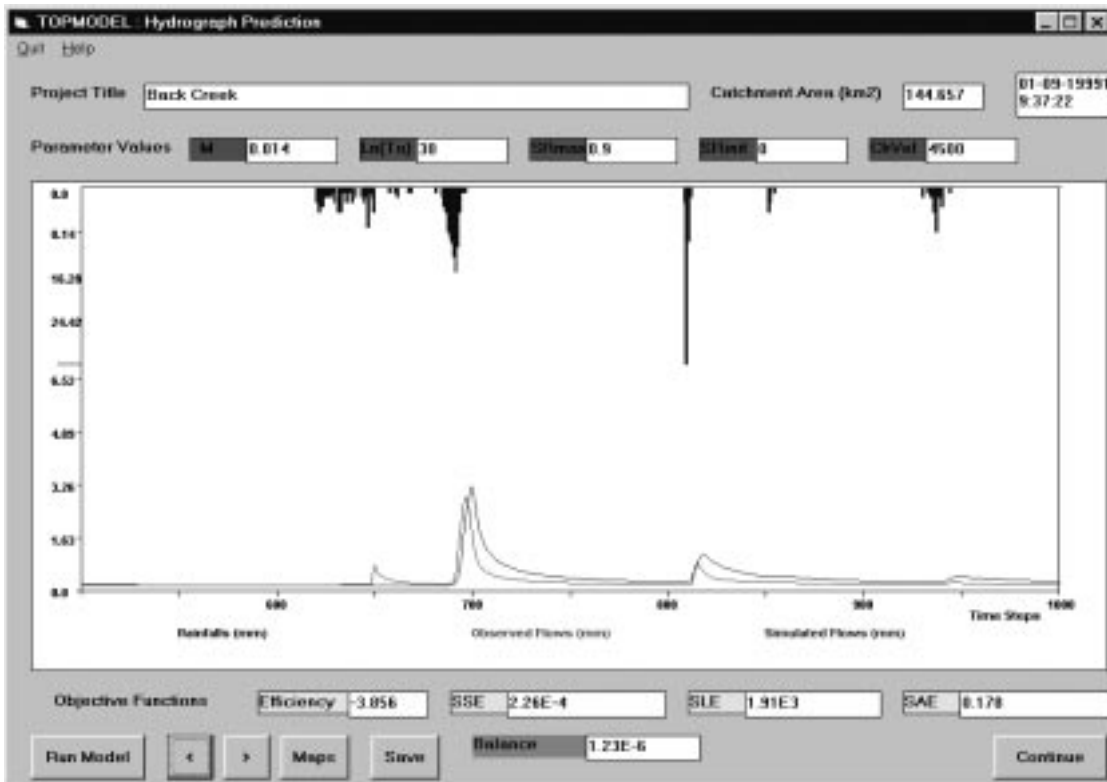


Figure I (4). September 1996 event; continuous TOPMODEL simulation.

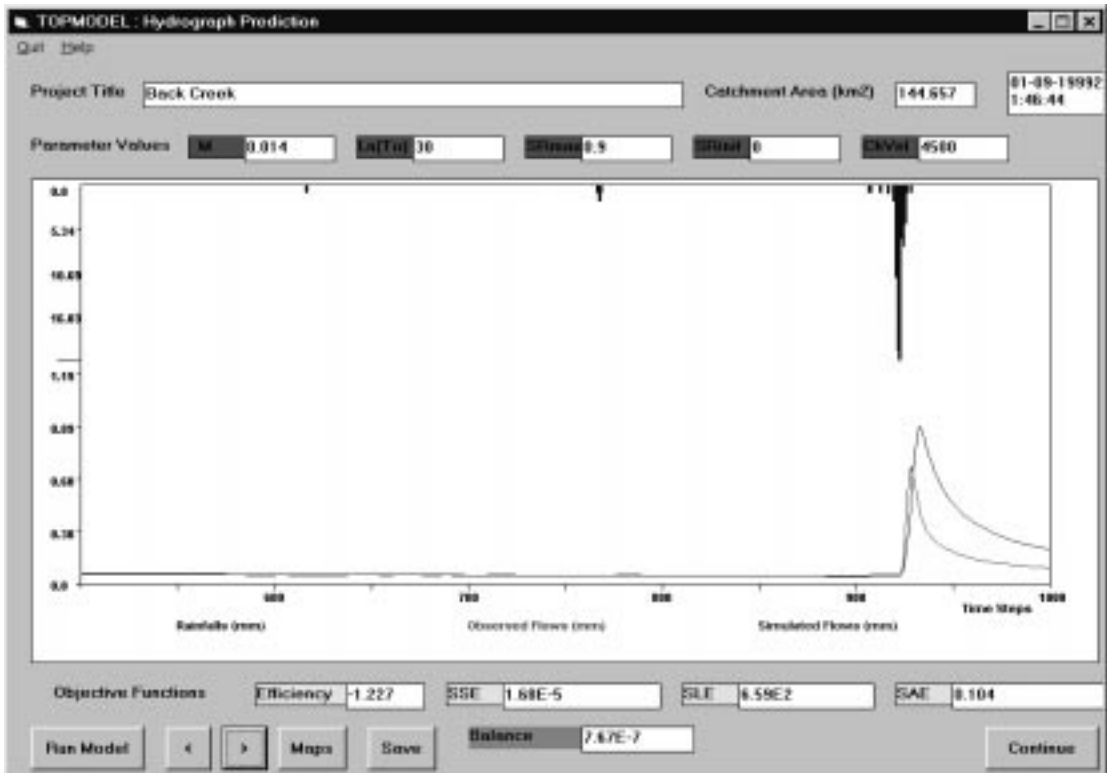


Figure I (5). November 1996 event; continuous TOPMODEL simulation.

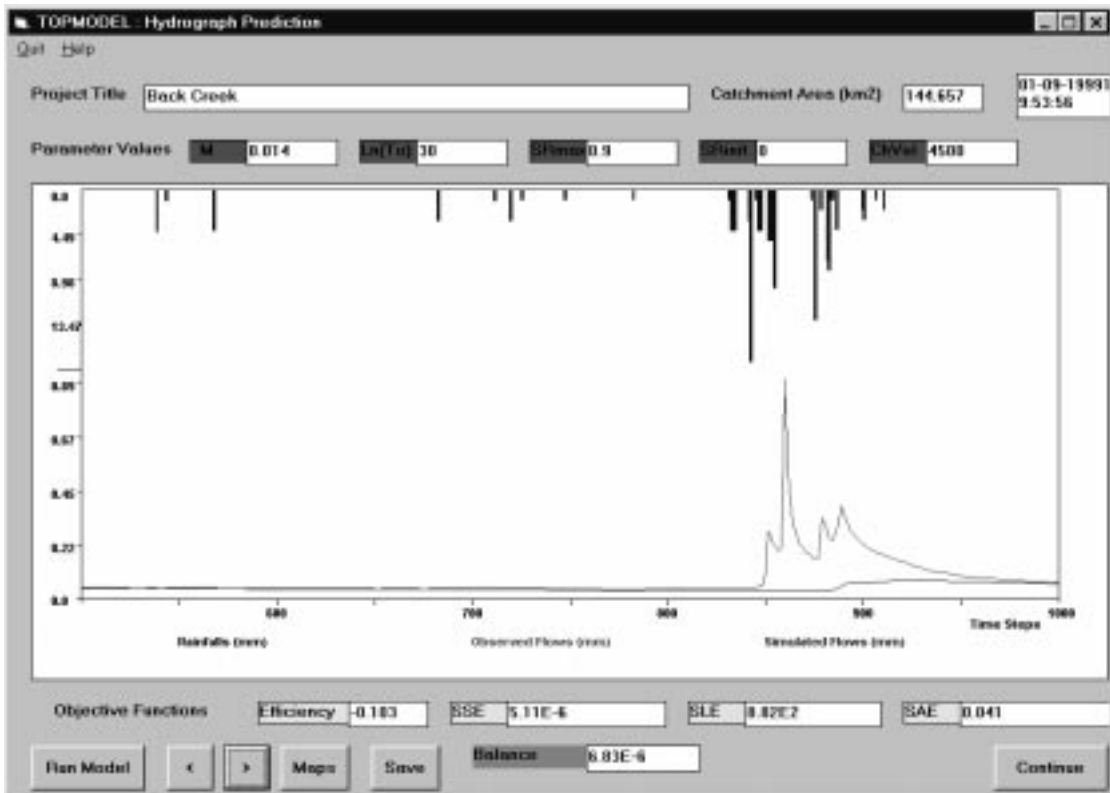


Figure I (6). June 1997 event; continuous TOPMODEL simulation.

# Appendix J

## Hydrographs for Water Years 1995, 1996, 1997, and the Beginning of 1998

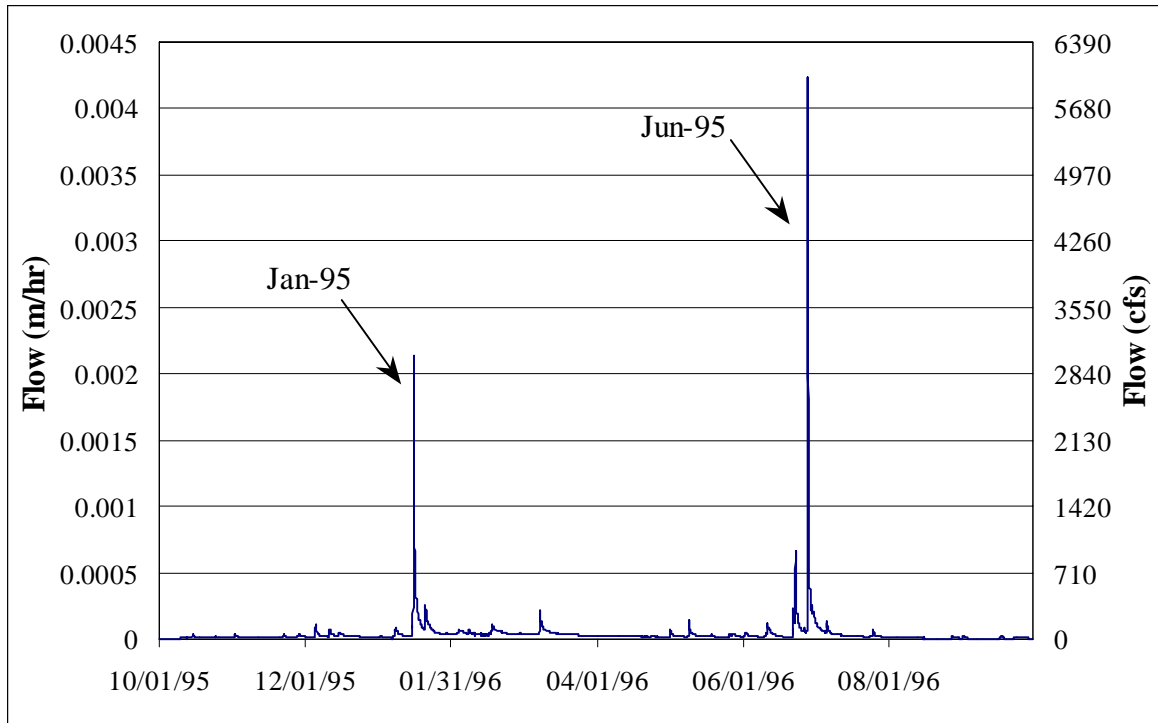


Figure J (1). 1995 water year with HEC-1 events identified.

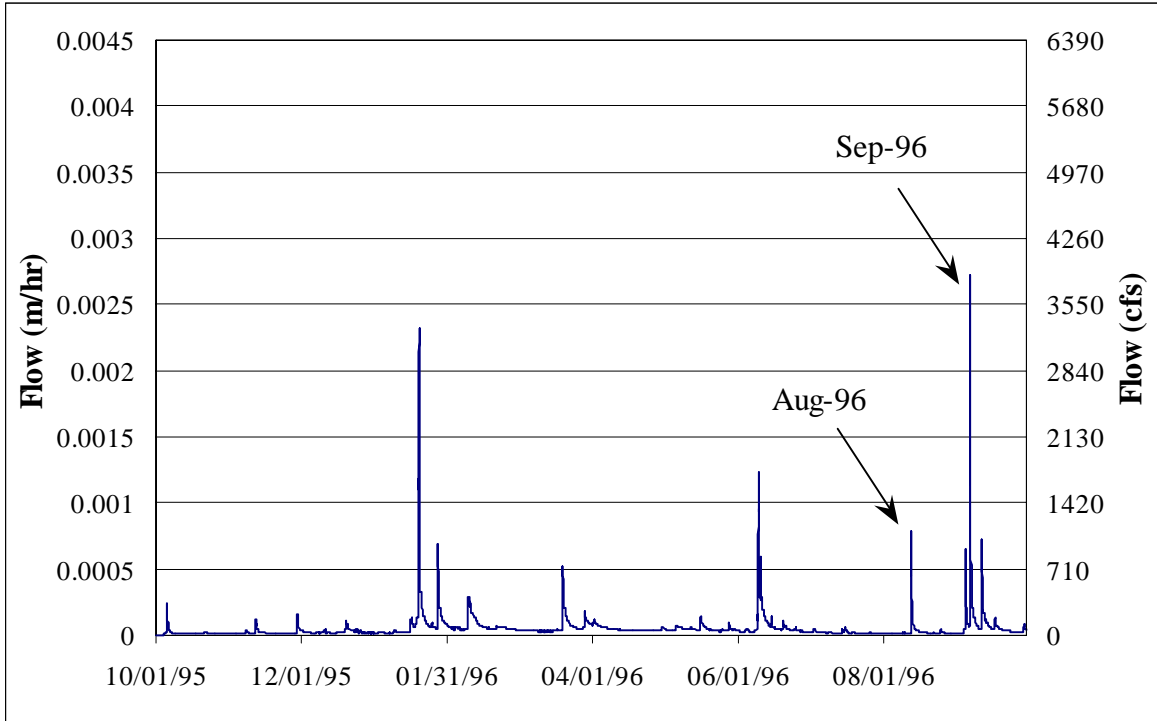


Figure J (2). 1996 water year with HEC-1 events identified.

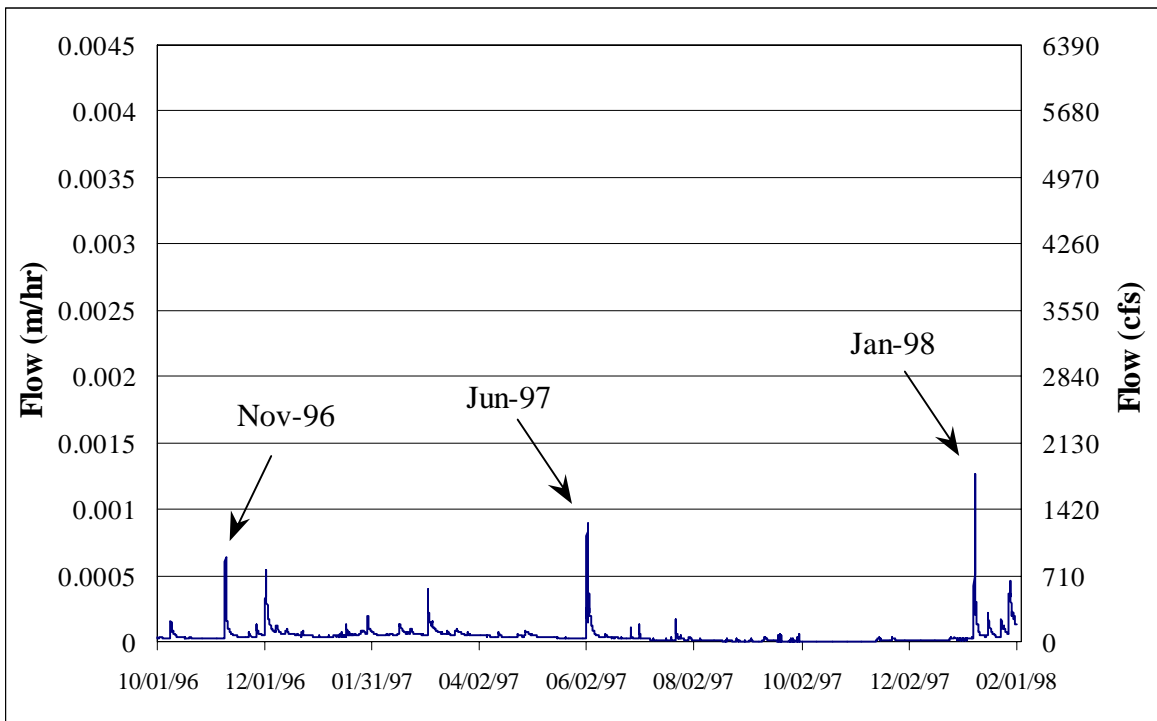


Figure J (3). 1997 and beginning of 1998 water years with HEC-1 events identified.

## Vita

Ryan Fedak was born on August 5, 1974 to Amelia and Andrew Fedak in Fairfax, Va. He graduated Woodbridge Senior High School in the spring of 1992 and began his studies at Virginia Tech the following fall. Mr. Fedak began his graduate studies in the fall of 1997 immediately after earning his undergraduate degree. Upon receiving his Master of Science degree, he will move to Atlanta and begin working for Moreland Altobelli Associates, Inc. In the near future, he hopes to travel to a developing country to undertake water-related service work.